PROTON TRANSFER AND COHERENT PHENOMENA IN MOLECULAR STRUCTURES WITH HYDROGEN BONDS

V. V. KRASNOHOLOVETS, P. M. TOMCHUK, and S. P. LUKYANETS

*Department of Theoretical Physics, Institute of Physics,
National Academy of Sciences, Kyïv, Ukraine*

CONTENTS

I. SPECIFIC PHYSICAL EFFECTS IN STRUCTURES WITH HYDROGEN BONDS

Hydrogen bonds and the motion of protons in hydrogen-bonded networks exhibit a great number of interesting physical effects, which, in turn, bring profound theoretical studies into being.

The most reliable information on the behavior of hydrogen bonds and proton motion in a hydrogen bond and through hydrogen-containing compounds yields X-ray diffraction, Raman and infrared (IR) spectra, nuclear magnetic resonance (NMR), absorption electron spectra, microwave and submicrowave spectroscopy, quasi-elastic neutron scattering (QENS), and rotational spectroscopy of supersonically expanded jets. The arrival of intense neutron sources has had a new dramatic impact on hydrogen bonding studies in solids [1]: Neutron diffraction and vibrational spectroscopy can also be performed with inelastic neutron scattering (INS) techniques. Besides, a very remarkable result has

recently been obtained by Isaacs et al. [2]: Studying high-momentum transfer inelastic (Compton) X-ray scattering of the hydrogen bond in ice I_h, they have revealed the Compton profile anisotropy that has reasonably been interpreted as the first direct experimental evidence for the substantial covalent character of the hydrogen bonds. The results obtained in Ref. 2 indeed demonstrate a high sensitivity of Compton scattering at the investigation of the phase of the electronic wave function. Thus, a pure classical (electrostatic) bonding model turns out to be inconsistent to describe the dynamics of the hydrogen bond, and that is why the role of quantum mechanical description of the behavior of the hydrogen bond is growing.

By means of the IR spectroscopy, Zundel [3–6] could show that various homoconjugated hydrogen bonds demonstrate a large proton polarizability. He found that in the case when a system of hydrogen bonds is completely structurally symmetrical, the whole system shows a large proton polarizability due to the strong coupling of proton motions.

Inelastic neutron scattering studies have shown [7–11] that many hydrogen-bonded crystals [potassium carbonate (i.e., $KHCO_3$), various polyanilines, $Ca(OH)_2$, and others] are characterized by the proton dynamics that is very decoupled from the backbone lattice.

The availability of the coherent proton tunneling and cooperative proton tunneling and transfer of four protons in hydrogen bonds of benzoic acids crystals (including dye doped) have been revealed by Trommsdorff and collaborators [12,13] by reading the electron spectra of the crystals.

Describing different techniques employed at the investigation of the motion of protons in hydrogen bonds, Fillaux [11] in particular notes that optical techniques are very sensitive to the hybridization state of valence electrons, which are largely unknown, and quantum calculations are not yet able to provide reliable values. On the contrary, the neutron scattering process is entirely attributable to nuclear interactions, and cross sections are independent of chemical bonding. It is interesting that the inelastic neutron scattering spectrum of the $KHCO_3$ cannot be described by conventional harmonic force fields because its protons are almost totally decoupled from surrounding heavy atoms, and it is also interesting that the dynamics of the protons are rather specified by localized modes in a fixed frame [11]. Similar results have been obtained for a whole series of molecular crystals, and this means that the description of the dynamics of molecular crystals based on the normal modes formalism should be reconsidered. Fillaux [14] has suggested that such a peculiar dynamics of protons might be resulted from quantum mechanics of a nonlocal sort.

At the same time, Trommsdorff [15] advocates low-temperature spectroscopy combined with single-molecule spectroscopy, calling them an exraordinal powerful tool to study the structure and dynamics in condensed phases. He

intimates that high-resolution optical spectroscopic methods make it possible to directly investigate some aspects of proton transfer reactions in which the proton displacement takes place by tunneling [15,16]. The observation of intramole-cular coherent proton tunneling has allowed the detailed theoretical examination and qualitative numerical calculations for such compounds as porphyrine, namalonaldehyde, topolone, and so on [15]. Intermolecular proton tunneling occurs in a great number of systems; as a rule, researchers talk about incoherent tunneling, which implies the direct influence of the thermal bath [15,17].

There is no energy difference in the symmetric double-well potential, and this gives rise to the direct proton tunneling, however, any asymmetry of the double-well potential creates the energy difference between vibrational levels. In this case one can infer that the tunneling motion should incorporate the vibrating energy of surrounding atoms. Indeed, it seems reasonable that when the proton moves, surrounding atoms should adjust to new equilibrium positions and hence the potential energy, or potential energy surface will govern the proton motion; in the general case it should incorporate the interaction with surrounding atoms including the rest protons and outside fields [18,19]. Theoretical consideration conducted in Refs. 20–22 [see also Refs. 23 (review paper) and 24] showed that the tunneling motion could occur when the tunneling motion of a proton is associated with phonons.

In particular, recent results [25] obtained by quasi-elastic neutron scattering are consistent with the fast localized motion of hydrogen associated with phonons within the hexagons formed by interstitial $g(Hf_2Mo_2)$ sites. Besides, the researchers [25] has also revealed the slower jump process corresponding to hopping of hydrogen from one hexagon to another, which has been proven by nuclear magnetic resonance measurements. The ratio of the characteristic hopping rates for the two jump processes is $\sim 10^3$ at 300 K.

A very peculiar dynamics has been revealed in the $Ca(OH)_2$ crystal by means of inelastic neutron scattering technique [26]. It has been found that anharmonic terms must be included, which mix the vibrational states of the OH and lattice modes. In particularly, the lattice modes have successfully been represented as the superposition of oxygen and proton synchronous oscillators, and it appears that the proton bending mode E_u is strongly coupled to the lattice modes. The contribution of the proton harmonic wave functions has been taken as the zero-order approximation.

Thus it seems that the whole variety of hydrogen-containing compounds might be subdivided to three conditionally independent groups. The first group embraces compounds that feature coherent proton tunneling, the second one covers compositions in which incoherent tunneling occurs, and the third one is intermediate between the first and second groups.

Other problems are associated with the motion of an excess proton through the network of hydrogen bonds (e.g., ice) or along a hydrogen-bonded chain.

Such a motion in many aspects is very different from the discussed above. We can mention here an early review paper by Morowitz [27] on biological systems considered as proton semiconductors, and we can also mention experimental work [28] on the first evidence for high conduction of protons along the interface between water and a polar lipid monolayer. A number of hydrogen-containing solids, such as lithium hydrazium sulfate $Li(N_2H_5)SO_4$, tri-ammonium hydrogen disulfate $(NH_4)_3H(SO_4)_2$, and others, exhibit the protonic conductivity three orders of magnitude greater along the c axis than in the perpendicular directions [29,30] (this is because of very long hydrogen-bonded chains, which are parallel to c axis and spread along the whole crystal [31,32]). Hydrogen-bonded chains are also present in many biological objects, in proton-conducting membrane proteins in particular [1,33–37]. The titled crystals together with other ones—for example, $(NH_4)_3H(SeO_4)_2$ [38–42] and $NH_4IO_3 \cdot 2HIO_3$ [43–48]—belong to superionic conductors due to abnormal high proton conductivity.

Modern inelastic neutron scattering technique has made it possible to discover free protons in solids [49]; that is, free protons have been found in manganese dioxides, coals, graphite nitric acid intercalation compounds, polypyrolles and polyanilines, and β-alumina. Perhaps the said compounds may be called protonic conductors as well, though in the solids the density of free protons is very small and the distribution of proton kinetic momentum is hidden by the zero-point oscillations of the host matrix [49].

In liquid phase, hydrogen atoms (or hydrogen bonds) display other peculiarities. For instance, the hydrogen bond structure of liquid water and alcohols is exemplified by the existence of three different species, as it follows from the infrared overtone spectra [50]: $OH_{nonbounded}$, $OH_{weak-cooperat.}$, and $OH_{strong-cooperat}$. By increasing the temperature, the content of strong cooperative hydrogen bonds decreases and a similar number of weak cooperative hydrogen bonds increases. Thus the difference spectra indicate identically the necessity to differ between three types of hydrogen-bonded interacting OH groups. In the next sections, we touch some other subtle structural characteristics of water.

Based on the nuclear magnetic resonance results, Huyskens [51,52] (see also Ref. 53) has corrected the ratio of a definite number of hydrogen bonds for a given number of molecules, $r_f = (1 - N_{H\text{-bond}}/N_{molecules})$, deduced for alcohol by Luck [54–56]. Huyskens has shown that the hydrogen bonds perpetually jump from one partner to another; in other words, molecules are completely inserted in a chain, acting at the same time in hydrogen bonding as proton donor and proton acceptor.

The arrangement of hydrogen bonds in hydrogen-containing compounds, which takes place in condensed phases (liquid, liquid crystal, and solid) due to the phase transition, is often accompanied by the appearance of open asso-ciates with their following polymerization, or clustering as it happens in

alkoxycyanobipheniles. A sophisticated theoretical analysis of the mechanism of dissociation of the cyclic dimmers accompanied by formation of opened chain-like associates and monomers has recently been proposed by Krasnoholovets and co-workers [57–62].

One more interesting aspect that we would like to mention has recently been emphasized by Gavrilov and Mukina [63]: Common to all protonated crystals with hydrogen bonds is the existence of distinguishing ranges of temperature, which are typical for crystals with weak hydrogen bonds (100 ± 10 K) and those with strong hydrogen bonds (210 ± 10, 260 ± 10, 380 ± 10 K).

In the next section we describe the most general approaches that are successfully employed at the theoretical study of the hydrogen behavior in compounds with hydrogen bonds. Then in the following sections we will show how some concrete problems are solved using methods developed in quantum mechanics, quantum field theory of solids, and statistical mechanics.

II.   QUANTUM MECHANICAL DESCRIPTION OF HYDROGEN-BONDED SYSTEMS

A.   Hydrogen Bond Vibrations

First consideration for the motion of the hydrogen atom in double-well potentials were proposed by Kovner and Chuenkov [64] and Hadzi [65]. However, the detailed analysis of the separability of the X—H stretching vibrations (with energy about 3000 cm^{-1}) from the hydrogen bond vibrations (with energy around 100 cm^{-1}) in the linear triatomic X—H$\cdots$Y system was carried out by Marechal and Witkowski [66].

Their attempt [66], rather successful, was aimed to fully explain the experimental infrared spectra. The normal stretching coordinates representing the X—H motion and the X—H$\cdots$Y motion were designated as q and Q, respectively (Fig. 1). The Hamiltonian describing such a system was written as

$$H(q,Q) = \frac{P^2}{2M} + \frac{p^2}{2m_{\mathrm{H}}} + U(q,Q) = \frac{P^2}{2M} + H_1(q,Q) \qquad (1)$$

Here P and p are the conjugate momenta of the coordinates Q and q, respectively; M and m_{H} are the masses of points described by the coordinates Q and q,
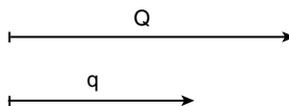
Figure 1. Q and q are normal coordinates.

respectively. $U(q, Q)$ is the potential energy for this motion. Using the fact that the oscillatory motion of the q coordinate is several tens faster than the oscillatory motion of the Q coordinate, the eigenfunctions Ψ of the Hamiltonian $H(q, Q)$ was expanded as

$$\Psi = \sum_n \alpha_n(Q)\phi_n(q, Q) \tag{2}$$

Thus $\phi_n(q, Q)$ is the wave function for the q motion when Q is fixed. The corresponding characteristic equation is

$$H\phi_n(q, Q) = \mathscr{E}_n(Q)\phi_n(q) \tag{3}$$

The wave function $\alpha_n(Q)$ for the Q motion is the characteristic of the equation

$$\left[\frac{P^2}{2M} + \mathscr{E}_n(Q) + \langle \varphi_n(q, Q)|\frac{P^2}{2M}|\phi_n(q, Q)\rangle_q\right]\alpha_n(Q) + \sum_{n,n_1}$$
$$\times \left[\langle \phi_n(q, Q)|\mathbf{P}|\phi_{n_1}(q, Q)\rangle_q \frac{\mathbf{P}}{M} + \langle \phi_n(q, Q)|\frac{P^2}{2M}|\phi_{n_1}(q, Q)\rangle_q\right]$$
$$\times \alpha_n(Q) = E\alpha_n(Q) \tag{4}$$

The function ϕ_n is reasonably approximated as a harmonic-oscillator function whose force constant k and equilibrium position q_0 depend on Q. Such an approximation signifies that the potential energy in expression (1) can be written as

$$U(q, Q) = \frac{1}{2}k(Q)[q - q_0(Q)]^2 + U'(Q) \tag{5}$$

Thus the frequency of the q motion is

$$\omega_H(Q) = \sqrt{k(Q)/m_H} \tag{6}$$

Here $\omega_H(Q)$ is equal to the X—H stretching mode when the hydrogen bonding is still not switched. This allows the calculation of the eigenvalues [66]

$$\mathscr{E}_n(Q) = \langle \varphi_n(q, Q)|H_1|\phi_n(q, Q)\rangle_q$$
$$= \left(n + \frac{1}{2}\right)\hbar\omega_H(Q) + \frac{1}{2}m_H\omega_H^2 q_0^2(Q) + U'(Q) \tag{7}$$

$$\langle \varphi_n(q, Q)|\frac{P^2}{2M}|\phi_n(q, Q)\rangle_q = \left(n + \frac{1}{2}\right)\frac{\hbar^2}{M}\left(\frac{d\omega}{dQ}\right)^2(1 - 4\mu) \tag{8}$$

where

$$\lambda(Q) = -q_0(Q)[m_H\omega_H(Q_0)/2\hbar]^{1/2}$$
$$\mu(Q) = [\omega_H(Q_0) - \omega_H(Q)]/2[\omega_H(Q_0) + \omega_H(Q)]$$

$$(9)$$

The other matrix elements involved in Eq. (4) are obtained [66] by using a Lippinkott–Schröder potential [67]. Using expressions (7) and (8), the following Hamiltonian can be derived:

$$H^{(n)} = \frac{P^2}{2M} + \left(n + \frac{1}{2}\right)\left[\hbar\omega_H(Q) + \frac{\hbar^2}{M}\left(\frac{d\lambda}{dQ}\right)^2(1 - 4\mu)\right]$$
$$+ \frac{1}{2}m_H\omega_H^2(Q)q_0^2(Q) + U'(Q)$$

$$(10)$$

The two main consequences follow from the Hamiltonian (10): (i) The difference between the Hamiltonians of the first excited state ($n = 1$) and the ground state ($n = 0$) for the q motion is

$$H^{(1)} - H^{(0)} \cong \mathrm{const} + B_HQ, \quad B_H = \hbar\left(\frac{d\omega_H}{dQ}\right)_{Q_0}$$

$$(11)$$

(ii) The isotope effect is characterized by the substitution $B_D = B_H/\sqrt{2}$.

Many carboxylic acids in gases and condensed states form dimers connected by a couple of hydrogen bonds (Fig. 2). The said acids are often treated as model systems for the study of spectra of hydrogen bonds [66], intermolecular
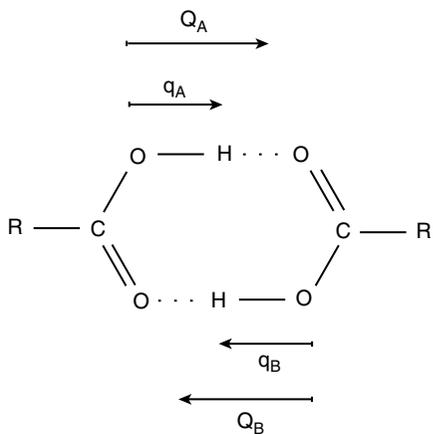
Figure 2. The cyclic planar carboxylic acid dimer.

hydrogen bonding and proton reactions [20–23], and rearrangement of hydrogen bonds [57–60].

The total Hamiltonian of a cyclic dimmer can be written as

$$H_{\text{total}} = H_A + H_B + H_{\text{int}} \tag{12}$$

where $H_{A(B)}$ is the Hamiltonian (1). The individual wave functions for the O—H stretching modes of bond A and B are taken as the basis wave functions. In the basis state the appropriate wave function is

$$\phi_0^l = \beta_0^l(Q_A, Q_B)\phi_0(q_A, Q_A)\phi_0(q_B, Q_B) \tag{13}$$

The corresponding effective Hamiltonian is

$$H_0 = \frac{P_A^2}{2M} + \frac{P_B^2}{2M} + \mathcal{E}_0(Q_A) + \mathcal{E}_0(Q_B) \tag{14}$$

The wave functions that specify a single excitation in the group O—H are

$$\begin{aligned}
\phi_1^l = {} & \beta_1^l(Q_A, Q_B) \quad \phi_1(q_A, Q_A) \quad \phi_0(q_B, Q_B) \\
& + \beta_1^{l'}(Q_A, Q_B) \quad \phi_0(q_A, Q_A) \quad \phi_1(q_B, Q_B)
\end{aligned} \tag{15}$$

Functions (15) split the effective Hamiltonian to

$$H^{\pm} = \frac{P_A^2}{2M} + \frac{P_B^2}{2M} + \mathcal{E}_1(Q_A) + \mathcal{E}_2(Q_B) \pm H_{\text{int}}(Q_A, Q_B)C_2 \tag{16}$$

where C_2 is the symmetry operator.

The transition probability from the l'th level of H_0 is defined as

$$D_l^{l'(\pm)} = \text{const}|\langle \beta_0^{l'}(Q_A, Q_B)|1 \mp C_2|\beta_l^{\pm}(Q_A, Q_B)\rangle_{Q_A+Q_B, Q_A-Q_B}|^2 \tag{17}$$

$D_l^{l'(\pm)}$ was computed [66] by a variational method; in the first approximation

$$D_{u,v}^{u',v'(\pm)} = \Gamma_{u,u'}^2 \left(\frac{B_{\text{H}}}{\sqrt{2M\hbar\omega_{\text{OO}}}} \right) \cdot (C_v^{v'(\pm)})^2 \tag{18}$$

Here l stands for the two indices u and v and $\Gamma_{u,u'}$ is the Franck–Condon factor. The calculated transition probability (18) was very successfully applied for the description of the experimental spectra for CD_3COOH and CD_3COOD [66].

The dependence of stretching vibrations of X—H on the length of the hydrogen bond is studied very well both theoretically and experimentally (see,

e.g., Refs. 68–70). However, the reasons of the bending vibrations of hydrogen bonds still remained unclosed so far. In Section II.E we will discuss a possible mechanism of such a behavior of the hydrogen bond.

B. Proton Transfer Incorporating Acoustic Phonons

The interconversion of the two tautomer forms of dimers (Fig. 2) by a concerted two proton transfer is governed by a double-well potential. In condensed phases the two possible tautomers are identical. Skinner and Trommsdorff [21] treated a model of crystalline benzoic acids in which the dynamics of each proton pair is uncorrelated with other pairs. Their model was based on a single double-minimum potential coupled to a thermal bath—that is, crystal vibrations. It was believed that in a condensed phase the crystal field breaks the symmetry of the two wells (Fig. 3). If Fig. 3 indeed represents the real situation when the proton transfer from the left well to the right one should take place at the participation of vibrations of the crystal; that is, phonons of some sort should activate the proton transfer. We would like to emphasize that this is the conventional viewpoint, which is widely employed by physicists.

For instance, a new method for dealing with phonon modes in path integrals was proposed by Sethna [71,72]. Using the path integrals and an instanton
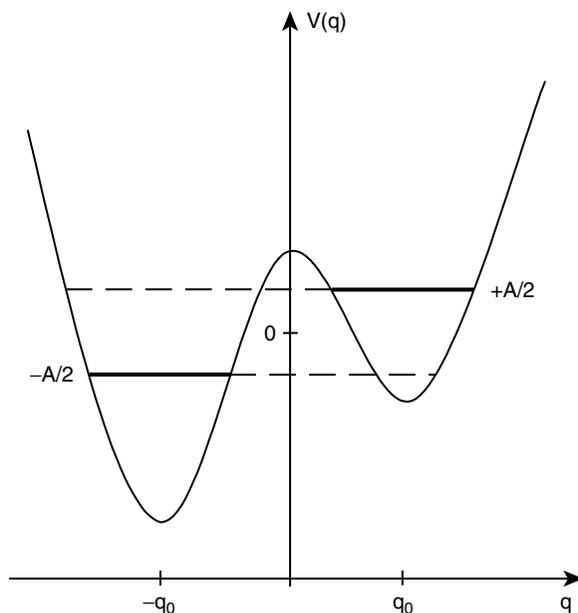
Figure 3. Asymmetric double-well potential $v(q)$. The minima are located at $\pm q_0$; the energy of the localized states $|\beta\rangle$ and $|\alpha\rangle$ are, respectively, $\pm A/2$.

calculation, he could construct a detailed theory of the tunneling event in the presence of phonons. The influence of dissipation on quantum coherence of a quantum mechanical particle that moves in a symmetric double-well potential and interacts with the environment by a phenomenological friction coefficient was considered by Bray and Moore [73]. Those methods are very interesting because they allow the quantitative calculation of rate constant which characterizes the process of tunneling in a double-well potential.

Using the mentioned approach [71–73], Skinner and Trommsdorff [21] started from the Hamiltonian

$$H = H_0 + H_{\text{ph}} + H' \tag{19}$$

Here

$$H_0 = T_q + v(q) \tag{20}$$

is the Hamiltonian for the proton coordinate q, and T_q and $v(q)$ are the kinetic energy and potential energy, respectively;

$$H_{\text{ph}} = T_Q + V(Q) \tag{21}$$

is the Hamiltonian of the crystalline coordinate Q, and T_Q and $V(Q)$ are the kinetic energy and potential energy, respectively;

$$H' = V(q, Q) \tag{22}$$

is the interaction potential energy.

The potential energy for proton coordinate written in the linear approximation is

$$v(q) = v_0(q) + \tilde{A}q \tag{23}$$

where $v_0(q)$ is a symmetric potential with minima at $\pm q_0$. For the symmetric case when $A = 0$, there are two lowest states $|\psi_1^0\rangle$ and $|\psi_2^0\rangle$ with an energy difference $E_2^0 - E_1^0 = J > 0$, which is also called the tunneling splitting. Setting $E_1^0 = -J/2$, one can choose new states $|\alpha\rangle = \frac{1}{2}(|\psi_1^0\rangle - |\psi_2^0\rangle)$ and $|\beta\rangle = \frac{1}{2}(|\psi_1^0\rangle + |\psi_2^0\rangle)$. The wave functions $\psi_\alpha(q) = \langle q \mid \alpha \rangle$ and $\psi_\beta(q) = \langle q \mid \beta \rangle$ are localized in the left and right wells, respectively, besides $\langle \alpha|q|\beta\rangle = 0$.

In such a presentation

$$H_0 = \left\| \begin{matrix} -A/2 & -J/2 \\ -J/2 & A/2 \end{matrix} \right\| \tag{24}$$

where $A \cong 2\tilde{A}q_0$ is the energy asymmetry between the localized levels (Fig. 3). The eigenvalues corresponding to the Hamiltonian (24) are

$$E_1 = -\frac{1}{2}\sqrt{A^2 + J^2}, \qquad E_2 = -E_1 \qquad (25)$$

In the framework of the model, the difference $E_2 - E_1$ is within the acoustic phonon bandwidth, and that is why Skinner and Trommsdorff [21] reasonably assumed that the longitudinal acoustic modes could influence the tunneling proton transfer. The interaction potential (22) was chosen in the form of the deformation potential approximation (see Ref. 74)

$$H' \cong \frac{1}{2}a\delta\rho(\mathbf{R})$$

$$\delta\rho(\mathbf{R}) = -\hbar \sum_{\mathbf{k}} \sqrt{\frac{\omega_{\mathbf{k}}\omega_{\mathrm{D}}}{N}}(\hat{b}_{\mathbf{k}}e^{i\mathbf{k}\mathbf{R}} + \hat{b}_{\mathbf{k}}^{+}e^{-i\mathbf{k}\mathbf{R}}) \qquad (26)$$

Here a is a dimensionless constant, $\delta\rho(\mathbf{R})$ is the density fluctuation of the medium at the position $\mathbf{R}$ (the center of symmetry of the benzoic acid dimer), ω_{D} is the Debye frequency, and N is the number of acoustic modes, $\omega_{\mathbf{k}} = v_{\mathrm{sound}}|\mathbf{k}|$, $\hat{b}_{\mathbf{k}}^{+}(\hat{b}_{\mathbf{k}})$ is the Bose operator of creation (annihilation of a acoustic phonon with the wave vector $\mathbf{k}$). In the localized representation we have

$$H_0 = \left\|\begin{matrix} -\delta A/2 & 0 \\ 0 & \delta A/2 \end{matrix}\right\| \qquad (27)$$

where $\delta A = a\delta\rho(\mathbf{R})$.

The second-order perturbation theory makes it possible to calculate the rate constant for the transition from the eigenstate $|\psi_m\rangle$ to $|\psi_l\rangle$ [21]:

$$k_{lm} = \frac{1}{\hbar^2}\int_{-\infty}^{\infty}\langle H_{lm}'^{+}(t)H_{lm}'\rangle e^{i\omega_{ml}t}dt \qquad (28)$$

where

$$\omega_{ml} = (E_m - E_l)/\hbar, \qquad H'(t) = e^{iH_{\mathrm{ph}}t/\hbar}H'e^{-iH_{\mathrm{ph}}t/\hbar}$$

$$\langle\ldots\rangle = \frac{\mathrm{Tr}\{e^{-H_{\mathrm{ph}}/k_{\mathrm{B}}T}\ldots\}}{\mathrm{Tr}\,e^{-H_{\mathrm{ph}}/k_{\mathrm{B}}T}}, \qquad H_{\mathrm{ph}} = \sum_{k}\hbar\omega_k\left(\hat{b}_k^{+}\hat{b}_k + \frac{1}{2}\right) \qquad (29)$$

For the chosen model ($l, m = 1, 2$), Skinner and Trommsdorff [21] calculated the rate constant

$$k_{21} = k_{21}^0 \cdot (n(\omega_{21}) + 1) \tag{30}$$

$$k_{21}^0 = k\omega_{21}, \qquad k = \frac{3\pi}{2}a^2\left(\frac{J}{\hbar\omega_D}\right)^2, \qquad n(\omega) = \frac{1}{e^{\hbar\omega/k_BT} - 1} \tag{31}$$

Rate constants k_{21} and k_{12} satisfy the detailed balance condition

$$k_{21}/k_{12} = e^{-\hbar\omega_{21}/k_BT} \tag{32}$$

The fundamental relaxation rate is

$$\frac{1}{\tau} = k_{12} + k_{11} = k_{21}^0\coth\frac{\hbar\omega_{21}}{2k_BT} \tag{33}$$

In Ref. 21 it was also considered the model of two interacting double wells coupled to a thermal bath. The problem was simplified by the consideration of two dimers separated by the dye molecule when the distance between the dimmers was about 1 nm. In this case the interaction Hamiltonian was approximated by

$$H' = \delta A \cdot (|\phi_4\rangle\langle\phi_4| - |\phi_1\rangle\langle\phi_1|) \tag{34}$$

where $|\phi_i\rangle$ ($i = 1, \ldots, 4$) are the basis states for the Hamiltonian H_0, which is the four-row matrix that includes parameters A and J determined above and a new one, $B \propto 2v_0q_0^2$. In the case when the inequality $J \ll |A \pm B|$ is not satisfied, H_0 can be diagonalized exactly [21]:

$$H_0 = \begin{Vmatrix} -A & -J/\sqrt{2} & 0 & 0 \\ -J/2 & -B & -J/\sqrt{2} & 0 \\ 0 & -J/\sqrt{2} & A & 0 \\ 0 & 0 & 0 & -B \end{Vmatrix} \tag{35}$$

The calculation of the rate constant for the model described by the Hamiltonians (35) and (34) results in [21]

$$k_{ij} = k_{ij}^0 \cdot (n(\omega_{ij}) + 1) \tag{36}$$

$$k_{ij} = k_{ij}^0 n(\omega_{ij}), \quad k_{ij}^0 = k\omega_{ij}\left(\frac{2\hbar\omega_{ij}}{J}\right)^2 [M_{3i}M_{3j} - M_{1i}M_{1j}]^2 \tag{37}$$

where M_{ij} are matrix elements for the eigenstates $|\psi_j\rangle$, which are functions of $|\phi_j\rangle$.

The rate constant (36) and (37) as a function of temperature correlated well with the experimental data obtained for the carboxylic acid protons of crystalline perprotobenzoic acid and ring-deuterobenzoic acids by nuclear magnetic resonance T_1 [75] and inelastic neutron scattering (for an analysis of the experiment see Refs. 76 and 77). It should be noted that some of the major parameters of the model (for instance, J) allowed the direct determination by fluorescence line narrowing technique.

The single-phonon absorption/emission is dominant at the low temperature limit when $A \gg k_B T$ and $a \gg 1$ (a is the dimensionless constant). When temperature increases, new factors begin to influence the proton transfer, namely, multiphoton processes and the tunneling through intermediate excited states.

In particular, in Ref. 78 the proton transfer dynamics of hydrogen bonds in the vicinity of the guest molecules has been studied by using a field-cyclic nuclear magnetic relaxometry (spin-lattice relaxometry). It has been revealed that the spin lattice relaxation incorporates the two major members:

$$T_1^{-1}(\omega) = T_1^{-1}(\omega)\big|_p + T_1^{-1}(\omega)\big|_g \tag{38}$$

The first member on the right in expression (38) is the relaxation rate caused by dimmers of the pure material. The second member arises from dynamics of the benzoic acid dimers contained within the range of the thiondigo quest molecule; $T_1^{-1}(\omega)\big|_g$ is stipulated by modulation of proton dipolar interaction induced by the proton transfer in the hydrogen bonds.

A very new methodology called the perturbative instanton approach has recently been developed by Benderskii et al. [79–84] for the description of tunneling spilling, which manifests itself in vibrational spectra of hydrogen containing nonrigid molecules. The mentioned studies allow the detailed consideration of resonances in tunneling splittings at the transverse frequency Ω close to the energy difference D between potential wells. Taking into account the asymmetry of the double-well potential, they chose the potential in the form (for simplicity we treat here only one-dimensional case) [82]

$$V = \frac{m\Omega^2 a_0^2}{8}(1 - X^2)^2 + \frac{3D}{4}X\left(1 - \frac{X^2}{3}\right) \tag{39}$$

The dimensionless asymmetry D has been assumed to be of the order of the semiclassical parameter γ^{-1} where

$$\gamma = \frac{m\Omega a_0^2}{2\hbar} \tag{40}$$

The corresponding Schrödinger equation is

$$\frac{d^2\psi}{dX^2} + \left[4\gamma\left(\varepsilon - \frac{3}{2}aX\left(1 - \frac{X^2}{3}\right)\right) - \gamma^2(1 - X^2)^2\right]\psi = 0 \qquad (41)$$

which includes the dimensionless parameters

$$\varepsilon = \frac{E}{\hbar\Omega}, \qquad a = \frac{D}{2\hbar\Omega} \qquad (42)$$

The solutions to Eq. (41) are [83]

$$\psi_0^L = D_{v_L}(-2\sqrt{\omega_L\gamma}(1 + X)), \quad \psi_0^R = D_{v_R}(-2\sqrt{\omega_R\gamma}(1 - X)) \qquad (43)$$

where

$$\omega_{L,D} = \left(1 \pm \frac{3a}{2\gamma}\right)^{1/2}, \qquad \varepsilon + a = \omega_L\left(v_L + \frac{1}{2}\right), \qquad \varepsilon - a = \omega_R\left(v_R + \frac{1}{2}\right) \qquad (44)$$

and $D_v(x)$ are parabolic cylinder functions. Then solutions (43) and (44) make it possible to obtain the equation for the instanton quantization [83], which, if the asymmetry is small ($a \ll 1$), is reduced to the rules

$$v_L = n + \chi_{nn}^-, \qquad v_R = n - 2a + \chi_{nn}^+ \qquad (45)$$

Here n is the integer and

$$\chi_{nn}^\pm = a \pm \sqrt{a^2 + (\chi_{nn}^0)^2} \qquad (46)$$

where the value

$$\chi_{nn}^0 = \frac{1}{\sqrt{2\pi}}\frac{2^{4n+2}\gamma^{n+1/2}}{n!}e^{-4/3\gamma} \qquad (47)$$

written in the dimensionless energy units is the tunneling splitting in the symmetric potential. The appropriate spectrum of energy eigenvalues is

$$\varepsilon_n^{L(R)} = n + \frac{1}{2} \mp \sqrt{a^2 + (\chi_{nn}^0)^2} \qquad (48)$$

The further complicated studies [83,84] have solved the quantum problem within the perturbative instanton approach generalized for excited states simulated above the barrier and for anharmonic transverse vibrations. The parameters of many-dimensional torsion–vibration Hamiltonians of some molecules (H_2O_2, malonaldehyde, etc.) have been derived. It has been shown that the torsion motion and bending vibrations are responsible for vibration-assisted tunneling and for significant dependence of the tunneling splittings on quantum numbers of transverse vibrations. The dependence of tunneling splittings on isotope effects of H/D and 13C/12C has also been calculated.

We have cited evidence supporting the proton transfer along hydrogen bonds; however, there are investigations carried out on other species, which bring forward an argument that the simple hydrogen-bonded dimer is favored over the proton transfer. For instance, the title of a review article by Legon [85] includes the following words: "Hydrogen bonding versus proton transfer." Based on so-called fast-mixing technique and pulsed-nozzle, Fourier-transform microwave spectroscopy (i.e., rotational spectroscopy of supersonic jets) Legon [85] has examined rotational spectra and spectroscopic constants of heterodimers in solid particles in gas mixtures in the series ($R_{3-n}H_nN \cdots HX$). Three possibilities have been analyzed, namely, the hydrogen-bonded form, a form with partial proton transfer, and a form with complete proton transfer. The conclusion has been drawn that the species $H_3N \cdots HX$ and $H_3P \cdots HX$ (where $X = F$, Cl, Br, and I) can all be described as the simple hydrogen-bonded type, without the need to invoke an appreciable extent of proton transfer (thus the double-well potential of the hydrogen bond is symmetric). And only the series $(CH_3)_3N \cdots HX$ (where $X = F$, Cl, Br, and I) has shown that the progressive weakening of the HX bond with respect to the dissociation products H^+ and X^- favors the ion pair.

C. Proton Polaron

In the case of the proton transfer, which takes place in the double-well potential, the potential energy (or potential energy surface) governs the proton motion and generally it incorporates the interaction with surrounding atoms including the rest protons and outside fields. Diffusion and mobility of hydrogen atoms and protons in compounds with hydrogen bonds allow the consideration very similar to the one described above. Indeed, since in compounds protons are characterized by localized wave functions, the motion of protons through the crystal should include the tunneling matrix element, or the tunneling (resonance) integral J and the possible interaction with the environment—that is, the thermal bath. By definition, the resonance integral is

$$J = \int \psi^*(\mathbf{r}_1) H \psi(\mathbf{r}_2) \, dV \tag{49}$$

where $\psi(\mathbf{r_i})$ is the proton wave function of a proton in the site described by the radius vector $\mathbf{r_i}$. The wave function $\psi(\mathbf{r_i})$ is compared to a ground state and H is the Hamiltonian, which includes the kinetic and potential energies of the proton.

The localized proton interacting with the corresponding ion (or atom) gives rise to its displacement from the equilibrium position, which in turn should lead to the lowering the potential energy of the atom. The problem is known as the displaced harmonic oscillator (see, e.g., Ref. 86). The classical function of Hamilton for the oscillator is

$$H = \frac{p^2}{2m} + \frac{m}{2}\omega^2 q^2 \tag{50}$$

The Schrödinger equation for the oscillator is

$$\left(-\frac{\hbar^2}{2m}\frac{d^2}{dq^2} + \frac{m}{2}\omega^2 q^2\right)\psi(q) = E\psi(q) \tag{51}$$

or in the dimensionless presentation

$$\frac{\hbar\omega}{2}\left(-\frac{d^2}{d\xi^2} + \xi^2\right)\psi(\xi) = E\psi(\xi) \tag{52}$$

where the dimensionless coordinate ξ is determined by the relation

$$q = \sqrt{\frac{\hbar}{m\omega}}\xi \tag{53}$$

One can introduce the Bose operators of creation (annihilation) of one oscillation, $\hat{b}^+(\hat{b})$:

$$\xi = \frac{1}{\sqrt{2}}(\hat{b} + \hat{b}^+), \quad \frac{d}{d\xi} = \frac{1}{\sqrt{2}}(\hat{b} - \hat{b}^+) \tag{54}$$

and then the Schrödinger equation (52) is transformed to

$$\hbar\omega\,\hat{b}^+\hat{b}\psi = \left(E - \frac{1}{2}\right)\psi \tag{55}$$

and the operators satisfy the commutation relation

$$\hat{b}\hat{b}^+ - \hat{b}^+\hat{b} = 1 \tag{56}$$

Now let the oscillator is subjected to the action of an outside force $\sqrt{2}\gamma\hbar\omega$, which is not time-dependent. Then Eq. (52) becomes

$$\frac{\hbar\omega}{2}\left(-\frac{d^2}{d\xi^2} + \xi^2 - \sqrt{2}\gamma\xi\right)\psi(\xi) = E\psi(\xi) \tag{57}$$

and in terms of operators $\hat{b}^+$ and $\hat{b}$, Schrödinger equation (55) changes to

$$[\hat{b}^+\hat{b} - \gamma(\hat{b}^+ + \hat{b})]\psi = \left[E/(\hbar\omega) - \frac{1}{2}\right]\psi \tag{58}$$

The solution of Eq. (58) is very simple. Equation (58) is satisfied by the operators

$$\hat{b} = \hat{\tilde{b}} + \gamma, \qquad \hat{b}^+ = \hat{\tilde{b}}^+ + \gamma \tag{59}$$

and instead of Eq. (58) we acquire

$$\hat{\tilde{b}}^+\hat{\tilde{b}}\varphi = \left[E/(\hbar\omega) - \gamma^2 - \frac{1}{2}\right]\varphi \tag{60}$$

where the new operators $\hat{\tilde{b}}^+$ and $\hat{\tilde{b}}$ obey the same commutation relation (56).

The displacement $-\gamma^2\hbar\omega$ of the potential energy of the oscillator directly indicates the possible strong interaction of a particle, which induced the displacement, with the vibrating lattice. First of all the charged particle should interact with polar modes—that is, optical phonons of the crystal studied. The detailed theory of the particle behavior resulted in the developing the small polaron theory for electrons was elaborated by Holstein [87] and Firsov [88]. The first theoretical research concerning the protonic small polaron was carried out later by Flynn and Stoneham [20], Fischer et al. [89], Roberts et al. [90], Klinger and Azizyan [91,92], and Tonks and Silver [93]. In the following sections we will widely use the small polaron model, applying it for the study of proton transport and rearrangements in systems with hydrogen bonds.

D. Proton Ordering

The necessity to analyze the phase transition in KH_2PO_4 crystals allowed Blinc [94–96] (see also Refs. 97 and 98) to construct the special pseudospin formalism describing the proton subsystem in many hydrogen-containing compounds.

So far we have dealt with the one-particle approximation, and the long-range proton interaction has not been taken into account. Experimental examination of ferroelectrics with hydrogen—that is, the KDP crystal (KH_2PO_4) and others (CsH_2AsO_4, $NH_4H_2AsO_4$, etc.)—showed that their physical properties are essentially caused by the proton subsytem (see, e.g., Blinc and Žecš [96]). The appearance of the soft mode in such crystals is associated with the parameter of

proton cooperation, or proton ordering. The corresponding theoretical model is the following. Protons being strongly localized along hydrogen bonds undergo anharmonic vibrations near equilibrium positions in the potential with two wells. The energy of the proton subsystem is presented in the form [96,98]

$$H_{\text{proton}} = \sum_l H_1(l) + \sum_{\substack{j,l \\ (l>j)}} H_2(jl) + \cdots \tag{61}$$

Here $H_1(l)$ corresponds to the part of the energy that depends on the configuration of the lth proton, and $H_2(jl)$ is the part of the energy that depends on the pair configuration of the lth and the jth protons. It is assumed that protons tunnel between two equilibrium positions (hence the double-well potential should be symmetric). In the presentation of second quantization in which the one-particle Hamiltonian $H_1(l)$ is diagonalized, the total Hamiltonian is written as

$$H_{\text{proton}} = \sum_\alpha E_\alpha \hat{a}^+_{\alpha,l} \hat{a}_{\alpha,l} + \sum_{\alpha,\beta,\gamma,\delta} v^{jl}_{\alpha\beta\gamma\delta} \hat{a}^+_{\alpha,l} \hat{a}_{\beta,l} \hat{a}^+_{\gamma,j} \hat{a}_{\delta,j} \tag{62}$$

where $\hat{a}^+_{\alpha,l}(\hat{a}_{\alpha,l})$ is the Fermi or Bose operator of the creation (annihilation) of a proton/deuteron in the lth position in the one-particle quantum state α where $\alpha = +, -$ (note that the ground state of a hydrogen atom in the potential with two minima is doublet).

The corresponding eigenfunctions (see Fig. 4)

$$\psi_+ = \frac{1}{\sqrt{2}} (\varphi_L + \varphi_R) \tag{63}$$

$$\psi_- = \frac{1}{\sqrt{2}} (\varphi_L - \varphi_R) \tag{64}$$

are symmetric and asymmetric linear combinations of wave functions localized in the left (φ_L) and the right (φ_R) equilibrium positions. The condition of the presence of a hydrogen atom in the hydrogen bond is expressed as

$$\hat{a}^+_{+,l} \hat{a}_{+,l} + \hat{a}^+_{-,l} \hat{a}_{-,l} = 1 \tag{65}$$

The operators $\hat{a}^+_{\alpha,i}(\hat{a}_{\alpha,i})$ make it possible to introduce the so-called pseudospin formalism that features the effective "spin-1/2" operators

$$S^x_l = \frac{1}{2} (\hat{a}^+_{+,l} \hat{a}^i_{+,l} - \hat{a}^+_{-,l} \hat{a}_{-,l}) \tag{66}$$

$$S^y_l = \frac{1}{2} (\hat{a}^+_{+,l} \hat{a}_{-,l} - \hat{a}^+_{-,l} \hat{a}_{+,l}) \tag{67}$$

$$S^z_l = \frac{1}{2} (\hat{a}^+_{-,l} \hat{a}_{-,l} + \hat{a}^+_{+,l} \hat{a}_{+,l}) \tag{68}$$
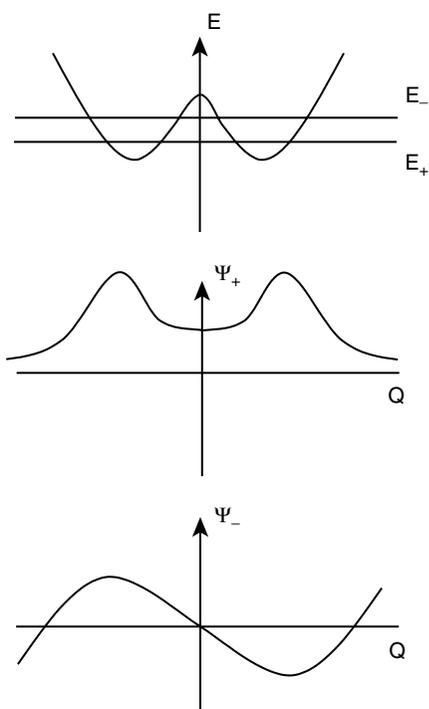
Figure 4. The basis state and proper functions for one-particle potential with two minima.

The pseudospin operators obey the known rules

$$[S_j^x, S_l^y]_- = i\delta_{jl}S_l^z; \ [S_j^y, S_l^z]_- = i\delta_{jl}S_l^x; \ [S_j^z, S_l^x]_- = i\delta_{jl}S_j^y \tag{69}$$

The operators of creation (annihilation) of a particle in symmetric quantum states, $\hat{a}_{+,l}^+(\hat{a}_{+,l})$, and in asymmetric ones, $\hat{a}_{-,l}^+(\hat{a}_{-,l})$, can be presented through the operators of creation and annihilation of a particle in the left and the right equilibrium positions in the hydrogen bond. Then one can express the pseudospin operators in the form

$$S_l^x = \frac{1}{2}(\hat{a}_{L,l}^+\hat{a}_{R,l} + \hat{a}_{R,l}^+\hat{a}_{L,l}) \tag{70}$$

$$S_l^y = \frac{1}{2}(\hat{a}_{L,l}^+\hat{a}_{R,l} - \hat{a}_{R,l}^+\hat{a}_{R,l}) \tag{71}$$

$$S_l^z = \frac{1}{2}(\hat{a}_{L,l}^+\hat{a}_{L,l} - \hat{a}_{R,l}^+\hat{a}_{R,l}) \tag{72}$$

It can be seen from expressions (70)–(72) that the *z* component of the pseudospin determines the operator of dipole momentum, the *y* component is the operator of

tunneling current, and the x component is the operator of proton tunneling. In other words, S^z characterizes the difference between the populations of the left and the right equilibrium positions and S^x characterizes the difference between the populations of symmetric and asymmetric states.

Thus the Hamiltonian of the proton subsystem becomes

$$H_{\text{proton}} \cong -\hbar\Omega \sum_l S_l^x - \frac{1}{2} \sum_{j,l} \mathscr{I}_{jl} S_j^z S_l^z \tag{73}$$

where the tunneling integral and the energy of proton interaction are, respectively,

$$\hbar\Omega \cong E_- - E_+ \tag{74}$$

$$\mathscr{I}_{jl} = -4\nu_{++--}^{jl} \tag{75}$$

In the mentioned approximation we have

$$H_{\text{proton}} \cong -\hbar\Omega \sum_l S_l^x - \frac{1}{2} \sum_{j,l} \mathscr{I}_{jl} \langle S_j^z \rangle S_l^z \tag{76}$$

The parameter $\sum_l \mathscr{I}_{jl} \langle S_l^z \rangle$ contains information on the collective proton coupling, and the order parameter $\langle S_l^z \rangle$ points to the degree of proton ordering.

The pseudospin methodology is widely used not only for the description of hydrogen containing ferro- and antiferroelectrics, but also for the study of many other systems with hydrogen bonds. In particular, the pseudospin methodology was applied by Silbey and Trommsdorff [99] for examining the influence of two-phonon process on the rate constant of molecular compounds. In the next sections we will also employ the pseudospin formalism for the investigation of some problems where protons are exemplified by the cooperative behavior.

E. Bending Vibrations of Hydrogen Bond

Perhaps the first theoretical model describing the three-dimensional pattern that makes it possible to explain correlations between dependences of stretching and bending vibrations of hydrogen bonds has been constructed by Rozhkov et al. [100]. Their research was based on a work by Isaacs et al. [101], who showed that hydrogen forms the covalent bond with two oxygen atoms. In the framework of adiabatic approximation, Rozhkov et al. [100] chose the model potential of the oxygen–hydrogen interaction in the form of the Morse potential:

$$V(\mathbf{r}) = D(e^{-2a(r-r_0)} - 2e^{-a(r-r_0)}) \tag{77}$$

where D, a, and r_0 are parameters of the potential. In a recent work by Isaacs et al. [101], it has been shown that the hydrogen atom forms the covalent bond with two oxygen atoms. Because of the model for the construction of the potential of hydrogen bond U, one more oxygen atom spaced at R along the x axis (i.e. the O$\cdots$O line) has been added. Therefore

$$U(\mathbf{r}) = V(\boldsymbol{\rho}, X + R/2) + V(\boldsymbol{\rho}, X - R/2) \qquad (78)$$

where X is the coordinate of the proton reckoned from the center of the hydrogen bond and $\boldsymbol{\rho}$ is the radius vector of hydrogen in the yz plane; that is, $\boldsymbol{\rho} = (X, Y)$.

Let us rewrite expression (2) explicitly:

$$U(\mathbf{r}) = D[e^{-2a(r_- - r_0)} + e^{-2a(r_+ - r_0)} - 2e^{-a(r_- - r_0)} - 2e^{-a(r_+ - r_0)}] \qquad (79)$$

where $r_\pm = \{(X \pm R/2)^2 + y^2 + z^2\}^{1/2}$. Coordinates of the minimum of the potential (3) are

$$X_0 = \pm \frac{1}{a}\operatorname{arccot}(e^{(R - R_c)/2}) \qquad (80)$$

where $y_0 = z_0 = 0$ and $R_c = (2r_0 + a^{-1}\ln 2)$ is the minimum length of the hydrogen bond at which the double-well potential is transformed to the one-dimensional one (note that the coordinates are defined from the condition grad U).

Having explained experimental dependences of frequencies of the stretching and bending vibrations on the length of hydrogen bond, Rozhkov et al. [100] have proposed to include one more parameter $b \neq a$ to the potential (77). They employed the method developed by Tanaka [69], which allowed the passage from the dynamics of a proton in an isolated hydrogen bond to the thermodynamics of a system of hydrogen bonds. The new parameter b becomes responsible for the curvature of the potential (77) in transversal directions. In so doing, ar is replaced for $[a^2 X^2 + b^2(y^2 + z^2)]^{1/2}$ in expression (77).

Using the perturbation theory developed in Ref. 102, one can choose the Hamiltonian of the three-dimensional oscillator with frequencies ω_v and ω_δ (stretching and bending, respectively) and a new equilibrium position x, which are vibration parameters of the free energy. In this case the free energy per hydrogen can be represented as

$$F = \langle U_0 \rangle + F_0 - \langle H_0 \rangle_0 \qquad (81)$$

$$F_0 = -k_B T \ln\left(2\sinh\frac{\hbar\omega_v}{k_B T}\right) - 2k_B T \ln\left(2\sinh\frac{\hbar\omega_\delta}{k_B T}\right) \qquad (82)$$

where

$$\langle \ldots \rangle_0 = \frac{\mathrm{Tr}\{\ldots e^{-H_0/k_\mathrm{B}T}\}}{\mathrm{Tr}\, e^{-H_0/k_\mathrm{B}T}} \tag{83}$$

For the calculation of $\langle U_0 \rangle$, one can put $\mathbf{r} = \mathbf{r}_0 + \mathbf{u}$, where $\mathbf{r}_0$ is the equilibrium position and $\mathbf{u}$ is the displacement. In the harmonic approximation we obtain

$$\langle e^{i\mathbf{k}\mathbf{u}} \rangle_0 = e^{-\frac{1}{2}\sum_i \langle k_i \rangle^2 \langle u_i \rangle^2} \tag{84}$$

Then the average value of a function $f(\mathbf{r})$ is

$$\langle f(\mathbf{r}) \rangle_0 = \frac{\int d\xi f(\mathbf{r}_0 + \xi)\exp\left(-\frac{1}{2}\sum_i \xi_i^2/\sigma_i^2\right)}{(2\pi)^{3/2}\sigma_x\sigma_y\sigma_z} \tag{85}$$

where $\sigma_i^2 = \langle u_i \rangle_0^2$ and $i = x, y, z$.

Setting $\langle U(\mathbf{r}) \rangle_0 = 2DW$, we obtain the dimensionless average potential

$$\begin{aligned} W &\cong e^{-2\xi_0+2\lambda}\, \frac{(\xi^2 - \chi^2)\cosh 2\chi + 2\mu(\xi\cosh 2\chi - \chi\sinh\chi)}{(\xi + 2\mu)^2 - \chi^2} \\ &\quad -2e^{-\xi_0+\lambda/2}\, \frac{(\xi^2 - \chi^2)\cosh 2\chi + \mu(\xi\cosh\chi - \chi\sinh\chi)}{(\xi + \mu)^2 - \chi^2} \end{aligned} \tag{86}$$

where $\xi = aR/2$, $\xi_0 = \xi - ar_0$, $\chi = ax$, $\lambda = a^2\sigma_v^2$, $\mu = b^2\sigma_\delta$, $\sigma_v \equiv \sigma_x$, and $\sigma_\delta = \sigma_y = \sigma_z$. In the harmonic approximation we obtain

$$\sigma_v^2 = \frac{\hbar\coth(\hbar\omega_v/k_\mathrm{B}T)}{2m\omega_v} \tag{87}$$

$$\sigma_\delta^2 = \frac{\hbar\coth(\hbar\omega_\delta/k_\mathrm{B}T)}{2m\omega_v} \tag{88}$$

where m is the proton/deuteron mass. Allowing for expressions (81)–(83) and (87) and (88), one can show that the minimization of the free energy, $\partial F/\partial\omega_{v,\delta}$, is reduced to the equations

$$\omega_v^2 = 2\Omega^2\, \partial W/\partial\lambda \tag{89}$$

$$\omega_\delta^2 = 2\Omega^2\, \partial W/\partial\mu \tag{90}$$

where

$$\Omega^2 = 2a^2D/m \tag{91}$$

Equations (13) and (14) along with the equation for determining the localization of hydrogen in the hydrogen bond,

$$\partial W/\partial x = 0 \qquad (92)$$

makes it possible to define the needed parameters.

Numerical calculations have been performed [100] using the simplex method [103]. Then calculated curves $\omega_v(R)$ and $\omega_\delta(R)$ and experimental dependences of $\omega_{v,\delta}$ as functions of R (see Ref. 70) have been superimposed for comparison. We would like to note that the agreement is indeed remarkable. The increase of the $\omega_\delta(R)$ observed with the shortened length of hydrogen bond has accounted for the increment of the rigidity of hydrogen bond in transverse directions. The strong fall of the curve $\omega_v(R)$, which takes place in the same region of R, is explained by the transformation of the potential (78) in the vicinity of the equilibrium position of the proton to the one-dimensional potential $U = a^4 x^4 D/4$ [104].

Thus the model of the three-dimensional hydrogen bond presented in Ref. 100 should be considered very realistic. The interaction between hydrogen bonds (or hydrogen-bonded chains), which is taken into account in the model, plays a key role in the behavior of the $\omega_v(R)$ and $\omega_\delta(R)$, especially in the range of small R that is typical for the strong hydrogen bond.

Another approach of O—H—O hydrogen bond dynamics is discussed in Appendix A; the approach also accurately reproduces the well-known dependence of the O—H stretching mode on the hydrogen bond length.

F. Tunneling Transition and Coupled Protons

Quantum effects and strong interactions with vibrating surrounding atoms complicate the detailed study of proton transfer in the hydrogen bond $AH \cdots B$. Owing to the small mass, quantum tunneling of the proton plays an important role at a symmetric double-well potential.

The study of the time scale of proton transfer has shown [110] that the transfer is specified by the residence time in a given well or by the frequency of excursions to other well. Besides, the proton oscillates within the local potential minimum of a given well with the period of 10^{-15} to 10^{-13} s, which is much shorter than the residence time. The thermal motion of the molecules should modulate the potential over a period of 10^{-13} to 10^{-11} s. Fillaux et al. [110] note that the vibration assisted tunneling mechanism [21] has emerged from extensive studies (mostly of carboxylic acid dimers) with nuclear magnetic resonance and quasi-elastic neutron scattering [111–114], which probe a time scale of the order of 10^{-9} s. This scale is significantly longer than that of proton dynamics. This means that the two mentioned methods provide only the

information averaged over many excursions of the proton between the two wells, and quantum effects are then not observed directly.

Vibrational spectroscopy measures atomic oscillations practically on the scale as the scale of proton dynamics, 10^{-15} to 10^{-12} s. Fillaux et al. [110] note that optical spectroscopies, infrared and Raman, have disadvantages for the study of proton transfer that preclude a complete characterization of the potential. (However, the infrared and Raman techniques are useful to observe temperature effects; inelastic neutron spectra are best observed at low temperature.) As mentioned in Ref. 110, the main difficulties arise from the non-specific sensitivity for proton vibrations and the lack of a rigorous theoretical framework for the interpretation of the observed intensities.

Inelastic neutron scattering spectroscopy is characterized by completely different intensities because the neutron scattering process is entirely attributable to nuclear interactions [110]: Each atom features its nuclear cross section, which is independent of its chemical bonding. Then the intensity for any transition is simply related to the atomic displacements scaled by scattering cross sections. And because the cross section of the proton is about one order of magnitude greater than that for any other atom, the method is able to record details of quantum dynamics of proton transfer.

As a rule, vibration dynamics of atoms and molecules is treated in the framework of harmonic force fields. In the model, eigenvalues are the normal frequencies, and eigenvectors determine displacements of atoms for each normal mode (see, e.g. Ref. 115) and the eigenvectors are related to the band intensities. However, transition moment operators are largely unknown for optical spectra, and therefore theoretical descriptions are remaining questionable. The inelastic neutron scattering technique allows the calculation of band intensities, because they are proportional to the mean-square amplitudes of atomic displacements scaled by nuclear cross sections [116–118]. This specified force fields and makes it possible to extract modes involving large proton displacements while contributions from other atoms can be ignored.

The inelastic neutron scattering spectra of potassium hydrogen carbonate ($KHCO_3$), some molecular crystals, and polymers have shown [8–11,110] that these compounds can be regarded as crystals of protons so weakly coupled to surrounding atoms that the framework of the atoms and ions can be virtually ignored. This allows one to support Fillaux's [119] quasi-symmetric double minimum potential along the proton stretching mode coordinate. In this case, proton transfer is associated with the pure tunneling transition, and the "phonon assistance" of proton tunneling is unnecessary. Thus proton tunneling is purely a local dynamics.

What is the reason for decoupling the proton dynamics from the crystal lattice revealed in a great number of compounds? Fillaux [119] has investigated the reason for this decoupling, supposing that the proton dynamics could be

Figure 5. Two identical harmonic oscillators.
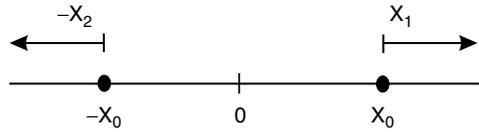
caused by the spin correlation for indistinguishable fermions according to the Pauli exclusion principle. He has considered the dynamics of a centrosymmetric pair of protons, assuming that the protons can be represented with identical harmonic oscillators with mass m moving along collinear coordinates x_1 and x_2 and coupled to one another (Fig. 5). The Hamiltonian was chosen in the form

$$H = \frac{1}{2m}(P_1^2 + P_2^2) + \frac{1}{2}m\omega_{0x}^2$$
$$\times [(x_1 - X_0)^2 + (x_2 + X_0)^2 + 2\gamma_x(x_1 - x_2)^2] \tag{93}$$

Here P_1 and P_2 are the momenta of the two oscillating masses; the harmonic frequency of the uncoupled oscillators at equilibrium positions $\pm X_0$ is ω_{0x}. The coupling potential proportional to γ_x depends only on the distance between equilibrium positions of the two oscillating masses at $\pm X_0' = X_0/(1 + 4\gamma_x)$.

A system of coupled oscillators can be expressed as linear oscillations of normal modes. The symmetric (x_s) and asymmetric (x_a) displacements of the two particles represent normal coordinates. The coordinates are defined with accuracy to an arbitrary factor, but frequencies and wave functions are independent of it. Normalized normal coordinates corresponding to an effective mass m are the following:

$$x_a = \frac{1}{\sqrt{2}}(x_1 + x_2), \qquad x_s = \frac{1}{\sqrt{2}}(x_1 - x_2) \tag{94}$$

$$P_a = \frac{1}{\sqrt{2}}(P_1 + P_2), \qquad P_s = \frac{1}{\sqrt{2}}(P_1 - P_2) \tag{95}$$

Substituting expressions (94) and (95) into the Hamiltonian (93), we get the Hamiltonian that includes separated normal modes, that is,

$$H = H_a + H_s + m\omega_{0x}^2 X_0^2 \frac{4\gamma_x}{1 + 4\gamma_x} \tag{96}$$

where

$$H_a = \frac{P_a^2}{2m} + \frac{1}{2}m\omega_a^2 x_a^2 \tag{97}$$

$$H_s = \frac{P_s^2}{2m} + \frac{1}{2}m\omega_s^2(x_s - \sqrt{2}X_0')^2 \tag{98}$$

Here, in expressions (97) and (98), the normal frequencies are

$$\omega_a = \omega_{0x}, \qquad \omega_s = \omega_{0x}\sqrt{1 + 4\gamma_x} \qquad (99)$$

The corresponding eigenfunctions and eigenvalues are (see also Ref. 120)

$$\psi_{\ln} = \psi_l(x_a) \cdot \psi_{sn}(x_s - \sqrt{2}X_0') \qquad (100)$$

$$E_{\ln} = \left(al + \frac{1}{2}\right)\hbar\omega_a + \left(sn + \frac{1}{2}\right)\hbar\omega_s \qquad (101)$$

Spins of the two protons are correlated in a singlet ($s = 0$) and a triplet ($s = 1$) state. The spatial part of the proton wave function, with respect to particle permutation, is symmetrical in the singlet state and antisymmetrical in the triplet state. Explicitly, the wave functions are

$$\Theta_{0\pm}(x_1, x_2) = \frac{1}{\sqrt{2}}\psi_{s0}(x_a)[\psi_{s0}(x_s - \sqrt{2}X_0') \pm \psi_{a0}(x_s + \sqrt{2}X_0')] \qquad (102)$$

If we drop the spin interaction and the tunneling resonance integral for two protons in a dimer, the energy of splitting for the singlet and triplet states become ignored. Hence the ground state remains degenerate similarly to the bosons.

If the proton oscillations are not coupled to the dimer oscillations, the dynamics can be modeled by symmetric and antisymmetric normal coordinates for proton modes (x_a, x_s) and for dimer modes (X_a, X_s). Then the total wave function is

$$\Xi_0(x_1, x_2; X_1, X_2) = \psi_{a0}(x_a)\psi_{s0}(x_s - \sqrt{2}X_0')\varphi_{a0}(x_a)\varphi_{s0}(x_s - \sqrt{2}X_0') \qquad (103)$$

If the nuclear spins are taken into account, the total vibrational wave function according to the Pauli principle becomes similar to function (103):

$$\Xi_{0\pm}(x_1, x_2; X_1, X_2) = \frac{1}{\sqrt{2}}\psi_{a0}(x_a)[\psi_{s0}(x_s - \sqrt{2}X_0')$$
$$\pm \psi_{s0}(x_s - \sqrt{2}X_0')]\varphi_{a0}(x_a)\varphi_{s0}(x_s - \sqrt{2}X_0'') \qquad (104)$$

In the case when the proton and dimer modes are coupled, the normal coordinates become linear combinations of the proton and dimer's atoms coordinates. Fermions and bosons are not distinguished, and we have a conflict with the Pauli principle: The two protons are not distinguished in the ground state.

Thus we can consider the two types of dynamics. The first one is usual, which is met in vibrational spectroscopy; in this case, normal coordinates

represent the mixture of fermion and boson displacements. The second one is based on the Pauli principle, namely, that there is no mixing of the normal coordinates for fermions and bosons and therefore the total wave function is factored:

$$\psi(x_i; X_i) = \psi(x_i)\Phi(X_i) \tag{105}$$

Thus Fillaux [119], assuming that the spin interaction is extremely weak, has argued that the factorization of the wave function must be regarded as a spin-related selection rule. The rule applies to pairs of coupling terms and to the mean distance between their equilibrium positions. This is treated as the fundamental justification of the localized proton modes introduced empirically to elucidate his previous observations [7–9].

The excited states, however, have no degeneracy, and that is why in this case the dynamics can be represented by conventional normal modes that can include the total number of atomic coordinates. The normal coordinates may be different in the ground and excited states; and because of that, the calculation of the scattering function can be more complicated with the analysis based on the normal mode approach.

The spin-related section rule can be proved by elastic neutron scattering measurements. In order to establish the specific fingerprint of the spin correlation, the scattering functions for the linear harmonic oscillator, for the double-well minimum function, and for pairs of coupled oscillators have been calculated in Ref. 119.

Considering the harmonic potential, Fillaux chooses the wave functions for an isolated harmonic oscillator along the x coordinate in the form [120]

$$\psi_n(x) = \left(\frac{a_x^2}{\pi}\right)^{1/4} \frac{1}{\sqrt{2^n n!}} H_n(a_x x) e^{-\frac{1}{2}a_x^2 x^2} \tag{106}$$

with

$$a_x^2 = \frac{m\omega_{0x}}{\hbar} = \frac{1}{2u_{0x}^2} \tag{107}$$

H_n is the Hermite polynomial of degree n, m is the oscillator mass, and u_{0x}^2 is the mean-square amplitude in the ground state. The scattering process, which is very important for the studies by the neutron techniques, is characterized by the scattering function

$$S(\mathbf{Q}, \omega) = |\langle \psi_{\text{fin}}(\mathbf{r})|\exp(i\mathbf{Q}\mathbf{r})|\psi_{\text{in}}(\mathbf{r})\rangle|^2 \delta(E_{\text{in,fin}} - \hbar\omega) \tag{108}$$

where $\psi_{in}(\mathbf{r})$ and $\psi_{fin}(\mathbf{r})$ are the proton wave functions in the initial and final states respectively, $E_{in,fin}$ is the energy of the transition, and $\hbar\omega$ is the neutron energy transfer.

In the case of the harmonic oscillator, the elastic scattering function has the form

$$S(\mathbf{Q}, \omega) = \exp(-Q_x^2, u_{0x}^2)\delta(\omega) \qquad (109)$$

A single particle in a symmetrical two-well potential is presented by the symmetric (0^+) and antisymmetric (0^-) substates. The difference between two corresponding energies $E_{0^-} - E_{0^+} = \hbar\omega_0$ represents the tunneling splitting. In the case of the high potential barrier, the corresponding wave functions are symmetrical and antisymmetrical combinations of the harmonic wave functions (106) centered at the minima of two wells, $\pm X_0$:

$$\psi_{0\pm}(x) = \frac{1}{\sqrt{2[1 \pm \exp(-a_x^2 X_0^2)]}} [\psi_0(x - X_0) \pm \psi_0(x + X_0)] \qquad (110)$$

The appropriate scattering functions, which characterize symmetric and antisymmetric combinations of harmonic wave functions, are [119]

$$S(Q_x, \omega)_{0^+0^+} = \frac{1}{1 + \exp(-X_0^2/2u_{0x}^2)}$$
$$\times \left| \left[\cos(Q_x X_0) + \exp\left(-\frac{X_0^2}{2u_{0x}^2}\right) \right] \exp\left(-\frac{Q_x^2 u_{0x}^2}{2}\right) \right|^2 \delta(\omega) \qquad (111)$$

$$S(Q_x, \omega)_{0^\mp 0^\mp} = \frac{1}{1 - \exp(-X_0^2/2u_{0x}^2)}$$
$$\times \left| i\sin(Q_x X_0)\exp\left(-\frac{Q_x^2 u_{0x}^2}{2}\right) \right|^2 \delta(\omega_0 \pm \omega) \qquad (112)$$

$$S(Q_x, \omega)_{0^-0^-} = \frac{1}{1 - \exp(-X_0^2/2u_{0x}^2)}$$
$$\times \left| \left[\cos(Q_x X_0) - \exp\left(-\frac{X_0^2}{2u_{0x}^2}\right) \right] \exp\left(-\frac{Q_x^2 u_{0x}^2}{2}\right) \right|^2 \delta(\omega) \qquad (113)$$

Here, the periodic terms are caused by interferences between waves scattered by the same proton at the two sites, and the exponent terms are stipulated by the overlapping the wave functions centered at $\pm X_0$.

Functions $S_{0^+0^+}$ and $S_{0^-0^-}$ are analogous to the optical fringes; functions $S_{0^+0^-}$ and $S_{0^-0^+}$ are associated with the tunneling transition at energy $\hbar\omega_{0^-}$.

The elastic incoherent scattering functions defined in expression (100) yields [119]

$$S(Q_x, \omega) = 2 \exp\left[-Q_x^2 \left(\frac{u_{0x}^2}{2\sqrt{1+4\gamma_x}} + \frac{u_{0x}^2}{2}\right)\right] \delta(\omega) \tag{114}$$

It is easily seen that the Gaussian profile in expression (114) is practically the same as for the harmonic oscillator (109). Consequently, isolated oscillators and coupled pairs of bosons are virtually are not distinguished.

Now let us look at the coupled fermions. Fillaux considers, as an example, the hydrogen molecule and argues that a similar pattern should take place for the oscillators in $KHCO_3$. The vibrational ground-state wave functions are

$$\Theta_{0\pm}(x_1, x_2) = \frac{1}{\sqrt{2}} [\psi_{s0}(x_1 - x_2 - R) \pm \psi_{s0}(x_1 - x_2 + R)] \tag{115}$$

where R_0 is the bond length. The part of the scattering function depending on the spatial coordinates is equal to

$$S(Q_x, \omega) = |\langle \Theta_{0\pm}(x_1, x_2)|e^{iQ_x x_1} \pm e^{iQ_x x_2}|\Theta_{0\pm}(x_1, x_2)\rangle|^2 \delta(\omega) \tag{116}$$

Thus in the case of the coupled fermions when the singlet and tripled states belong to the same molecular species, the corresponding scattering functions are

$$S(Q_x, \omega)_{0^+0^+} = 2\cos^2(Q_x X_0') \left[\cos(Q_x X_0') + \exp\left(-\frac{X_0'^2}{2u_{0x}^2}\right)\right]^2$$
$$\times \exp\left[-Q_x^2\left(\frac{u_{0x}^2}{2\sqrt{1+4\gamma_x}} + \frac{u_{0x}^2}{2}\right)\right]\delta(\omega) \tag{117}$$

$$S(Q_x, \omega)_{0\pm0\mp} = 2\sin^4(Q_x X_0')^2 \times \exp\left[-Q_x^2\left(\frac{u_{0x}^2}{2\sqrt{1+4\gamma_x}} + \frac{u_{0x}^2}{2}\right)\right]\delta(\omega) \tag{118}$$

$$S(Q_x, \omega)_{0^-0^-} = 2\cos^2(Q_x X_0') \left[\cos(Q_x X_0') - \exp\left(-\frac{X_0'^2}{2u_{0x}^2}\right)\right]^2$$
$$\times \exp\left[-Q_x^2\left(\frac{u_{0x}^2}{2\sqrt{1+4\gamma_x}} + \frac{u_{0x}^2}{2}\right)\right]\delta(\omega) \tag{119}$$

As can be seen from expressions (117)–(119), quantum interference leads to the modulation of the Gaussian profiles by the $\cos^2(Q_x, X_0')$ and $\sin^4(Q_x, X_0')$ terms.

Thus the dynamics of the coupled oscillators is a function of their quantum nature. In the case of bosons, the dynamics is described by usual spatial symmetric and antisymmetric normal modes; but in the case of fermions, spin–spin

correlations result in a singlet and triplet state. In crystalline ground state, owing to the Pauli principle the proton dynamics is the dynamics of fermions and it is virtually decoupled from the dynamics of bosons—that is, O, C, N, and so on, atoms.

The further study of pairs of coupled oscillators, both theoretical and experimental, has been performed on the potassium hydrogen carbonate crystal, $KHCO_3$, and its deuterated analog, $KDCO_3$, by Ikeda and Fillaux [121]. It has been shown in their research that (i) the proton dynamics in fact is amenable to the harmonic oscillator and in the ground state is largely decoupled from the lattice; (ii) classical normal coordinates apply only to coupled pairs of bosons; (iii) coupled pairs of fermions must be regarded as singlet and triplet states, and the spin correlation for indistinguishable protons gives rise to quantum interference; and (iv) deuteron and lattice dynamics are correlates.

An interesting study concerning the tunneling of protons has been conducted by Willison [122], who has treated the phenomenon of sonoluminescence in liquid water just as caused by the proton tunneling between oxygens of nearest water molecules (see Appendix B).

III. TRANSPORT PROPERTIES OF HYDROGEN-BONDED COMPLEXES: POLARONS AND POLARITONS IN SYSTEMS WITH HYDROGEN BONDS

A. Orientational-Tunneling Model of One-Dimensional Molecular System

Proton transport along a hydrogen-bonded chain strongly depends on structural peculiarities of the chain. In Ref. 135 the description of proton transport has been based on the proton transfer process that involves the Grotthus mechanism with the further reorientation caused by ''tumbling'' (vibrational and/or librational) of the neighboring ionic group. In other words, the first step of the transport process consists of ionic defect motion, and the next one is accompanied by occurrence of the so-called orientational defect. Their existence is accepted in models considering proton transport in ice and the orientational relaxation rates of icy substances. Perhaps the first experimental study of the orientational (Bjerrum) defect charge was carried out by Hubman [136] based on the measuring the dielectric constant of ammonia-doped ice. In I_h ice, the energy of the Bjerrum defects was determined [137] by relaxation of the surrounding neighbors when the defects were forming.

The model proposed by Stasyuk et al. [135] describes the chain of hydrogen bonds connecting by ionic groups. The model is a development of their previous ''pseudo-spins reduced basis model'' [138], which took into account only the motion of a proton along the hydrogen bond. Reference 135 discusses the orientational degrees of freedom, which make it possible to include rotations

of covalent bonds connecting protons with ionic groups. The quasi-one-dimensional chain with L- and D-Bjerrum proton defects (for a discussion about the defects see, e.g., Ref. 139) as well as the chain with only one proton have been considered. The energy levels, polarization, and susceptibility of the proton subsystem that features a small number of hydrogen bonds have also been investigated. It has been shown that the thermodynamic properties of such molecular systems change strongly with the change of orientational motion frequency and external electric field strength.

Stasyuk et al.'s model is the following. Let the molecular system $AH \cdots CH \ldots CH \cdots B$ contain a chain of N hydrogen bonds between the ions or ionic groups C (Fig. 6). A and B denote ions or ionic groups placed on the ends of the chain. Stasyuk et al. [135] proceed from the concept implying the availability of a double-well potential for each bond. The ionic defect represents the motion of a proton within a single hydrogen bond between the two heavy ions. The orientational defects allow a proton to move along a chain. In the approach, there are only two lowest proton states in a bond and only two different orientational positions for the covalent bond. The starting Hamiltonian presented in the second quantization form is based on wave functions ψ_a and ψ_b of the lowest proton states in the left (a) and right (b) minima of the double-well potential:

$$H = H_A + \sum_{l=1}^{N-1} H_l + H_B + H_{\text{tun}} + H_{\text{rot}} + H_C + H_{\mathscr{E}} \qquad (120)$$

The short-range interaction's part of the Hamiltonian includes three terms:

$$
\begin{aligned}
H_A &= \varepsilon_A(1 - n_{1,a}) + w_A n_{1,a} \\
H_l &= w'(1 - n_{l,b})(1 - n_{l+1,a}) + w n_{l,b} n_{l+1,a} + \varepsilon(1 - n_{k,b}) n_{l+1,a} \\
&\quad + \varepsilon(1 - n_{l,b}) n_{l+1,a} + \varepsilon n_{l,b}(1 - n_{l+1,a}) \\
H_B &= \varepsilon_B(1 - n_{N,b}) + w_B n_{N,b}
\end{aligned}
\qquad (121)
$$
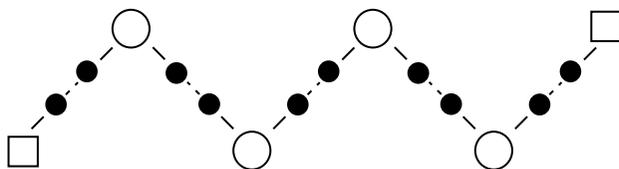
Figure 6. Scheme of the hydrogen-bonded chain. The arrows show the direction of the motion of a proton. (From Ref. 136.)
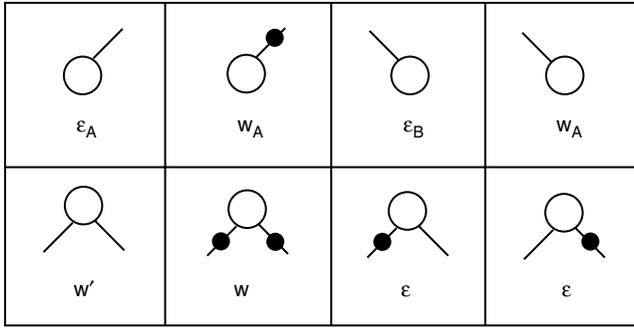
Figure 7. Proton configurations near ionic groups and the proton energies. (From Ref. 136.)

where $\varepsilon, \varepsilon_{A,B}, w, w', w_{A,B}$ are the energies of proton configurations in the potential minima nearest to the ionic groups (Fig. 7); $n_{l,\mu}$ are the occupation numbers of protons in the positions $\mu = a, b$ in the bond $k(k = 1, \ldots, N)$.

The tunneling energy H_{tun} is presented in the form

$$H_{\text{tun}} = \Omega_A(\hat{a}_{1,a}^+\hat{a}_{1,b} + \hat{a}_{1,b}^+\hat{a}_{1,a}) + \Omega_B(\hat{a}_{N,a}^+\hat{a}_{N,b} + \hat{a}_{N,b}^+\hat{a}_{N,a})$$
$$+ \Omega_0 \sum_{l=2}^{N-1} (\hat{a}_{l,a}^+\hat{a}_{l,b} + \hat{a}_{l,b}^+\hat{a}_{l,a}) \tag{122}$$

where $\hat{a}_{l,\mu}^+(\hat{a}_{l,\mu})$ are the proton creation (annihilation) operators—that is, Fermi operators. The tunneling frequencies of the outer and inner bonds are Ω_A, Ω_B, and Ω_0, respectively. The effect associated with the orientational motion is described by the term

$$H_{\text{rot}} = \Omega_{\text{rot}} \sum_{l=1}^{N-1} (\hat{a}_{l,b}^+\hat{a}_{l+1,a} + \hat{a}_{l+1,a}^+\hat{a}_{l,b}) \tag{123}$$

where Ω_{rot} is characterized by the pseudo-tunneling effect. The term

$$H_{\text{C}} = U \sum_{l=1}^{N-1} n_{l,a}n_{l,b} + V \sum_{l=1}^{N} (1 - n_{l,a})(1 - n_{l,b}) \tag{124}$$

corresponds to the energy of Coulomb repulsion between two protons in the hydrogen bond, the first term, and between free electron pairs without protons, the second term (this is so-called lone pairs [138,140]). The last term in expression (120)

$$H_{\mathscr{E}} = e\mathscr{E} \sum_{l=1}^{N} \sum_{\mu=\{a,b\}} R_{l,\mu}n_{l,\mu} \tag{125}$$

describes the interaction between a proton with charge e and the external electric field $\mathscr{E}$; $R_{l,\mu}$ is the distance between the left edge of the chain and the corresponding potential well (l, μ).

In the case of a symmetric system, some parameters are reduced to the following: $\Omega_A = \Omega_B = \Omega$, $\varepsilon_A = \varepsilon_B = \tilde{\varepsilon}$, and $w_A = w_B = \tilde{w}$.

There exist 2^{2N} many-particle states in a chain with N bonds, namely, $|r\rangle = |n_{1,a}, \ldots, n_{N,b}\rangle$, where $n_{k,\mu} = \{0, 1\}$ is the number of protons in the position $\mu = \{a, b\}$ in the lth bond. In this case the Hamiltonian expressed in terms of the Hubbard operators $X^{r,r'} = |r\rangle\langle r'|$ acting on the basis $|r\rangle$ decomposed into $(2N + 1)$ pairs that correspond to the various values of the proton number $n = \sum_{l,\mu} n_{l,\mu} = 0, 1, \ldots, 2N$:

$$H = H^0 \oplus H^1 \oplus \cdots \oplus H^{2N} \tag{126}$$

The eigenvalues of these Hamiltonians give the energy spectrum of the system studied. Short-range proton correlations and a strong Coulomb interaction between protons in a bond could result in the equilibrium distribution of protons without high-energy proton configurations [138]. Similarly, the Hubbard-type interaction can also be excluded. Let us write, for example, the basis for $|r\rangle$ for $N = 2$:

$$
\begin{aligned}
c_{0,a} &= X^{1,2} + X^{3,6} + X^{4,7} + X^{5,8} + X^{9,12} + X^{10,13} + X^{11,14} + X^{15,16} \\
c_{1,a} &= X^{1,4} - X^{2,7} - X^{3,9} + X^{5,11} + X^{6,12} - X^{8,14} - X^{10,15} + X^{13,16} \\
c_{0,b} &= X^{1,3} - X^{2,6} + X^{4,9} + X^{5,10} - X^{7,12} - X^{8,13} + X^{11,15} - X^{14,16} \\
c_{1,b} &= X^{1,5} - X^{2,8} - X^{3,10} - X^{4,11} + X^{6,13} + X^{7,14} + X^{9,15} - X^{12,16}
\end{aligned}
\tag{127}
$$

The Hamiltonian decomposes into five terms:

$$H = H_2^0 \oplus H_2^1 \oplus H_2^2 \oplus H_2^3 \oplus H_2^4 \tag{128}$$

where

$$H_2^0 = a_2^0 \cdot \hat{1} \tag{129}$$

$$
\begin{aligned}
H_2^1 = {} & ((b - a) + \mathscr{E}(M_a + M_{ab}))X^{2,2} + M_a\mathscr{E}(X^{3,3} - X^{4,4}) \\
& + ((b - a) - \mathscr{E}(M_a + M_{ab}))X^{5,5} + \Omega(X^{2,3} + X^{3,2}) \\
& + \Omega(X^{4,5} + X^{5,4}) + \Omega_{\text{rot}}(X^{3,4} + X^{4,3}) + a_2^1 \cdot \hat{1}
\end{aligned}
\tag{130}
$$

$$H_2^2 = [U + V + \mathscr{E}(2M_a + M_{ab})]X^{6,6} + M_{ab}(X^{7,7} - X^{10,10})$$
$$+ (b - a)X^{8,8} + [J - (b - a)]X^{9,9} + \Omega(X^{8,10} + X^{5,4})$$
$$+ \Omega(X^{9,10} + X^{10,9}) + \Omega_{\text{rot}}(X^{6,7} + X^{7,6})$$
$$+ \Omega_{\text{rot}}(X^{10,11} + X^{11,10}) + a_2^2 \cdot \hat{1} \tag{131}$$

$$H_2^3 = [U + J - (b - a) + \mathscr{E}(M_a + M_{ab})]X^{12,12} + (U + \mathscr{E}M_a)X^{13,13}$$
$$+ (U - \mathscr{E}M_a)X^{14,14} + [U + J - (b - a) - \mathscr{E}(M_a + M_{ab})]X^{15,15}$$
$$+ \Omega(X^{12,13} + X^{13,12}) + \Omega(X^{14,15} + X^{15,14})$$
$$+ \Omega_{\text{rot}}(X^{13,14} + X^{14,13}) + a_2^3 \cdot \hat{1} \tag{132}$$

$$H_2^4 = (2U + J)X^{16,16} + a_2^4 \cdot \hat{1}$$

Here $(b - a) = (\tilde{w} - \tilde{\varepsilon}) - (\varepsilon - w')$ is the difference between energies of proton configurations at the first and last ionic groups (A and B) and an internal potential well (C). The value $a_2^2 = \tilde{w} + \tilde{\varepsilon} + \varepsilon$ determines the energy of domain walls at the ends of the chain (due to the fact that the boundary of the chain is characterized by other parameters than the internal part). The other parameters a_i^j are the following:

$$a_2^0 = a_2^2 - (\tilde{w} - \tilde{\varepsilon}) - (\varepsilon - w')$$
$$a_2^1 = a_2^2 - (\tilde{w} - \tilde{\varepsilon})$$
$$a_2^3 = a_2^2 + (\tilde{w} - \tilde{\varepsilon})$$
$$a_2^4 = a_2^2 + (\tilde{w} - \tilde{\varepsilon}) + (\varepsilon - w')$$

The parameter $J = w + w' - 2\varepsilon$ is the effective short-range interaction between the protons near an ionic group; $M_a = -eR_a$, $M_{ab} = -eR_{ab}$, where R_a is the distance between the ionic group and the neighboring potential well and R_{ab} is the distance between two neighboring wells of the double minimum potential. Note that for a chain with any finite number of N, the corresponding Hamiltonian can be written in the same way.

The equation for eigenvalues and eigenvectors of the Hamiltonian (126)

$$\sum_{r'} \langle r|H|r' \rangle u_{rr'} = \lambda_\mu u_{r\mu} \tag{134}$$

allows one to obtain the energy spectrum of the system.

The dielectric susceptibility χ of proton subsystem can be expressed via the Green function

$$\chi(\omega) = -\frac{2\pi}{\hbar} \langle\langle P \mid P \rangle\rangle_\omega \tag{135}$$

where $P = -e \sum_{l,\mu} R_{l,\mu} n_{l,\mu}$ is the operator of electric dipole momentum of protons in the chain. The Hamiltonian represented on the basis $|\tilde{r}\rangle = \sum_r u_{rr'} |r'\rangle$ has the diagonal form

$$\tilde{H} = \sum_p \lambda_p \tilde{X}^{p,p} \tag{136}$$

where the operator $\tilde{X}^{p,p}$ is determined by the unitary transformation of Hubbard operators $X^{p,p}$,

$$X^{r,r'} = \sum_{\mu,\nu} u_{r\mu}^* \tilde{X}^{\mu,\nu} u_{\nu r'} \tag{137}$$

The equation of motion of the operator $\tilde{X}^{\mu,\nu}$ is the following:

$$i\hbar \frac{\partial}{\partial t} \tilde{X}^{\mu,\nu} = [\tilde{X}^{\mu,\nu}, \tilde{H}]_t = (\lambda_\nu - \lambda_\mu)\tilde{X}^{\mu,\nu} = \lambda_{\nu\mu} \tilde{X}^{\mu,\nu} \tag{138}$$

This allows the determination of the susceptibility of the proton subsystem,

$$\chi(\omega) = \sum_{\mu<\nu} 2\tilde{P}_{\mu\nu}^2 \lambda_{\nu\mu} \frac{\langle \tilde{X}^{\mu\mu} - \tilde{X}^{\nu\nu} \rangle}{(\hbar\omega)^2 - \lambda_{\nu\mu}^2} \tag{139}$$

where the operator of dipole moment constructed on the basis $|r'\rangle$ is equal to

$$\tilde{P}_{\mu\nu} = \sum_{l,l'} u_{\mu l} \langle l|P|l'\rangle u_{l'\nu}^* \tag{140}$$

and the average occupation number of state $|\mu\rangle$ is defined as

$$\langle \tilde{X}^{\mu\mu} \rangle = \frac{e^{-\beta\lambda_\mu}}{\sum_\nu e^{-\beta\lambda_\nu}} \tag{141}$$

The energy spectrum and the susceptibility, for instance, for a short chain with the number of ions $N = 2$ and two protons ($n = 2$) in the two hydrogen

bonds have been calculated in Ref. 135. In this case the system studied is described by the Hamiltonian (131) and the corresponding eigenvalues are

$$
\begin{aligned}
\lambda_{1,2} &= \frac{1}{2}(U + V \pm q_-) + \mathscr{E}(M_a + M_{ab}) + a_2^2 \\
\lambda_3 &= (b - a) + a_2^2 \\
\lambda_4 &= J - (b - a) + a_2^2 \\
\lambda_{5,6} &= \frac{1}{2}(U + V \pm q_+) - \mathscr{E}(M_a + M_{ab}) + a_2^2
\end{aligned}
\tag{142}
$$

where

$$
q_\pm = \sqrt{(U + V \mp 2\mathscr{E}M_a)^2 + 4\Omega_{\text{rot}}^2}
\tag{143}
$$

The examination of the spectrum (142) as a function of Ω_{rot} that features the proton's orientational motion and at $\mathscr{E} = 0$ shows that the behavior of the system is specified by two regimes. At $\Omega_{\text{rot}} < \Omega_{\text{rot}}^*$, where $\Omega_{\text{rot}}^* = \{(b - a)^2 - (U + V)(b - a)\}^{1/2}$, the ground state corresponds to the location of the domain wall in the center of the chain when the protons are found in potential wells near the outer ionic groups A and B. At $\Omega_{\text{rot}} > \Omega_{\text{rot}}^*$ one of the protons is localized at an internal ion. The appropriate static susceptibility at low temperature becomes

$$
\chi = \begin{cases} 0, & \Omega_{\text{rot}} < \Omega_{\text{rot}}^* \\ 2\frac{M_a^2}{q}\left(1 - \frac{U^2}{q^2}\right), & \Omega_{\text{rot}} > \Omega_{\text{rot}}^* \end{cases}
\tag{144}
$$

Numerical calculations performed for the system $N = n = 2$, $N = n = 3$, and $N = n = 4$ have shown [135] that χ as a function of Ω_{rot} is smoothed in the vicinity of Ω_{rot}^* and that the value of Ω_{rot}^* shifts to the low frequency region with the increase of N.

The statistical sum for the considering system ($N = n = 2$) is equal to

$$
\begin{aligned}
Z = {} & e^{-(b-a)/k_{\text{B}}T} + e^{-(J-(b-a))/k_{\text{B}}T} + 2e^{-(U+V)/2k_{\text{B}}T} \\
& \times \left(e^{-\mathscr{E}(M_a + M_{ab})/k_{\text{B}}T}\cosh\frac{q_-}{2k_{\text{B}}T} + e^{\mathscr{E}(M_a + M_{ab})/k_{\text{B}}T}\cosh\frac{q_+}{2k_{\text{B}}T} \right)
\end{aligned}
\tag{145}
$$

The average dipole moment is obtained from expression (145)

$$
\langle P \rangle = -\frac{\partial F}{\partial \mathscr{E}}
\tag{146}
$$

where the free energy is given by

$$F = -\frac{\ln Z}{k_{\mathrm{B}}T} \tag{147}$$

Explicitly,

$$\langle P \rangle = -2 \frac{e^{-(U+V)/2k_{\mathrm{B}}T}}{Z} \{ e^{-\mathscr{E}(M_a+M_{ab})/k_{\mathrm{B}}T} \xi_- - e^{\mathscr{E}(M_a+M_{ab})/k_{\mathrm{B}}T} \xi_+ \} \tag{148}$$

$$\xi_{\pm} = (M_a + M_{ab})\cosh\frac{q_{\pm}}{2k_{\mathrm{B}}T} + M_a \frac{U + V \mp 2\mathscr{E}M_a}{q_{\pm}} \sinh\frac{q_{\pm}}{2k_{\mathrm{B}}T} \tag{149}$$

Expressions from (145) to (149) allows one to obtain the analytical expression for the static susceptibility,

$$\chi(\mathscr{E}) = \frac{e^{-(U+V)/2k_{\mathrm{B}}T}}{Z^2} \{ e^{-\mathscr{E}(M_a+M_{ab})/k_{\mathrm{B}}T}\xi_- - e^{\mathscr{E}(M_a+M_{ab})/k_{\mathrm{B}}T}\xi_+ \}^2$$
$$+ \frac{e^{-(U+V)/2k_{\mathrm{B}}T}}{Z} \{ e^{-\mathscr{E}(M_a+M_{ab})/k_{\mathrm{B}}T}\eta_- - e^{\mathscr{E}(M_a+M_{ab})/k_{\mathrm{B}}T}\eta_+ \} \tag{150}$$

where

$$\eta_{\pm} = \frac{2}{k_{\mathrm{B}}T}(M_a + M_{ab})^2 - M_a^2 \left(\frac{U + V \mp 2\mathscr{E}M_a}{q_{\pm}}\right)^2 \cosh\frac{q_{\pm}}{2k_{\mathrm{B}}T}$$
$$- 4\frac{M_a^2}{q_{\pm}} \left[1 - \left(\frac{U + V \mp 2\mathscr{E}M_a}{q_{\pm}}\right)^2 \right] \sinh\frac{q_{\pm}}{2k_{\mathrm{B}}T} \tag{151}$$

Expressions (142), (148), and (150) allow the consideration of the energy spectrum, the dipole moment, and the susceptibility on the field strength $\mathscr{E}$. A numerical inspection of the spectrum performed in Ref. 135 has shown that the ground state is reconstructed at $\mathscr{E} = \mathscr{E}_2 = (U + V)/2M_a$. The transfer of all the protons along the field to an appropriate edge of the chain induces D defects at this edge, and consequently L defects appear at the opposite edge. This changes the inclination of the dipole moment $\langle P \rangle$ as a function of $\mathscr{E}$ just at $\mathscr{E} = \mathscr{E}_2$. An anomaly of susceptibility $\chi(\mathscr{E})$ appears at $\mathscr{E} = \mathscr{E}_2$ as well. Besides, it has been concluded that the motion of protons along the chain under an electric field is very sensitive to the value of Ω_{rot}. In the general case, the peculiar value $\mathscr{E}_2$ depends on the number of ions in the chain [135],

$$\mathscr{E}_2 = \frac{U + V}{2(N - 1)M_a} \tag{152}$$

The appearance of high-energy proton configurations, D and L defects, has occurred at $\mathscr{E} > \mathscr{E}_2$, which is caused by the increasing the dipole moment of the proton subsystem with the gain of the number of hydrogen bonds.

The motion of L defects has been treated in detail in the case $N = 3$ and $n = N - 1$. The energy spectrum as a function of Ω_{rot} has been obtained analytically at $\mathscr{E} = 0$ and $\Omega = 0$. Two peculiarities have been found in the spectrum at the parameters $\Omega_{\text{rot}}^{(1)} = -(b - a)$ and $\Omega_{\text{rot}}^{(2)} = -(b - a)/(\sqrt{2} - 1)$. The rearrangement of the spectrum influences the behavior of the susceptibility: $\chi(\Omega_{\text{rot}})$ decreases with $\Omega_{\text{rot}} > \Omega_{\text{rot}}^{(2)}$, and this takes place at the arbitrary number of hydrogen bonds. With the increase of the number of hydrogen bonds, the distance between $\Omega_{\text{rot}}^{(1)}$ and $\Omega_{\text{rot}}^{(2)}$ becomes smaller. Applying an external field leads to the proton transfer along the field and the migration of an L defect in the opposite direction. Thus an L defect is localized at the left edge of the chain, and all the protons occupy the right potential wells in the remaining $(N - 1)$ double-well potentials. In other words, the protons are ordered and therefore the left domain wall should appear between the first bond with an L defect and the second left bond. Meanwhile the right domain wall is formed at the right edge; that is, a D defect is created at the right edge of the chain. By the estimation [135], D and L defects may be realized at value $\mathscr{E}$, which decreases with the growing the number of hydrogen bonds.

As an example of an object with more than one L defect, the chain with N hydrogen bonds and only one proton has been studied [135]. They have considered the energy spectrum as a function of the field $\mathscr{E}$ at the fitted parameters $(b - a), \Omega, \Omega_0, M_a, M_{ab}$ and various values of Ω_{rot}. The susceptibility falls within two regions that are specified by $\Omega_{\text{rot}} < -(b - a)$ and $\Omega_{\text{rot}} > -(b - a)$. The $(N - 1)$ energy levels form the energy band with the increase of N. A peculiarity revealed in the behavior of $\langle P \rangle$ and χ at $\Omega_{\text{rot}} > -(b - a)$ has been related to the motion of a delocalized proton from the inner hydrogen bond toward the outer bond along the applied field.

B. Proton Ordering Model

A number of hydrogen-containing compounds, such as lithium hydrazium sulfate $Li(N_2H_5)SO_4$ (LiHzS), tri-ammonium hydrogen disulfate $(NH_4)_3H(SO_4)_2$ (TAHS), and others, exhibit an anisotropy of the protonic electrical conductivity σ at temperatures $T \geq 300$ K: along the c axis the σ_c is about 10^3 larger than in the perpendicular directions [29,30]. This effect is stipulated by long hydrogen-bonded chains that spread along the c axis along the whole crystal. Thus the relatively large σ_c is caused by the motion of protons along hydrogen-bonded chains. The large proton mobility of ice is explained by the net of hydrogen bonds [140]. The comparatively high proton conductivity was observed also in proton-conducting proteins [141–143], which also connected with proton transfer along the hydrogen-bonded chains.

Having understood the microscopic mechanism of the motion of protons in the hydrogen-bonded network and along the hydrogen-bonded chain, we should know first the behavior of the proton subsystem in the aforementioned compounds. The compounds are characterized by the complicated structure of the primitive cell, and many of them possess typical ferroelectric properties caused by the presence of hydrogen bonds. Experimental studies (see, e.g., Refs. 144 and 145) specify a significant role of the proton subsystem in proton superionic phase transitions in a group of crystals $M_3H(XO_4)_2$ (where $M = K$, Rb, Cs, MH$_4$; $X = Se$, S), which indicates the prime importance of the consideration of a hydrogen bond network and its rearrangement at the number of phase transitions of the crystals [42]. For instance, the structural X-ray studies [146,147] revealed the following phase transition sequence in the $(NH_4)_3H(SeO_4)_2$ crystal [42]: superionic phase I (with trigonal symmetry R$\bar{3}$m), superionic phase II (space group R$\bar{3}$), ferroelastic phase III (triclinic symmetry C$\bar{1}$ or P$\bar{1}$, with small deviations from monoclinic), ferroelastic phase IV (monoclinic symmetry Cc) with the transition temperatures 332 K, 302 K, 275 K, 181 K, and 101 K, respectively.

In a series of works by Salejda and Dzhavadov [148] and Stasyuk et al. [38–42], a microscopic description of the phase transitions in $(NH_4)_3H(SeO_4)_2$ has been proposed. The results obtained have been compared with those obtained from the Landau phenomenological theory. The original Hamiltonian has been presented in a bilinear form

$$H_{\text{int}} = \frac{1}{2} \sum_{m,m';f,f'} \Phi_{ff'}(mm') n_{mf} n_{m'f'} \tag{153}$$

where $n_{mf} = 0$ or 1 is the occupation number of a proton in position f of unit cell m; $\Phi_{ff'}(mm')$ denotes the energy of pair interaction. The Hamiltonian of the proton subsystem includes, in addition to expression (153), the sum of single-particle energies

$$H_0 = \sum_{m,f} (E - \mu) n_{mf} \tag{154}$$

The chemical potential μ of the proton subsystem at the given number of protons is determined from condition

$$\sum_{m;f} \bar{n}_{mf} = \bar{n} \tag{155}$$

where $\bar{n}$ is the number of protons per unit cell, which for $(NH_4)_3 \cdot H(SeO_4)_2$-type crystals one can put $\bar{n} = 1$. In the mean-field approximation

$$H_{\text{MF}} = U_0 + \sum_{m;f} \gamma_f(m) n_{mf} + \sum_{m;f} (E - \mu) n_{mf} \tag{156}$$

where

$$U_0 = -\frac{1}{2} \sum_{m,m';f,f'} \Phi_{ff'}(mm')\bar{n}_{mf}\bar{n}_{m'f'} \qquad (157)$$

we obtain

$$\gamma_f(m) = \sum_{m';f'} \Phi_{ff'}(mm')\bar{n}_{m'f'} \qquad (158)$$

The statistical sum Z and thermodynamic potential Ω for the system with the Hamiltonian (156) are defined as

$$Z = \mathrm{Tr}\, e^{-H_{\mathrm{MF}}/k_{\mathrm{B}}T} = \prod_{m;f} \sum_{n_f=\{0,1\}} e^{-(\gamma_f(m)+E-\mu)n_m/k_{\mathrm{B}}T} e^{-U_0/k_{\mathrm{B}}T} \qquad (159)$$

$$\Omega = -k_{\mathrm{B}}T \ln Z = U_0 - k_{\mathrm{B}}T \sum_{m;f} \ln\left(1 + e^{-(\gamma_f(m)+E-\mu)/k_{\mathrm{B}}T}\right) \qquad (160)$$

Thus, the mean number of protons per unit cell obeys the Fermi–Dirac statistics

$$\bar{n}_{mf} = \left(e^{(\gamma_f(m)+E-\mu)/k_{\mathrm{B}}T} + 1\right)^{-1} \qquad (161)$$

Let us now represent the mean number of protons $\bar{n}_{mf}$ as follows:

$$\bar{n}_{mf} = \frac{1}{3}\bar{n} + \delta\bar{n}_{mf} \qquad (162)$$

where $\delta\bar{n}_{mf}$ is the deviation from the mean proton occupation number. The three components can be represented in the form [38]

$$\delta\bar{n}_{m1} = \frac{1}{\sqrt{2}}ue^{i\mathbf{k}_3\mathbf{R}_m} + \frac{1}{\sqrt{6}}v$$

$$\delta\bar{n}_{m2} = -\frac{1}{\sqrt{2}}ue^{i\mathbf{k}_3\mathbf{R}_m} + \frac{1}{\sqrt{6}}v \qquad (163)$$

$$\delta\bar{n}_{m3} = -\frac{2}{\sqrt{6}}v$$

The presentation (163) makes it possible to obtain the observed occupations of proton positions ($\bar{n}_{m1} = 1$, $\bar{n}_{m2} = 0$, $\bar{n}_{m3} = 0$ or $\bar{n}_{m1} = 0, \bar{n}_{m2} = 1, \bar{n}_{m3} = 0$) for

the saturation values of order parameters u and v: $u = \pm 1/\sqrt{2}$ and $v = 1/\sqrt{6}$, where

$$u = \pm \frac{1}{\sqrt{2}} \langle n_{m1} - n_{m2} \rangle, \qquad v = \frac{1}{\sqrt{6}} \langle n_{m1} + n_{m2} - 2n_{m3} \rangle \qquad (164)$$

The resulting orderings are induced by the irreducible representation $A_g(\tau_1)$ of the wave vector group $G_{\mathbf{k}_i}$ as well as by the representation $E_g(\tau_3 + \tau_5)$ of the point group $G_{\mathbf{k}_7=0}$. Indeed, in a general case the deviation can be written as

$$\delta \bar{n}_1 = \frac{1}{\sqrt{2}} [u_3 e^{i\mathbf{k}_3 \mathbf{R}_m} - u_2 e^{i\mathbf{k}_2 \mathbf{R}_m}] + \frac{1}{3}(\eta + \zeta)$$

$$\delta \bar{n}_2 = \frac{1}{\sqrt{2}} [u_1 e^{i\mathbf{k}_1 \mathbf{R}_m} - u_3 e^{i\mathbf{k}_3 \mathbf{R}_m}] + \frac{1}{3}(\varepsilon^2 \eta + \varepsilon \zeta) \qquad (165)$$

$$\delta \bar{n}_3 = \frac{1}{\sqrt{2}} [u_2 e^{i\mathbf{k}_2 \mathbf{R}_m} - u_1 e^{i\mathbf{k}_1 \mathbf{R}_m}] + \frac{1}{3}(\varepsilon \eta + \varepsilon^2 \zeta)$$

where $\varepsilon = e^{i2\pi/3}$; the variables

$$\eta = \bar{n}_1 + \varepsilon \bar{n}_2 + \varepsilon^2 \bar{n}_3$$
$$\zeta = \bar{n}_1 + \varepsilon^2 \bar{n}_2 + \varepsilon \bar{n}_3 \qquad (166)$$

are transformed according to the E_g representation under point group operations. Setting

$$\eta = |\eta| e^{i\psi}, \qquad \zeta = |\eta| e^{-i\psi} \qquad (167)$$

we obtain

$$\eta + \zeta = 2|\eta| \cos \psi$$

$$\varepsilon^2 \eta + \varepsilon \zeta = 2|\eta| \cos \left(\psi - \frac{2\pi}{3} \right) \qquad (168)$$

$$\varepsilon \eta + \varepsilon^2 \zeta = 2|\eta| \cos \left(\psi - \frac{4\pi}{3} \right)$$

The choice $|\eta| = \sqrt{3/2} v$, $\psi = \{\frac{1}{3}\pi; \ \pi; \ \frac{1}{3}\pi\}$ corresponds to the orientation states with vectors $\mathbf{k}_3 = \frac{1}{2}\mathbf{b}_3$, $\mathbf{k}_1 = \frac{1}{2}\mathbf{b}_1$, and $\mathbf{k}_2 = \frac{1}{2}\mathbf{b}_2$, respectively.

The same proton occupation in each unit cell occurs in phase IV. Hence the change in symmetry of the proton distribution in phase IV, in comparison with phase II, may be formally connected with one of irreducible representations of group $G_{\mathbf{k}=0}$, if only the proton subsystem is taken into account.

For the basis (n_1, n_2, n_3), only a two-dimensional irreducible representation E_g becomes suitable. In this case the expressions for the deviations $\delta \mathbf{n}_f$ can be derived from Eqs. (165) with restriction to uniform terms. The values $|\eta| = 1$ and $\psi = 0, \frac{2}{3}\pi, \frac{2}{3}\pi$ correspond to three orientation states with $\mathbf{n}_{mf} = (1,0,0)$, $(0,1,0)$, $(0,0,1)$, respectively. Thus, Eqs. (165) for the deviations of proton occupation numbers include the cases of all three phases (II, III, and IV). The representation of $\delta \mathbf{n}_f$ in the form of Eqs. (163) allows one to describe not only the ordering to an orientation state with vector $\mathbf{k}_3$ of phase III (at $u \neq 0$ and $v \neq 0$), but also the ordering with $\mathbf{n}_{mf} = (0,0,1)$ for phase IV (with $u = 0$, $v \neq 0$ and saturation value $v = -2/\sqrt{6}$).

Equations (163) allow one to derive equations for the proton mean occupation numbers and thermodynamic functions in the mean-field approximation. Substituting variables $\delta \bar{n}_{mi}$ where $i = 1, 2, 3$ into Eqs. (157)–(159), we get

$$\gamma_1(m) = \gamma_0 + av + be^{i\mathbf{k}_3\mathbf{R}_m}u$$
$$\gamma_2(m) = \gamma_0 + av - be^{i\mathbf{k}_3\mathbf{R}_m}u \qquad (169)$$
$$\gamma_3(m) = \gamma_0 - 2av$$

Here

$$\gamma_0 = \frac{1}{3}\bar{n}\sum_{f'}\Phi_{ff'}(0)$$

$$a = \frac{1}{\sqrt{6}}[\varphi_{11}(0) - \varphi_{12}(0)] \qquad (170)$$

$$b = \frac{1}{\sqrt{2}}[\varphi_{11}(\mathbf{k}_3) - \varphi_{12}(\mathbf{k}_3)]$$

where the following designation is used:

$$\varphi_{ff'}(\mathbf{k}) = \sum_{m'}\Phi_{ff'}(mm')\,e^{i\mathbf{k}\cdot(\mathbf{R}_m - \mathbf{R}_{m'})} \qquad (171)$$

which is the Fourier transform of the proton interaction matrix. Then instead of expression (157) we have

$$U_0 = -\frac{N}{2}\gamma_0 - \frac{N}{2}\sqrt{6}av^2 - \frac{N}{2}\sqrt{2}bu^2 \qquad (172)$$

The symbols u and v here play the role of proton order parameters. Then the thermodynamic equilibrium conditions $\partial\Omega/\partial\bar{n}_{mf} = 0$ and $\partial F/\partial\bar{n}_{mf} = 0$ are

rewritten with respect to the parameters u and v as follows:

$$\frac{\partial}{\partial u}\left(\frac{1}{N}F\right) = 0, \qquad \frac{\partial}{\partial v}\left(\frac{1}{N}F\right) = 0 \qquad (173)$$

With the explicit form of the free energy F as a function of order parameters u and v,

$$\frac{1}{N}F = \frac{1}{N}U_0 - k_{\mathrm{B}}T\left[\ln\left(1 + \frac{1}{y}e^{-(av+bu)/k_{\mathrm{B}}T}\right)\right.$$
$$\left. + \ln\left(1 + \frac{1}{y}e^{-(av-bu)/k_{\mathrm{B}}T}\right) + \ln\left(1 + \frac{1}{y}e^{2av/k_{\mathrm{B}}T}\right)\right] + \mu\bar{n} \quad (174)$$

where $y = e^{(E-\mu+\gamma_0)/k_{\mathrm{B}}T}$, one derives the following equations for u and v:

$$u = \frac{1}{\sqrt{2}}\left[\frac{1}{ye^{(av+bu)/k_{\mathrm{B}}T} + 1} - \frac{1}{ye^{(av-bu)/k_{\mathrm{B}}T} + 1}\right]$$
$$v = \frac{1}{\sqrt{26}}\left[\frac{1}{ye^{(av+bu)/k_{\mathrm{B}}T} + 1} - \frac{1}{ye^{(av-bu)/k_{\mathrm{B}}T} + 1} - \frac{Z}{ye^{-2av/k_{\mathrm{B}}T} + 1}\right] \qquad (175)$$

The parameter y is deduced from the equation

$$\frac{1}{ye^{(av+bu)/k_{\mathrm{B}}T} + 1} - \frac{1}{ye^{(av-bu)/k_{\mathrm{B}}T} + 1} - \frac{Z}{ye^{-2av/k_{\mathrm{B}}T} + 1} = \bar{n} \qquad (176)$$

which follows from Eq. (161). For the sake of simplicity, let $\bar{n} = 1$. The solution to Eqs. (175) and (176) and the analysis of extrema of the function F has been performed numerically [38]. It has been found that a first-order transition to phase IV takes place at $b = \sqrt{3}\,a$ with $u = 0$ and $v \neq 0$. At $b > \sqrt{3}a$ a transition to the ordered state corresponding to phase III with $u \neq 0$ and $v \neq 0$ occurs. Tricritical takes place at $(b/a)_{\mathrm{c}} = 2.07$ and $T_{\mathrm{c}} = 0.65a$ when the transition to phase III changes from first to second. At $b/a = (b/a)^* = \sqrt{3}$ all three absolute minima of free energy coexist (at $T < T_{\mathrm{c}}$) having equal depth.

C. Proton Conductivity at the Superionic Phase Transitions

The rearrangement of the hydrogen-bonded network at the superionic phase transitions studied in the framework of the lattice-gas-type model, which has been described in the previous subsection, makes it possible to evaluate the main aspects of proton conductivity in the mentioned compounds.

Let us treat the proton dynamics starting from the modified Hamiltonian (153), that is [149,150],

$$H_{\text{int}} = \frac{1}{2} \sum_{m,m';f,f'} \Phi_{ff'}(mm') n_{mf} n_{m'f'} - \mu \sum_{m;f} n_{mf} \qquad (177)$$

where $n_{mf} = \{0,1\}$ is the proton occupation number for position f in the primitive unit cell with the coordinate $\mathbf{R}_m$, $\Phi_{ff'}(mm')$ is the energy of proton interactions, and μ denotes the chemical potential that determines the average proton concentration.

The formation of a hydrogen bond induces the deformation of the XO_4 group [151–153], which leads to the shortening of the distance between the vertex oxygens $O(2)'$ and $O(2)''$. In its turns, this localizes the proton, resulting in the typical polaron effect described in Section II.C. Thus the appearance of the polaron means the increase of the activation energy for the bond breaking and the hopping of the proton to another localized position in the lattice.

The potential energy of the oxygen subsystem in the harmonic approximation is given by expression

$$\phi = \phi_0 + \sum_{m,m'} \sum_{k,k'} \sum_{\alpha,\beta} \phi_{\alpha\beta}(mk; m'k') u_\alpha(mk) u_\beta(m'k') \qquad (178)$$

where $k = 1, 2$ is the sublattice number of the mth unit cell and the force constants

$$\phi_{\alpha\beta}(mk; m'k') = \frac{\partial^2}{\partial u_\alpha(mk) \partial u_\beta(m'k')}\bigg|_0 \qquad (179)$$

The matrices $\phi_{\alpha\beta}(mk; m'k')$ for the $M_3H(X0_4)_2$ class of crystals are represented as follows [149]:

$$\phi(m1; m + \mathbf{a}_1, 2) = \begin{pmatrix} a & c \\ c & a + 2/\sqrt{3} \end{pmatrix}$$

$$\phi(m1; m + \mathbf{a}_2, 2) = \begin{pmatrix} a & -c \\ -c & a + 2/\sqrt{3} \end{pmatrix}$$

$$\phi(m1; m + \mathbf{a}_3, 2) = \begin{pmatrix} a + \sqrt{3}c & c \\ c & a - 2/\sqrt{3} \end{pmatrix} \qquad (180)$$

$$\phi(mk; mk) = \begin{pmatrix} h & 0 \\ 0 & h \end{pmatrix}$$

If we consider only displacements of the O(2) oxygens in (x, y)-plane, we gain the dynamic matrix

$$D(\mathbf{k}) = \begin{pmatrix} D^{11} & D^{12} \\ D^{21} & D^{22} \end{pmatrix} \tag{181}$$

where

$$D^{12} = \begin{pmatrix} a(e^{i\mathbf{ka}_1} + e^{i\mathbf{ka}_2}) + (a + \sqrt{3}c)e^{i\mathbf{ka}_3} & c(e^{i\mathbf{ka}_1} - e^{i\mathbf{ka}_2}) \\ c(e^{i\mathbf{ka}_1} - e^{i\mathbf{ka}_2}) & \begin{matrix} (a + 2\sqrt{3}c)(e^{i\mathbf{ka}_1} + e^{i\mathbf{ka}_2}) \\ + (a - \sqrt{3}c)e^{i\mathbf{ka}_3} \end{matrix} \end{pmatrix}$$

$$D^{11}(\mathbf{k}) = D^{22}(\mathbf{k}) = \begin{pmatrix} h & 0 \\ 0 & h \end{pmatrix}, \qquad D^{21}(\mathbf{k}) = D^{12}(-\mathbf{k}) \tag{182}$$

Thus the determination of the normal vibration modes is reduced to the evaluation of the vibration frequencies and polarization vectors of the matrix $D(\mathbf{k})$. For instance, in the case $\mathbf{k} = 0$ we have

$$\omega_{1/3}(0) = h + (3a + \sqrt{3}c), \qquad \omega_{2/4}(0) = h - (3a + \sqrt{3}c) \tag{183}$$

$$u_1 = \frac{1}{\sqrt{2}} \begin{pmatrix} 1 \\ 0 \\ 1 \\ 0 \end{pmatrix}, \qquad u_2 = \frac{1}{\sqrt{2}} \begin{pmatrix} 0 \\ -1 \\ 0 \\ 1 \end{pmatrix}$$

$$u_3 = \frac{1}{\sqrt{2}} \begin{pmatrix} 0 \\ 1 \\ 0 \\ 1 \end{pmatrix}, \qquad u_4 = \frac{1}{\sqrt{2}} \begin{pmatrix} -1 \\ 0 \\ 1 \\ 0 \end{pmatrix} \tag{184}$$

The solutions (183) and (184) point to the existence of the two different types (in- and antiphase) of the oxygen vibrations with different frequencies.

The change of the proton potential on the hydrogen bond caused by the antiphase vibrations of the oxygens results in the shortening of the bond length. Hence the modes $j = 2$ and $j = 4$ are treated as having the coordinates of polarization vectors $\mathbf{u}_2$ and $\mathbf{u}_4$ approximated by their values at $\mathbf{k} = 0$. Thus the interaction of the protons with the oxygen vibrations can be represented in the second quantization form

$$H_{\text{pr-ph}} = \sum_{m;f} \sum_{\mathbf{k},j} \tau_{mf}(\mathbf{k}j)(\hat{b}_{\mathbf{k}j} + \hat{b}_{\mathbf{k}j}^+) n_{mf} \tag{185}$$

where $\hat{b}_{\mathbf{k}j}^{+}(\hat{b}_{\mathbf{k}j})$ is the Bose operator of phonon creation (annihilation) in the jth branch with the wave vector $\mathbf{k}$. The coefficients $\tau_{mf}(\mathbf{k}j)$ are given in Ref. 150. The vibration energy of the oxygen subsystem is

$$H_{\mathrm{ph}} = \sum_{\mathbf{k},j} \hbar\omega_j(\mathbf{k})\hat{b}_{\mathbf{k}j}^{+}\hat{b}_{\mathbf{k}j} \tag{186}$$

Neglecting the intrabond proton potential, the proton transport process is considered as the dynamical breaking and formation of the hydrogen bonds connected to the HXO$_4$ ionic group rotations. This signifies that the tunneling integral is presented as follows [149]:

$$H_{\mathrm{tun}} = \Omega_{\mathrm{rot}} \sum_{m;f\neq f'} \{\hat{a}_{mf}^{+}\hat{a}_{mf'} + \hat{a}_{m+a_f-a_{f'},f}^{+}\hat{a}_{mf'}\} + h.c. \tag{187}$$

Here $\hat{a}_{mf}^{+}(\hat{a}_{mf})$ is the operator of proton creation (annihilation) in a position that is characterized by indices m and f defined above. Ω_{rot} is the transfer integral that describes the interbond proton hopping as a quantum tunneling. Once again we would like to emphasize that the parameter Ω_{rot} does not characterized the direct overlapping of the wave functions of protons located at the nearest sites. Ω_{rot} is associated with the rotational motion of ion groups, which in the first approximation one can consider as a proton ''tunneling'' of some sort.

Applying the canonical transformation $\tilde{H} = e^{iS}He^{-iS}$ used in the theory of small polaron (see, e.g., Ref. 88), we obtain instead of the Hamiltonians (185)–(187)

$$\tilde{H} = -\tilde{\mu}\sum_{m,f} n_{mf} + \frac{1}{2}\sum_{m,m';f,f'} \tilde{\Phi}_{ff'}(mm')n_{mf}n_{m'f'}$$

$$+ \sum_{\mathbf{k},j} \hbar\omega_j(\mathbf{k})\hat{b}_{\mathbf{k}j}^{+}\hat{b}_{\mathbf{k}j} + \tilde{H}_{\mathrm{tun}} \tag{188}$$

$$\tilde{H}_{\mathrm{tun}} = \Omega_{\mathrm{rot}}\sum_{m;f\neq f'} \{\hat{a}_{mf}^{+}\hat{a}_{mf'}X_{ff'}(mm)$$

$$+ \hat{a}_{m+a_f-a_{f'},f}^{+}\hat{a}_{mf'}X_{ff'}(m+a_f-a_{f'},m)\} + h.c. \tag{189}$$

Here the band narrowing factor is

$$X_{ff'}(mm') = e^{-\sum_{\mathbf{k},j}\Delta\tau_{ff'}(mm';\mathbf{k}j)(\hat{b}_{\mathbf{k}j}+\hat{b}_{\mathbf{k}j}^{+})/\hbar\omega_j(\mathbf{k})}$$

$$\Delta\tau_{ff'}(mm';\mathbf{k}j) = \tau_{mf}(\mathbf{k}j) - \tau_{m'f'}(\mathbf{k}j) \tag{190}$$

the proton chemical potential is

$$\tilde{\mu} = \mu + \sum_{\mathbf{k},j} \frac{|\tau_{mf}(\mathbf{k}j)|^2}{\hbar\omega_j(\mathbf{k})} \tag{191}$$

and the proton energy renormalized due to the polaron shift is

$$\tilde{\Phi}_{ff'}(mm') = \Phi_{ff'}(mm') - 2\sum_{\mathbf{k},j} \frac{\tau_{mf}(\mathbf{k}j)\tau_{m'f'}(-\mathbf{k}j)}{\hbar\omega_j(\mathbf{k})} \tag{192}$$

Proton conductivity of the systems studied has been considered in the framework of the Kubo linear response theory [154], i.e., the conductivity has been written as

$$\sigma(\omega,T) = \frac{1}{\mathscr{V}} \int_0^\infty \mathrm{d}t e^{i(\omega+i\varepsilon)t} \int_0^\infty \mathrm{d}\lambda \langle J(t-i\hbar\lambda)J(0)\rangle \tag{193}$$

here $\mathscr{V}$ is the effective volume of the crystal studied, the proton current is given by

$$J = \frac{e}{i\hbar}[H,x] = \frac{e\Omega_{\mathrm{rot}}}{i\hbar}\sum_m \sum_{f\neq f'} \mathbf{R}_{ff'}[\hat{a}_{mf}^+\hat{a}_{mf'}X_{ff'}(mm)$$
$$+ \hat{a}_{m+a_f-a_{f'},f}^+\hat{a}_{mf'}X_{ff'}(m+a_f-a_{f'},m)] + h.c. \tag{194}$$

where $x = \sum_{m,f} n_{mf}\mathbf{r}_{mf}$ is the proton polarization operator and the vector connected the centers of hydrogen bonds is equal to $\mathbf{R}_{ff'} = \mathbf{R}_{ff'}(mm) = \mathbf{r}_{mf} - \mathbf{r}_{mf'}$.

Using the procedure with the deformation of integration counter in the complex plane proposed in Ref. 155, Pavlenko and Stasyuk [149,150] have arrived at the following result:

$$\sigma(\omega) = \frac{e^2\Omega_{\mathrm{rot}}^2}{\hbar^2}\frac{2\sqrt{\pi}}{\mathscr{V}}\frac{\sinh(\hbar\omega/2k_\mathrm{B}T)}{\hbar\omega/2}e^{-5E_0/(12k_\mathrm{B}T)}$$
$$\times \tilde{\tau}\sum_{f,f'} \mathbf{R}_{ff'}^2 \bar{n}_f(1-\bar{n}_{f'})e^{\hbar\alpha_{ff'}/(2k_\mathrm{B}T)}e^{-\tau^2(\omega+\alpha_{ff'})^2} \tag{195}$$

where $\alpha_{ff'} = \Phi_0(1-\bar{n}_f+\bar{n}_{f'})/2\hbar$ and

$$\Phi_0 = \Phi_{12}(m,m+\mathbf{a}_1-\mathbf{a}_2) = \Phi_{12}(m,m+\mathbf{a}_1-\mathbf{a}_3) = \Phi_{12}(m,m+\mathbf{a}_1-\mathbf{a}_3)$$

are the interaction energy matrix elements presented in the approximation of nearest neighbors.

The activation energy has the form

$$E_a^{ff'} = \frac{5}{12}E_0 - \frac{1}{4}\Phi_0 \cdot (1 - \bar{n}_f + \bar{n}_{f'}) + \frac{3}{80}\Phi_0^2 \cdot (1 - \bar{n}_f + \bar{n}_{f'})^2/E_0 \qquad (196)$$

which includes the contribution from different transfer processes. The first term in expression (196) is the typical polaronic part, and the next two terms are caused by the interproton interaction and proton ordering. $E_a^{ff'}$ changes with the temperature T as the proton ordering $\bar{n}_f$ is a function of T.

The temperature dependence of the different phonon-activated transfer processes is defined by the redistribution of proton occupancies $\bar{n}_j$ of three sublattices ($j = 1, 2, 3$). For example, in the web-superionic phase the hydrogen-bonded network is disordered, and that is why the system is exemplified by only one activation energy, $E_a^0 = \frac{5}{12}E_0 - \frac{1}{4}\Phi_0 + \frac{3}{80}\Phi_0^2/E_0$.

At low temperature, in phase III the saturation is realized (or $\bar{n}_2 = 1$ and $\bar{n}_1 = \bar{n}_3 = 0$); in this case, $E_a^{23} = \frac{5}{12}E_0 - \frac{1}{4}\Phi_0 + \frac{3}{80}\Phi_0^2/E_0$ and $E_a^{12} = E_a^{13} = \frac{5}{12}E_0$, which typically holds for the strong polaron effect. In phase IV, the ordering features the components $\bar{n}_3 = 1$ and $\bar{n}_1 = \bar{n}_2 = 0$, and then the activation energy is $E_a^{31} = E_a^{32} = \frac{5}{12}E_0$. Therefore, in ordered phases, the activation energy is always higher than in the superionic phase that agrees with the experiments [155,156].

A numerical calculation of the conductivity (195) has been performed in Refs. 149 and 150 at different sets of parameters. The energy of activation estimated in Ref. 149 varied from 0.288 to 0.32×10^{-19} J, while the experimentally obtained value was approximately $0.48 \cdot 10^{-19}$ J. The better fit to the experimental data as mentioned in Ref. 149 could be possible if the additional short-range proton correlations would be taken into account.

Short-range proton correlations have been introduced in the starting Hamiltonian in Ref. 150; that is, the Hubbard operators describing the energy of the hydrogen bond configuration with two possible protons have entered a new term in the total Hamiltonian of the system studied, namely,

$$J \sum_{m,f} (X_{mf}^{ab} + X_{mf}^{ba}) \qquad (197)$$

where J is the usual resonance integral that has been added to the term that described the reorientational "tunneling" motion of protons (187). $X_{mf}^{ab} = |p\rangle_{mf} \langle q|_{mf}$ are the projection Hubbard operators, constructed on states

$$\begin{aligned}
|0\rangle_{mf} &= |00\rangle_{mf} \quad &\text{(there is no hydrogen bond)} \\
|a\rangle_{mf} &= |10\rangle_{mf} \quad &\text{(proton is in the left well)} \qquad (198) \\
|b\rangle_{mf} &= |01\rangle_{mf} \quad &\text{(proton is in the right well)}
\end{aligned}$$

In particular, this allows the representation of the operators of occupation of hydrogen bonds through the Hubbard operators

$$n_{mf} = X_{mf}^{aa} + X_{mf}^{bb} \tag{199}$$

The numerical estimate [150] of the proton conductivity (195) derived in the framework of the model described above is in good agreement with the experimental results. This is the direct theoretical justification of the experimentalists' remark [152,153,157] that the reorientation of ion groups should assist the proton transport in some superionic conductors.

D. Polaronic Conductivity Along a Hydrogen-Bonded Chain

In Section A, we have already considered the approach that includes the movement of two types of faults: ionic state (positive or/and negative) and Bjerrum faults. It has been suggested (see also, e.g., Refs. 158–160) that the drift of the ionic state (i.e., strictly speaking, an excess proton or proton hole) along the ordering chain changes the polarization of each site and therefore changes the polarization of the whole chain.

Thus, for the motion of the next state along the chain it is necessary to repolarize the chain into its initial state, which can be achieved by Bjerrum-fault transfer. The semiphenomenological theory of proton transfer along the hydrogen-bonded chain of the ice-like structure, developed in Ref. 161, includes the influence of longitudinal acoustic vibrations of the chain sites on the proton subsystem. Reference 162, in which the dynamics of the ionic state formation in the hydrogen-bonded chains is considered, resembles roughly Ref. 161.

One more approach based on the small polaron concept regarding the description of the motion of protons along a hydrogen-bonded chain, which allows the detailed calculation of the proton electric conductivity, was proposed in Refs. 163–165. In Ref. 163 the ionic state transfer along the weak hydrogen-bonded chain was treated. In that paper, expressions for the proton current density are derived in the small polaron model with allowance for the strong ionic coupling with intrasite vibrations of the nearest-neighbor A—H groups, $\nu(AH) \approx 10^{14}$ Hz (the weak coupling slightly decreases the A—H group longitudinal vibrations frequency, it is characterized by a large equilibrium distance $A \cdots A$, 0.29 nm $\leq r_{A\cdots A} \leq$ 0.34 nm [166], and, therefore, the proton is strongly localized in the potential well near one of the A atoms). However, as was mentioned in Ref. 167 (see also Ref. 3), the necessary reason for the proton transfer in the hydrogen-bonded chain was the large proton polarizability of hydrogen bonds. This polarizability is typical for the strong hydrogen bonds,

which are specified by Ref. 167: (i) a considerable drop of the longitudinal vibrations ν (AH) from 6×10^{13} Hz to 3×10^{12} Hz in comparison with the previous mentioned 10^{14} Hz; (ii) a short equilibrium distance A...A, 0.25 nm $\leq r_{A...A} \leq 0.28$ nm; and (iii) a small height of the energy barrier between two wells, $E_w \ll h\nu_0$ ($\nu_0 \sim 10^{14}$ Hz, the proton frequency in an isolated well). The consequence of the above-mentioned facts is the proton delocalization and the appearance of optical polarization vibrations of it in the hydrogen bond with frequency $\nu = (3.6 \text{ to } 6) \times 10^{12}$ Hz $\approx k_B T/h$, where $T \approx 300$ K. These conditions have been well known for many years (see, e.g., Ref. 168). Besides, numerical calculations by Scheiner [168] show that in a chain with the number of bonds exceeding four, the influence of marginal effects upon the excess proton located on the middle molecule can almost be neglected.

Let us suppose that the strong hydrogen-bonded chain is absolutely ordered either by a strong external electric field $\mathscr{E}$ or by the asymmetrical arrangement of side bonds (Fig. 8). Then we assume that thermally activated structural defects in a hydrogen-bonded chain (like those in ice) are practically excluded (in the similar structure system—that is, ice—the concentration of Bjerrum faults is 5×10^{-7} per molecule H_2O, and the concentration of ions is 10^{-12} per molecule H_2O [159]).

Let us consider the migration of a charge carrier—that is, of an ionic state (an excess proton or a proton hole)—assuming that the chain does not change the polarization after a charge carrier has passed along it (Fig. 9). This is true if, firstly, the charge carrier lifetime τ_0 on the lth site considerably exceeds the time $\delta\tau$ required for hopping from the neighboring $(l-1)$th site, and, secondly, the initial polarization recovers on the $(l-1)$th site for times less than or of the order of τ_0. Such an approach assumes that the Bjerrum fault, which follows the ionic state, is removed by the repolarization of the $(l-1)$th site before an ionic state can pass to the next site. This Bjerrum-fault turning can be caused by electrical momenta of the neighboring ordered A—H chain groups. If we treat the case of a strong longitudinal field $\mathscr{E}$ (for instance, $\mathscr{E} = 10^7$ to 10^8 V/m), the
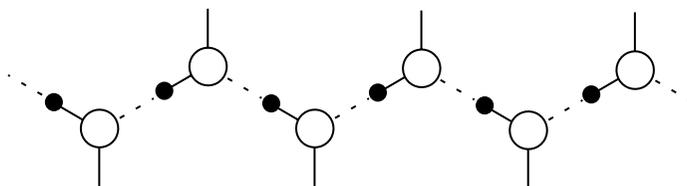
Figure 8. Chain of hydrogen bonds in longitudinal electric field $\mathscr{E}$; ◯ is atom A, where A = O, N, F; ● is H; ----- is hydrogen bond;——is covalent bond.
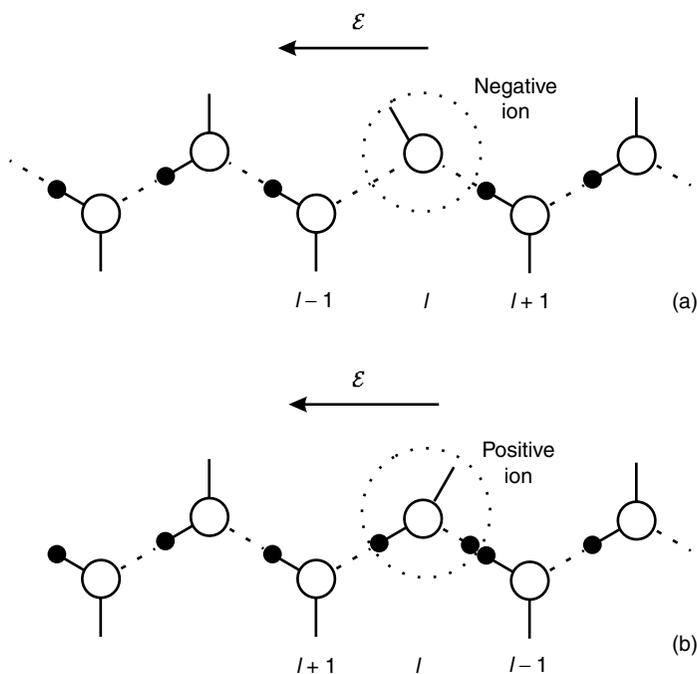
Figure 9. (a) Ionic state $(-)$ moves to the right; this corresponds to the motion of the chain protons to the left. (b) Ionic state $(+)$ moves to the left; this corresponds to the movement of chain protons to the left, too.

initial polarization of the A—H$\cdots$A complex broken in the neighborhood of the ion recovers both under the influence of the large total polarization of other ordered chain links and under the influence of the field itself. The fact that the total polarization of the ordered chains is large in the electric field is a consequence of the strong polarizability of hydrogen bonds. The latter, if we neglect the coupling of separate O—H$\cdots$O complexes, was shown in earlier works by Zundel and collaborators [169,170]. They demonstrated that in field $\mathscr{E} = 10^7$ to 10^8 V/m the strong hydrogen bond polarizability is of the order of 10^{-28} m^3. This value exceeds the polarizability of the isolated $(H_3O)^+$ ion and water molecules by 10^2 times.

Thus in view of the aforementioned reasons, for times $t \geq \tau_0$ we can ignore the local changes of the chain polarization while an ionic state moves along it, and imagine the latter as is shown in Fig. 9.

In the small concentration of charge carriers the hydrogen-bonded chain Hamiltonian can be written as

$$H = H_0 + H_1 + H_{\text{tun}} \tag{200}$$

$$H_0 = \sum_l E \hat{a}_l^+ \hat{a}_l + \sum_q \hbar\omega_0(q)\left(\hat{b}_q^+ \hat{b}_q + \frac{1}{2}\right)$$

$$- \sum_{l,q} \hbar\omega_0(q)\hat{a}_l^+ \hat{a}_l[u_l(q)\hat{b}_q^+ + u_l^*(q)\hat{b}_q] \tag{201}$$

$$H_{\text{tun}} = \sum_{l,m} J(R_m)\hat{a}_{l+m}^+ \hat{a}_l \tag{202}$$

where E is the quasi-particle energy in the site; $\hat{a}_l^+ (\hat{a}_l)$ is the charge carrier creation (annihilation) Fermi operator in the lth site; $\hat{b}_q^+ (\hat{b}_q)$ is the optical phonon creation (annihilation) Bose operator with momentum q and frequency $\omega_0(q)$; the tunneling Hamiltonian operator (202) is taken as perturbance; $J(R_m)$ is the wave-function overlap integral of charge carriers responsible for the carrier intersite hopping;

$$u_l(q) = N^{-1/2} e^{iqR_l}[u_1 e^{-iqg} + u_0 + u_2 e^{iqg}]$$

is a dimensionless quantity characterizing the displacement of protons in the nearest-neighbor $(l-1)$th and $(l+1)$th sites (as well as that of the lth site, in the case when the carrier is an excess proton) due to polarization of carrier interaction with the proton vibrations on the hydrogen bonds to the left (to the right) of it; u_0 is a constant responsible for the carrier interaction with the lth site proton (in case when the charge carrier is a proton hole, then $u_0 \equiv 0$); g is the chain constant; $R_l = lg$, where l is the site index; and N is the number of chain sites.

The operator H_2 introduced in expression (200) corresponds to a possible optical and acoustical phonon interaction in the chain (this is because AH groups of which the chain is constructed would be treated as external, and then the entire compound governs the behavior of the A atoms embedded in the chain; see also the next subsection). In the adiabatic approximation, it is expressed in the following way:

$$H_2 = \sum_k \hbar\omega_{\text{ac}}(k)\left(\hat{B}_k^+ \hat{B}_k + \frac{1}{2}\right)$$

$$+ \hbar\chi \sum_{l;k,q} n_l[u_l(q)\hat{b}_q^+ + u_l^*(q)\hat{b}_q][v_l(k)\hat{B}_k^+ + v_l^*(k)\hat{B}_k] \tag{203}$$

where the second term describes the reverse influence of displaced protons ($u_l(q)$ value) of the $(l-1)$th and $(l+1)$th sites upon the ion located in the lth site which has induced these displacements. The interaction results in the attraction of the ion itself to the $(l+1)$th site proton (Fig. 9). In expression (203), $\hat{B}_k^+ (\hat{B}_k)$ stands for an acoustical phonon creation (annihilation) Bose operator with momentum k and frequency $\omega_{ac}(k)$; $\upsilon_l(k)$ is the dimensionless site vibration amplitude; χ is the constant of possible interaction of acoustic and optical phonons with charged fault (in s^{-1}); and $n_l = \langle \hat{a}_l^+ \hat{a}_l \rangle$ is the number of carriers in the chain (below we put $\langle n_l \rangle = n = $ const).

The Hamiltonian (203) is diagonalized in the operators $\hat{b}_q$, $\hat{B}_k$ by the Bogolyubov–Tyablikov canonical transformation [171,172]. The diagonalization results are (see Appendix C)

$$H = \tilde{H}_0 + H_{tun} \tag{204}$$

$$\tilde{H}_0 = \sum_l E\hat{a}_l^+ \hat{a}_l + \sum_{l=1}^{2} \sum_q \hbar\Omega(q)\left(\hat{b}_l^+(q)\hat{b}_l(q) + \frac{1}{2}\right)$$

$$- \sum_{\alpha=1}^{2} \sum_{l;q} \hbar\Omega(q)\hat{a}_l^+ \hat{a}_l[\tilde{u}_{\alpha l}(q)\hat{b}_\alpha^+(q) + \tilde{u}_{\alpha l}^*(q)\hat{b}_\alpha(q)] \tag{205}$$

Here

$$\Omega_{1,2}(q) = \left\{ \frac{1}{2}(\omega_0^2(q) + \omega_{ac}^2(q)) \pm \frac{1}{2}\left[(\omega_0^2(q) - \omega_{ac}^2(q))^2 \right.\right.$$

$$\left.\left. + 4\chi^2 n^2 |u_q|^2 |\upsilon_q|^2 \omega_0^2(q)\omega_{ac}^2(q)\right]^{1/2} \right\}^{1/2} \tag{206}$$

$$\tilde{u}_{\alpha l}(q) = 2u_l(q) \begin{cases} \dfrac{\omega_0^2(q)}{\Omega_1(q)[\Omega_1(q) + \omega_0(q)]} & (\alpha = 1) \\[2mm] \dfrac{\Omega_2(q) - \omega_{ac}(q)}{\chi n |u_q||\upsilon_q|} & (\alpha = 2) \end{cases} \tag{207}$$

where u_q and υ_q are defined by $u_l(q)$ and $\upsilon_l(q)$, respectively, divided by $N^{-1/2}\exp(iqR_l)$.

Let us note that with the variation of χ from zero to the maximally permissible value $\chi_{max} = [\omega_0(q)\omega_{ac}(q)]^{1/2}/2n|u_q||\upsilon_q|$, the frequencies $\Omega_{1,2}(q)$ change within

$$\omega_0(q) < \Omega_1(q) < \sqrt{\omega_0^2(q) + \omega_{ac}^2(q)}, \qquad \omega_{ac}(q) > \Omega_2(q) > 0 \tag{208}$$

χ_{max} corresponds to $\Omega_2(q) = 0$.

In the Hamiltonian (205) the operator $\hat{b}_1^+(q)(\hat{b}_1(q))$ describes the creation the creation (annihilation) of an optical phonon with frequency $\Omega_1(q)$ and takes into account the polarizing influence of the charged fault on proton subsystem. The operator $\hat{b}_2^+(q)(\hat{b}_2(q))$ corresponds to creation (annihilation) of an acoustic phonon with frequency $\Omega_2(q)$ relative to new equilibrium site positions; in this case the renormalized acoustic phonons become also polarizational ones. This is taken into account in the last term of the Hamiltonian $\tilde{H}_0$ describing the ionic state interaction with the new optical and acoustical vibrations of the chain.

Let us now consider the proton current in the hydrogen-bonded chain studied. With the use of the unitary operator

$$S = \sum_{\alpha=1}^{2} \sum_{l;q} \hat{a}_l^+ \hat{a}_l [\tilde{u}_{\alpha l}(q)\hat{b}_\alpha^+(q) - \tilde{u}_{\alpha l}^*(q)\hat{b}_\alpha(q)] \qquad (209)$$

we perform the canonical transformation $\bar{H} = e^{-S}\tilde{H}e^{S}$, which is diagonalized with an accuracy to terms of fourth order in the Fermi operator:

$$\bar{H}_0 = \sum_l \bar{E}\hat{a}_l^+ \hat{a}_l + \sum_{\alpha=1}^{2} \sum_q \hbar\Omega_\alpha(q)\left[\hat{b}_\alpha^+(q)\hat{b}_\alpha(q) + \frac{1}{2}\right] \qquad (210)$$

where

$$\bar{E} = \bar{E}_l = E - \sum_{\alpha=1}^{2} \sum_q \Omega_\alpha(q)|\tilde{u}_{\alpha l}(q)|^2 \qquad (211)$$

(the second term on the right-hand side is the so-called polaron shift). The operator $\bar{H}_0$ is site-diagonal and characterizes stationary states of the system, and it resembles the small polaron Hamiltonian with allowance for $\bar{H}_1 = e^{-S}H_1 e^{S}$ (the Hamiltonian H_1 is assumed to be a perturbation). But, since $\bar{H}_0$ includes in addition to polarizational also optical renormalized phonons, operator (204)—or, more exactly $\bar{H}_0 + \bar{H}_1$—would be more properly called Hamiltonian for a polaron–condenson whose binding energy is defined by (211).

Let us calculate the proton current density of I due to hopping (at room temperature). On calculating I, we apply the method based on the usage of the statistical operator, proposed earlier by Hattori [173] for another type of systems. Setting $J(R_m) \ll k_B T$ where $k_B T \approx 300$ K, with accuracy to terms of order $J^2(R_m)$ we have for the current density

$$I = \mathrm{Tr}(\rho_\mathscr{E} j) \qquad (212)$$

The current density operator is

$$j_{\mathscr{E}} = \frac{e}{\mathscr{V} i\hbar} \left[\sum_l R_l \hat{a}_l^+ a_l, H_1 \right] = \frac{e}{i\hbar} \sum_{l,m} J(R_m)(R_{l+m} - R_l) \hat{a}_{l+m}^+ a_l \qquad (213)$$

where $\mathscr{V}$ is an effective volume occupied by a carrier in the chain and the operator $\rho_{\mathscr{E}}$ is the density matrix (or statistical operator) correction due to the interaction with the external field $\mathscr{E}$:

$$\rho_{\mathscr{E}} = -\frac{i}{\hbar} \int_{-\infty}^t d\tau \, \exp\left[-\frac{i}{\hbar}(t - \tau)(H + H_{\mathscr{E}}) \right] [H_{\mathscr{E}}, \rho_1]$$

$$\times \exp\left[\frac{i}{\hbar}(t - \tau)(H + H_{\mathscr{E}}) \right] \qquad (214)$$

Here the field Hamiltonian is

$$H_{\mathscr{E}} = -e\mathscr{E} \sum_l R_l \hat{a}_l^+ \hat{a}_l \qquad (215)$$

and the correction to the statistical operator is

$$\rho_1 = -\frac{e^{-\tilde{H}_0/k_B T}}{\mathrm{Tr} e^{-\tilde{H}_0/k_B T}} \int_0^{1/k_B T} d\lambda e^{\lambda \tilde{H}_0} H_{\mathrm{tun}} e^{-\lambda \tilde{H}_0} \qquad (216)$$

Expression (212) is reduced to

$$I = \frac{\mathscr{E}}{\mathscr{V} \, \mathrm{Tr} e^{-\tilde{H}_0/k_B T}} \int_0^\infty d\tau \int_0^{1/k_B T} d\lambda \mathrm{Tr}\{ e^{-\tilde{H}_0/k_B T} e^{\tilde{H}_0 \lambda} j(-\tau) e^{-\tilde{H}_0 \lambda} j \} \qquad (217)$$

$$j(-\tau) = \exp\left[-\frac{i}{\hbar} \tau(\tilde{H}_0 + H_{\mathscr{E}}) \right] j \exp\left[\frac{i}{\hbar} \tau(\tilde{H}_0 + H_{\mathscr{E}}) \right] \qquad (218)$$

Using the invariability of the trace, we perform the canonical transformation in expression (217) by means of quantum mechanical thermal averaging over Fermi operators with an accuracy to terms linear in the carrier concentration, and then averaging over the phonon bath, we obtain [165]

$$I = \mathscr{E} e^2 g^2 J^2 n h^{-2} \int_0^\infty d\tau \int_0^{1/k_B T} d\lambda \exp\left(\frac{i}{\hbar} \tau e \mathscr{E} g \right) \exp\left(-2 \sum_l S_{T,\alpha} \right)$$

$$\times \left\{ \exp \sum_{\alpha;q} |\Delta^{(\alpha)}(q)|^2 \operatorname{cosech} \frac{\hbar \Omega_\alpha(q)}{2k_B T} \cos\left[\left(\tau - \frac{i\hbar}{2k_B T} + i\hbar\lambda \right) \Omega_\alpha(q) \right] \right\}$$

$$(219)$$

where the constant of charge carrier (i.e., proton) coupling with optical ($\alpha = 1$) and acoustical ($\alpha = 2$) phonons is

$$S_{T,\alpha} = \frac{1}{2} \sum_q |\Delta^{(\alpha)}(q)|^2 \coth \frac{\hbar \Omega_\alpha(q)}{2k_B T} \tag{220}$$

$$|\Delta^{(\alpha)}(q)|^2 = 4|u_q|^2 \frac{2}{N} (1 - \cos qg) \begin{cases} \dfrac{\omega_0^4(q)}{\Omega_1^2(q)[\Omega_1(q) + \omega_0(q)]^2} & (\alpha = 1) \\[4mm] \dfrac{[\Omega_2(q) - \omega_{ac}(q)]^2}{\chi^2 n^2 |u_q|^2 |v_q|^2} & (\alpha = 2) \end{cases} \tag{221}$$

In view of the comparatively large mass, a proton drifting along the hydrogen-bonded system resembles a classical particle; therefore in order to obtain expression (219), we have performed the following simplifications. The assumption mentioned above is that the overlap integral is $J(R_m) \ll k_B T$, and for $\delta E = E - \bar{E} > \hbar \Omega_1(q) \geq \hbar \omega_0(q) \sim k_B T$ the inequality $J(R_m) \ll \delta E$ is valid. This shows that on drifting along the chain a proton hops only to neighboring sites. Under these conditions the overlap integral is nonzero only between nearest neighbors, $J(g) = J = $ const. Besides, in expression (217) after averaging over Fermi operators, terms with $R_{l+m} - R_l = g$ are nonzero in the sums over l and m. Let us also note that the assumed condition $J \ll k_B T$ enables us to take into account the field $\mathscr{E}$ to practically any order in expressions (217) and (219).

In the small polaron theory the coupling constant S_T is much greater than 1, which allows the calculation of integrals in expression (219) [165]

$$I = 2^{3/2} \pi^{1/2} egn J^2 \hbar^{-2} e^{-\frac{E_a}{k_B T}} \left[\sum_{\alpha;q} |\Delta^{(\alpha)}(q)|^2 \Omega_l^2(q) \, \text{cosech} \frac{\hbar \Omega_\alpha(q)}{2k_B T} \right]^{-1/2}$$

$$\times \sinh \frac{eg\mathscr{E}}{2k_B T} \exp\left(-\frac{(eg\mathscr{E})^2}{\sum_{\alpha;q} |\Delta^{(\alpha)}(q)|^2 \hbar^2 \Omega_l^2(q) \, \text{cosech} \frac{\hbar \Omega_\alpha(q)}{2k_B T}} \right) \tag{222}$$

where n is the polaron concentration and the activation energy of polaron hops is

$$E_a = \frac{1}{k_B T} \sum_{\alpha;q} |\Delta^{(\alpha)}(q)|^2 \tanh \frac{\hbar \Omega_\alpha(q)}{4k_B T} \tag{223}$$

An analysis conducted in Ref. 165 has shown that the phonon–phonon interaction that is described by the constant χ does not virtually influence $S_{T,1}$. However, the interaction leads to a considerable coupling of a polaron with

acoustic phonons, and therefore the value of $S_{T,2}$ is able to reach $S_{T,1}$ (in the case when the concentration of protons is not very small).

A hydrogen-bonded chain with no temperature-activated free charge carriers is a dielectric. But charge carriers can be injected by the external electric field. Such a situation corresponds to the case of space-charge-limited proton current. A number of materials, including ice crystals—that is, a system with a hydrogen-bonded network—exhibit stationary proton injection currents [174]. Thus the space-charge-limited proton current can be found in hydrogen-bonded chains. To calculate the current, we start from the following equations [175]:

$$I = en\mu(\mathscr{E})\mathscr{E} \tag{224}$$

$$\frac{d\mathscr{E}}{dx} = \frac{en}{\varepsilon_0\varepsilon} \tag{225}$$

where $\mu(\mathscr{E})$ is the carrier mobility, ε is dielectric constant of the system studied, and ε_0 is the dielectric constant of free space. In Eqs. (224) and (225) we usually ignore the diffusion current, because the connection of the current with the local field is the same as that with the field average.

Let us calculate the space-charge-limited density of proton current $I \cdot \mu(\mathscr{E})$ needed for this purpose is obtained from the right-hand side of formula (222) divided by $en\mathscr{E}$. Putting en from Eq. (224) into Eq. (225), we arrive at the differential equation

$$\mu(\mathscr{E}')\mathscr{E}'\,d\mathscr{E}' = \frac{I}{\varepsilon_0\varepsilon}\,dx \tag{226}$$

Here $0 \le \mathscr{E}' \le \mathscr{E}$, where $\mathscr{E}$ is the applied field; $0 \le x \le L$, where L is the screening length of the charge in the chain. The solution to Eq. (226) with account for expression (223) is [165]

$$
\begin{aligned}
I = {} & \frac{2^{5/2}\pi^{1/2}\varepsilon_0}{\hbar^2 e}\frac{\varepsilon k_B T J^2}{L}\left(\cosh\frac{e\mathscr{E}g}{2k_B T} - 1\right) \\
& \times \frac{\exp(-E_a/k_B T)}{\left[\sum_{\alpha;q}|\Delta^{(\alpha)}(q)|^2\Omega_\alpha^2(q)\,\mathrm{cosech}\frac{\hbar\Omega_\alpha(q)}{2k_B T}\right]^{1/2}}
\end{aligned}
\tag{227}
$$

The electrical conductivity σ is easy defined by expression (217) or (221) for I because, by definition, $I = \sigma(\mathscr{E})\mathscr{E}$.

Experimental values of conductivity σ_c at room temperature in the $Li(N_2H_5)SO_4$ and $(NH_4)_3H(SO_4)_2$ crystals (i.e., conductivity along hydrogen-bonded chains) are equal to $0.23 \times 10^{-8}\ \Omega^{-1}\,cm^{-1}$ [29] and $5 \times 10^{-8}\ \Omega^{-1}\,cm^{-1}$ [30], respectively. Choosing reasonable values of three major parameters J, S_T,

and Ω, we obtain [165] the same values of σ by derived expressions (223) and (227). Moreover, expressions (223) and (227) correlate well with the measured proton conductivity of proton-conducting membrane proteins (see Refs. 33 and 34).

E.   The Anharmonicity Influence

In complex compounds including proton-conducting proteins the hydrogen-bonded chain is formed by means of AH groups, the position of which is rather rigidly fixed by the side chemical bonds. Therefore the distances between the sites (AH groups) and, thus, the chain rigidity appear to be functions of external parameters—that is, thermostat functions. In other words, if we neglect a comparatively weak influence of the light H atoms upon the vibrations of A atoms, then the A atom participation in acoustic vibrations of the molecular chain will be entirely environmental, with A atoms being rigidly connected to the environment by the side chemical bonds. Therefore, these acoustic vibrations appear to be external with respect to the chain. Owing to this fact, a bilinear connection of the acoustic vibrations with the longitudinal optical polarizational phonons (the chain proton vibrations on the hydrogen bonds) responsible for the proton formation appears. On calculating the proton conductivity, all these peculiarities of a hydrogen-bonded chain have been taken into account.

Apart from the bilinear connection between acoustic and optical vibrations, the usual phonon anharmonicity takes place in the chain. The acoustic vibrations modulate the distances between A atoms and thus influence the frequency of proton vibrations on hydrogen bonds. The proton vibration frequency can be presented as

$$\omega(q) \to \omega_q + \frac{\partial \omega}{\partial U_q(r)} \delta U_q(r) \tag{228}$$

where $U_q(r)$ is the coordinate of the normal acoustic vibrations of the chain. The calculation of the second member in expression (228) results in an addendum of the type

$$H' = \sum_q (\kappa_q \hat{B}_q^+ + \kappa_q^* \hat{B}_q) \hat{b}_q^+ \hat{b}_q \tag{229}$$

appearing in the Hamiltonian that describes the motion of an excess proton (or proton hole) along a hydrogen-bonded chain; here κ_q is the anharmonicity constant, $\hat{B}_q^+(\hat{B}_q)$ is the acoustic phonon creation (annihilation) operator, and $\hat{b}_q^+(\hat{b}_q)$ is the analogous optical phonon operator.

In Ref. 176 the estimation of anharmonicity on the proton conductivity, neglecting the bilinear phonon–phonon interaction, has been calculated. The proton current density is obtained from expression (219); in this formula we

should now formally put $\nu \to 1$, $|\Delta^{(\nu)}(q)| \to |\Delta_q|$, $S_{T1} \to S_T$, and $\Omega_1(q) \to \omega_q$ $[1 + (\kappa_q \hat{B}_q^+ + \kappa_q^* \hat{B}_q)]$, and the thermal averaging after Gibbs should be additionally performed:

$$\frac{e^{-\frac{1}{k_{\mathrm{B}}T} \sum_q \hbar\Omega_q \left(\hat{B}_q^+ \hat{B}_q + \frac{1}{2}\right)}}{\mathrm{Tr}\, e^{-\frac{1}{k_{\mathrm{B}}T} \sum_q \hbar\Omega_q \left(\hat{B}_q^+ \hat{B}_q + \frac{1}{2}\right)}} \tag{230}$$

where $\hbar\Omega_q$ is the energy of the thermal vibration quantum—that is, the lattice acoustic phonon energy. As a result, we gain

$$I = 2^{3/2}\pi^{1/2}\hbar^{-2} engJ^2 \sinh\frac{e\mathscr{E}g}{2k_{\mathrm{B}}T}$$

$$\times\, e^{-E_{\mathrm{a}}/k_{\mathrm{B}}T}\left[\sum_q |\Delta(q)|^2 \omega_q^2 \mathrm{cosech}\frac{\hbar\omega_q}{2k_{\mathrm{B}}T}\right]^{-1/2}$$

$$\times \exp\left\{\sum_q |\kappa_q|^2 |\Delta_q|^2 \left(\frac{\hbar\omega_q}{2k_{\mathrm{B}}T}\right)^2 \mathrm{cosech}^4\frac{\hbar\omega_q}{2k_{\mathrm{B}}T}\right.$$

$$\left.\times \left(1 - \mathrm{cosech}\frac{\hbar\omega_q}{2k_{\mathrm{B}}T}\right)^2 \coth\frac{\hbar\Omega_q}{2k_{\mathrm{B}}T}\right\} \tag{231}$$

Expression (231) is correct at $\mathscr{E} < 10^8$ V/m and $|\kappa_q| \ll 1$. Setting $\kappa_q = 0$, we arrive at the current density derived in the pure small polaron theory [88].

If we put $|\kappa_q| = 0.1$, $|\Delta_q| = 20\text{–}30$, and $\omega_q = 2\pi \cdot 6 \times 10^{12}$ s^{-1} and T is around room temperature, we can estimate the last term exponential factor in expression (231) by

$$\exp\left\{\alpha \coth\frac{\hbar\Omega}{2k_{\mathrm{B}}T}\right\} \tag{232}$$

where α varies from 10^{-3} to 10^{-2} and Ω is a typical frequency of the acoustic phonons conditioning the anharmonicity. Since the charge carriers (protons or proton holes) in a hydrogen-bonded chain should be described by strongly localized functions (see also Kittel [177]), they should also interact with the shortest wave vibrations. Let us take as the Debye value $\Omega_{\mathrm{Debye}} = (1 \text{ to } 5)\times 10^{12}$ s^{-1}, then we can assume that $\Omega = (0.01 \text{ to } 0.1)\Omega_{\mathrm{Debye}}$. Substituting these values into expression (232), we get a rough estimation of the last exponential factor in I (231): $e^{0.2}$ to e^1.

Thus, the adduced estimation shows that under the indicated values of parameters the anharmonicity can appreciably influence the proton current in compounds with hydrogen-bonded chains.

F. Influence of Coulomb Correlations and the Electric Field Local Heterogeneities on Proton Conductivity

Nonlinear transfer and transport phenomena in hydrogen-bonded chains can be caused not only by a strong coupling of moving protons with the chain sites, but also by the relative large concentration of charge carriers in the chain. The model proton polaron Hamiltonian, which takes into account proton–proton correlation in the chain, can be written as [178]

$$H = H_0 + H_{\text{tun}} \tag{233}$$

$$H_0 = \sum_l E\hat{a}_l^+ \hat{a}_l + \sum_q \hbar\omega_q \left(\hat{b}_q^+ \hat{b}_q + \frac{1}{2} \right)$$

$$- \sum_q \hbar\omega_q \hat{a}_l^+ \hat{a}_l [u_l(q)\hat{b}_q^+ + u_l^*(q)\hat{b}_q] + \sum_{l,m} U_{lm}\hat{a}_l^+ \hat{a}_l \hat{a}_m^+ \hat{a}_m \tag{234}$$

$$H_{\text{tun}} = \sum_l J(mg)\hat{a}_{l+m}^+ \hat{a}_l + h.c. \tag{235}$$

Here once again $\hat{a}_l^+ (\hat{a}_l)$ is the Fermi operator of charge carrier creation (annihilation) in the lth site, E is the quasi-particle (i.e., polaron) energy in the site, $\hat{b}_q^+ (\hat{b}_q)$ is the optical phonon creation (annihilation) Bose operator with the momentum q and the frequency ω_q, U_{lm} is the energy of the Coulomb repulsion among the carriers sitting in the l and m sites, operator (235) is the tunnel Hamiltonian assumed to be perturbation, $J(mg)$ is the resonance overlap integral, $u_l(q)$ is the dimensionless value characterizing the displacement of protons in the $(l-1)$th and $(l+1)$th sites by the carrier located in the lth site, and $R_l = lg$, where l is the site ordinal index and g is the chain constant.

It should be noted that the Coulomb correlations among the carriers on one site should have been taken into account in the Hamiltonian H in the general case, yet we assume that the energy of such interaction is too large and thus the Hamiltonian in Eqs. (233)–(235) describes the carrier migration along the lower Hubbard band (about Hubbard correlations see, e.g., Ref. 173).

To derive the current density, we apply the method employed in the previous subsection. Thus we proceed from the formula [cf. with Eq. (212)]

$$I = \text{Tr}(\rho_{\text{tot}} j) \simeq \text{Tr}(\rho_{\mathscr{E}} j) \tag{236}$$

where ρ_{tot} is the system total statistical operator and j is the operator of current density. The operator ρ_{tot} satisfies the equation of motion

$$i\hbar \frac{\partial \rho_{\text{tot}}}{\partial t} = i\hbar \frac{\partial \rho_{\mathscr{E}}}{\partial t} = [H_{\text{tot}}, \rho] \tag{237}$$

where

$$H_{\text{tot}} = H + H_{\mathscr{E}}, \qquad H_{\mathscr{E}} = H_{\mathscr{E}}^{(0)} + H_{\mathscr{E}}^{(1)} \tag{238}$$

$$\rho_{\text{tot}} = \rho + \rho_{\mathscr{E}} \tag{239}$$

Here the operator $H_{\mathscr{E}}$ describes the interaction with the field $\mathscr{E}$ and

$$H_{\mathscr{E}}^{(0)} = -e\mathscr{E} \sum_l R_l \hat{a}_l^+ \hat{a}_l$$

$$H_{\mathscr{E}}^{(1)} = -e\mathscr{E} \sum_{l,m} \mathscr{L}(mg) \hat{a}_{l+m}^+ \hat{a}_l \tag{240}$$

$\rho \simeq$ const is the statistical operator of the system studied, when the field is absent, in linear approximation $\rho = \rho_0 + \rho_1$:

$$\rho_0 = \frac{e^{-H_0/k_{\text{B}}T}}{\text{Tr}\, e^{-H_0/k_{\text{B}}T}} \tag{241}$$

$$\rho_1 = -\frac{e^{-H_0/k_{\text{B}}T}}{\text{Tr}\, e^{-H_0/k_{\text{B}}T}} \int_0^{1/k_{\text{B}}T} d\lambda e^{\lambda H_0} H_{\text{tun}} e^{-\lambda H_0} \tag{242}$$

$\rho_{\mathscr{E}}$ is the correlation to ρ due to the interaction $H_{\mathscr{E}}$ [$\rho_{\mathscr{E}}$ is directly derived from Eq. (237)]:

$$\rho_{\mathscr{E}} = -\frac{i}{\hbar} \int_{-\infty}^t d\tau e^{-i\frac{t-\tau}{\hbar}H_{\text{tot}}} [H_{\mathscr{E}}, \rho] e^{i\frac{t-\tau}{\hbar}H_{\text{tot}}} \tag{243}$$

In the case where hopping motion is involved, the density operator j is written as

$$j = \frac{e}{\mathscr{V} i\hbar} [H_{\text{tun}}, \Re] \tag{244}$$

where $\mathscr{V}$ is an effective volume occupied by a carrier in the chain and (in the general case) the coordinate operator is expressed as

$$\Re = \sum_l R_l \hat{a}_l^+ \hat{a}_l + \sum_{l,m} \mathscr{L}(mg) \hat{a}_{l+m}^+ \hat{a}_l \tag{245}$$

It should be noted that in expression (245) and, therefore, in expressions (240) we have neglected the coordinate dependence of the phonon subsystem (i.e., indirect transitions have been dropped). Then, with allowance for expressions (235) and

(245) we obtain the following from commutation (244) for j:

$$j = j^{(0)} + j^{(1)} \tag{246}$$

$$j^{(0)} = \frac{e}{\mathcal{V} i \hbar} \sum_{l,m} J(mg)(R_{l+m} - R_l) \hat{a}_{l+m}^+ \hat{a}_l \tag{247}$$

$$j^{(1)} = \frac{e}{\mathcal{V} i \hbar} \sum_{l,m,n} [J(ng)\mathcal{L}((m-n)g) - J((m-n)g)\mathcal{L}(ng)] \hat{a}_{l+m}^+ \hat{a}_l \tag{248}$$

In the Hamiltonian H_{tot} contained in expression (243), we neglect the operator H_1; such an approximation corresponds to the calculation of I with the accuracy of $J^2(g)$. Besides, in H_{tot} in expression (243) the operator $H_{\mathcal{E}}^{(1)}$ can also be neglected; in this case the criterion that it be small can be derived as follows. Let us formally expand in expression (243) $\exp[\pm i(t-\tau)(H_0 + H_{\mathcal{E}}^{(0)} + H_{\mathcal{E}}^{(1)})/\hbar]$ in a series in the operator $H_{\mathcal{E}}^{(1)}$ with restriction to the first members of the expansion. Then the corrections proportional to $J^2(mg)e\mathcal{E}\mathcal{L}(g)$ will appear in the current density. Hence as we neglect the members proportional to $J^3(g)$, acquire the following restriction on the parameters of the operator $H_{\mathcal{E}}^{(1)}$:

$$e\mathcal{E}\mathcal{L}(g) \leq J(g) \tag{249}$$

Note that the function $\mathcal{L}(g)$ characterizes the site neighborhood in which the meaning of the electric field is different from the applied field $\mathcal{E}$; that is, just $\mathcal{L}(g)$ is responsible for the electric field local heterogeneity.

With allowance for the above-mentioned facts, the current density I can be presented as the sum of three terms:

$$I = I_0 + I_1 + I_2 \tag{250}$$

where

$$I_0 = \text{Tr}(\rho_{\mathcal{E}}^{(0)} j^{(0)}) \tag{251}$$

$$I_1 = \text{Tr}(\rho_{\mathcal{E}}^{(1)} j^{(0)}) \tag{252}$$

$$I_2 = \text{Tr}(\rho_{\mathcal{E}}^{(0)} j^{(1)}) \tag{253}$$

$$\rho_{\mathcal{E}}^{(0,1)} = -\frac{i}{\hbar} \int_{-\infty}^{t} d\tau e^{-i\frac{t-\tau}{\hbar}(H_0 + H_{\mathcal{E}}^{(0)})} [H_{\mathcal{E}}^{(0,1)}, \rho_{(1,0)}] e^{i\frac{t-\tau}{\hbar}(H_0 + H_{\mathcal{E}}^{(0)})} \tag{254}$$

By means of the unitary operator

$$S = \sum_{l;q} \hat{a}_l^+ \hat{a}_l [u_l(q)\hat{b}_q^+ - u_l^*(q)\hat{b}_q] \tag{255}$$

we perform the canonical transformation $\bar{H}_0 = e^{-S}H_0 e^S$, diagonalizing the Hamiltonian with respect to the phonon variables

$$\bar{H}_0 = \sum_l \bar{E}\hat{a}_l^+\hat{a}_l + \sum_q \hbar\omega_q\left(\hat{b}_q^+\hat{b}_q + \frac{1}{2}\right) + \sum_{l,m} \bar{U}_{lm}\hat{a}_l^+\hat{a}_l\hat{a}_m^+\hat{a}_m \qquad (256)$$

Here $\bar{E}$ is the carrier coupling energy on the site including the polaron shift, and $\tilde{U}_{lm}$ is the energy including not only the Coulomb correlations but also the correlations according for phonon exchange,

$$\bar{E} = E_l = E - \sum_q \hbar\omega_q|u_l(q)|^2 \qquad (257)$$

$$\bar{U}_{lm} = \bar{U}_{ml} = U_{lm} - \sum_q \hbar\omega_q\mathrm{Re}[u_l(q)u_l^*(q)] \qquad (258)$$

According to expressions (227) and (254), we get for the current density I_0 [178]

$$I_0 = \frac{\mathscr{E}}{\mathscr{V}\,\mathrm{Tr}\,e^{-H_0/k_\mathrm{B}T}}\mathrm{Tr}\left\{e^{-H_0/k_\mathrm{B}T}\int_0^\infty d\tau e^{-i\frac{\tau}{\hbar}(H_0+H_\mathscr{E}^{(0)})}\right.$$
$$\left.\times \int_0^{1/k_\mathrm{B}T} d\lambda e^{\lambda H_0}j^{(0)}e^{-\lambda H_0}e^{-i\frac{\tau}{\hbar}(H_0+H_\mathscr{E}^{(0)})}j^{(0)}\right\} \qquad (259)$$

Calculating the integrals and performing thermal averaging over the phonon subsystem in expression (259), we obtain [178]

$$I_0 \simeq 2^{3/2}\pi^{1/2}\hbar^{-2}ngJ^2\sinh\frac{e\mathscr{E}g}{2k_\mathrm{B}T}$$
$$\times e^{-E_\mathrm{a}/k_\mathrm{B}T}\left[\sum_q |\Delta(q)|^2\omega_q^2\,\mathrm{cosech}\,\frac{\hbar\omega_q}{2k_\mathrm{B}T}\right]^{-1/2}$$
$$\times e^{\bar{U}/2k_\mathrm{B}T}\exp\left(-\frac{(eg\mathscr{E}-\bar{U})^2}{2\sum_q|\Delta(q)|^2\hbar^2\omega_q^2\,\mathrm{cosech}\,\frac{\hbar\omega_q}{2k_\mathrm{B}T}}\right) \qquad (260)$$

Here n is concentration of polarons and E_a is the activation energy [see expression (223)].

Making use of the explicit form of the commutator $[H_\mathscr{E}^{(1)}, \rho_0]$, we gain for the current density I_1 instead of (252) and (254)

$$I_1 = -\frac{i}{\hbar}\int_{-\infty}^0 d\tau \frac{1}{\mathscr{V}\,\mathrm{Tr}e^{-H_0/k_\mathrm{B}T}}\mathrm{Tr}\left\{e^{i\frac{\tau}{\hbar}(H_0+H_\mathscr{E}^{(0)})}\right.$$
$$\left.\times\left[-e\mathscr{E}\sum_{l,m}\mathscr{L}(mg)\hat{a}_{l+m}^+\hat{a}_l, e^{-H_0/k_\mathrm{B}T}\right]e^{-i\frac{\tau}{\hbar}(H_0+H_\mathscr{E}^{(0)})}j^{(0)}\right\} \qquad (261)$$

The calculation of the right-hand side of (261) is analogous to that in the case of I_0. The final expression is [178]

$$I_1 \simeq \sqrt{2\pi}\hbar^{-2}ne\mathscr{E}\mathscr{L}gJe^{-E_a/k_BT}\left[\sum_q |\Delta(q)|^2\omega_q^2 \operatorname{cosech} \frac{\hbar\omega_q}{2k_BT}\right]^{-1/2}$$

$$\times e^{\bar{U}/k_BT}(1 - e^{(3\bar{U}-e\mathscr{E}g)/2k_BT})\exp\left(-\frac{(eg\mathscr{E}-\bar{U})^2}{2\sum_q|\Delta(q)|^2\hbar^2\omega_q^2 \operatorname{cosech} \frac{\hbar\omega_q}{2k_BT}}\right) \quad (262)$$

Since the theory, which is developing, is applied to strongly localized heavy charge carriers (i.e., protons), we have performed the calculations in the limiting transition $l \to 1$, reflecting the fact that protons hop only to nearest sites. In this approximation, the contribution of I_2 to the total current density can be neglected [178]. Thus, the total current is

$$I_{tot} = I_0 + I_1 \quad (263)$$

where I_0 and I_1 are given by expressions (260) and (262), respectively.

Let us calculate the space-charge-limited density of proton current (263). In this case the polaron potential energy changes from site to site within the chain and, being due to the field, remains smaller than the value of the Coulomb repulsion between the carriers, U (the latter obstructs the filling of a chain by carriers by definition). The value of the Coulomb correlation energy is limited by the inequalities $J \ll \bar{U} < E - \bar{E}$, where $J \ll k_BT$ and the polaron shift energy $E - \bar{E}$ can be approximately identical to the fault (ionic state) activation energy within a chain, its value being of the order of 10–$15\,k_BT$ [29,158,160]. Since $\mathscr{L}$ describes the neighborhood into which the carrier arrives after its hopping from the nearest neighbor at distances between the sites smaller than g, the inequality

$$e\mathscr{E}g < \bar{U} \quad (264)$$

should be considered as the criterion of validity of the small carrier concentration approximation. At such values of the field $\mathscr{E}$ the contribution of Coulomb correlations to the Hamiltonian (229) may be dropped [formally it corresponds to $\bar{U} = 0$ in expressions for current (260) and (262)].

To derive the space-charge-limited density of proton current that takes into account the local heterogeneities, which is given by the parameter $\mathscr{L}$, we proceed from Eq. (225) and the equation

$$I = I_0 + I_1 = en[\mu_0(\mathscr{E}) + \mu_1(\mathscr{E})]\mathscr{E} \quad (265)$$

where $\mu_0(\mathscr{E})$ is the carrier mobility without allowance for local changes of the field; $\mu_1(\mathscr{E})$ is a correction to $\mu_0(\mathscr{E})$ with allowance for local changes of the field. With $\mathscr{E} \leq 10^8$ V/cm the mobilities are [178]

$$\mu_0(\mathscr{E}) = 2J\mathscr{E}^{-1}\sinh(e\mathscr{E}g/2k_{\mathrm{B}}T)M \tag{266}$$

$$\mu_1(\mathscr{E}) = e\mathscr{L}\exp(-e\mathscr{E}g/2k_{\mathrm{B}}T)[1 - \exp(-e\mathscr{E}g/k_{\mathrm{B}}T)]M \tag{267}$$

where

$$M = \sqrt{2\pi}\hbar^{-2}gJ\exp(-E_{\mathrm{a}}/k_{\mathrm{B}}T)\left[\sum_q |\Delta(q)|^2\omega_q^2\operatorname{cosech}\frac{\hbar\omega_q}{2k_{\mathrm{B}}T}\right]^{-1/2} \tag{268}$$

Solving equations (225) and (265), we derive the needed current density. It is convenient to write the solution in terms of the effective electroconductivity

$$\sigma(\mathscr{E}) = \sigma_0(\mathscr{E}) + \sigma_1(\mathscr{E})$$

$$= \frac{2^{5/2}\pi^{1/2}\varepsilon_0\varepsilon k_{\mathrm{B}}T}{\hbar^2 eL}\frac{\exp(-E_{\mathrm{a}}/k_{\mathrm{B}}T)}{\left[\sum_q |\Delta(q)|^2\omega_q^2\operatorname{cosech}\frac{\hbar\omega_q}{2k_{\mathrm{B}}T}\right]^{1/2}}$$

$$\times \left(\frac{\cosh(e\mathscr{E}g/2k_{\mathrm{B}}T)}{\mathscr{E}} + \frac{k_{\mathrm{B}}T}{J}\frac{\mathscr{L}}{g}F(\mathscr{E})\right) \tag{269}$$

where

$$F(\mathscr{E}) = 1 - \left(1 + \frac{e\mathscr{E}g}{2k_{\mathrm{B}}T}\right)e^{-\frac{e\mathscr{E}g}{2k_{\mathrm{B}}T}} - \frac{1}{9}\left[1 - \left(1 + \frac{3e\mathscr{E}g}{2k_{\mathrm{B}}T}\right)e^{-\frac{3e\mathscr{E}g}{2k_{\mathrm{B}}T}}\right] \tag{270}$$

An analysis of the results obtained shows [178] that the correction $\sigma_1(\mathscr{E})$ in (269) reaches the value of $\sigma_0(\mathscr{E})$ at the field $\mathscr{E} > 10^6$ V/m and at the ratio $\mathscr{L}/g = 0.001$ to 0.05.

Thus, considering the transport phenomenon in a hydrogen-bonded chain in an electric field $\mathscr{E} > 10^6$ V/m, the calculation of the local field changes from the value of the applied field becomes essential if $\mathscr{L}/g \geq 0.01$ (however, $\mathscr{L}/g \ll 1$). The Coulomb correlations must be accounted for at large values of the field, but are not likely to considerably change the general trend of the curve $\sigma(\mathscr{E})$, yet influence quantitative estimates of the values $\sigma_0(\mathscr{E})$ and $\sigma_1(\mathscr{E})$.

G.   External Influences on the Proton Conductivity

Let us consider following Ref. 179 the character and value of the change of the hydrogen-bonded chain proton conductivity under the influence of light (two

cases can be treated: absorption by a polaron and absorption by a chain) and ultrasound.

As is known from electron small polaron theory [88], transitions of charge carriers from site to site are possible not only due to phonon activation but owing to the action of light (so-called intraband absorption). With this regard the adiabatic transition of a carrier from the ground state of the lth site to the ground state of the $(l + 1)$th site occurs through an interval of excited states. Assume that an excited virtual state is described by function $|l'\rangle$. The matrix element of such a process, corresponding to second order of perturbation theory, can be written as

$$\frac{\langle l|e\tilde{\mathscr{E}}(t) \cdot \mathbf{r}|l'\rangle\langle l'|e\tilde{\mathscr{E}}(t) \cdot \mathbf{r}|l+1\rangle}{E' - E} = \frac{(\mathbf{d} \cdot \tilde{\mathscr{E}}(t))^2}{\Xi}\hat{a}_{l+1}^+\hat{a}_l \qquad (271)$$

Here $e\tilde{\mathscr{E}}(t) \cdot \mathbf{r}$ is the potential energy of a charge carrier, $\tilde{\mathscr{E}}(t) = \tilde{\mathscr{E}}_0 \cos \Omega t$ is the variable electric field (in dipole approach), $\mathbf{r}$ is the charge carrier coordinate in a unit cell between the lth site and the $(l + 1)$th site, $\Xi = E' - E$ is the difference between the energies of the carrier in excited and ground states, $\mathbf{d}$ is the dipole transition moment, and $\hat{a}_l^+ (\hat{a}_l)$ is the creation (annihilation) Fermi operator of a charge carrier in the lth site.

With regard to these radiation transitions, the Hamiltonian of the system available in the direct external electric field can be written in the small carrier concentration approximation as

$$H = H_0 + H_{\text{tun}} + H_{\mathscr{E}} + H_{\tilde{\mathscr{E}}} \qquad (272)$$

$$H_0 = \sum_l E\hat{a}_l^+\hat{a}_l + \sum_q \hbar\omega_q\left(\hat{b}_q^+\hat{b}_q + \frac{1}{2}\right)$$

$$- \sum_q \hbar\omega_q\hat{a}_l^+\hat{a}_l[u_l(q)\hat{b}_q^+ + u_l^*(q)\hat{b}_q] \qquad (273)$$

$$H_{\text{tun}} = \sum_l J\hat{a}_{l+1}^+\hat{a}_l + h.c. \qquad (274)$$

$$H_{\mathscr{E}} = -e\sum_l R_l\hat{a}_l^+\hat{a}_l \qquad (275)$$

$$H_{\tilde{\mathscr{E}}} = \sum_l \frac{(\mathbf{d} \cdot \tilde{\mathscr{E}}_0)^2}{2\Xi}\hat{a}_{l+1}^+\hat{a}_l + h.c. \qquad (276)$$

Here $H_0 + H_{\text{tun}}$ is the small polaron Hamiltonian, $H_{\mathscr{E}}$ describes the correlation between the carriers and the applied field $\mathscr{E}$, $H_{\tilde{\mathscr{E}}}$ is the operator describing intraband transitions conditioned by light absorption, E is the carrier coupling

energy in the site, J is the resonance integral, and $R_l = lg$, where l is the site index and g the chain constant.

Let us calculate the correction to the proton polaron direct current density conditioned by light-induced transitions between the sites. This photocurrent calculation is analogous to that of the correction to the drift activation current carried out in the previous subsection [the analogy lies in the fact that operator (276) is similar to the correction to the Hamiltonian if the electric field is taken into account, with the correction being nondiagonal on the operator of the coordinate; see expression (236)].

The current density sought for is obtained according to

$$I_{\tilde{\mathscr{E}}} = [\mathrm{Tr}(\rho_{\mathscr{E}}^{(1)} j^{(2)}) + \mathrm{Tr}\,(\rho_{\mathscr{E}}^{(2)} j^{(1)})] \tag{277}$$

Here

$$\rho_{\mathscr{E}}^{(1,2)} = -\frac{i}{\hbar} \int_{-\infty}^{0} d\tau e^{-i\frac{t-\tau}{\hbar}(H_0+H_{\mathscr{E}})} [H_{\mathscr{E}}, \rho_{\mathrm{tun}}^{(1,2)}] e^{i\frac{t-\tau}{\hbar}(H_0+H_{\mathscr{E}})} \tag{278}$$

is the corresponding correction to the statistic operator of the system conditioned by the correlation (276), where

$$\rho_{\mathrm{tun}}^{(1,2)} = -\frac{e^{-H_0/k_{\mathrm{B}}T}}{\mathrm{Tr}\,e^{-H_0/k_{\mathrm{B}}T}} \int_0^{1/k_{\mathrm{B}}T} d\lambda e^{\lambda H_0} H_{\mathrm{tun},\tilde{\mathscr{E}}} e^{-\lambda H_0} \tag{279}$$

and

$$j^{(1,2)} = \frac{e}{\mathscr{V} i\hbar} \left[\sum_l R_l \hat{a}_l^+ \hat{a}_l, H_{\mathrm{tun},\tilde{\mathscr{E}}} \right] \tag{280}$$

is the current density operator.

The calculation of the density current (277) is very similar to that carried out in the previous subsection. The final expression is

$$I_{\tilde{\mathscr{E}}} = \sqrt{2\pi} \hbar^{-2} eng J \frac{(\mathbf{d} \cdot \tilde{\mathscr{E}}_0)^2}{2\Xi} \sinh \frac{e\mathscr{E}g}{2k_{\mathrm{B}}T}$$
$$\times \frac{\exp(-E_{\mathrm{a}}/k_{\mathrm{B}}T)}{\left[\sum_q |\Delta(q)|^2 \omega_q^2 \cosech \frac{\hbar\omega_q}{2k_{\mathrm{B}}T} \right]^{-1/2}} \tag{281}$$

where n is the carrier concentration in the chain, E_{a} is the polaron hopping activation energy [see expression (223)], and $|\Delta(q)|^2$ is the coupling function.

The resulting proton current density (which includes the drift activation current), considered in the two previous subsections and photocurrent (281) is

$$I_{\tilde{\mathscr{E}}} = \sqrt{2\pi}\hbar^{-2}engJ\left(2J + \frac{(\mathbf{d}\cdot\tilde{\mathscr{E}}_0)^2}{2\Xi}\right)\sinh\frac{e\mathscr{E}g}{2k_BT}$$

$$\times\frac{\exp(-E_a/k_BT)}{\left[\sum_q|\Delta(q)|^2\omega_q^2\text{cosech}\frac{\hbar\omega_q}{2k_BT}\right]^{-1/2}} \qquad (282)$$

If the dipole transition moment $\mathbf{d}$ is comparatively large and the value $(\mathbf{d}\cdot\tilde{\mathscr{E}}_0)^2/2\Xi$ is of the order of J (recall that $J \sim (10^{-4}$ to $10^{-2})k_BT$, where $T \simeq 300$ K), then expression (282) gives a considerable increase of the current. With this regard the stationary photocurrent for $\mathscr{E} < 10^8$ V/m below room temperature is linear with the constant field $\mathscr{E}$ and quadratic with the amplitude of the variable field $\tilde{\mathscr{E}}_0^2$.

The maximum $|\mathbf{d}|$ is reached in the region of the polaron resonance absorption with radiation frequency $\Omega \approx 4E_a/\hbar$, where the width of the absorption curve is proportional to $\sqrt{E_ak_BT}$ [88,89]. According to data [165,180,181], $E_a = 3$–20 k_BT for systems with hydrogen-bonded chains. Therefore, the frequency interval $\Omega = 2\pi \times 1$–6×10^{14} s^{-1} should correspond to the proton polaron absorption in a hydrogen-bonded chain.

If we consider proton vibrations of a chain on hydrogen bonds as vibrations of individual oscillators with the typical frequency $\omega_0 \approx 2\pi \times 5 \times 10^{12}$ s^{-1}, then under the influence of infrared radiation with frequency ω_0, resonance absorption should be observed. A wide absorption band in the crystal LiN_2H_5 SO_4 with maximum in the region ω_0 has really been observed experimentally [180]. Strongly correlated vibrations of protons of the hydrogen-bonded chain, which result in a large proton polarizability of the chain, were observed by Zundel and collaborator [see, e.g., Ref. 6 (review article); this effect is considered in the following subsections.

The power absorbed by protons vibrating on hydrogen bonds in a chain can be considered as that absorbed by N oscillators, the cooperative effect being neglected [182]

$$\mathscr{P} = N\frac{\frac{e^2}{m}\tilde{\mathscr{E}}_0^2\eta\tilde{\omega}^2\cos\vartheta}{(\tilde{\omega}^2 - \omega_0^2)^2 + 4\eta^2\tilde{\omega}^2} \qquad (283)$$

Here e is the elementary charge, m is the proton mass, $\tilde{\mathscr{E}}_0$ is the amplitude of the electromagnetic wave with frequency $\tilde{\omega}$, ϑ is the angle between the dipole axis

(i.e., the hydrogen-bonded chain) and the vector $\tilde{\mathscr{E}}_0$, and η is the absorption coefficient (the half-width of the absorption band). The absorbed energy can cause the heating of chain protons and, therefore, the increase of optical phonon temperature: $T \rightarrow T^* > T$. Since in the first approximation the phonon heating is proportional to the temperature difference—that is, $P = C(T^* - T)$ [183], where C is a constant—then assuming $\mathscr{P} = P$ with resonance ($\tilde{\omega} = \omega_0$), we get

$$T^* = T + \alpha(\omega_0)\tilde{\mathscr{E}}_0^2 \qquad (284)$$

where $\alpha(\omega_0) = (4m\eta C)^{-1}Ne^2\cos\vartheta$.

With the above-mentioned parameter values of a hydrogen-bonded chain, with regard to anharmonicity (231) and heating (284) we obtain for the current density instead of (283)

$$I = 2^{3/2}\pi^{1/2}\hbar^{-2}engJ^2 \sinh\frac{e\mathscr{E}g}{2k_BT^*}$$

$$\times e^{-E_a/k_BT}\left[\sum_q |\Delta(q)|^2\omega_q^2\text{cosech}\frac{\hbar\omega_q}{2k_BT^*}\right]^{-1/2}$$

$$\times \exp\left\{\sum_q |\kappa_q|^2|\Delta_q|^2\left(\frac{\hbar\omega_q}{2k_BT^*}\right)^2\text{cosech}^4\frac{\hbar\omega_q}{2k_BT^*}\right.$$

$$\left.\times \left(1 - \text{cosech}\frac{\hbar\omega_q}{2k_BT^*}\right)^2\coth\frac{\hbar\Omega_q}{2k_BT}\right\} \qquad (285)$$

Here T is the temperature of acoustic phonons (thermostat), T^* is the temperature of optical phonons (284), the anharmonicity constant $|\kappa_q|$ is much less than 1, and Ω_q is the frequency of acoustic phonons; it is possible to assume $\Omega_q = (10^{-2}$ to $10^{-1})\Omega_{\text{Debye}}$. The coupling between the optical and acoustic phonons is strongest near Ω_{Debye}; and because of this, for sufficiently large anharmonicity, $|\kappa_q| \geq 10^{-2}$ even at $T = T^*$, the last exponential multiplier can be approximated by the exponent below, with the dispersion being neglected:

$$\exp\left\{2|\kappa|^2|\Delta|^2\frac{(10^{-2} \text{ to } 10^{-1})\hbar\Omega_{\text{Debye}}}{\hbar\omega_0}\left(\frac{T^*}{T}\right)^2\right\} \qquad (286)$$

Hence it is clear that an increase of the temperature of the optical phonons T^* activating the charge carrier hopping leads to an increase of the proton current

density (285). Such a stimulation mechanism remains working until the heating (284) is small in comparison with the polaron shift energy $\approx |\Delta|^2 \hbar \omega_0$ (the coupling function $|\Delta|^2 \approx 20$).

Let us now treat the influence of ultrasound (hypersound) on the proton mobility in the hydrogen-bonded chain. The impact of ultrasound on free electrons weakly connected with matrix vibrations (e.g., metals and nonpolar semiconductors) has been studied in detail (see, e.g., Ref. 184). The effect of ultrasound on the diffusion of atoms in a solid has also been studied in detail (see, e.g., Ref. 185).

While considering the influence of sound on the mobility of protons, their peculiar position should be taken into account, because in a solid they are specified both by the quantum features (the availability of the overlap integral between the nearest-neighbor sites in crystal with hydrogen bonds) and by classical ones (a large mass and hence a usual diffusion in metals and nonpolar semiconductors). The peculiar position occupied by the charge carriers in a hydrogen-bonded chain enables us to point out a specific mechanism of the proton conductivity stimulation by ultrasound.

The overlap integral J securing the carrier tunneling through the barrier between the two neighboring polaron wells in the quasi-classical approximation has the following appearance:

$$J \simeq E \exp\left\{ -\frac{2}{\hbar} \int_0^a dx \sqrt{2m^*[V(x) - K]} \right\} \tag{287}$$

where a is the potential barrier width, m^* is the effective mass of a carrier in a chain, $V(x)$ is the potential energy, and K is the kinetic energy of a carrier. Since the proton mass is much larger than that of the electron, the absolute value of the exponential function is not small (compare with Ref. 186). The probability of tunneling between polaron wells depends on the barrier width, which can be modulated in turn by an external ultrasound in this case.

The sites of hydrogen-bonded chains are rigidly fixed by the side chemical bonds in various compounds. That is why the distances between the sites and, therefore, the chain rigidity are functions of external parameters related to it— that is, the thermostat functions. In that event, longitudinal vibrations of the chain sites imposed by the matrix lead to periodical oscillations of the barrier width a between the neighboring polaron wells. If the barrier becomes thinner— that is, if $a \rightarrow a - \delta a$—the overlap integral

$$J \rightarrow J \exp\left(\frac{2}{\hbar} \langle R \rangle \delta a \right) \tag{288}$$

where $\langle R \rangle$ is the average meaning of the integrand $\sqrt{2m^*[V(x) - K]}$ in expression (287). The displacement of a can be quantized on the acoustic phonon operators: $\delta a \to \sum_q (\alpha_q \hat{B}_q^+ + \alpha_q^* \hat{B}_q)$. Then, performing quantum mechanical thermal averaging in expression (288) we have

$$\tilde{J} = J\exp\left\{\frac{\langle R \rangle}{\hbar}\sum_q |\alpha_q|^2 \coth\frac{\hbar\Omega_q}{2k_{\rm B}T}\right\} \tag{289}$$

where Ω_q is the acoustic phonon frequency with the wave number q.

On switching on ultrasound with the wave vector directed along the chain, the vibration amplitudes of framework atoms will be already defined in the chain not by temperature of the medium but by the ultrasound source intensity. In this case we have instead of expression (289)

$$\tilde{J}(A, \Omega_{\rm sound}) = J\exp\left\{\frac{\langle R \rangle}{\hbar}\delta a\left(1 + |\zeta(\Omega_{\rm sound})|^2 \frac{A}{\delta a}\right)\right\} \tag{290}$$

where $|\zeta(\Omega_{\rm sound})|^2$ is a constant characterizing the interaction between ultrasound with frequency $\Omega_{\rm sound}$ and the chain framework vibrations, and A is the ultrasound amplitude. The results obtained, (289) and (290), also agree qualitatively with the behavior of the proton tunnel frequency in the complex $O-H\cdots O$ of the KH_2PO_4 crystal considered in Refs. 187 and 188 when the pressure and temperature were taken as external factors.

Since the value δa is under the exponential sign, even a small correction to it should lead to a considerable change of the overlap integral. In fact, it is clearly seen from expression (290) that the correction $|\zeta(\Omega_{\rm sound})|^2 A$ caused by ultrasound to δa brings about a considerable increase of the vibration amplitude of chain framework atoms. This amplifies the modulation of the distance between the neighboring polaron wells. Moreover, since the expression for the proton current density is proportional to J^2 when external effects are not available [see, for instance, expressions (222) or (231)], the replacement of this value for $\tilde{J}^2(A, \Omega_{\rm sound})$ including an exponential dependence on the ultrasound amplitude should result in an appreciable exponential growth of the current (at least, by several times).

Of course, expression (290) is correct only in cases when tunneling of a quasi-particle (i.e., proton polaron), through the barrier takes place for times shorter than the period of the barrier oscillations. The amplitude of ultrasound vibrations in this situation should not exceed some critical $A_{\rm c}$ under which the warning-up of the chain is essential (in particular, the critical power of ultrasound for biotissues varies from 10^{-2} to 10^{-1} W/cm^2).

H.   Vibration Fluctuations of a Resonance Integral in the Polaron Problem

In the small polaron model a charge carrier that is strongly connected with a site locally deforms the crystal lattice and a consequence of the deformation is the induction of the interaction of the carrier with polarized optical phonons. For the most part, the impact of the phonon subsystem is reduced to the renormalization of the coupling energy. Considering the phonon subsystem in terms of second quantization makes it possible to take into account some peculiarities associated with external factors such as temperature, electromagnetic field, and ultrasound. Phonons are able to modulate the resonance overlap integral, which results into the effective thinning of the barrier between two polaron wells. In turn it leads to a significant increase of the current density (see previous sections and also Ref. 189).

A small proton polaron is different in some aspects from the electron polaron; that is, the hydrogen atom is able to participate in the lattice vibrations in principle (in any case it is allowable for excited states; see Section II.F), but the electron cannot. This means that one more mechanism of phonon influence on the proton polaron is quite feasible. That is, phonon fluctuations would directly influence wave functions of the protons and thereby contribute to the overlapping of their wave functions. In other words, phonons can directly increase the overlap integral in concept. Such an approach allows one to describe the proton transfer without using the concept of transfer from site to site through an intermediate state.

For instance, a similar approach was developed by Kagan and Klinger [190]. They studied the fluctuating diffusion through barrier (coherent) and over barrier (incoherent) of ^{3}He atoms in the crystal of ^{4}He atoms. In other words, the tunnel integral was treated as a matrix element constructed not only on wave functions y_l and y_m of diffusing ^{3}He atoms (l and m are the radius vectors of the lattice sites between which the quantum diffusion occurs), but also on wave functions j_{ln} and j_{mn} of vibrating motion of the crystal where n is the number of occupation of an excited state. The intersite diffusion of particles, which took into account diagonal phonon transitions, was treated in detail in Ref. 190, but the method of calculation did not allow them to investigate the contribution of off-diagonal phonon transfers.

Another approach has been proposed in Ref. 191. The approach is based on the model of small polaron and makes it possible to extend the range of the model. In particular, it includes the influence of vibration wave functions on the tunnel integral and provides a way of the estimation of diagonal and off-diagonal phonon transfers on the proton polaron mobility. It turns out that the one phonon approximation is able significantly to contribute to the proton mobility. Therefore, we will further deal with matrix elements constructed on

the phonon function $\varphi(\mathbf{q}) = \hat{b}_{\mathbf{q}}^{+}\varphi_{\mathbf{q}}(0)$ and will examine only the first excited state with $\nu = 1$.

In the approximation of small concentration of carriers we can write the polaron Hamiltonian as follows:

$$H = H_0 + H_{\text{tun}} + H_{\mathscr{E}} \tag{291}$$

$$H_0 = \sum_{\mathbf{l}} E\hat{a}_{\mathbf{l}}^{+}\hat{a}_{\mathbf{l}} + \sum_{\mathbf{q}} \hbar\omega_{\mathbf{q}}\left(\hat{b}_{\mathbf{q}}^{+}\hat{b}_{\mathbf{q}} + \frac{1}{2} \right)$$

$$- \sum_{\mathbf{q}} \hbar\omega_{\mathbf{q}}\hat{a}_{\mathbf{l}}^{+}\hat{a}_{\mathbf{l}}[u_{\mathbf{l}}(\mathbf{q})\hat{b}_{\mathbf{q}}^{+} + u_{\mathbf{l}}^{*}(\mathbf{q})\hat{b}_{\mathbf{q}}] \tag{292}$$

$$H_{\text{tun}} = \sum_{\mathbf{l},\mathbf{m}} \sum_{\mathbf{k},\mathbf{q}} \hat{b}_{\mathbf{k}}^{+}\varphi_{\mathbf{k}}^{*}(0)J_{\mathbf{lm}}\hat{a}_{\mathbf{l}}^{+}\hat{a}_{\mathbf{m}}\hat{b}_{\mathbf{q}}\varphi_{\mathbf{q}}(0) + h.c. \tag{293}$$

Here E is the energy of connection of a carrier with the lth site; $u_{\mathbf{l}}(\mathbf{q}) = ue^{i\mathbf{q}\cdot\mathbf{l}}$, where u is the dimensionless constant, which characterizes the degree of local deformation of the lattice by a carrier. The tunnel Hamiltonian (293) includes in addition the overlapping the phonon functions $\hat{b}_{\mathbf{q}}\varphi_{\mathbf{q}}(0)$ and $\hat{b}_{\mathbf{k}}^{+}\varphi_{\mathbf{k}}(0)$ as we conjecture that the proton polaron engages in the lattice vibration as well (hence $J_{\mathbf{lm}}$ becomes a function of the momentum $\mathbf{q}$ and/or $\mathbf{k}$, too). In the present form, Eq. (293), the total number of phonons is not kept; however, we imply that the phonons are absorbed and emitted by polarons and thus their total number remains invariable. Let us introduce the designation

$$V_{\substack{\mathbf{lm} \\ \mathbf{kq}}} = \varphi_{\mathbf{k}}^{*}(0)J_{\mathbf{lm}}\varphi_{\mathbf{q}}(0) \tag{294}$$

Then the tunnel Hamiltonian (293) changes to

$$H_{\text{tun}} = \sum_{\mathbf{l},\mathbf{m}} \sum_{\mathbf{k},\mathbf{q}} V_{\substack{\mathbf{lm} \\ \mathbf{kq}}} \hat{a}_{\mathbf{l}}^{+}\hat{a}_{\mathbf{m}}\hat{b}_{\mathbf{q}}^{+}\hat{b}_{\mathbf{q}} + h.c. \tag{295}$$

The Hamiltonian $H_{\mathscr{E}}$ in expression (291) has the form

$$H_{\mathscr{E}} = -e\sum_{\mathbf{l}} \mathscr{E} \cdot \mathbf{l}\hat{a}_{\mathbf{l}}^{+}a_{\mathbf{l}} \tag{296}$$

and describes the behavior of the field $\mathscr{E}$ on a proton polaron located in the lth site.

The diagonalization of the Hamiltonian H_0 (292) by phonon variables is realized by the canonical transformation

$$\bar{H}_0 = e^{-S}H_0 e^{S}, \qquad S = \sum_{\mathbf{l};\mathbf{q}} \hat{a}_{\mathbf{l}}^{+}\hat{a}_{\mathbf{l}}[u_{\mathbf{l}}(\mathbf{q})\hat{b}_{\mathbf{q}}^{+} - u_{\mathbf{l}}^{*}(\mathbf{q})\hat{b}_{\mathbf{q}}] \tag{297}$$

Under the transformation (297) the Hamiltonian (1) is transformed to

$$\bar{H} = \bar{H}_0 + \bar{H}_{\text{tun}} + H_{\mathscr{E}} \tag{298}$$

$$\bar{H}_0 = \sum_{\mathbf{l}} \left(E - \sum_{\mathbf{q}} |u|^2 \hbar\omega_{\mathbf{q}} \right) \hat{a}_{\mathbf{l}}^+ \hat{a}_{\mathbf{l}} + \sum_{\mathbf{q}} \hbar\omega_{\mathbf{q}} \left(\hat{b}_{\mathbf{q}}^+ \hat{b}_{\mathbf{q}} + \frac{1}{2} \right) \tag{299}$$

$$\bar{H}_{\text{tun}} = \sum_{\mathbf{l,m}} \sum_{\mathbf{k,q}} V_{\substack{\mathbf{lm}\\ \mathbf{kq}}} \hat{a}_{\mathbf{l}}^+ \hat{a}_{\mathbf{m}} \hat{\Phi}_{\mathbf{lm}}(0) e^{-S} \hat{b}_{\mathbf{q}}^+ \hat{b}_{\mathbf{q}} e^{S} + h.c. \tag{300}$$

where

$$\hat{\Phi}_{\mathbf{lm}}(0) = \exp\left\{ \sum_{\mathbf{q}} \hat{a}_{\mathbf{l}}^+ \hat{a}_{\mathbf{m}} [\Delta_{\mathbf{lm}}(\mathbf{q}) \hat{b}_{\mathbf{q}}^+ - \Delta_{\mathbf{lm}}^*(\mathbf{q}) \hat{b}_{\mathbf{q}}] \right\} \tag{301}$$

$$\Delta_{\mathbf{lm}}(\mathbf{q}) = u_{\mathbf{l}}(\mathbf{q}) - u_{\mathbf{m}}(\mathbf{q}) \tag{302}$$

With regard for the rules of transformation of the operator functions $\hat{b}_{\mathbf{q}}^+$ and $\hat{b}_{\mathbf{q}}$ [88,192], the Hamiltonian $\bar{H}_{\text{tun}}$ can be presented in the form

$$\bar{H}_{\text{tun}} = \sum_{\mathbf{l,m}} \sum_{\mathbf{k,q}} V_{\substack{\mathbf{lm}\\ \mathbf{kq}}} \hat{a}_{\mathbf{l}}^+ \hat{a}_{\mathbf{m}} \hat{M}_{\substack{\mathbf{lm}\\ \mathbf{kq}}} \hat{\Phi}_{\mathbf{lm}}(0) + h.c. \tag{303}$$

where the following designation has been introduced:

$$\hat{M}_{\substack{\mathbf{lm}\\ \mathbf{kq}}} = -\frac{\partial^2}{\partial\Delta_{\mathbf{lm}}(\mathbf{q})\partial\Delta_{\mathbf{lm}}^*(\mathbf{k})} - \sum_{\mathbf{l'}} u_{\mathbf{l'}}^*(\mathbf{q}) \frac{\partial}{\partial\Delta_{\mathbf{lm}}^*(\mathbf{q})}$$

$$+ \sum_{\mathbf{m'}} u_{\mathbf{m'}}^*(\mathbf{q}) \frac{\partial}{\partial\Delta_{\mathbf{lm'}}(\mathbf{q})} + \sum_{\mathbf{l',m'}} u_{\mathbf{l'}}^*(\mathbf{q}) u_{\mathbf{m'}}(\mathbf{k}) \tag{304}$$

Let us now calculate the current density of proton polarons by setting $|V_{\substack{\mathbf{lm}\\ \mathbf{kq}}}| \ll \hbar\omega_{\mathbf{q}}$, E, $k_{\text{B}}T$. We start from the expression

$$I = \text{Tr}(\rho_{\text{tun}}, j) \tag{305}$$

where the correction to the statistical operator of the system studied caused by the operator $\bar{H}_{\text{tun}}$ (303) has the form

$$\rho_{\text{tun}} = -\frac{i}{\hbar} \int_{-\infty}^{t} d\tau e^{-i(t-\tau)\bar{H}_0/\hbar} [\bar{H}_{\text{tun}}, \rho_0] e^{i(t-\tau)\bar{H}_0/\hbar} \tag{306}$$

the undisturbed statistical operator is equal to

$$\rho_0 = \frac{e^{-\bar{H}_0/k_{\rm B}T}}{{\rm Tr}\, e^{-\bar{H}_0/k_{\rm B}T}} \tag{307}$$

and the operator of current density is

$$j = \frac{e}{\mathscr{V}\, i\hbar}\left[\bar{H}_{\rm tun}, \sum_{\bf l} {\bf l}\hat{a}_{\bf l}^{+}\hat{a}_{\bf l}\right] \tag{308}$$

($\mathscr{V}$ is the effective volume of the crystal which contains one polaron). Substituting expressions from (306) to (308), the current density (305) can be written as

$$\mathbf{I} = \frac{1}{\hbar^2\,{\rm Tr}\, e^{-\bar{H}_0/k_{\rm B}T}}\int_0^{\infty} d\tau\,{\rm Tr}\left\{\left\{e^{-\bar{H}_0/k_{\rm B}T}\bar{H}_{\rm tun}\left(-\frac{i}{\hbar}\tau\right)\left[j\left(-\frac{1}{k_{\rm B}T}\right)-j\right]\right\}\right. \tag{309}$$

where the following designations of the operators are introduced:

$$\bar{H}_{\rm tun}\left(-\frac{i}{\hbar}\tau\right) = e^{-\frac{i}{\hbar}\tau(\bar{H}_0+H_{\mathscr{E}})}\bar{H}_{\rm tun}e^{\frac{i}{\hbar}\tau(\bar{H}_0+H_{\mathscr{E}})} \tag{310}$$

$$j\left(-\frac{1}{k_{\rm B}T}\right) = e^{-\frac{1}{k_{\rm B}T}(\bar{H}_0+H_{\mathscr{E}})}je^{\frac{1}{k_{\rm B}T}(\bar{H}_0+H_{\mathscr{E}})} \tag{311}$$

Then the following transformations can be performed in expression (309):

$$\mathbf{I} = \frac{1}{\mathscr{V}\hbar^2\,{\rm Tr}\, e^{-\bar{H}_0/k_{\rm B}T}}\int_0^{\infty} d\tau\,{\rm Tr}\left\{e^{-\bar{H}_0/k_{\rm B}T}\cdot\sum_{{\bf l},{\bf m},{\bf l}',{\bf m}'}\sum_{{\bf k},{\bf q},{\bf k}',{\bf q}'}\underset{{\bf k}{\bf q}}{V_{{\bf l}{\bf m}}}\underset{{\bf k}'{\bf q}'}{V_{{\bf l}'{\bf m}'}}({\bf l}-{\bf m})\right.$$

$$\times\,\hat{a}_{\bf l}^{+}\hat{a}_{\bf m}\hat{a}_{{\bf l}'}^{+}\hat{a}_{{\bf m}'}\left[\underset{{\bf k}{\bf q}}{\hat{M}_{{\bf l}{\bf m}}}\hat{\Phi}_{{\bf l}{\bf m}}\left(-\frac{i}{\hbar}\tau\right)\underset{{\bf k}'{\bf q}'}{\hat{M}_{{\bf l}'{\bf m}'}}\hat{\Phi}_{{\bf l}'{\bf m}'}\left(-\frac{1}{k_{\rm B}T}\right)e^{-e\mathscr{E}\cdot({\bf l}-{\bf m})/2k_{\rm B}T}\right.$$

$$\left.-\,e^{-5e\mathscr{E}\cdot({\bf l}-{\bf m})/2k_{\rm B}T}\underset{{\bf k}{\bf q}}{\hat{M}_{{\bf l}{\bf m}}}\hat{\Phi}_{{\bf l}{\bf m}}\left(-\frac{i}{\hbar}\tau\right)\underset{{\bf k}'{\bf q}'}{\hat{M}_{{\bf l}'{\bf m}'}}\hat{\Phi}_{{\bf l}'{\bf m}'}(0)\right]\right\}$$

$$= \frac{1}{\hbar^2\,{\rm Tr}\, e^{-\bar{H}_0/k_{\rm B}T}}\sum_{{\bf l},{\bf m}}\sum_{{\bf k},{\bf q}}e^{-\bar{H}_0/k_{\rm B}T}\frac{\hat{a}_{\bf l}^{+}\hat{a}_{\bf l}}{\mathscr{V}}({\bf l}-{\bf m})|\underset{{\bf k}{\bf q}{\bf l}}{V_{{\bf l}{\bf m}}}|^2(\underset{{\bf k}{\bf q}}{\hat{M}_{{\bf l}{\bf m}}})^2$$

$$\times\int_0^{\infty} d\tau\left\{\hat{\Phi}_{{\bf l}{\bf m}}\left(-\frac{i}{\hbar}\tau\right)\hat{\Phi}_{{\bf m}{\bf l}}\left(-\frac{1}{k_{\rm B}T}\right)e^{-e\mathscr{E}\cdot({\bf l}-{\bf m})/2k_{\rm B}T}\right.$$

$$\left.-\,\hat{\Phi}_{{\bf l}{\bf m}}\left(-\frac{i}{\hbar}\tau\right)\hat{\Phi}_{{\bf m}{\bf l}}(0)e^{-5e\mathscr{E}\cdot({\bf l}-{\bf m})/2k_{\rm B}T}\right\} \tag{312}$$

[here the structure of the operator $\hat{\Phi}_{\mathbf{lm}}(x)$ is defined by formulas (310) and (311)]. Preserving in expression (312) only members approximated by nearest neighbors, we then carry out the thermal averaging and integrate over τ. As a result we obtain

$$\mathbf{I} = \frac{\mathscr{E}}{|\mathscr{E}|}\frac{2^{3/2}\pi^{1/2}ng}{\hbar^2}\sinh\frac{e\mathscr{E}g}{k_BT}\sum_{\mathbf{k},\mathbf{q}}|V_{\mathbf{kq}}|^2\hat{M}_{\mathbf{qk}}^2$$

$$\times\frac{\exp(-E_a/k_BT)}{[\sum_{\mathbf{q}'}|\Delta(\mathbf{q}')|^2\omega_{\mathbf{q}'}^2\operatorname{cosech}\hbar\omega_{\mathbf{q}'}]^{1/2}} \tag{313}$$

where the activation energy is equal to

$$E_a = k_BT\sum_{\mathbf{q}'}|\Delta(\mathbf{q}')|^2\tanh(\hbar\omega_{\mathbf{q}'}/4k_BT) - 3e\mathscr{E}g/2 \tag{314}$$

Here the following designations are introduced: n is the concentration of polarons, g is the lattice constant, $V_{\mathbf{lm}\atop\mathbf{kq}} \to V_{\mathbf{ll+g}\atop\mathbf{kq}} = V_{\mathbf{kq}}$,

$$\Delta_{\mathbf{lm}}(\mathbf{q}) \to \Delta_{\mathbf{l+g}}(\mathbf{q}) = \Delta(\mathbf{q}), \text{ and } \hat{M}_{\mathbf{lm}\atop\mathbf{qk}} \to \hat{M}_{\mathbf{ll+g}\atop\mathbf{qk}} = \hat{M}_{\mathbf{qk}}$$

Let us analyze the result obtained in Eq. (313) neglecting the dependence of values on wave vectors $\mathbf{q}$ and $\mathbf{k}$. The elements of operator $\hat{M}^2$ can be written in agreement with expression (304) as below:

$$\hat{M}^2 \propto \left\{\frac{\partial^4}{\partial|\Delta|^4}, \quad \pm|u|^2\frac{\partial^2}{\partial|\Delta|^2}, \quad u\frac{\partial^3}{\partial|\Delta|^3}, \quad |u|^4\right\} \tag{315}$$

On the other hand, in expression (313) the structure of the term (as a function of parameter $|\Delta|$), which falls under the influence of the operator $\hat{M}^2$, has the form

$$f(|\Delta|) \propto \frac{1}{|\Delta|}\exp(-C|\Delta|^2), \qquad 0 < C < 1 \tag{316}$$

Taking into account the inequalities $\hbar\omega < k_BT$ and $|u|^2 \approx |\Delta|^2 \gg 1$, we can compare all the terms of the series $\hat{M}^2f(|\Delta|)$. It is easy to see that the term proportional to $|u|^4$ is maximal in expression (315); the other ones are one to several orders of magnitude smaller. Thus, we can retain only one, with the biggest term proportional to $|u|^4$ in the series (315). Then setting $|u|^2 \approx |\Delta|^2$ and assuming that $e\mathscr{E}g < k_BT$ (it is correct until $\mathscr{E} \leq 10^7$ V/m and for moderate

temperatures, see Ref. 88 for details), we finally obtain instead of expression (313)

$$
I = \frac{\mathscr{E}}{|\mathscr{E}|} \frac{2^{3/2}\pi^{1/2}ng}{\hbar^2} \sinh\frac{e\mathscr{E}g}{k_{\mathrm{B}}T} |V|^2|\Delta|^4
$$

$$
\times \frac{\exp(-E_{\mathrm{a}}/k_{\mathrm{B}}T)}{[|\Delta|^2\omega^2\mathrm{cosech}(\hbar\omega/2k_{\mathrm{B}}T)]^{1/2}} \tag{317}
$$

Expression (317) for the current density is distinguished from that derived in the standard model of small polaron [see, e.g., formula (227)] only by multiplier $|\Delta|^4$. However, in the theory of small polaron is assumed that $|\Delta|^2$ significantly exceeds the unit. Consequently, the result obtained makes it possible to spread the framework of the small polaron model very considerably. The inclusion of phonon transitions is culminated in the renormalization of the overlap integral,

$$
J \to V = J|\Delta|^2 \tag{318}
$$

Therefore, in cases when the value of J is too small, the proton conductivity can still be very substantial due to the fluctuating absorption and radiation of phonons by charged carriers. This allows also the application of the approach developed above to compounds in which hopping of heavy carriers occurs by comparatively distant structural groups (for example, 0.4 to 0.8 nm, which takes place in some superionic crystals).

I.   An Example of Superionic Conductivity: The $NH_4IO_3 \cdot 2NHIO_3$ Crystal

The crystal of ammonium triiodate was investigated by different methods: X-ray diffraction analysis [193], neutronography [194], polarization optical techniques [195], differential scanning calorimetry and vibrational spectroscopy [196], and nuclear quadrupole resonance [197]. In Refs. 193 and 195 it was established that at a temperature above $T_0 = 213$ K, this is a superionic crystal with a conductivity of the protonic type ($\sigma \simeq 10^{-5}$ $\Omega^{-1}\mathrm{cm}^{-1}$ at 300 K [193]). Transition to the superionic state is accompanied by anomalies in permittivity and conductivity, characteristic of phase transition of the second kind [195], but the polarization-optical changes indicate that at $T = T_0$ the symmetry of the crystal does not change. Neutronographic investigation [194] revealed the presence of a system of bifurcated hydrogen contacts. In view of this fact, transition to the superionic state was attributed to disordering of the protonic subsystem (at $T > T_0$). Raman spectroscopy studies [196,198] demonstrated that ordering of the protonic subsystem actually occurs at a much lower temperature T_c, which lies in the range of about 120–125 K and is accompanied by doubling of the unit cell volume.

Indeed, the results obtained in Refs. 196 and 198 have shown that the phase diagram of ammonium triiodate $NH_4IO_3 \cdot 2HIO_3$ crystal is essentially more complicated than was assumed previously: In addition to the second-order transition to the high proton conductivity state at the temperature $T_c = 213$ K, the differential scanning calorimetry examinations has revealed two transitions at the temperatures $T_1 = 365.6$ K (first-order transition) and at $T_c^1 = 365.6$ K (second-order transition). Starting from general theoretical views, Puchkovska and Tarnavski [196] have proposed the symmetry of crystal phases which agrees with the results of investigations of the vibrational spectra of the crystal. Apparently the new phase 3 existing in the narrow temperature range from $T_c^1 = 365.6$ to $T_c^2 = 211.6$ K is a metastable phase, and therefore it was not found previously in the dielectric and conductivity measurements [195]. Metastable phases have been revealed also in other proton conductors. For instance, in Ref. 199, transitions between stable and metastable phases in the ammonium hydrogen selenates NH_4HSeO_4 and ND_4SeO_4 were discussed.

The finding of several phase transitions in triiodate ammonium allows the examination of another proton conductor, the $KIO_3 \cdot 2HIO_3$ crystal, which at room temperature has the same structure as triiodate ammonium and whose dielectric properties and temperature dependencies are similar to the latter [200,201].

Having understood the mechanism of the motion of protons in the $NH_4IO_3 \cdot 2HIO_3$ crystal, the investigation of the far-infrared absorption spectrum (in the region from 60 to 400 cm^{-1}) and the Raman spectrum (in the region from 600 to 800 cm^{-1}) has been performed [46]. The temperature behavior of the vibration spectra has been studied in the range from 77 to 300 K. The Raman spectra have been obtained from a polycrystalline samples on a DFS-24 (LOMO) spectrometer. The fragments of these spectra discussed herein are illustrated in Fig. 10. Figure 11 shows the IR spectra recorded by a FIS-3 spectrometer (Hitachi, Japan). The temperature of the sample was stabilized with the help of an "Utrex" K-23 thermostabilization system (Institute of Physics, Kyiv) with an accuracy of ± 1 K.

Measurements performed revealed anomalous behavior of (a) the Raman-active mode with a frequency of ≈ 756 cm^{-1} (Fig. 10) and (b) an infrared-active mode with a frequency of ≈ 99 cm^{-1} (Fig. 11). The intensities of these modes in the superionic phase are virtually constant, but at $T < T_0$ the first of them increases in accordance with the law $|(T - T_0)/T_0|^{1/2}$, whereas the second of these modes decreases in accordance with the same law.

The conductivity of the crystal in Arrhenius coordinates is represented by a straight line, and the activation energy is evaluated from the conductivity plot as a function of temperature, $E_a \simeq 46$ kJ/mol [193]. The activation energy, assessed from broadening of the PMR band in accordance with the Waugh–Fedin relation, proved to be equal to $E_a^{(2)} \simeq 33.1$ kJ/mol [193,202]. Investigation of
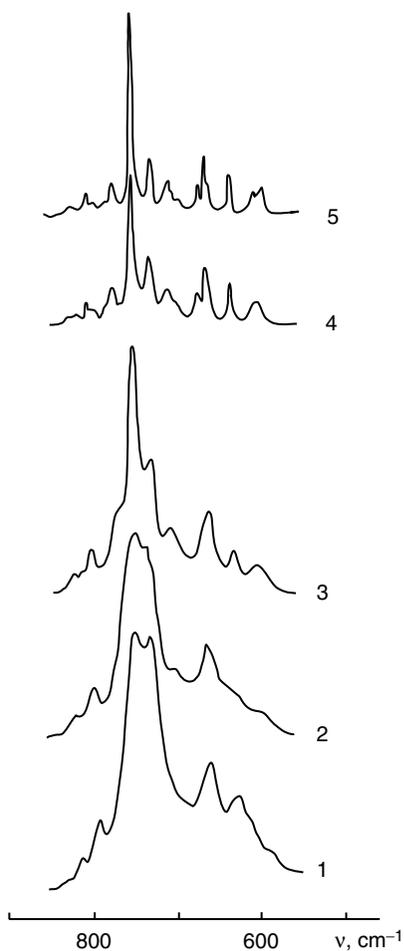
Figure 10. Raman spectrum of the $NH_4IO_3 \cdot 2HIO_3$ crystal in the region of stretching vibrations of the I–O group as a function of temperature: 297 (1), 216 (2), 185 (3), 125 (4), 77 K (6). (From Ref. 46.)

the spin-lattice relaxation gives an activation energy of $E_a^{(1)} \simeq 8.8$ kJ/mol (at $T > T_0$) [202], and the value $E_a^{(1)}$ determined by this procedure characterizes exclusively the hopping mobility of the protons. Such an appreciable spread of activation energy values measured by different methods suggests that the conductivity in ammonium triiodate is governed by two different mechanisms with the activation energies $E_a^{(1)}$ and $E_a^{(2)}$ ($E_a^{(1)} + E_a^{(2)} \simeq E_a$). Therefore, it is natural to suppose that anomalous modes with frequencies of 99 and 756 cm^{-1} found in Ref. 46 are directly connected with the two competing protonic conductivity mechanisms.
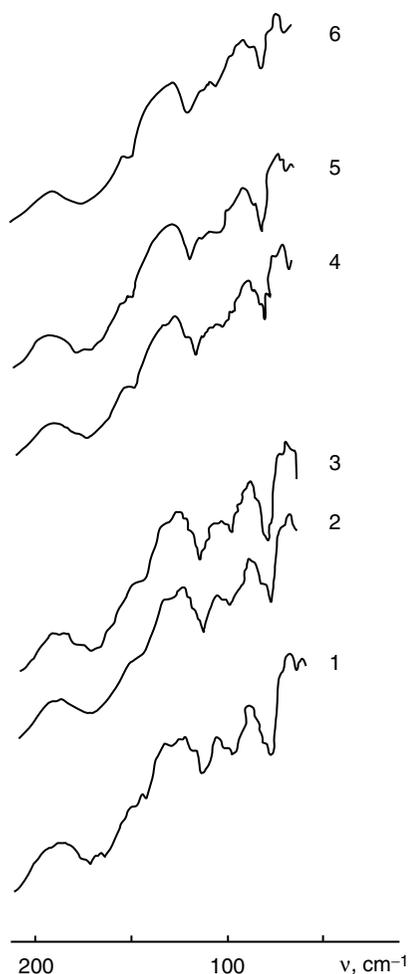
Figure 11. Infrared absorption spectrum of the $NH_4IO_3 \cdot 2HIO_3$ crystal in the region of the lattice vibrations as a function of temperature: 132 (1), 172 (2), 182 (3), 227 (4), 245 (5), 286 K (6). (From Ref. 46.)

The presence of the polar mode oriented in the direction of maximum conductivity gives grounds to postulate the feasibility of the polaronic mechanism of motion of the protons in this crystal. As was shown in the previous subsection (see also Refs. 57,58, and 191) the proton can traverse a comparatively large distance between the nearest sites of the protonic sublattice (0.4 to 0.8 nm) with the participation of vibrational quanta, that is, phonons; the virtual absorption of such a quantum can appreciably increase the resonance integral of overlapping of the wave functions of the proton on the nearest sites; see expression (318).

As we pointed out above, not only the low-frequency mode (99 cm^{-1}), but also the high-frequency mode (756 cm^{-1}), is involved in the protonic conductivity. The criterion for the low-frequency polaronic conductivity is the inequality $\hbar\omega < 2k_BT$, where ω is the frequency of the phonons; $\omega = 99$ cm^{-1} falls under the inequality at $T > 50$ K. At the inequality $\hbar\omega > 2k_BT$, which holds true for the mode with a frequency of 756 cm^{-1}, the standard model of the mobility of the small is not valid; therefore, this case should be treated separately.

Let us apply expression (317) for the calculation of the proton current density associated with the hopping mobility of protons. Neglecting the dispersion in expression (317) and assuming that the applied electric field $\mathscr{E}$ is small, we can write the hopping current density as follows:

$$I = \frac{2^{3/2}\pi^{1/2}e^2ng^2}{\hbar^2k_BT}|V|^2|\Delta^{(1)}|^4$$
$$\times \frac{\exp(-E_a/k_BT)}{[|\Delta^{(1)}|^2\omega_1^2\mathrm{cosech}(\hbar\omega_1/2k_BT)]^{1/2}} \tag{319}$$

where the activation energy is (314)

$$E_a^{(1)} \simeq k_BT|\Delta^{(1)}|^2\tanh(\hbar\omega_1/4k_BT) \tag{320}$$

Here $|\Delta^{(1)}|^2$ is the coupling constant, which ties protons in the polar low-frequency mode ($\omega_1 = 99$ cm^{-1}); n is the proton concentration, and g the lattice constant.

As is well known from the small polaron theory [88], in the region of moderate temperatures the contribution made by the band mechanism to the polaronic current is considerably smaller than the contribution made by the hopping conductivity. However, this result was obtained in approximation of low-frequency phonons, when $\hbar\omega < 2k_BT$. At the same time, the polaronic conductivity can be considered for the opposite case as well (in any case, for heavy carriers, such as protons) [163] when the energy of the phonons exceeds the thermal energy k_BT. Then, it follows that the ratio of the hopping and band conductivities satisfies the inequality in favor of the band mechanism $(I_{\mathrm{band}} \gg I_{\mathrm{hop}})|_{\hbar\Omega \gg k_BT}$. Consequently, it is reasonable to calculate the density of the band polaronic current I_{band}, brought about by mode with a frequency $\omega_2/2\pi = 756$ cm^{-1}, and to compare the result obtained with that for the hopping current I_{hop} (319) where the role of the activating system is played by the low-frequency mode with $\omega_1/2\pi = 99$ cm^{-1}.

It is convenient to start from the canonical form of the polaron Hamiltonian $\bar{H} = e^{-S}He^{S}$ written in the momentum presentation

$$\bar{H} = \bar{H}_0 + \bar{H}_{\text{tun}} \tag{321}$$

$$\bar{H}_0 = \sum_{\mathbf{k}} E(\mathbf{k})\hat{a}_{\mathbf{k}}^+ \hat{a}_{\mathbf{k}} + \sum_{\mathbf{q}} \hbar\omega_{2\mathbf{q}} \left(\hat{b}_{\mathbf{q}}^+ b_{\mathbf{q}} + \frac{1}{2} \right) \tag{322}$$

$$\bar{H}_{\text{tun}} = \sum_{\mathbf{k},\mathbf{k}'} \hat{a}_{\mathbf{k}'}^+ \hat{a}_{\mathbf{k}} \frac{1}{N} \sum_{\mathbf{l},\mathbf{m}} V_{\mathbf{lm}\atop \mathbf{kk}'} \hat{\Phi}_{\mathbf{lm}} e^{i(\mathbf{k}-\mathbf{k}')\mathbf{l} - i\mathbf{k}'\mathbf{m}'} \tag{323}$$

Here

$$E(\mathbf{k}) = -E_{\text{p}} + 2\langle V \rangle e^{-S_T} \cos \mathbf{kg} \tag{324}$$

is the energy of band polaron where the first term

$$E_{\text{p}} = \sum_{\mathbf{q}} |u_{\mathbf{q}}|^2 \hbar\omega_{2\mathbf{q}} \tag{325}$$

is the polaron shift—that is, the energy gap that separates the narrow polaron band [the second term in Eq. (324)] from the valence zone. The phonon operator is expressed as

$$\hat{\Phi}_{\mathbf{lm}} \equiv \hat{\Phi}_{\mathbf{lm}}(0) = \exp\left\{ \sum_{\mathbf{q}} [\Delta_{\mathbf{lm}}^{(2)}(\mathbf{q})\hat{b}_{\mathbf{q}}^+ - \Delta_{\mathbf{lm}}^{(2)*}(\mathbf{q})\hat{b}_{\mathbf{q}}] \right\} - e^{-S_T} \tag{326}$$

$$\Delta_{\mathbf{lm}}^{(2)}(\mathbf{q}) = u_{\mathbf{l}}(\mathbf{q}) - u_{\mathbf{m}}(\mathbf{q}) \tag{327}$$

and $u_{\mathbf{l}}(\mathbf{q}) = ue^{i\mathbf{lq}}$, where u is the dimensionless constant ($|u|^2 \gg 1$) that characterizes the degree of local deformation of the crystal by the carrier with respect to its interaction with the high-frequency mode, $\omega_2/2\pi = 756 \text{ cm}^{-1}$. The matrix element $V_{\mathbf{lm}\atop \mathbf{kk}'}$ in the tunnel Hamiltonian (323) has been defined in the previous subsection, expression (294). The value $\langle V \rangle$ in expression (324) is the thermal average of the aforementioned matrix element (we do not define concretely the phonon mode which leads to the increase of the resonance integral because as it will be seen from the following consideration the parameter $\langle V \rangle$ will drop out of the net result). $\hat{a}_{\mathbf{k}}^+ (\hat{a}_{\mathbf{k}})$ is the Fermi operator of creation (annihilation) of a phonon with the wave vector $\mathbf{k}$; the constant of proton–phonon coupling is [see Eq. (220)]

$$S_T = \frac{1}{2} \sum_{\mathbf{q}} |\Delta^{(2)}(\mathbf{q})|^2 \coth \frac{\hbar\omega_{2\mathbf{q}}}{2k_{\text{B}}T} \tag{328}$$

By definition [88] (see also Ref. 164), the operator of density of the band current is equal to

$$j_{\text{band}} = \frac{e}{\mathscr{V} i\hbar} \left[i \sum_{\mathbf{k},\mathbf{k}'} \left(\frac{\partial}{\partial \mathbf{k}} \delta_{\mathbf{k},0} \right) \hat{a}_{\mathbf{k}+\mathbf{k}'}^{+} \hat{a}_{\mathbf{k}'}, \bar{H}_0 \right]$$

$$= \frac{e}{\mathscr{V} \hbar} \sum_{\mathbf{k},\mathbf{k}'} \hat{a}_{\mathbf{k}}^{+} \hat{a}_{\mathbf{k}} \frac{\partial}{\partial \mathbf{k}} E(\mathbf{k}) \tag{329}$$

Performing here the thermal averaging, we obtain the following equation for the density of band current:

$$I_{\text{band}} = \frac{e}{\mathscr{V} \hbar} \sum_{\mathbf{k},\mathbf{k}'} \langle \hat{a}_{\mathbf{k}}^{+} \hat{a}_{\mathbf{k}} \rangle \frac{\partial}{\partial \mathbf{k}} E(\mathbf{k}) \tag{330}$$

where the brackets $\langle \ldots \rangle$ just mean the thermal averaging. The average value $\langle \hat{a}_{\mathbf{k}}^{+} \hat{a}_{\mathbf{k}} \rangle$ of the operator of number of quasi-particles in the polaron band is defined from the kinetic equation

$$\left(i\hbar \frac{\partial}{\partial t} + ie\mathscr{E} \right) \langle \hat{a}_{\mathbf{k}}^{+} \hat{a}_{\mathbf{k}} \rangle = -\langle [\bar{H}_{\text{tun}}, \hat{a}_{\mathbf{k}}^{+} \hat{a}_{\mathbf{k}}] \rangle \tag{331}$$

When we uncouple the commutator on the left-hand side of Eq. (331), nondiagonal corrections to the operator $\hat{a}_{\mathbf{k}}^{+} \hat{a}_{\mathbf{k}}$ appear. A correction $\hat{a}_{\mathbf{k}'}^{+} \hat{a}_{\mathbf{k}}$ caused by the electric field $\mathscr{E}$ and the interaction with phonons can be defined from the equation of motion

$$\left(i\hbar \frac{\partial}{\partial t} + E(\mathbf{k}') - E(\mathbf{k}) \right) \hat{a}_{\mathbf{k}'}^{+} \hat{a}_{\mathbf{k}} + [H_{\mathscr{E}}, \hat{a}_{\mathbf{k}'}^{+} \hat{a}_{\mathbf{k}}] = [\bar{H}_{\text{tun}}, \hat{a}_{\mathbf{k}'}^{+} \hat{a}_{\mathbf{k}}] \tag{332}$$

where the field operator $\bar{H}_{\mathscr{E}}$ (296) written in $\mathbf{k}$-presentation has the form

$$\bar{H}_{\mathscr{E}} = ie\mathscr{E} \sum_{\mathbf{k}'} \left(\frac{\partial}{\partial \mathbf{k}} \delta_{\mathbf{k},0} \right) \hat{a}_{\mathbf{k}+\mathbf{k}'}^{+} \hat{a}_{\mathbf{k}'} \tag{333}$$

With regard to Eq. (332) we derive from Eq. (331) the kinetic equation for the function $f(\mathbf{k}, t) = \langle \hat{a}_{\mathbf{k}}^{+} \hat{a}_{\mathbf{k}} \rangle$ which describes the quasi-particle distribution,

$$\frac{\partial f}{\partial t} + \frac{e\mathscr{E}}{\hbar} \frac{\partial f}{\partial \mathbf{k}} = \sum_{\mathbf{k}'} [f(\mathbf{k}, t) - f(\mathbf{k}', t)] W_{\mathscr{E}}(\mathbf{k}', \mathbf{k}) \tag{334}$$

where $W_{\mathscr{E}}(\mathbf{k}', \mathbf{k})$ is the transitions probability that is given by the expression

$$
W_{\mathscr{E}}(\mathbf{k}', \mathbf{k}) = 2\langle V \rangle \hbar^{-2} \int_0^\infty d\tau \langle \hat{\Phi}_{\mathbf{g}}(\tau) \hat{\Phi}_{\mathbf{g}}(0) \rangle
$$
$$
\times \exp\left\{ -e + i\hbar^{-1} \int_0^\tau d\tau' [E(\mathbf{k}' - e\mathscr{E}\mathbf{g}/\hbar) - E(\mathbf{k} - e\mathscr{E}\mathbf{g}/\hbar)] \right\} \quad (335)
$$

Let us represent the distribution function in the form

$$
f(\mathbf{k}, t) \simeq f^{(0)}(\mathbf{k}) + f^{(1)}(\mathbf{k}, t) \quad (336)
$$

where $f^{(0)}$ is the unperturbed distribution function and $f^{(1)}$ is a correction to it. Substituting f from expression (336) into Eq. (334), we get

$$
f^{(1)}(\mathbf{k}, t) \simeq \frac{1}{\sum_{\mathbf{k}'} W_{\mathscr{E}}(\mathbf{k}', \mathbf{k})} \frac{e}{\hbar} E(\mathbf{k}) \frac{\partial f^{(0)}}{\partial \mathbf{k}} \quad (337)
$$

Rewriting expression (330) in terms of the result (337), we obtain

$$
I_{\text{band}} = \frac{e^2}{\hbar} \sum_{\mathbf{k}} \left(\sum_{\mathbf{k}'} W_{\mathscr{E}}(\mathbf{k}', \mathbf{k}) \right)^{-1} \frac{\partial f^{(0)}(\mathbf{k})}{\partial \mathbf{k}} \frac{\partial E(\mathbf{k})}{\partial \mathbf{k}} \quad (338)
$$

First of all, let us calculate the value $W_{\mathscr{E}}(\mathbf{k}', \mathbf{k})$ (335). Allowance for the narrowness of the polaron band means that we can put $E(\mathbf{k}' - e\mathscr{E}\mathbf{g}/\hbar) \simeq E(\mathbf{k} - e\mathscr{E}\mathbf{g}/\hbar)$. This assumption reduces the calculation of the integral to the integration over τ carried out in expression (309). The final result is

$$
W_{\mathscr{E}}(\mathbf{k}', \mathbf{k}) \simeq \frac{2\pi^{1/2} \langle V \rangle^2}{\hbar^2 S_T^{1/2} \omega_2} e^{-S_T} e^{-e\mathscr{E}g/\hbar\omega_2} \quad (339)
$$

Substituting $W_{\mathscr{E}}(\mathbf{k}', \mathbf{k})$ from (339) to expression (338), setting the Boltzmann distribution for the population of polarons in the band, $f^{(0)}(\mathbf{k}) = \exp(-E(\mathbf{k})/k_B T)$, and not taking the dispersion into account, we finally arrive at the density of band proton current:

$$
I_{\text{band}} = \frac{e^2 g^2 n \mathscr{E} \omega_2 |\Delta^{(2)}|^2 \exp(-|\Delta^{(2)}|^2/2)}{2^{1/2} \pi^{1/2} k_B T} \exp(-|\Delta^{(2)}|^2 \hbar\omega_2/k_B T) \quad (340)
$$

(when deriving expression (340), we have taken into account that in the range from low to room temperature $\coth(\hbar\omega_2/2k_B T) \simeq 1$ and that the inequality $e\mathscr{E}g/\hbar\omega_2 \ll 1$ holds right up to $\mathscr{E} \sim 10^9$ V/m).

The experimental protonic conductivity versus temperature dependence curves $\sigma(T)$ are described in Refs. 193 and 195 by the simple Arrhenius law

$$\sigma(T) = \frac{\text{const}}{T} \exp\left(-\frac{E_a}{k_B T}\right)$$

in which the parameters const and E_a are determined empirically irrespective of the microscopic characteristics of the crystal. In our present consideration we derive formulas for polaronic conductivity $\sigma_{\text{hop}}(T) = I_{\text{hop}}/\mathscr{E}$ and $\sigma_{\text{band}}(T) = I_{\text{band}}/\mathscr{E}$ [where I_{hop} and I_{band} imply expressions (319) and (340) respectively], proceeding from the notion of small proton polaron. The expressions for $\sigma_{\text{hop}}(T)$ and $\sigma_{\text{band}}(T)$ will now can be compared with the experimental dependence $\sigma(T)$.

In expressions (319) and (340) the lattice constant g equals 0.8 nm, the concentration of bifurcated protons (between two hydrogen bonds of the cell) per unit volume, n, is approximately 4×10^{27} m^{-3}, and the frequencies $\omega_1 = 2\pi \times 99$ cm^{-1} and $\omega_2 = 2\pi \times 756$ cm^{-1} are expressed in s^{-1}. The coupling constant $|\Delta^{(1)}|^2$ connected the charge carrier with the vibrations of the crystal characterized by ω_1 can easily be found by comparing the calculated value of the activation energy (320) with the experimental value $E_a^{(1)} \simeq 8.8$ kJ/mol; from the equation thus formed we get $|\Delta^{(1)}|^2 \simeq 25$. Analogously, by comparing the exponential term $|\Delta^{(2)}|^2 \hbar\omega_2$ from expression (340) with the experimental value of the activation energy $E_a^{(2)} \simeq 33.1$ kJ/mol, we obtain the coupling constant of the carrier with the mode of collective vibrations of the IO$_3$ pyramids: $|\Delta^{(2)}|^2 \simeq 4$. Only one parameter of the theory—namely, the tunnel integral to the second power $|V|^2$—remains indeterminate.

Figure 12 shows the experimental curve for conductivity $\sigma(T)$ in the direction of maximum mobility of the protons [193] and the plots of the band and hopping polaron conductivity versus T dependence curves ($\sigma_{\text{hop}}(T)$ and $\sigma_{\text{band}}(T)$, respectively), constructed in conformity with Eqs. (319) and (340); the tunnel integral is assumed to be equal to $|V| = 10^{-26}$ J. As can be seen from Fig. 12, for the adopted parameter values, based on the experimental values of the frequencies of optically active modes $\omega_1 = 2\pi \times 99$ cm^{-1} and $\omega_2 = 2\pi \times 756$ cm^{-1} and on the activation energies $E_a^{(1)} \simeq 8.8$ kJ/mol and $E_a^{(2)} \simeq 33.1$ kJ/mol, the calculated total conductivity $\sigma_{\text{hop}}(T) + \sigma_{\text{band}}(T)$ is qualitatively consistent with the experimental value of the conductivity $\sigma(T)$ in the region $T > T_0 = 213$ K. Furthermore, from Fig. 12 it seen that in the region $T > T_0$ the band polaron conductivity prevails (the activation of carriers to the band is effected by the mode with the frequency of 756 cm^{-1}), whereas the hopping polaron conductivity activated by the mode with the frequency of 99 cm^{-1} should prevail in the region of $T < T_0$.
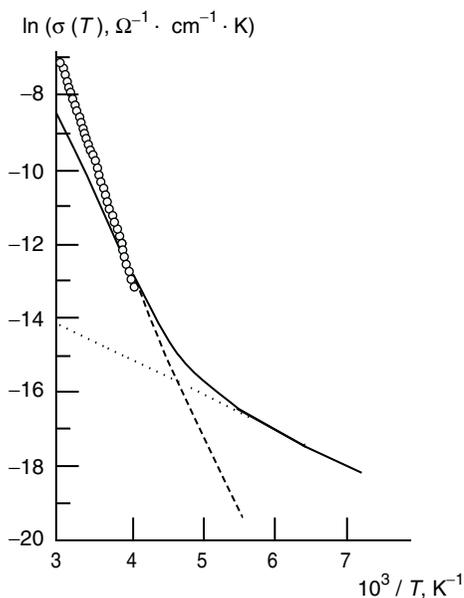
Figure 12. Conductivity of the $NH_4IO_3 \cdot 2HIO_3$ crystal as a function of the reciprocal temperature: the experimental dependence ($\bigcirc$) in the direction of maximum conductivity of the crystal; the dependence charts of hopping conductivity ($\cdots\cdots$) and of band conductivity (-----), plotted in accordance with Eqs. (319) and (340), respectively. The continuous curve is a plot of the total conductivity $\sigma_{hop} + \sigma_{band}$ as a function of the reciprocal temperature T^{-1}. (From Ref. 46.)

Thus, the polaronic mechanism of the superionic conductivity in the crystal of ammonium triiodate, which we propose in this chapter, is yet another, novel conception in the range of the known [149,150,203,204] modernized models of the hopping and continuous diffusion.

At the same time it is interesting to understand why the intracellular 756 cm^{-1} mode influences the proton conductivity. As we mentioned above, the polarized optical 99-cm^{-1} mode activates the proton mobility in the range $T_c < T < T_0$, where $T_c = 120$ K and $T_0 = 213$ K. However, the intracellular 756-cm^{-1} mode is not polarized; nevertheless, it is responsible for the proton mobility for $T > T_0$. With $T > T_c = 120$ K, these two modes demonstrate an anomalous temperature behavior and the intracellular mode begins to intensify [47]. It is the intensification of the cellular mode with T, which leads to its strong coupling with charge carriers in the crystal studied. A detailed theory of the mixture of the two modes is posed in Appendix D.

K. Polariton Effect in Crystals with Symmetric O$\cdots$H$\cdots$O Hydrogen Bonds

Up to now there is still no complete information on the mechanisms of ν(XH) stretching vibration band broadening in the infrared spectra of hydrogen-bonded systems. Among these systems the most intriguing seem to be those with strong

hydrogen bonds, when the effect is fairly pronounced and increases up to continuous absorption of several thousands wavenumbers. According to Hadzi [205], "With hydrogen bonds stronger than, for instance, those in carboxylic dimers the absorption pattern in the region above 1600 cm^{-1} is very peculiar. Instead of one, more or less structured, X—H stretching band there appear several, most often three bands. . . . This type of spectrum has been designated (i) and the bands A, B, C may be taken as characteristic of a class of very strong hydrogen bonds." So far there is a large amount of experimental data on the spectroscopic behavior of strong hydrogen bonds (the $R_{O\cdots O}$ distance ranging from 0.254 to less than 0.248 nm) [206–210], and the results obtained are related mainly to liquids and solids. The origin of the ABC structure could be explained by anharmonic coupling between the stretching high frequency X—H$\cdots$X and low frequency X$\cdots$X motions, called the strong-coupling theory [66], which we discussed in Section II.A. The substructure of shape of the ABC region can also be described by anharmonic resonance interactions with other intramolecular vibrations and Fermi resonance [211].

The hydrogen bond potential for the systems with strong hydrogen bonds is expected to be a single- or two-minima potential with comparably deep minima and low barriers, so that the proton may be considered localized in the deeper well. Furthermore, with hydrogen bond strength increasing, the redistribution of the relative intensity of thee bands is observed (the intensity of the band A decreases, whereas that of the B and particularly C band increases) along with the band A lowering in frequency [209]. Thus, for the very short hydrogen bonds the ν(XH) stretching band developed into "very strong and broad absorption culminating somewhere between 600 and 1200 cm^{-1}" [66] with sharp low-frequency edge. Furthermore, according to Hadzi [205], these spectra classified as (ii) have led to later diffraction studies. Several models have been proposed [211,212] for the description of the continuos absorption, though an explanation of such spectroscopic behavior of strong symmetrical hydrogen bonds is still questioned. It is likely that different mechanisms contribute more or less to the proton behavior in solids with strong hydrogen bonds that we propose could contribute to the knowledge of the ν(XH) shaping mechanisms under various conditions.

Let us consider molecular excitations in a system with strong hydrogen bonds, which is under the light radiation according to Ref. 213.

The existence of hydrogen bonds with a high polarizability often leads to the formation of a wide extended band in the infrared absorption spectra. This is especially clearly manifested in compounds with strong hydrogen bonds when the distance between oxygen atoms $R_{O\cdots O} \leq 0.25$ nm. Hence, the motion of a proton located at the center of a O$\cdots$H$\cdots$O bridge will cause strong modulation of the cell dipole moment. When incident light is applied to a crystal, those polarized proton oscillations will be coupled with falling photons

forming polaritons. In such a case, high-frequency intermolecular vibrations will interact just with polaritons.

High-frequency intermolecular vibrations and their interaction with optical phonons are described by the Hamiltonian [214,215]

$$H_0 = \sum_n E_n^f(0)\hat{a}_n^{f^+}\hat{a}_n^f + \frac{1}{\sqrt{N}}\sum_{n,\mathbf{k}} \hbar\chi_{\mathbf{k}}^{nf}\hat{a}_n^{f^+}\hat{a}_n^f(\hat{b}_{\mathbf{k}} + \hat{b}_{-\mathbf{k}}^+)$$
$$+ \sum_{\mathbf{k}} \hbar\Omega(\mathbf{k})\hat{b}_{\mathbf{k}}^+\hat{b}_{\mathbf{k}} \tag{341}$$

Here $E_n^f(0)$ refers to the fth excited state of a free molecule in the crystal; $\hat{a}_n^f + (\hat{a}_n^f)$ is the Bose operator of creation (annihilation) of an intramolecular vibrational excitation in the nth molecule; $\hbar\Omega(\mathbf{k})$ refers to the energy of an optical phonon with the wave vector $\mathbf{k}$ connected with proton oscillations in the $O\cdots H\cdots O$ bridge; $\hat{b}_{\mathbf{k}}^+(\hat{b}_{\mathbf{k}})$ is the Bose operator of phonon creation (annihilation); and $\hbar\chi_{\mathbf{k}}^{nf}$ is the coupling energy between the molecular excitation and phonons.

The most important feature of the present model refers to the strong interaction between the incident photons and molecular excitations. Such a model seems to be one more mechanism that explains the appearance of the extended wing in the $\nu(OH)$ infrared absorption.

The Hamiltonian of photon–phonon interaction has the form [171]

$$H = \frac{1}{2}\sum_{\mathbf{k}} H_{\mathbf{k}} \tag{342}$$

$$H_{\mathbf{k}} = \hbar\omega(\mathbf{k})(\hat{\alpha}_{\mathbf{k}}^+\hat{\alpha}_{\mathbf{k}} + \hat{\alpha}_{-\mathbf{k}}^+\hat{\alpha}_{-\mathbf{k}}) + \hbar\Omega_l(\hat{b}_{\mathbf{k}}^+\hat{b}_{\mathbf{k}} + \hat{b}_{-\mathbf{k}}^+\hat{b}_{-\mathbf{k}})$$
$$- D_{\mathbf{k}}[(\hat{\alpha}_{\mathbf{k}}^+ - \hat{\alpha}_{-\mathbf{k}})(\hat{b}_{\mathbf{k}}^+ + \hat{b}_{-\mathbf{k}}) + (\hat{\alpha}_{-\mathbf{k}}^+ - \hat{\alpha}_{\mathbf{k}})(\hat{b}_{-\mathbf{k}}^+ + \hat{b}_{\mathbf{k}})] \tag{343}$$

Here the interaction $\hbar\omega_{\mathbf{k}}$ is the energy of an incident photon with the wave vector $\mathbf{k}$, and $\hat{\alpha}_{\mathbf{k}}^+(\hat{\alpha}_{\mathbf{k}})$ the Bose operator of creation (annihilation) of the photon; the interaction matrix is

$$D_{\mathbf{k}} = -D_{\mathbf{k}}^* = -\frac{i}{2}\sqrt{\frac{\Omega_l\omega(\mathbf{k})(\varepsilon_0 - \varepsilon_\infty)}{\varepsilon_0\varepsilon_\infty}} \tag{344}$$

and neglecting the dispersion we can assume that in expressions (343) and (344) $\Omega(\mathbf{k}) = \Omega_l$ (hereafter Ω_l and Ω_t are well-known threshold frequencies for longitudinal and transversal optical modes, respectively; see, e.g., Ref. 171). The diagonalization of the Hamiltonian (343) is done by transition to new operators [171]

$$\hat{\beta}_{\mu\mathbf{k}} = u_{\mu_1}\hat{\alpha}_{\mathbf{k}} + u_{\mu_2}\hat{b}_{\mathbf{k}} - v_{\mu_1}\hat{\alpha}_{-\mathbf{k}}^+ - v_{\mu_2}\hat{b}_{-\mathbf{k}}^+ \tag{345}$$

where u_{μ_j} and v_{μ_j} are four real functions that should be determined ($\mu = 1, 2$; $j = 1, 2$).

The diagonalized Hamiltonian has the form

$$H_{\mathbf{k}} = \sum_{\mu=1}^{2} \hbar\omega_{\mu}(\mathbf{k})\hat{\beta}_{\mu\mathbf{k}}^{+}\hat{\beta}_{\mu\mathbf{k}} \tag{346}$$

The operator $\hat{\beta}_{\mu\mathbf{k}}$ satisfies the Bose commutation condition

$$[\hat{\beta}_{\mu\mathbf{k}}, \hat{\beta}_{\mu'\mathbf{k}}^{+}] = \delta_{\mu\mu'} \tag{347}$$

The following equalities are valid:

$$v_{\mu_1} = \frac{\omega_{\mu}(\mathbf{k}) - \omega(\mathbf{k})}{\omega_{\mu}(\mathbf{k}) + \omega(\mathbf{k})}u_{\mu_1}, \qquad v_{\mu_2} = \frac{\Omega_l - \omega(\mathbf{k})}{\Omega_l + \omega(\mathbf{k})}u_{\mu_2} \tag{348}$$

allowing one to eliminate v_{μ_1} and v_{μ_2}. These functions satisfy the equations

$$\sum_{s=1}^{2} (u_{\mu s}u_{\eta s} - v_{\mu s}v_{\eta s}) = \delta_{\mu\eta} \tag{349}$$

Equations (348) and (349) lead to the following equations for quantities $u_{\mu s}$ and $v_{\mu s}$:

$$u_{11}u_{21}\left[1 - \frac{(\omega_1 - \omega(\mathbf{k}))(\omega_2 - \omega(\mathbf{k}))}{(\omega_1 + \omega(\mathbf{k}))(\omega_2 + \omega(\mathbf{k}))}\right]$$
$$+ u_{12}u_{22}\left[1 - \frac{(\Omega_l - \omega_1)(\Omega_l - \omega_2)}{(\Omega_l + \omega_1)(\Omega_l + \omega_2)}\right] = 0 \tag{350}$$

$$u_{11}^2\left[1 - \left(\frac{\omega_1 - \omega(\mathbf{k})}{\omega_1 + \omega(\mathbf{k})}\right)^2\right] + u_{12}^2\left[1 - \left(\frac{\Omega_l - \omega_1}{\Omega_l + \omega_1}\right)^2\right] = 1 \tag{351}$$

$$u_{21}^2\left[1 - \left(\frac{\omega_2 - \omega(\mathbf{k})}{\omega_2 + \omega(\mathbf{k})}\right)^2\right] + u_{22}^2\left[1 - \left(\frac{\Omega_l - \omega_2}{\Omega_l + \omega_2}\right)^2\right] = 1 \tag{352}$$

One of the four quantities $u_{\mu s}$ and $v_{\mu s}$ is the free parameter; let $u_{12} = 1$. Then solving Eqs. (350)–(352), one can rewrite the phonon operator $(\hat{b}_{\mathbf{k}}^{+} + \hat{b}_{-\mathbf{k}})$ in the

interaction term of the Hamiltonian (341) via polariton operators $\hat{\beta}_{1,2\mathbf{k}}$

$$
\begin{aligned}
(\hat{b}_{\mathbf{k}}^+ + \hat{b}_{-\mathbf{k}}) = \frac{\Omega_l + \omega_1}{2\omega_1 u_{12}} \Bigg\{ &(\hat{\beta}_{1\mathbf{k}} + \hat{\beta}_{1,-\mathbf{k}}^+) \\
&- \left[\frac{u_{11}}{u_{12}} \frac{\omega(\mathbf{k})(\Omega_l + \omega_1)}{\omega_1(\omega_1 + \omega(\mathbf{k}))} - \frac{u_{21}}{u_{22}} \frac{\omega(\mathbf{k})(\Omega_l + \omega_2)}{\omega_2(\omega_2 + \omega(\mathbf{k}))} \right] \\
&\times \left[\frac{u_{11}}{u_{12}} \frac{\omega(\mathbf{k})(\Omega_l + \omega_1)}{\omega_1(\omega_1 + \omega(\mathbf{k}))} \right] (\hat{\beta}_{1\mathbf{k}} + \hat{\beta}_{1,-\mathbf{k}}^+) \\
&- \frac{u_{11}}{u_{22}} \frac{\omega(\mathbf{k})(\Omega_l + \omega_2)}{\omega_2(\omega_1 + \omega(\mathbf{k}))} (\hat{\beta}_{2\mathbf{k}} + \hat{\beta}_{2,-\mathbf{k}}^+) \Bigg] \Bigg\}
\end{aligned}
\tag{353}
$$

Here $\omega(\mathbf{k}) = ck$ and the frequencies of polariton branches are

$$
\omega_{1,2}^2(\mathbf{k}) = \frac{1}{2\varepsilon_\infty} \left(\varepsilon_0 \Omega_t^2 + c^2 k^2 \pm [(\varepsilon_0 \Omega_t^2 + c^2 k^2)^2 - 4\varepsilon_\infty c^2 \Omega_t^2 k^2]^{1/2} \right)
\tag{354}
$$

At small k these two solutions are reduced to

$$
\omega_1^2(\mathbf{k}) = \frac{c^2 k^2}{\varepsilon_\infty}
\tag{355}
$$

$$
\omega_2^2(\mathbf{k}) = \Omega_t^2 \frac{\varepsilon_0}{\varepsilon_\infty} + \frac{c^2 k^2}{\varepsilon_\infty} = \Omega_l^2 \frac{c^2 k^2}{\varepsilon_\infty}
\tag{356}
$$

In approximation $ck \gg \Omega_l$, Ω_t, Eq. (353) becomes

$$
(\hat{b}_{\mathbf{k}}^+ + \hat{b}_{-\mathbf{k}}) = \frac{\Omega_l - \Omega_t}{8\sqrt{\Omega_t \Omega_l}} \sqrt{ck} (\hat{\beta}_{2\mathbf{k}} + \hat{\beta}_{2,-\mathbf{k}}^+)
\tag{357}
$$

When obtaining Eq. (357), we let $\Omega_l > \Omega_t$ at least by several times. Hence, instead of the exciton–phonon Hamiltonian (341), one can turn to the exciton–polariton Hamiltonian:

$$
\begin{aligned}
H_0 = &\sum_n E_n^f(0)\hat{a}_n^{f+} \hat{a}_n^f + \frac{1}{\sqrt{N}} \sum_{n,\mathbf{k}} \kappa_{\mathbf{q}} \hbar \omega_2(\mathbf{k}) \hat{a}_n^{f+} \hat{a}_n^f (\hat{\beta}_{2\mathbf{k}} + \hat{\beta}_{2,-\mathbf{k}}^+) \\
&+ \sum_{\mathbf{k}} \hbar \omega_2(\mathbf{k}) \hat{\beta}_{2\mathbf{k}}^+ \hat{\beta}_{2\mathbf{k}}
\end{aligned}
\tag{358}
$$

where the effective coupling function is

$$
\kappa_{\mathbf{k}} = \tilde{\chi}_{\mathbf{k}}^{nf} \frac{\Omega_l - \Omega_t}{8\sqrt{\Omega_t \Omega_l}} \sqrt{ck}
\tag{359}
$$

and $\tilde{\chi}_{\mathbf{k}}^{nf}$ is the dimensionless function of exciton–phonon interaction. The Hamiltonian (18) is diagonalized over $\hat{\beta}_{2\mathbf{k}}$ by means of the well-known transformation [214]

$$\hat{a}_n^f = \hat{A}_n^f e^{-\hat{\sigma}_n^f} \tag{360}$$

$$\hat{\beta}_{2\mathbf{k}} = \hat{B}_{\mathbf{k}} - \sum_n \hat{A}_n^{f+} \hat{A}_n^f \frac{1}{\sqrt{N}} \kappa_{\mathbf{k}}^* \tag{361}$$

$$\hat{\sigma}_n^f = \frac{1}{\sqrt{N}} \sum_{\mathbf{k}} (\kappa_{\mathbf{k}}^* \hat{B}_{\mathbf{k}}^+ - \kappa_{\mathbf{k}} \hat{B}_{\mathbf{k}}) \tag{362}$$

where $\hat{\sigma}_n^{f+} = -\hat{\sigma}_n^f$. Consequently, the Hamiltonian is transformed to

$$H = \sum_n \varepsilon_n^f \hat{A}_n^{f+} \hat{A}_n^f + \sum_{\mathbf{k}} \hbar\omega_2(\mathbf{k}) \hat{B}_{\mathbf{k}}^+ \hat{B}_{\mathbf{k}} \tag{363}$$

$$\varepsilon_n^f = E_n^f(0) - \frac{1}{N} \sum_{\mathbf{k}} |\kappa_{\mathbf{k}}|^2 \hbar\omega_2(\mathbf{k}) \tag{364}$$

Having analyzed infrared absorption spectra, let us calculate the absorption coefficient $K(\omega)$ (see, e.g., Refs. 215 and 216):

$$G_n^f(t) = \langle\langle \hat{a}_n^f(t), \hat{a}_n^{f+}(0) \rangle\rangle \tag{365}$$

The time-dependent operators $\hat{A}_n^f$ and $\hat{B}_{\mathbf{k}}$ are as follows:

$$\hat{A}_n^f(t) = \hat{A}_n^f e^{-i\varepsilon_n^f t}, \qquad \hat{B}_{\mathbf{k}}(t) = \hat{B}_{\mathbf{k}} e^{-i\omega_2(\mathbf{k})t} \tag{366}$$

Equation (365) changes to [211,214]

$$G_n^f(t) = -i\theta(t) \langle \exp[-\hat{\sigma}_n^f(t)] \exp[\hat{\sigma}_n^f(0)] \rangle_0 \exp(-i\varepsilon_n^f t) \tag{367}$$

where

$$\theta(t) = \begin{cases} 0, & \text{if } t < 0 \\ 1, & \text{if } t \geq 0 \end{cases} \tag{368}$$

The correlation function from Eq. (367) is reduced to

$$\langle \exp[-\hat{\sigma}_n^f(t)] \exp[\hat{\sigma}_n^f(0)] \rangle_0 = [g_n^f(t)] \tag{369}$$

where the coupling function is expressed as

$$g_n^f(t) = \frac{1}{N} \sum_{\mathbf{k}} |\kappa_{\mathbf{k}}|^2 \{(n_{\mathbf{k}} + 1)e^{-i\omega_2(\mathbf{k})t} + n_{\mathbf{k}} e^{i\omega_2(\mathbf{k})t} - (2n_{\mathbf{k}} + 1)\} \tag{370}$$

Here $n_{\mathbf{k}}$ is the quantity of polarons and is defined by an external light source. In our case the intensity of the source is small, of the order of 10 μW. Therefore one would expect that the value of $n_{\mathbf{k}}$ is near unity of smaller.

The overall result for the Fourier component of the Green function, Eq. (367), is

$$G_n^f(\omega) = -i \int_t^\infty dt \exp[i(\omega - \varepsilon_n^f + i\gamma)t + g_n^f(t)] \tag{371}$$

where γ is a positive parameter that describes the adiabatic switching of exciton–polaron interaction. Furthermore, one should take into account that the coupling constant is small, $\tilde{\chi} \ll 1$. Hence, the function $g_n^f(t)$ in Eq. (370) can be expanded into a Taylor series; and for the absorption coefficient, one can gain (only two terms of expanding are saved)

$$K(\omega) \propto \mathrm{Im}\, i \int_t^\infty dt\, e^{i(\omega - \varepsilon_n^f + i\gamma)t} \left[1 + \tilde{\chi}^2 \left(\left(\frac{\Omega_l - \Omega_t}{8\sqrt{\Omega_t \Omega_l}} \right)^2 \sum_{\mathbf{k}} \left(\sqrt{ck}\right)^2 e^{-ickt} + \cdots \right) \right] \tag{372}$$

Here at the expansion we have put $n_{\mathbf{k}} = 1$, and $\tilde{\chi}_{\mathbf{k}}$ is taken in the step form: $\tilde{\chi}_{\mathbf{k}} = \tilde{\chi}$ if $k_0 \le k \le k_{max}$ and $\tilde{\chi}_{\mathbf{k}} = 0$ for all other k; that is, we believe that the exciton–phonon interaction is effective only in the region between phonon wavenumbers $k_0 = 50\ \mathrm{cm}^{-1}$ and $k_{max} = 200\ \mathrm{cm}^{-1}$. Note that we have also made an extrapolation of the function $\kappa_{\mathbf{k}}$, expression (359), from large values of k to small values.

Integrating over t, we gain from Eq. (372)

$$K(\omega) = K_0(\omega) + K_1(\omega) \tag{373}$$

$$K_0(\omega) \propto \frac{\gamma}{(\omega - \varepsilon_n^f)^2 + \gamma^2} \tag{374}$$

$$K_1(\omega) \propto \frac{\tilde{\chi}^2 (\Omega_l - \Omega_t)^2}{64 \Omega_l^2 \Omega_t} \gamma \sum_{\mathbf{k}} \frac{ck}{(\omega - \varepsilon_n^f - ck)^2 + \gamma^2} \tag{375}$$

Let us make a transfer in Eq. (375) from summation over $\mathbf{k}$ to integration:

$$\sum_{\mathbf{k}} \frac{ck}{(\omega - \varepsilon_n^f - ck)^2 + \gamma^2} = I(\omega) = \frac{2\pi}{ck_0} 2 \int_1^{k_{max}/k_0} \frac{x\, dx}{(\Xi - x)^2 + (\gamma/ck_0)^2} \tag{376}$$

where k_0 and k_{max} are effective lower and upper values of the wavenumber; moreover, in Eq. (376) the following parameter is introduced:

$$\Xi = \frac{\omega - \varepsilon_n^f}{ck_0} \tag{377}$$

The integral $I(\omega)$ in expression (376) can easily be taken:

$$
I(\omega) = \frac{1}{2}\ln\left|\frac{(ck_{max})^2 - 2(\omega - \varepsilon_n^f)ck_{max} + (\omega - \varepsilon_n^f)^2 + \gamma^2}{(ck_0)^2 - 2(\omega - \varepsilon_n^f)ck_0 + (\omega - \varepsilon_n^f)^2 + \gamma^2}\right|
$$
$$
+ \frac{\omega - \varepsilon_n^f}{\gamma}\left(\arctan\frac{ck_{max} - (\omega - \varepsilon_n^f)}{\gamma} - \arctan\frac{ck_0 - (\omega - \varepsilon_n^f)}{\gamma}\right) \qquad (378)
$$

Thus, the correction to the absorption coefficient $K_0(\omega)$ (373) takes the form

$$
K_1(\omega) \propto \frac{\pi}{16}\tilde{\chi}^2\frac{(\Omega_l - \Omega_t)^2}{\Omega_l^2\Omega_t}\gamma I(\omega) \qquad (379)
$$

Utilizing expressions (374) and (379), we can calculate the absorption coefficient (373) as a function of the following parameters: the constant of exciton–phonon coupling $\tilde{\chi}$, the longitudinal phonon frequency Ω_l (that is, the proton stretching frequency in the hydrogen bridge $O\cdots H\cdots O$), the transversal phonon frequency Ω_t (that is, the bending proton frequency in the bond $O\cdots H\cdots O$), the effective boundary values of the polariton branch ck_0 and ck_{max}, and the damping constant γ. Numerical calculations of the absorption coefficient $K(\omega)$ have been performed while varying all of these parameters [213]. The spectra calculated have shown very significant deviations of the $\nu(OH)$ band from the Lorentzian profile (i.e., when $\tilde{\chi} = 0$).

In order to check the validity of the suggested approach, we have applied theoretical results to the OH stretching band-shape modeling for the α-modification of the acid potassium iodate $KIO_3\cdot HIO_3$ crystal (the spectra of the said crystal have been recorded in Ref. 217). The α-modification of the $KIO_3\cdot HIO_3$ crystal is known to exhibit ferroelectric behavior [218]. The structure is monoclinic with space group $P2_1/c$ in the paraelectric phase, and is assumed to change to $P2_1$ below the Curie temperature $T_c = 223$ K. The principal feature of the crystal structure of α-$KIO_3\cdot HIO_3$, as revealed by inelastic neutron scattering [219], is a short $O-H\cdots O$ hydrogen bond ($O\cdots O$ distance about 0.249 nm) linking two iodate ions. In the paraelectric phase, the symmetric $O\cdots H\cdots O$ hydrogen bond takes place).

In Fig. 13 the experimental spectrum of the α-$KIO_3\cdot HIO_3$ crystal in the $\nu(OH)$ region and the calculated spectrum [by formulas (373), (374), and (379)] are presented. It is easy to see that the theoretical curve gives a fairly good fitting of the experimental spectrum. The negligible deviation of the experimental and calculated spectra observed in the middle part of the figure may be explained by the overlapping of the $\delta(OH)$ absorption band in this region of the spectrum.

Thus the inclusion of the polariton part into the absorption coefficient of a solid with strong symmetric hydrogen bonds predicts that instead of the narrow
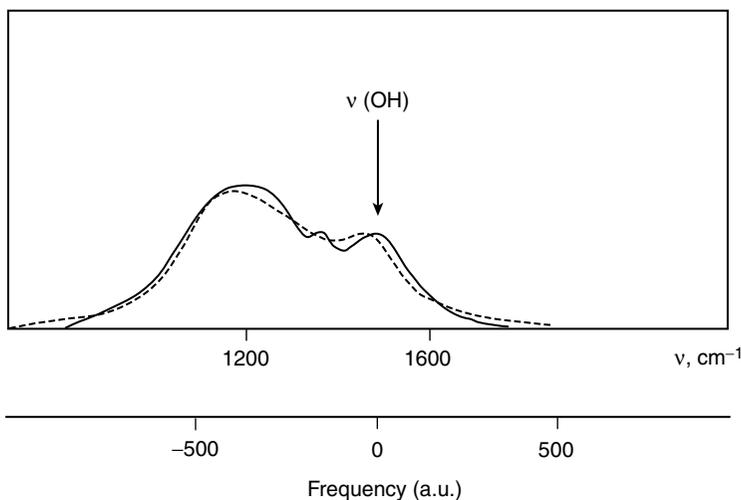
Figure 13. Infrared absorption spectrum of the α-$KH(IO_3)_2$ crystal in the $\nu(OH)$ stretching region (——) and the numerically calculated spectrum (-----). The values of the fitting parameters (in cm^{-1}) are: $\Omega_l = 200$, $\Omega_t = 50$, $ck_0 = 10$, $ck_{max} = 500$, $\gamma = 100$. The dimensionless coupling constant $\tilde{\chi} = 0.008$. (From Ref. 214.)

high-frequency OH stretching band, a very strong broad absorption should appear in the frequency region below 1200 cm^{-1}. The theory described can be applied to the analysis of any real crystal that includes strong symmetric hydrogen bonds.

IV.   BACTERIORHODOPSIN CONSIDERED FROM THE MICROSCOPIC PHYSICS STANDPOINT

A.   Active Site of Bacteriorhodopsin and the Proton Path

Bacteriorhodopsin is a membrane protein, which is present in the purple membrane of *Halobacterium halobium*. Bacteriorhodopsin is an energy-transducing molecule operating as a light-driven molecular generator of proton current: It transports protons from the cytoplasmic to the extracellular side of the membrane [220]. Upon light excitation, the light-adapted form of bacteriorhodopsin undergoes a cycle of chemical transformations including at least five intermediates, K, L, M, N, and O (and the ground state, bR), with absorption bands covering almost all the visible range [221,222].

Henderson et al. [223] presented a detailed pattern of the structure of bacteriorhodopsin using high-resolution cryoelectron microscopy. Using X-ray and neutron diffraction techniques, Dencher et al. [224–227] could decode the

secondary and tertiary structure of bacteriorhodopsin during the photocycle. Nevertheless, we should emphasize that the resolution is still restricted by several tenths of a nanometer. The most important amino acid residues of bacteriorhodopsin molecule participating in a protein–chromophore interaction have been determined by methods of genetic engineering (see, e.g., Refs. 228–230).

It is now firmly established that the primary light-induced processes include a very fast shift of electron density along the protonated Schiff base retinal and its all-*trans*–13-*cis* isomerization, leading to the formation of the first stable intermdiate K [231] which stores about one-third of the absorbed light energy [232]. Resonance Raman and Fourier transform-infrared (FT-IR) spectroscopies have provided significant information about the nature of the alternations of the retinal and of neighboring amino acids residues constituting an active site during the bacteriorhodopsin photocycle. Various intermediates have been stabilized, and FT-IR difference spectra of the intermediates have been taken (see, e.g., Refs. 6, 222, 230, and 233). The key changes involve Tyr 185, Asp 85, Asp 96, Asp 212, Glu 204, and very plausible Tyr 57.

Different aspects of bacteriorhodopsin functioning have been studied early [35–37, 223, 233–249]. However, as a rule, the researchers have described the mechanism of proton transport phenomenologically, though the analysis of the results taken from the FT-IR difference spectra yielded detailed descriptions of the proton state in a proton pathway in all of the above-mentioned intermediates (see, e.g., Zundel [6]).

Below we propose a microscopic model of the light-induced proton transport in bacteriorhodopsin, which is based on the active site model proposed in Refs. 6, 35–37, 233, and 248. Namely, we shall analyze the influence of the charge separation in the excited chromophore on a set of proton absorption bands covering almost all the visible range [221,222].

Henderson et al. [223] presented a detailed pattern of the structure of bacteriorhodopsin using high-resolution cryoelectron microscopy. Using X-ray and neutron diffraction techniques, Dencher et al. [224–227] could decode the secondary and tertiary structure of bacteriorhodopsin during the photocycle. Nevertheless, we should emphasize that the resolution still shows transitions in the active site (protonation of counterions, deprotonation of Schiff base, and reprotonation of counterions), leading to a metastable state of the protein.

Since bacteriorhodopsin is a chromoprotein complex, a change in the interaction between the Schiff base of retinal-chromophore and the protein-opsin, taking place in the active site, plays a central role in light energy conversion and membrane color regulation. Opsin consists of a single polypeptide chain of 248 amino acids residues. It forms seven transmembrane segments, A–G, having α-helical secondary structure. The tertiary structure of these transmembrane segments determined by electron microscopy [223] is
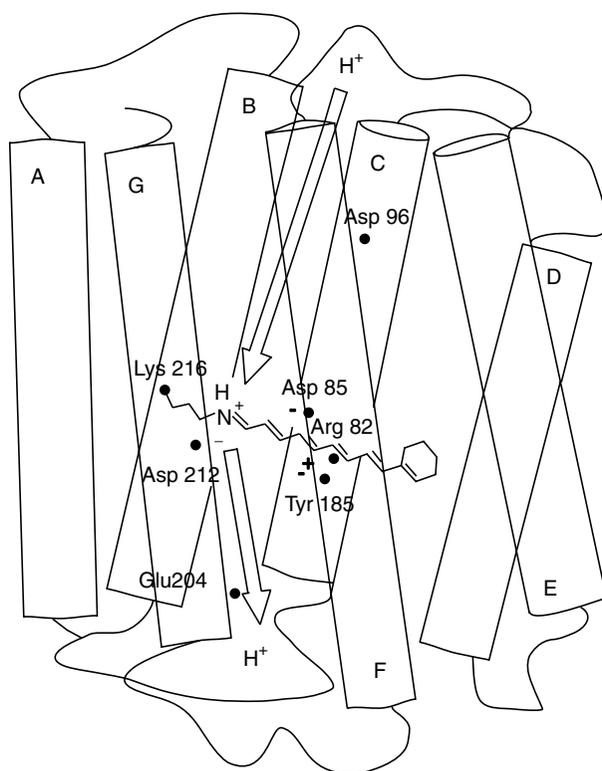
Figure 14.   Spatial model of bacteriorhodopsin structure. (From Ref. 37.)

shown schematically in Fig. 14. The retinal covalently bound via the protonated Schiff base to the amino acid residue Lys 216 [220] in the middle of the G segment is also shown in Fig. 14. The retinal long axis is inclined at an angle of about 20° relative to membrane plane [250]. The β-ionone ring of the retinal points away from the cytoplasmic side of the membane [251]. Two orientations of the N—H bond of the retinal are possible [238,246]: The N—H bond may point toward either the cytoplasmic or the extracellular side of the membrane. Experimental data on photocycle kinetics [238] show that both these orientations may occur in the native membrane. Henceforth, we will consider only one orientation state, shown in Fig. 14.

    Figure 14 also shows the amino acid residues playing a key role in the proton transport: Asp 85, Asp 212, and Tyr 185 with negatively charged terminal groups that are counterions with respect to the positively charged protonated Schiff base; Asp 85 and Asp 96 are inner proton acceptor and donor, respectively; Arg 82 favors the deprotonation of the retinal Schiff base. The data

on light-induced FT-IR difference spectroscopy indicate that aspartic and tyrosine acid terminal groups undergo the largest changes during the bacteriorhodopsin photocycle [6,252,253]. Zundel and co-workers [6,233,241, 254] constantly noticed that the proton pathway includes tyrosines and structural water. And at the end of the pathway, Glu 204 is present [6,230,255].

The principal structure of the outlet proton channel is now considered as being composed of water molecules and the terminal −OH group of Asp 212, Glu 204 and, possibly, tyrosine(s). In contrast, the inlet channel has hydrophobic side chains of amino acid residues, except for the polar side chain of Asp 96 which is positioned about 0.1 nm from the Schiff base and about 0.6 nm from the cytoplasmic end of the C segment [224]. One or two water molecules close to the Schiff base [256–258] perhaps play a structure forming role and promote the proton dynamics.

The light-induced isomerization of the retinal shifts the protonated Schiff base into a new environment. A subsequent charge separation triggers the rearrangement of the active site, resulting in determination of the connection of the proton with the retinal Schiff base down to the critical value when the Schiff's base proton is transferred to Asp 85.

The measurements carried out by light-induced FT-IR difference spectroscopy indicate that the bR → K transition is accompanied by the protonation of Tyr 185 ($-O^- \rightarrow -OH$) [259–261] and the creation of new H bonds [233,6]. These bonds are formed between the protonated Schiff base and the terminal group of Asp 85, as well as between the terminal groups of Asp 212 and Tyr 185. The protonation of Tyr 185 can easily be explained using the results of quantum chemical calculations of the charge distribution in the intermediate K [262]. In accordance with these results, the negative charge is increased near the C_{14} of 13-*cis*-retinal, which is located close to the terminal group of Tyr 185 (Fig. 15). This suggests that the negative charge favors H^+ transfer from the terminal group $-NH_3^+$ of Arg 82 to that of Tyr 185 via the side chain of Asp 212, because the negative charge of its terminal group is partially neutralized by the positive charge concentrated near C_{15} and the side chain of Lys 216 (Fig. 15b).

FT-IR spectrometric measurements [252,263] show that Asp 96 undergoes deprotonation ($-COOH \rightarrow -COO^-$) during the K → L transition. From our point of view, this process can be understood if one considers the positive charge at the C_{15} of 13-*cis*-retinal and the side chain of Lys 216 (Fig. 16). It is obviously favors the deprotonation process for the terminal group of Asp 96. In turn, the appearance of the negative charge distant from the active side can promote changes in the protein structure (leading, in particular, to a variation in geometry and strength of the H bonds [245]), which have been observed experimentally [264–269].

The protonated Schiff base of all-*trans*-retinal in the ground state has a pK_a greater than 13 [270], which provides its strong connection with the retinal by
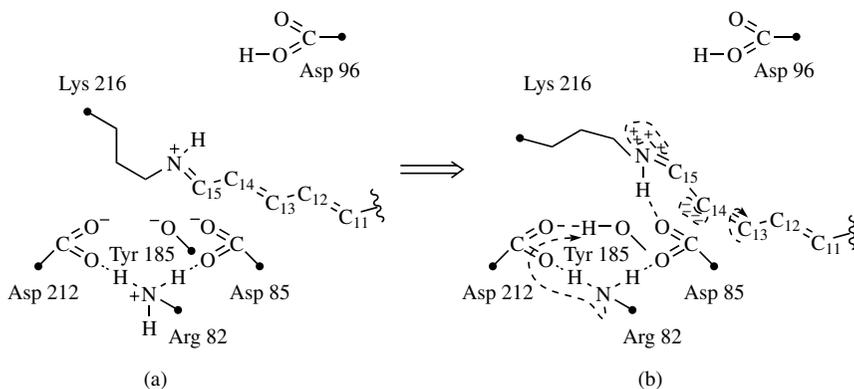
Figure 15. Scheme of the active site changes at the transition from the ground state bR (a) to the intermediate K (b). (From Ref. 37.)

means of an electrostatic attractive interaction between the positive protonated Schiff base and negative counterions. Charge separation in the active site taking place after the all-*trans*–13-*cis* isomerization of the retinal makes the connection of the proton with the Schiff base weaker. This naturally results in a decrease in the pK_a value for the Schiff's base proton.

At the L $\rightarrow$ M transition, two protons neutralize the counterions [233]: One proton transfers from the Schiff base to the terminal group of Asp 85 [271,272], and another transfers from the terminal group of Tyr 185 to that of Asp 212 [273]. Note that this process follows the deprotonation of Asp 96, including an additional negative charge on the terminal group −COOH of Asp 85 and Asp 212. This is the mechanism of additional decrease of the Schiff's base
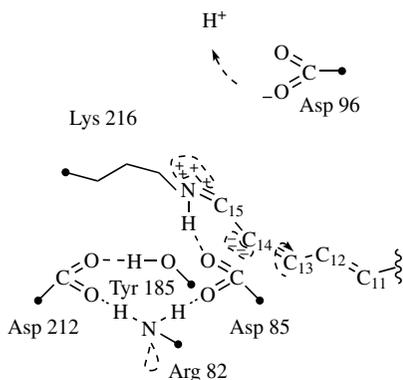
Figure 16. Scheme of the active site for the intermediate L. (From. Ref. 37.)

proton pK_a down to the critical value (≈ 3 [274]), at which the proton transfers from the Schiff base to the terminal group of Asp 85. This process, in turn, decreases the charge separation in the active site and thereby increases the acceptor property of Asp 212. The proton from Tyr 185 is then captured by this acceptor (Fig. 17a).

In the next stage of the L → M transition the terminal group of Asp 96 is reprotonated. This is followed by deprotonation of the Schiff base, which becomes less positive than that in the ground state of the retinal. Hence, the inductive interaction between the Schiff base and Asp 96 decreases; as a result, Asp 96 is able to resume its initial state (−COOH).
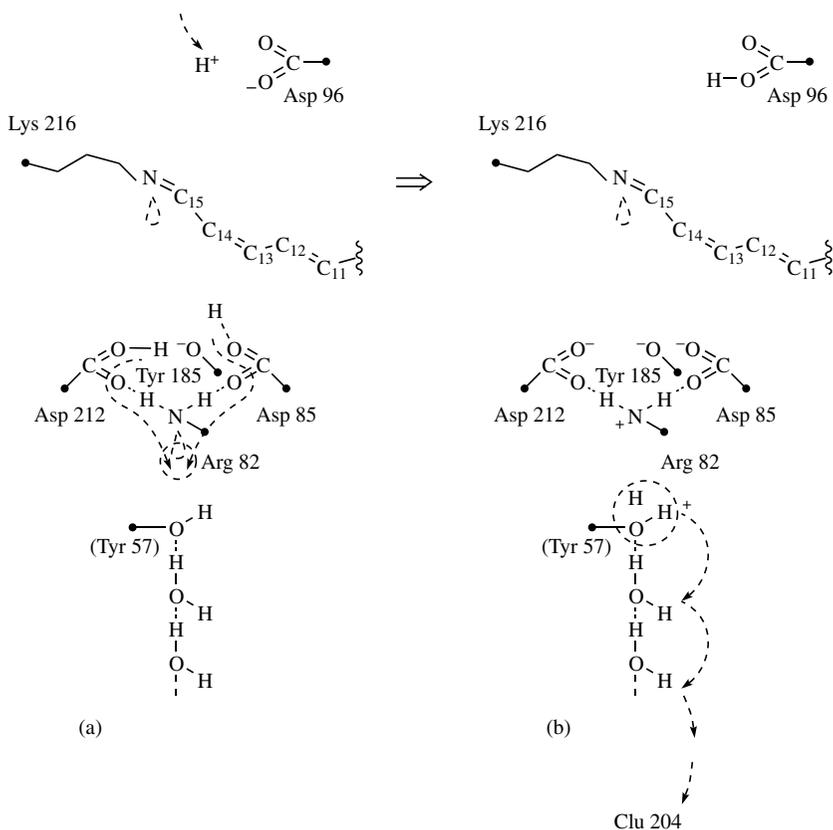
Figure 17. Scheme of the active site changes during the L → M transition. (a) Formation of the hydrogen-bonded chain at the moment before the reprotonation of Arg 82. (b) Reconstruction of the active site (see Figure 15a) and the excess proton hopping motion along the hydrogen-bonded chain. (From Ref. 37.)

The dominant effect in the proton transport is due to changes in protein structure (see also Refs. 258, 275, and 276). These structural changes lead to the formation of a hydrogen bond between the amino acid residues (Asp 85–Arg 82–Asp 212), holding a proton of the Schiff base, and the outlet proton channel to the terminal group $-NH_2$ of Arg 82 (Fig. 17a). This is supported by data from Ref. 233. The most possible candidate for the formation of this hydrogen bond is terminal group of Tyr 57.

B. Light-Excited Retinal and Evolution of Excitations in the Retinal

After light with energy $\hbar\omega \simeq 213$ kJ/mol (or $85k_B T$, where $T = 300$ K) has been absorbed by retinal in bacteriorhodopsin, the retinal transfers to the excited state ($^1B_u \leftarrow S_0$ transition [238]) and electron density is shifted along the retinal polyene chain toward the nitrogen atom over a few femtoseconds. This provides a large change in the retinal dipole momentum $\Delta\mu \approx 13.5$ D, which has been confirmed using second harmonic generation and two-photon absorption experiments [277,278].

Let us treat the process of retinal excitation ($\pi \rightarrow \pi^*$ electron transition) and its subsequent relaxation into the vibronic subsystem.

One of the main elements of the retinal molecule is a polyene chain that is long enough. The absorption band of such a chain lies in visible range (see, e.g., Ref. 279); therefore just the polyene chain is responsible for the absorption by $\lambda_{max} = 570$ nm. The spectra of polyenes are characterized by a vibrational structure of the main absorption band. In bacteriorhodopsin retinal, this structure is on the band of absorption with $\lambda_{max} = 419$ nm [280]. Therefore, the main, more intensive band of observing the vibrational structure on the main absorption band is attributed probably to the stronger interaction of the excited π-electronic (π^*-electronic) cloud in bacteriorhodopsin with a polar environment (in this case the energy of the π^*-electronic cloud is a little bit higher than in the previous case, and therefore the energy is nearer to energies of the protein polar groups' vibration). These facts indicate that when considering the kinetics of the π-electronic cloud, we must take into account the connection of the cloud with vibration of the conjugate chain nuclei. Experiments on the isolated retinal have enabled us to conclude [35] that a *cis–trans* distribution occurs on vibration-excited levels. And the effective intersystem transition at these levels plays a substantial role.

Now we will discuss the characteristics of the vibrational and π-electronic subsystems of the chain of coupled C=C bonds [35]. An isolated C=C group undergoes high-frequency valence (intramolecular) vibration, $\Omega = 2\pi \times 5 \times 10^{13}$ s^{-1}. The groups in the polyene chain are interconnected by σ bonds (the vibrational frequency of the carbon atoms in the isolated C—C group equals about $2\pi \times 2 \times 10^{13}$ s^{-1}), hence the virtual vibrational quantum interchange is substantial. By such a strong bond the spectrum of intramolecular vibrations of

the retinal polyene chain is formed in an energetic band with a width $2\hbar\Omega$. On the other hand, in the polyene chain the absolute meaning of the resonance integral of the electron overlap in the C=C bond may be evaluated by the value $\hbar M = (4\text{–}6) \times 10^{-19}$J (therefore, $M = 2\pi \times (6\text{–}9) \times 10^{14}$ s^{-1}), and the resonance integral of the π-electron overlap between two nearest groups C=C can be evaluated by the value $0.7\hbar M$. The magnitude of the resonance integral of π electrons in the lowest excited states should be at least as much as one mentioned above. Consequently, the width of the π^*-electronic cloud energetic band (excitonic band) can be assumed to be equal to $2\hbar M$; the vibrational band comes out to $2\hbar\Omega$, and the inequality $2\hbar M \gg 2\hbar\Omega$ holds true.

The electronic excitation in the retinal is coherent [35], and this means that the interaction of excited electrons with retinal's vibrations is small. That is, the energy of exciton–vibration interaction $\hbar\chi$ is much smaller than the excitonic and vibrational bands, $\hbar\chi \ll 2\hbar\Omega \ll 2\hbar M$.

The Hamiltonian of intramolecular collective vibrations of the quasi-one-dimensional system of coupled C=C bonds can be written as

$$H_{\text{vib}} = \sum_l \hbar\Omega \hat{B}_l^+ \hat{B}_l + \sum_{l,m} \hbar\delta\Omega_{l-m} \hat{B}_l^+ \hat{B}_m \tag{380}$$

where Ω is a characteristic vibrational frequency of carbon atoms (sites) in polyene chain, $\hat{B}_l^+ (\hat{B}_l)$ is the Bose creation (annihilation) operator of an vibrational quantum in the lth site, and $\delta\Omega_{l-m}$ is an exchange frequency of the virtual vibrational quantum between the lth and the mth sites.

To diagonalize the Hamiltonian (380), let us go from the site representation to the momentum representation of the creation (annihilation) operators of vibrations through the transform $\hat{B}_l = N^{-1/2} \sum_q \hat{B}_q \exp(-iqR_l)$. Here N is a number of carbon atoms in the chain; $R_l = lg_0$, where g_0 is a distance between the nearest C atoms; we suppose $g_0 = r_{\text{C=C}} \approx r_{\text{C–C}}$—that is, $g_0 = 0.135$ to 0.146 nm. In the momentum representation the Hamiltonian

$$H_{\text{vib}} = \sum_q \hbar\Omega_q \left(\hat{B}_q^+ \hat{B}_q + \frac{1}{2} \right) \tag{381}$$

Here $\hat{B}_q^+ (\hat{B}_q)$ is the Bose creation (annihilation) operator of the collective intensive vibrational quantum with an energy of $\hbar\Omega_q$ and quasi-momentum of $\hbar q$.

The excitonic Hamiltonian

$$H_{\text{exc}} = \sum_k \hbar\varepsilon_k \hat{A}_k^+ \hat{A}_k \tag{382}$$

where $\hat{A}_k^+ (\hat{A}_k)$ is the Fermi creation (annihilation) operator of a coherent exciton in the band having the energy $\hbar\varepsilon_k$ and quasi-momentum $\hbar k$.

In the case of the coherent vibronic state excitations, we shall take into account a change of the frequency of the collective vibrations in the polyene chain caused by the exciton excitation:

$$\Omega_q \rightarrow \Omega_q + \frac{\partial \Omega_q}{\partial N_q} \delta N_q$$

Next, we pass to the operators of the exciton-state occupation numbers $\delta N_q \rightarrow \hat{N}_q = \hat{A}_q^+ \hat{A}_q$ and replace $\partial \Omega_q / \partial N_q \rightarrow \Delta \Omega_q$.

The total Hamiltonian of the system under consideration assumes as

$$H = H_0 + H_1 \tag{383}$$

$$H_0 = \sum_q H_{0q} = \sum_q \left\{ \hbar \varepsilon_q \hat{A}_q^+ \hat{A}_q + \hbar \Omega_q \left(\hat{B}_q^+ \hat{B}_q + \frac{1}{2} \right) \right.$$

$$\left. + \hbar \Delta \Omega_q \hat{A}_q^+ \hat{A}_q \left(\hat{B}_q^+ \hat{B}_q + \frac{1}{2} \right) \right\} \tag{384}$$

$$H_1 = \sum_{k,q} \left\{ \hbar \chi_q \hat{B}_q \hat{A}_{k-q}^+ \hat{A}_k + \hbar \chi_q^* \hat{B}_q^+ \hat{A}_k^+ \hat{A}_{k-q} \right\} \tag{385}$$

If we neglect the exciton–vibration interaction (i.e., the operator H_1), the wave functions of collective vibrations and of coherent excitonic states of the retinal molecule (they are specified by quasi-momentum $\hbar q$ and are the proper functions of the Hamiltonian H_{0q}) form an orthonormal basis

$$|q; f_q, \mu_q\rangle = \frac{1}{\sqrt{\mu_q!}} (\hat{B}_q^+)^{\mu_q} (\hat{A}_q^+)^{f_q} |q; 0, 0\rangle \tag{386}$$

where $f_q = 0, 1$; $\mu_q = 0, 1, \ldots$; $|q; 0, 0\rangle$ is the vector of a ground state and describes the system without quasi-particles.

Let us consider the kinetics of the excitonic excitation in the retinal using the method of nonequilibrium statistical operator [281]. We denote the statistical operator of the system by $\rho(t)$ and shall study the evolution of its following matrix elements:

$$\mathcal{N}_{qq}(t) = \text{Tr}\{\rho(t) \hat{B}_q^+ \hat{B}_q\}$$
$$\rho_{kk}(t) = \text{Tr}\{\rho(t) \hat{A}_k^+ \hat{A}_k\} \tag{387}$$
$$\underset{qq}{P_{kk}}(t) = \text{Tr}\{\rho(t) \hat{A}_k^+ \hat{A}_k \hat{B}_q^+ \hat{B}_q\}$$

Here $\mathcal{N}_{qq}(t)$ is a nonequilibrium function of the excitations distribution in vibrational subsystem at the moment of time t; matrix elements $\rho_{kk}(t)$ determine

a probability of existence at the moment of t of the π-electronic cloud in an excited state with a quasi-momentum $\hbar k$ and with an energy $\hbar \varepsilon_k$; matrix elements $P_{kk}(t)$ describe a coupling between the π^*-electronic cloud and the vibrational subsystem.

The equation of evolution of the matrix elements $\mathcal{N}_{qq}(t)$ has the form

$$i\hbar \frac{\partial \mathcal{N}_{qq}(t)}{\partial t} = -\text{Tr}\{\rho^{(0)}(t)[H_0, \hat{B}_q^+ \hat{B}_q]\}$$

$$-\frac{i}{\hbar} \lim_{\eta \to 0} \int_{-\infty}^{t} d\tau e^{\eta \tau} \text{Tr}\{\rho^{(0)}(t)[H_1(\tau), [H_1, \hat{B}_q^+ \hat{B}_q]]\} \qquad (388)$$

Similar equations are derived for $\rho_{kk}(t)$ and $P_{kk}(t)$. In Eq. (389), $\rho^{(0)}(t)$ is statistical operator of the excitonic vibrational system (retinal) in thermostat (protein) in the absence of interaction H_1; the operator $H_1(\tau)$ equals $\exp(i\tau H_0/\hbar)H_1 \exp(-i\tau H_0/\hbar)$. From Eq. (388) and from similar equations for $\rho_{kk}(t)$ and $P_{kk}(t)$ with regard to expressions (383) to (385), we derive the following system of the differential coupling equations:

$$\frac{\partial}{\partial t} \mathcal{N}_{qq}(t) = \sum_k v_{kq}(t) \left\{ \rho_{kk}(t) + P_{k-q,k-q}(t) - P_{kk}(t) \right\} \qquad (389)$$

$$\frac{\partial}{\partial t} \rho_{kk}(t) = \sum_k v_{kq}(t) \left\{ -\rho_{kk}(t) + \rho_{k-q,k-q}(t) \right.$$

$$\left. -2P_{kk}(t) + P_{k-q,k-q}(t) + P_{k+q,k+q}(t) \right\} \qquad (390)$$

$$\frac{\partial}{\partial t} P_{kk}(t) = v_{kq}(t) \left\{ \rho_{k-q,k-q}(t) + 3[P_{k-q,k-q}(t) - P_{kk}(t)] \right\} \qquad (391)$$

In the equations derived, the terms containing products of four and more Fermi operators $\hat{A}_q$ and $\hat{A}_q^+$ are omitted. Besides, when deriving the equations, in $H_1(\tau)$ the uncoupling of the operator products have been made:

$$2\hat{A}_q^+ \hat{A}_q \hat{B}_q^+ \hat{B}_q|_{\tau} \to \langle \hat{A}_q^+ \hat{A}_q \rangle_{\tau} \hat{B}_q^+ \hat{B}_q|_{\tau} + \langle \hat{B}_q^+ \hat{B}_q \rangle_{\tau} \hat{A}_q^+ \hat{A}_q|_{\tau}$$

$$= \rho_{qq}(\tau) \hat{B}_q^+ \hat{B}_q|_{\tau} + \mathcal{N}_{qq}(\tau) \hat{A}_q^+ \hat{A}_q|_{\tau} \qquad (392)$$

It is admissible if

$$\rho_{qq}(\tau)|\Delta \Omega_q| < \varepsilon_q, \Omega_q, \qquad \mathcal{N}_{qq}(\tau)|\Delta \Omega_q| < \varepsilon_q, \Omega_q \qquad (393)$$

In Eqs. (389)–(392) the function of a momentary exciton–vibration interaction is

$$v_{kq}(t) = |\chi_q|^2 \frac{\tilde{\Omega}_q(t)}{[\tilde{\varepsilon}_{k-q}(t) - \tilde{\varepsilon}_k(t)]^2 - \tilde{\Omega}_q^2(t)} \qquad (394)$$

where

$$\tilde{\varepsilon}_k(t) = \varepsilon_k + \Delta\Omega_k\left[\mathscr{N}_{kk}(\tau) + \frac{1}{2}\right], \qquad \tilde{\Omega}_q(t) = \Omega_q + \Delta\Omega_q\rho_{qq}(t) \qquad (395)$$

The inclusion of the term $\hbar\Delta\Omega_q\hat{A}_q^+\hat{A}_q\hat{B}_q^+\hat{B}_q$ in the Hamiltonian (384) makes it possible to avoid a singularity in expression (394) at certain values of k and q. Note that in expression (394), $v_{kq}(t) > 0$ when $q\pi/2g_0$. A choice of the function of exciton–vibration interaction as

$$\chi_q = \begin{cases} \chi > 0, & q \geq \pi/2g_0 \\ 0, & q \leq \pi/2g_0 \end{cases} \qquad (396)$$

satisfies the demands mentioned above.

The initial conditions for equations (389)–(391) are

$$\rho_{kk}(t)\big|_{t=0} = \delta_{k0}, \qquad \mathscr{N}_{qq}(t)\big|_{t=0} = P_{kk}_{qq}(t)\big|_{t=0} = 0 \qquad (397)$$

Now let us pass to the Laplace transformation over time variable t in Eqs. (390)–(391):

$$\rho_{kk}^L(p) = \int_0^\infty e^{-pt}\rho_{kk}(t)\,dt, \qquad P_{kk}^L_{qq}(p) = \int_0^\infty e^{-pt}P_{kk}_{qq}(t)\,dt \qquad (398)$$

For this purpose we should multiply both sides in Eqs. (390) and (391) by e^{-pt} and integrate over t from 0 to ∞. As a result, we get the equations

$$p\rho_{kk}^L(p) - \rho_{kk}(t)\big|_{t=0} = \sum_q v_{kq}\big\{ -\rho_{kk}^L(p) + \rho_{k-q,k-q}^L(p)$$
$$- 2P_{kk}^L_{qq}(p) + P_{k-q,k-q}^L_{\bar{q},q}(p) + P_{k+q,k+q}^L_{\bar{q},q}(p)\big\} \qquad (399)$$

$$P_{kk}^L_{qq}(p) - P_{kk}_{qq}(t)\big|_{t=0} = v_{kq}\big\{\rho_{k-q,k-q}^L(p) + 3[P_{k-q,k-q}^L_{\bar{q},q}(p) - P_{kk}^L_{qq}(p)]\big\} \qquad (400)$$

Here the neglecting of the dependence of v_{kq} on t occurs owing to relationships (393) and (395). With the help of Eq. (400), correlators $P_{kk}^L_{qq}(p)$ in Eq. (399) can be eliminated, and after that the inverse Laplace transform can be made. This brings us to equation

$$\frac{\partial}{\partial t}\rho_{kk}(t) = -\sum_q \tilde{v}_{kq}\{\rho_{kk}(t) + \rho_{k-q,k-q}(t)\} \qquad (401)$$

where $\tilde{v}_{kq} = v_{kq}(1 + 1/9)^{-1}$; below we set $\tilde{v}_{kq} \simeq v_{kq} \simeq \bar{v}$.

Let us substitute now the difference $[P_{k-q,k-q}(t) - P_{kk}(t)]$ from Eq. (391) into Eq. (389) and then perform uncoupling $P_{kk}(t) \rightarrow \rho_{kk}(t)\mathcal{N}_{qq}(t)$. The term $(\partial/\partial t)\rho_{kk}(t)$ on the left-hand side of Eq. (390) can now be replaced by the right-hand side of Eq. (401). Then for the function $R(t) = \sum_k \rho_{kk}(t)$ and for the characteristic function $\mathcal{N}(t) = \mathcal{N}_{qq}(t)|_{max}$ we obtain the following equations:

$$\frac{\partial}{\partial t}R(t) = -2N\bar{v}R(t) \tag{402}$$

$$\frac{\partial}{\partial t}\mathcal{N}(t) = \frac{1}{N}[2N\bar{v}t + \ln(3 - e^{-2N\bar{v}t})](3 - e^{-2N\bar{v}t}) \tag{403}$$

In the retinal the number of sites, N, is 12 and $\bar{v} \ll \Omega$; and because of $\Omega = 2\pi \times 5 \times 10^{13}$ s^{-1} and $M \geq 2\pi \times 5 \times 10^{14}$ s^{-1}, it is possible to set $v \simeq 2 \times 10^{13}$ s^{-1}. The characteristic time of vibration relaxation of the electronic excitation has an order 10^{-13} to 10^{-12} s [282]. In this case for the light-excited retinal in bacteriorhodopsin, according to experimental data [283] we have $t = t_{rel} = 7 \times 10^{-13}$ s^{-1}. Thus, according to Eq. (402) $R(t_{rel}) = 0$. Then from Eq. (403) we derive the distribution function, which is not in equilibrium, of collective intramolecular vibrations of the retinal at the moment of t_{rel}:

$$\mathcal{N}(t_{rel}) \simeq \frac{2}{3}\bar{v}t_{rel} \simeq 10 \tag{404}$$

The distribution function (404) is much greater than the Planck distribution function

$$\frac{1}{e^{\hbar\Omega/k_B T} - 1} \simeq e^{-\hbar\Omega/k_B T} \ll 1 \tag{405}$$

which characterized vibrations of sites in retinal before the photon absorption (we recall that $\hbar\Omega \simeq 85\,k_B T$, $T = 300$ K). The function $\mathcal{N}(t)$ can be written formally in the form of the Planck function written for more high effective temperature T^*, $[\exp(\hbar\Omega/k_B T^*) - 1]^{-1}$. Then at the moment t_{rel} the effective temperature is expressed as

$$T^* = \frac{\hbar\Omega}{k_B \ln(11/10)} \simeq 80\,T \tag{406}$$

Thus the energy passed into the vibrational subsystem is equal to $\hbar\Omega\mathcal{N}(t_{rel}) \simeq 80\,k_B T$; that is, virtually all the total energy of the absorbed photon ($85\,k_B T$) has passed on to the vibrational subsystem by the time of $t = t_{rel}$.

Clearly, the excited π^*-electron subsystem should introduce a significant charge distribution in polyene chain of the retinal. It is the charge separation that plays an important role in the destabilization of the excited retinal. In fact, the initial all-*trans* conformation of the retinal is stabilized by an attractive

electrostatic interaction between the protonated Schiff base and nearby nega-tively charged residues (counterions). In contrast, the electronic excitation of the retinal generating a negative charge near the retinal Schiff base destabilizes the all-*trans* conformation; as a consequence, fast torsional vibrations can be initiated [284–286]. The frequency of these vibrations can estimated from a simple scheme of repulsive electrostatic interaction between the π^*-electron cloud, having an effective charge of e^*, and the counterions, with a general of e. We can get an evaluation of the energy of this interaction by the expression

$$W = \frac{ee^*}{4\pi\varepsilon_0\varepsilon r} \tag{407}$$

where $e^* \approx 0.1e$ [262], $r \approx 0.5$ nm, and $\varepsilon \approx 3$. Thus the vibrational frequency is $\nu = W/h \approx 10^{13}$ s^{-1}, which is consistent with the data of Ref. 238. Hence we can conclude that the π^* electron relaxes via the induced torsional vibrations of the retinal. The intensity of these vibrations is increased, as is readily seen from the consideration given above; and, finally, picosecond isomerization from all-*trans* to the 13-*cis* conformation of the retinal takes place.

The light-induced 13-*cis*-retinal of bacteriorhodopsin features a strained state with separated charges: An additional dipole almost perpendicular to the retinal long axis arises after *trans–cis* isomerization (see Fig. 15b). Thus, part of the absorbed photon energy is stored. The energy difference between the 13-*cis* and all-*trans* conformations of the retinal amounts to $\Delta U \approx 65$ kJ/mol [287].

C. Proton Ejection

A broad structureless absorption band in the infrared spectrum (1700–2800 cm^{-1}) observed for the intermediate L by Zundel and co-workers [6,238,288] was unambiguously interpreted as proton collective fluctuations occurring in the outlet proton channel. In this channel, charges are shifted within less than a picosecond [250,289]; and an uninterrupted hydrogen bond, which features a large proton polarizability [6], is formed. Thus the outlet channel in the intermediate L makes up the hydrogen-bonded chain whose polarization periodi-cally changes: OH $\cdots$ OH $\cdots$ OH $\ldots$ $\rightleftarrows$ HO $\cdots$ HO $\cdots$ HO... As we mentioned in Ref. 37, such collective proton vibrations in the hydrogen-bonded chain could be considered as longitudinal polarized optical phonons with a frequency of more than 10^{12} Hz.

Figure 17a demonstrates the state of the hydrogen-bonded chain (possible terminal group of Tyr 57 followed by water molecules) and that of the active site before an excess proton enters the outlet channel. At this moment, the terminal group $-NH_2$ of Arg 82 appears to be connected with two other protons of the terminal groups of Asp 85 and Asp 212. These two protons destabilize the active site because they both pretend to occupy (indirectly) the vacancy in the terminal group of Arg 82. In the next step, these protons occupy the vacancy,

and the initial states of Asp 85, Asp 212, and Arg 82 residues are resumed. However, one of the transferred protons becomes coupled with Arg 82 while another proton is in excess. This can be regarded as a short-lived ion state ($\tau_0 \approx 10^{-6}$ s; see, e.g., Ref. 34), located at the site of the hydrogen-bonded chain neighboring Arg 82 (Fig. 5b). It is obvious that the excess proton strongly interacts with the collective fluctuations of the hydrogen bonds or in other terms with polarized optical phonons. This enables us to apply the concept of the proton polaron, which has been discussed in the previous sections, to the problem of proton transport in bacteriorhodopsin, because during the L $\rightarrow$ M transition the excess proton finds itself in a strongly polarized outlet channel.

The polaron state may be created on any site of the hydrogen-bonded chain along which the excess proton moves. In this state, the charge carrier is coupled with a chain site for a time τ_0, leading to a local deformation of the chain. Figure 18 illustrates the excess proton hopping motion along the outlet hydrogen-bonded chain as a set of polaron wells. The positively charged terminal group $-NH_3^+$ of Arg 82 has to set the direction of the excess proton motion from the active site to the extracellular surface of the membrane. Hence, this proton drifts under the electrostatic field of the group $-NH_3^+$.

We can write the Hamiltonian of the excess proton in the hydrogen-bonded chain in the form

$$H = H_0 + H_{\text{tun}} + H_{\mathscr{E}} \tag{408}$$

$$H_0 = \sum_l E\hat{a}_l^+\hat{a}_l + \sum_q \hbar\omega_q\left(\hat{b}_q^+\hat{b}_q + \frac{1}{2}\right)$$
$$- \sum_l \hat{a}_l^+\hat{a}_l\hbar\omega_q[u_l(q)\hat{b}_q^+ + u_l^*(q)\hat{b}_q] \tag{409}$$

$$H_{\text{tun}} = \sum_l J\hat{a}_{l+1}^+\hat{a}_l + h.c. \tag{410}$$

$$H_{\mathscr{E}} = -\mathscr{E}\sum_l R_l\hat{a}_l^+\hat{a}_l \tag{411}$$
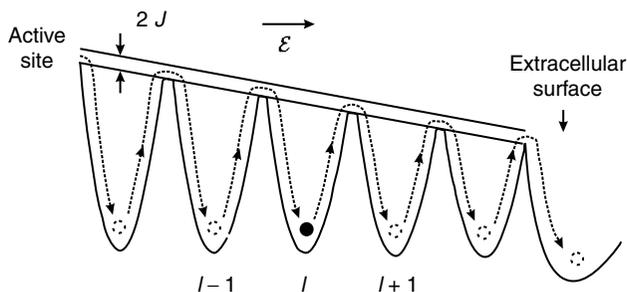

Figure 18. Hopping motion of the excess proton in the system of polaron wells. $2J$ is width of the narrow polaron band; $\mathscr{E}$ is the pulling electric field. (From Ref. 37.)

where H_0 is the basic small polaron Hamiltonian containing energy operators for the excess charge carrier [first term in expression (409)], polarized vibrations of the hydrogen-bonded chain [that is, optical phonons; second term in expression (409)], and a local deformation induced by the excess proton [third term in expression (409)]; H_{tun} is the tunnel Hamiltonian describing the proton motion from site to site, and $H_{\mathscr{E}}$ is the electric field Hamiltonian depicting the change in the proton potential energy along the chain. In expression (409), E is the coupling energy of the excess proton with the lth site of the chain; $\hat{a}_l^+(\hat{a}_l)$ is the Fermi operator of creation (annihilation) of the charge carrier in the lth site; and $\hat{b}_q^+(\hat{b}_q)$ is the Bose operator of creation (annihilation) of the optical phonon with the cycle frequency ω_q and wavenumber q; $u_l(q) = u\exp(iql)$, where u is the dimensionless constant responsible for the coupling between the excess proton and the lth site; J is the resonance integral that characterizes the overlapping of wave functions of the excess proton in neighboring sites; and $R_l = lg$, where l is the site number in the chain and g the chain constant.

The calculation of the proton current is reduced to the method described in Section III. The density of the hopping proton current is given by

$$I = \text{Tr}(\rho_{\mathscr{E}} j) \tag{412}$$

where $\mathscr{V}$ is the effective volume of the chain and the statistical operator $\rho_{\mathscr{E}}$ and the operator of current density are determined as follows:

$$j = \frac{e}{\mathscr{V} i\hbar}[H_{\mathscr{E}}, H_{\text{tun}}] \tag{413}$$

$$\rho_{\mathscr{E}} = \frac{i}{\hbar}\int_{-\infty}^{t} d\tau e^{-\frac{i}{\hbar}(t-\tau)(H_0+H_{\mathscr{E}})}[H_{\mathscr{E}}, \rho_{\text{tun}}]e^{\frac{i}{\hbar}(t-\tau)(H_0+H_{\mathscr{E}})} \tag{414}$$

where

$$\rho_1 = \rho_0 \int_0^{1/k_BT} d\lambda e^{\lambda H_0} H_1 e^{-\lambda H_0}, \qquad \rho_0 = \frac{e^{-H_0/k_BT}}{\text{Tr}\, e^{-H_0/k_BT}} \tag{415}$$

After calculations and leaving out the phonon dispersion, we obtain the following expression for the density current of the outlet proton channel of bacteriorhodopsin [37]:

$$I = 2^{2/3}\pi^{1/3}\frac{eg}{\mathscr{V}\hbar^2\omega}\sinh\frac{e\mathscr{E}g}{2k_BT}\frac{\exp(-E_a/k_BT)}{[2u^2\,\text{cosech}\,(\hbar\omega/k_BT)]^{1/2}} \tag{416}$$

where the activation energy is expressed as

$$E_a = 2k_BTu^2\tanh(\hbar\omega/4k_BT) \tag{417}$$

Let us present the current density I on the left-hand side of expression (416) in the form $I = e/At_{eject}$, where A is the area of cross section of the chain and t_{eject} is the time of proton drift along the chain. Since $\mathcal{V} = AL$, where L is the chain length, we can derive from expression (417) the expression for the time drift of excess proton in the chain under consideration:

$$t_{eject} = 2^{-3/2}\pi^{-1/2}\frac{L}{g}\frac{\hbar^2\omega}{J^2}e^{E_a/k_B T}\frac{\left[2u^2\operatorname{cosech}\left(\hbar\omega/k_B T\right)\right]^{1/2}}{\sinh(e\mathscr{E}g/2k_B T)} \qquad (418)$$

All the parameters in expression (418) can be readily estimated. In the proton polaron concept there are only two free parameters: the coupling function, written here as u^2, and the resonance integral J. Their orders of magnitude are known from the general model of small polarons. Here we can set $u^2 = 15$ and $J = 0.9 \times 10^{-2}k_B T$. The phonon frequency can be put equal to $\omega = 2\pi \times 6 \times 10^{12}$ s^{-1}, as we discussed above; and in this case $\hbar\omega = k_B T$, where $T = 300$ K. Then the activation energy E_a equals $7.35k_B T$. The excess proton energy in the field of the active site effective charge $e\mathscr{E}g$ has been chosen to be equal to 10^7 V/m, which is typical for living cells. Finally, setting the number of the chain sites $L/g = 5$, we gain from expression (418)

$$t_{eject} \approx 80\,\mu s \qquad (419)$$

This estimation is consistent with experimental data [290] according to which the time of proton ejection equals 76 μs. In Ref. 230 it is pointed out that at pH 7, the proton appears at the surface with a time constant of about 80 μs. Thus, the theory presented herein is in good agreement with the available experiments.

V. MESOMORPHIC TRANSFORMATIONS AND PROTON SUBSYSTEM DYNAMICS IN ALKYL- AND ALKOXYBENZOIC ACIDS

A. Molecular Associates

Mesomorphism of alkyl- and alkoxybenzene acids, which can be either smectic or nematic types, was explained [291] by aggregation of their molecules via intermolecular hydrogen bonds in cyclic dimers (hereafter we will use abbreviations nABA and nAOBA for alkyl- and alkoxybenzene acids, respectively, where n determines the number of C atoms in the alkyl radical). Experimental investigations of the dynamics of hydrogen bonds in the vicinity of the phase transitions have been performed in a series of works (see, e.g., Ref. 292). It was shown early [291,293] that in the infrared spectrum new bands appear with heating of the solid-state phase well in advance of the melt point.

This is testimony to a partial dissociation of cyclic dimers with the formation of open associates and monomers. In Refs. 57, 58, 60 the quantitative estimations of the relative number of different building blocks as functions of temperature and phase of the sample have been made. For reference, the infrared spectra of n-carbonic and perftoralkylbenzoic acids, which do not possess mesomorphic properties, have been studied as well.

The absorption infrared spectra of nABA ($n = 1$–9) and nAOBA ($n = 3$–12) have been measured in the spectral range from 100 to 4000 cm^{-1}(± 3 cm^{-1}) and in the temperature interval from 100 to 550 K (± 1 K) [57,58,60]. The assignment of the spectral infrared bands to the vibrations of atoms of the dimer ring (Fig. 2) has been made based on calculations of frequencies and shapes of normal coordinates performed for dimers of homologies of carbon acids [292]. Vibrations of the parareplaced benzoic acid and its alkyl radical have been interpreted on the basis of calculations carried out in Refs. 294 and 295, respectively. The maxima recorded at 2900 cm^{-1} (ν_{OH} band), 1692 cm^{-1} ($\nu_{C=O}$ band), and 940 cm^{-1} (ρ_{OH} band) for all phases of the ABA and AOBA are direct evidence for the connection of molecules ABA and AOBA via hydrogen bonds.

In the crystal state ($T = 300$ K), molecules of AOBA are united into centrosymmetrical dimers by means of a pair of hydrogen bonds ($R_{O\cdots O} = 0.2629$ nm). For short homologies ($n \leq 5$) the packing of molecules in the crystal is caused by the interaction between the rings of benzoic acids (Fig. 19a). The layer packing of molecules with more long alkyl radicals ($n \geq 6$) stems from the interaction between methylene chains aligned parallel to each other (Fig. 19b). The distance between benzoic acids from the nearest layers equals 0.45 nm. The packing of molecules in the ABA crystal has a similar nature.

The enthalpy of hydrogen bond in cyclic dimers (Fig. 20a) in the ABA and AOBA is equal to -35.3 ± 0.8 kJ/mol per hydrogen bond at $T = 300$ K. For the quantitative estimation of the enthalpy the Iogansen method [296] has been applied, which is based on the analysis of the shift of the frequency of twisting vibration ρ_{OH} and that of the gravity center of the ν_{OH} band of associates with relation to the corresponding shifts for monomers. The determination of frequencies $\rho_{OH}^{(mon)}$ and $\nu_{OH}^{(mon)}$ of ABA and AOBA monomers, which are needed for the calculation of the enthalpy, has been performed by the infrared spectra of ABA and AOBA measured in the solution of CCl_4 and the gaseous state in the temperature range from 540 to 550 K. The frequencies prove to be 612 and 3550 cm^{-1}, respectively, practically for all the acids studied.

As it follows from the infrared spectra, only cyclic dimers are present in the crystal state on cooling to 100 K. In this state, the bond energy of the hydrogen bond has been determined to be 36 ± 1 kJ/mol at 100 K and 34 ± 1 kJ/mol at 300 K. The crystals, on being heated, exhibit the appearance of a new band (920–925 cm^{-1}) well before the transition to a metaphase. The intensity of the band increases with T, and the maximum of the band slightly moves to low
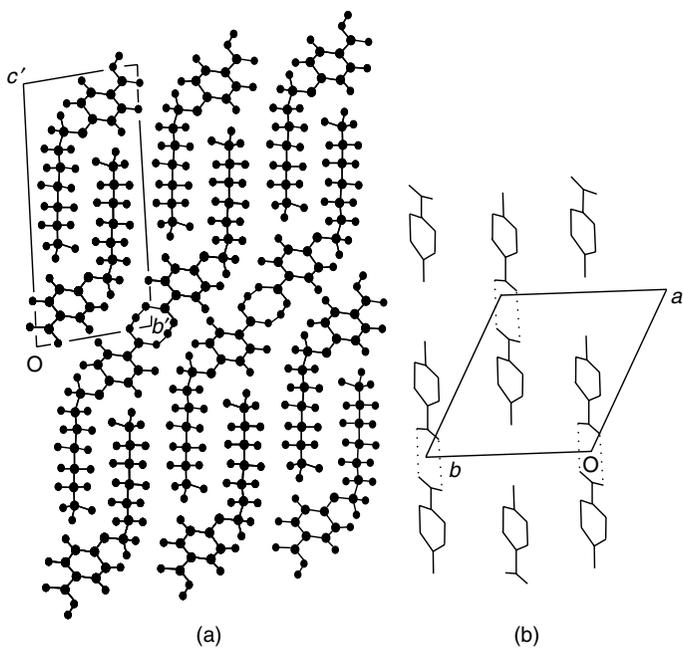
Figure 19. (a) Molecular stacking in the crystal state of the 7AOBA in the projection on the *a* axis. (b) The crystal structure of toluil acid in the projection on the *c* axis. (From Ref. 57.)
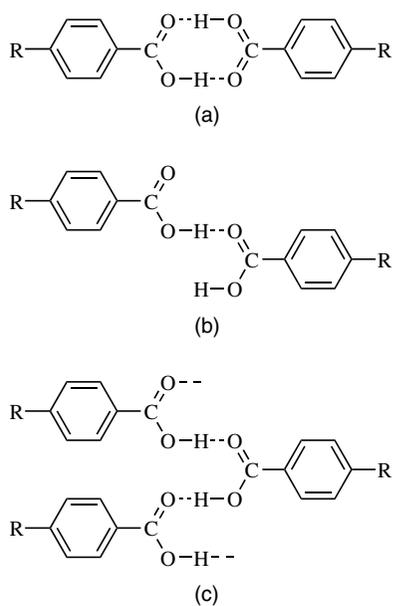
Figure 20. Possible types of hydrogen-bonded associates: (a) Cyclic dimer, (b) open dimer, and (c) chain associate. (From Ref. 58.)

frequencies. Coincidentally with this band, one more band with the maximum at 1710 cm^{-1}, a wide shoulder (3300 cm^{-1}), and new bands in the range from 500 to 700 cm^{-1} appear as well. Taking into account peculiarities of the crystal structure of the 7AOBA and low intensities of the bands caused by the absorption of unbound hydroxyl group OH (612 and 3550 cm^{-1}), it is necessary to suggest that three or more molecules take part in the formation of such associates (Fig. 20c). An appraisal of the enthalpy of hydrogen bond of the formed chain associates by the Iogansen's frequency rule [296] yields magnitude -31.5 ± 0.8 kJ/mol. Near the phase transition from the solid crystal to the liquid crystal, the quantity of open associates accounts for 30% of the total number of nAOBA (nABA) molecules; a small part of monomers is available as well.

Heating over the melting temperature is accompanied by amplification of the intensity of bands resulted from monomers (612, 1730, and 3550 cm^{-1}) and decay of the intensity of bands stemming from cyclic dimers (940, 1690, and 2900 cm^{-1}). That is, with heating, cyclic dimers dissociate into monomers; the quantity of open associates holds constant in the framework of the mesophase (Fig. 21). These clusters (i.e., open associates), which feature a certain order
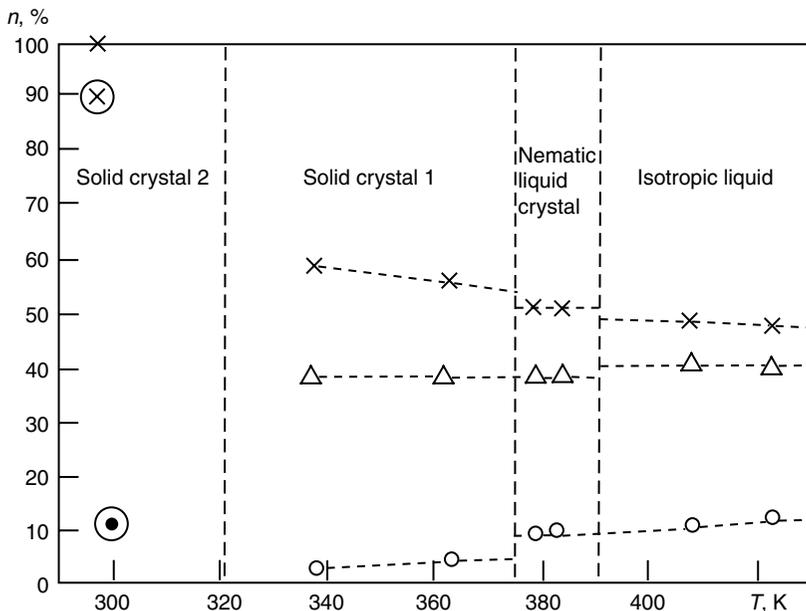
Figure 21. Relative content of cyclic dimers ($\times$), open associates ($\triangle$), and monomers ($\bigcirc$) in different phase states of the 7AOBA; ($\otimes$, $\odot$) are the data for dilution of the 7AOBA in CCl$_4$. The vertical dashed lines correspond to the phase transition temperatures. (From Ref. 57.)

parameter, set conditions for a smectic layer type of the mesophase. In particular, electron paramagnetic resonance spectroscopy also points to the formation of polymer hydrogen-bonded associates in the mesophase of 9AOBA [297].

Cyclic dimers, open associates, and monomers exist also in the liquid state; however, with temperature the dynamic equilibrium is shifted to monomers. Note that a more simple pattern of the molecular structure is set with dissolving of the acids studied in CCl_4: Only cyclic dimers and monomers are found at equilibrium, and the quantity of monomers increases with dilution of the solution or with its heating; open associates do not arise. The enthalpy of hydrogen bond of dimer molecules in the solution is approximately the same as in the crystal at the same temperature.

What is the reason for the transformation of hydrogen bonds revealed at the phase transitions in the homology series studied? Bernal's hypothesis [298] indicates that it is the character of packing of molecules in the crystal state which determines the possibility of mesophase formation and its type. In the case of nAOBA-type benzoic acids with short alkyl radicals ($n \leq 5$), the ordering of molecules ("piles") is determined by the interaction between benzoic rings. If the radicals are longer, the intermolecular interaction between methylene chains fixes the layer packing of cyclic dimers (Fig. 20). The conjugation of π electrons of benzoic acids with those of carbonyl groups dictates the flat structure of the cyclic dimer core. With melting, the liquid crystal is formed: in the first case nematic and in the second case smectic. The distance between benzoic rings of neighboring dimers is 0.45 nm. In similar manner, the nABA crystals are constructed [57,58,60].

B.   Rearrangement of Hydrogen Bonds: Mechanism of Open Associates Formation

Let us consider the process of disruption of a pair of hydrogen bonds, which have connected two nABA (or nAOBA) molecules into a dimer, and the following formation of one crossed hydrogen bond combining two nABA molecules which previously have been unconnected. The problem can be reduced to the model below. Let two hydrogen bonds from two nearest dimer rings is characterized by two-well potentials (Figure 20a) whose parameters are given (see Section II). It would seem that the dynamics of the crystal net of hydrogen bonds, which are marked by two-well potentials, can be investigated in principle in the framework of the Ising pseudospin model (see Section II.D). However, in our case there is reliable experimental evidence of the origination of "crossed" hydrogen bonds that characterize the creation of open associates discussed in the previous subsection.

It is reasonable to assume that at the phase transition "solid crystal 1 → solid crystal 2" that is close to the phase transition "solid crystal → liquid crystal" the intradimer hydrogen bonds are in a predissociate state. This state can be

unstable with respect to the proton transfer from the dimer to a new spatial position that corresponds to a "crossed" hydrogen bond. Such a transfer can be activated by two types of intradimer vibrations of the proton [292]: (i) $\rho(O \cdots H) = 30\text{--}50$ cm^{-1} (in plane of the dimer ring), which is transversal to the $O \cdots O$ line of the dimer; (ii) $\alpha_{\perp}(O \cdots H) = 30\text{--}50$ cm^{-1} (normal to the dimer plane).

Let us employ now the small polaron model for the consideration of proton transfer from the intradimer state to the interdimer one (Fig. 20a and Fig. 20b, respectively) [57]. The initial Hamiltonian can be written in the form

$$H = H_0 + H_{\text{tun}} \tag{420}$$

$$H_0 = \sum_{l=1}^{2} E_l \hat{a}_l^+ \hat{a}_l + \sum_{\alpha;\mathbf{q}} \hbar\omega_{\alpha\mathbf{q}} \left(\hat{b}_{\alpha\mathbf{q}}^+ \hat{b}_{\alpha\mathbf{q}} + \frac{1}{2} \right)$$

$$- \sum_{\alpha=1}^{2} \hat{a}_l^+ \hat{a}_l \sum_{\alpha;\mathbf{q}} \hbar\omega_{\alpha\mathbf{q}} [u_\alpha(\mathbf{q}) \hat{b}_{\alpha\mathbf{q}}^+ + u_\alpha^*(\mathbf{q}) \hat{b}_{\alpha\mathbf{q}}] \tag{421}$$

$$H_{\text{tun}} = V_{12}(\hat{a}_1^+ \hat{a}_2 + \hat{a}_2^+ \hat{a}_1) \tag{422}$$

Here H_0 is the Hamiltonian that includes the bond energy of a proton in the intradimer ($E_1 < 0$) and interdimer ($E_2 < 0$) hydrogen bonds (we suppose that $|E_2| > |E_1|$), the energy of phonons, and the interaction of the proton with the lattice phonons. H_{tun} is the tunnel Hamiltonian that provides for proton transfer between two types of the hydrogen bonds. $\hat{a}_l^+(\hat{a}_l)$ is the Fermi operator of creation (annihilation) of hydrogen atom in the intradimer ($l = 1$) and interdimer ($l = 2$) hydrogen bond, respectively; $\hat{b}_{\alpha\mathbf{q}}^+(\hat{b}_{\alpha\mathbf{q}})$ is the Bose operator of creation (annihilation) of a lattice polarized optical phonon, which belongs to the lth branch, with the energy $\hbar\omega_{\alpha\mathbf{q}}$ and the wave vector $\mathbf{q}$; $u_l(\mathbf{q}) = u_l \exp(i\mathbf{q} \cdot \mathbf{l})$, where u_l is the dimensionless value that characterizes the displacement of the pair of oxygens $O \cdots O$, which form the hydrogen bond, from their initial equilibrium positions due to the localization of the hydrogen atom H between them (u_1 refers to the intradimer hydrogen bond, and u_2 refers to the interdimer hydrogen bond). The matrix element from expression (422) is determined as

$$V_{12} = \int d\mathbf{r} \langle \Phi | \psi_1^* W \psi_2 | \Phi \rangle \tag{423}$$

where W is the potential that specifies two possible positions (1 and 2) of the hydrogen atom, intradimer and interdimer, respectively (Fig. 22); ψ_1 and ψ_2 are wave functions of the hydrogen atom, which are localized at the aforementioned position;

$$|\Phi\rangle = \hat{B}^+ \Phi_0, \qquad \langle \Phi | = \hat{B}\Phi_0 \tag{424}$$

Figure 22. Disruption of two hydrogen bonds connecting two *n*ABA (or *n*AOBA) molecules into the dimer and the formation of one crossed hydrogen bond, which unifies two previously unconnected *n*ABA (or *n*AOBA)—that is, the transition of a hydrogen atom from the intradimer state to the inerdimer state. (From Refs. 57 and 58.)
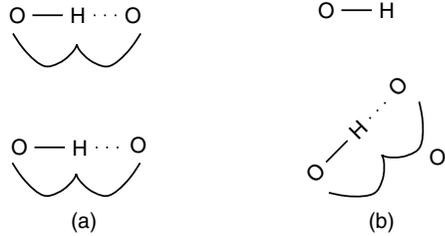
are quantized site functions that describe the superposition of intradimer vibrations $\rho(O \cdots H)$ and $\alpha_\perp(O \cdots H)$, and $\hat{B}^+(\hat{B})$ is the Bose operator of creation (annihilation) of these vibrations.

By analogy with the operator of current density, considered in the previous sections, we can introduce the operator of proton transfer density between the two different types of hydrogen bonds:

$$j = \frac{1}{\mathscr{V} i\hbar} \left[H_{\text{tun}}, \sum_{l=1}^{2} R_l \hat{a}_l^+ \hat{a}_l \right] \tag{425}$$

In expression (425) $R_2 - R_1 = g$ where the g is the length of proton jump.

The equation of motion of the statistical operator, which describes the system studied, is

$$i\hbar \frac{\partial \rho}{\partial t} = [H, \rho] \tag{426}$$

If we assume that H_{tun} is a perturbation $(|V| \ll \hbar\omega_{l\mathbf{q}}, |E_{1,2}|, k_B T)$, we derive from Eq. (426), setting in the first approximation $H_{\text{tun}} = 0$, that

$$\rho_0 = \frac{e^{-H_0/k_B T}}{\text{Tr} e^{-H_0/k_B T}} \tag{427}$$

The correction to ρ_0 caused by the interaction Hamiltonian (422) is

$$\rho_{\text{tun}} = -\frac{i}{\hbar} \int_{-\infty}^{t} d\tau e^{-i\frac{t-\tau}{\hbar}H_0} [H_{\text{tun}}, \rho_0] e^{i\frac{t-\tau}{\hbar}H_0} \tag{428}$$

Expressions (425) and (428) make it possible to calculate the proton transfer density by the following formula, which is known also from the previous sections:

$$I = \text{Tr}(\rho_{\text{tun}} j) \tag{429}$$

(here $\mathscr{V}$ is the effective volume of the molecular system in question; see Fig. 22). The overall result is [57] (see also Ref. 36)

$$I = 2^{3/2}\pi^{1/2}\hbar^{-2}n_{\text{ass}}g|V|^2 \sinh\frac{|\bar{E}_1|-|\bar{E}_2|}{k_BT}\exp\left(-\frac{E_a}{k_BT}\right)$$

$$\times \left[\sum_\alpha |\Delta|^2\omega_\alpha^2\text{cosech}(\hbar\omega_l/k_BT)\right]^{-2} \tag{430}$$

where n_{ass} is the concentration of associates and

$$E_a = k_BT\sum_\alpha |\Delta|^2 \tanh\frac{\hbar\omega_\alpha}{4k_BT} - \frac{3}{2}(|\bar{E}_1|-|\bar{E}_2|) \tag{431}$$

is the activation energy. In expressions (430) and (431) we have neglected the dispersion, put $|\Delta|^2 = u_1^2 - u_2^2$, and written the renormalized energies $\bar{E}_1$ and $\bar{E}_2$ of polaron shift for the two types of hydrogen bonds.

Let us estimate I for the mesomorphic 7AOBA crystal. Parameters can be chosen as follows [57,58,60]. The temperature of phase transition "solid crystal $2 \rightarrow$ solid crystal 1," $T = T_c$, is 320 K (see Fig. 21); the distance g is 0.26 nm; and the energy difference $|\bar{E}_1| - |\bar{E}_2|$ equals $2k_BT_c$. The major contribution to the activation transition in the small polaron model is introduced by low-frequency polarized phonons and hence the inequality $2k_BT > \hbar\omega_l$ should be held. In our case there are two comparatively intensive polarized vibrations of the benzoic ring: $\gamma(\text{CCC}) = 175 \text{ cm}^{-1}$ and $\beta(\text{CCH}) = 290 \text{ cm}^{-1}$. The degree of deformation of the dimer ring (Fig. 20a) is described by the constant $|\Delta|^2$; this parameter characterizes the bandwidths in infrared absorption spectra of the proton subsystem at frequencies $\omega_1 = \gamma(\text{CCC})$ and $\omega_2 = \beta(\text{CCH})$. In addition, the bandwidths have significant dependence on the length of radicals (in particular, the replacement of radical H for $(\text{CH}_2)_4\text{CH}_3$ leads to the bandwidth broadening of 1.5 in the cyclic dimers of carbonic acids [299]). Since by definition $|\Delta|^2 \gg 1$, we can set $|\Delta|^2 = 40$ (during which the polaron shift $|\Delta|^2\hbar\omega_{1,2}$ is still too small by comparison with the bond energy $|E_{1,2}| \approx 4 \text{ eV}$). The concentration of p-alkyl acids in a dish was $4 \times 10^{21} \text{ cm}^{-3}$; in the "solid-state 1" phase the concentration of open associates was 40% of this value (see Fig. 21). Therefore, the concentration of open associates, which is entered in expression (430), is $n_{\text{ass}} = 1.6 \times 10^{21} \text{ cm}^{-3}$.

The square of matrix element

$$|V|^2 = \int\int d\mathbf{r}\,d\mathbf{r}'|\psi_1(\mathbf{r})|^2|\psi_2(\mathbf{r})|^2\langle\langle\Phi|W|\Phi\rangle\rangle^2 \tag{432}$$

remains the most undetermined value. Symbols $\langle\langle\ldots\rangle\rangle$ mean the thermal averaging by the statistical operator P, where

$$P = \frac{\exp[-\hbar\Omega(\hat{B}^+\hat{B} + \frac{1}{2})/k_\mathrm{B}T]}{\mathrm{Tr}\,\exp[-\hbar\Omega(\hat{B}^+\hat{B} + \frac{1}{2})/k_\mathrm{B}T]} \tag{433}$$

The averaging (433) reduces the matrix element (432) to the form

$$|V|^2 = V_0^2 \coth^2 \frac{\hbar\Omega}{2k_\mathrm{B}T_c} \tag{434}$$

Let us set here $\Omega = 2\pi \times 40\ \mathrm{cm}^{-1}$—that is, the mean value of frequency for the superposition of the intradimer vibrations $\rho(\mathrm{O}\cdots\mathrm{H})$ and $\alpha_\perp(\mathrm{O}\cdots\mathrm{H})$. Thus the matrix element V_0, which is constructed only on proton wave functions $\psi_{1,2}(\mathbf{r})$, is the fitting parameter. With regard to the numerical values of Ω and T_c, we get from expression (434): $V \simeq 11.6\,V_0$. In as much as the following inequalities should be held, $V_0 \ll \hbar\Omega$, $\hbar\omega_{1,2}$, $k_\mathrm{B}T$, we can put $V_0 = 10^{-23}\ \mathrm{J}$ (i.e., $\simeq 10^{-2}\,k_\mathrm{B}T_c$).

Using expression (430) for the proton transfer density I, we can readily write the expression for the proton transfer rate

$$K = I\mathscr{A} \tag{435}$$

where $\mathscr{A}$ is the effective area of the cross section of reaction channel characterizing the interaction of transferring proton with an oxygen of the neighboring dimer.

Note that as follows from expression (430) in the range close to the phase transition, the temperature dependence of proton transfer rate (435) is expressed as $T^{1/2}\exp(-\mathrm{const}/T)$. Here, the first factor is responsible for the creation of open associates, and it prevails over the second one for $T > T_c$. Below T_c in the first factor the exponent $1/2$ remains; however, the absolute value of the second factor increases, which accounts for the lack of open associates in the "solid state 2" phase in this temperature range.

If we set $\mathscr{A} \sim 0.1 \times 0.1\ \mathrm{nm}^2$ and insert numerical values of all the parameters mentioned above into expression for I (430), we will obtain from expression (435) the following meaning of the proton transfer rate:

$$K \sim 10^{-2}\ \mathrm{s}^{-1} \tag{436}$$

On the other hand, in the experiments [57,58,60] the samples, when heated to T_c (see Fig. 21), exhibited open associates whose formation was completed in

two to three minutes. Thus in fact the calculated value of K qualitatively agrees with the experimental value.

The number of acids merging into polymer associates varied from 2 to 7 and could extend to even higher numbers. Thus such a polymerization is similar to some kind of the clusterization of alkyl- and alkoxybenzoic acids in the solid state. We will return to this problem in Section VIII.

VI.   QUANTUM COHERENT PHENOMENA IN STRUCTURES WITH HYDROGEN BONDS

A.   Mesoscopic Quantum Coherence and Tunneling in Small Magnetic Grains and Ordered Molecules

Over a period of years there has been considerable interest in the phenomenon of mesoscopic quantum tunneling and coherence revealed in various small-size systems. In particular, the phenomenon has been observed in optically trapped ions [300,301], superconductors in which the order parameter shows the phase difference across Josephson junctions [302], spin-domains in atomic Bose–Einstein condensates [303], and mesoscopic magnetic clusters and grains [304]. Many physical properties of small-size systems being governed by quantum effects are radically distinguished from properties of macroscopic samples. Besides the usual one-particle quantum effects (for instance, tunneling), some low-dimension structures demonstrate a correlated quantum behavior of several particles such as the mesoscopic tunneling of a cooperative magnetic moment observed by the magnetic relaxation measurements in magnetic molecules and small grains [305–308] (note that a mechanism of magnetization reversal was originally proposed by Bean and Livingston [309] much earlier).

Coffey and co-workers [310–312] have conducted detailed studies of the wideband dielectric response of polar molecules and the rotational motion of single-domain ferromagnetic particles in the presence of an external magnetic field with regard to the inertia of the particles. In particular, Coffey and co-workers have developed a generalized approach based on the transformed Langevin equation, which allowed them to calculate the dipole moment of tagged molecules and investigate its motion followed by oscillations of the applied field. They have examined [313,314] the rotational Brownian motion of two- and three-dimensional rotators and have shown how the Langevin equation is transformed into an equation for the dipole moment. The contribution of single-domain particle inertial effects to resonance in ferrofluids has also been analyzed [315]. The study [316] of the nonaxially symmetric asymptotic behavior of a potential having minima at $\theta = (0, \pi)$ at the escape from the left to the right of the potential allowed the precise calculation of the prefactor in the

Néel–Brown model; however, the nonlinear field effects have also been very significant. The further search for the accurate description of the macroscopic quantum tunneling of magnetization **M** needs correct asymptotic formulas for the reversal time for magnetocrystalline anisotropy potentials, which have been calculated by Coffey and collaborators as well [315–318].

Similar mesoscopic quantum effects take place also in short hydrogen-bonded chains and in small clusters, which include hydrogen bonds. The phenomenon of large proton polarizability and fast oscillations of the polarization of the chain were studied experimentally by Zundel and co-workers [6,249,288,289]. A theoretical study of macroscopic tunneling of the chain polarization has been conducted in Refs. 319–322.

To gain a better understanding the collective proton dynamics, let us consider an isolated chain schematically shown in Fig. 23. The proton subsystem is found here in the degenerate ground state, and the chain as a whole can take two configurations with different proton polarizations of hydrogen bonds. The mesoscopic quantum tunneling of polarization from one configuration to the other one stems from quasi-one-dimensional proton sublattice dynamics [319]. However, the rotating motion of ionic or orientational defects might relieve the degeneration of polarization in principle as well [161,323–325]. In this instance we meet the over-barrier reconstruction of polarization of the chain,
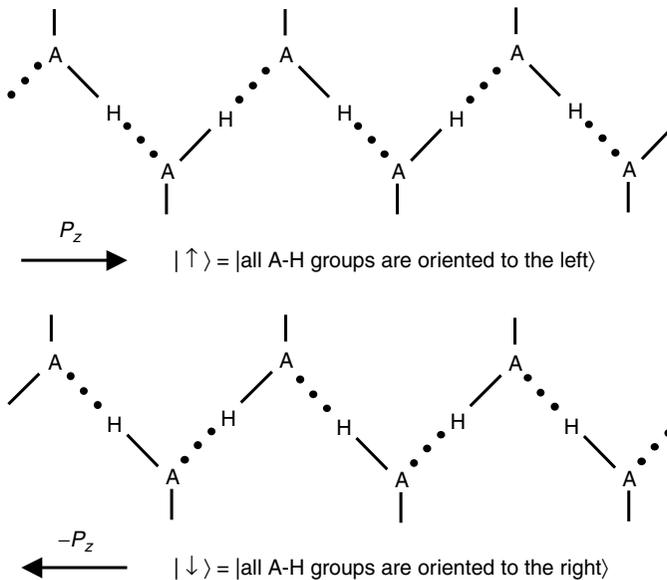

Figure 23. Two configurations of the hydrogen-bonded chain, which are characterized by opposite polarizations. (From Ref. 319.)

and the corresponding solution in terms of a soliton formation is similar to the Bloch wall in ferromagnetics, which is typical for rather macroscopic samples. Traditionally, small clusters are single domains in which the total polarization is fixed and features two equilibrium orientations along and against the principal axis of the chain (Fig. 23). Let us denote these configurations of the chain by symbols $|\uparrow\rangle$ and $|\downarrow\rangle$. Our goal is to demonstrate a possibility of the spontaneous tunnel transformation of a short chain (or a single domain) from configuration $|\uparrow\rangle$ to configuration $|\downarrow\rangle$. Such a behavior of the chain means that protons in the hydrogen bonds coherently move from the left side to the right side; or, in other words, the total chain polarization tunnels between the two opposite directions P_z and $-P_z$, as shown in Fig. 23.

Let us turn to the main properties of the energy spectrum, which should help us to shed light on the chain polarization transition and a role of the Coulomb interaction that realizes the phenomenon. In the simplest case of an isolated hydrogen-bonded chain, the Hamiltonian H of the proton subsystem can be written in the form of two parts: (a) the potential energy H_C corresponding to the Coulomb interaction between protons and (b) the kinetic energy H_{tun} describing the tunneling transfer of a proton along the hydrogen bond:

$$H = H_C + H_{tun} \tag{437}$$

$$H_C = U \sum_l (\hat{a}_{R,l}^+ \hat{a}_{R,l} \hat{a}_{L,l+1}^+ \hat{a}_{L,l+1}) \tag{438}$$

$$H_{tun} = J \sum_l (\hat{a}_{R,l}^+ \hat{a}_{L,l} + \hat{a}_{L,l}^+ \hat{a}_{R,l}) \tag{439}$$

Here $\hat{a}_{R(L),l}^+ (\hat{a}_{R(L),l})$ is the Fermi operator of creation (annihilation) of a proton in the left (right) well of the two-well potential of the lth hydrogen bond, J is the overlap, or tunnel integral, and U the Coulomb repulsion energy between protons in the neighbor hydrogen bonds. At first let us assume that tunnel integral J is smaller than Coulomb interaction U, so that our Hamiltonian can be represented only by the potential part $H = H_C$ that corresponds to the zero order of the perturbation theory. The energy spectrum has a simple structure (Fig. 24a). The doubly degenerated ground state corresponds to the two chain configurations $|\uparrow\rangle = |10, 10, \ldots, 10\rangle$ and $|\downarrow\rangle = |01, 01, \ldots, 01\rangle$; that is, the protons are oriented to the left or to the right. Excited states of the chain stipulated by unordered proton configurations in the hydrogen bonds (e.g., $|01, 10, \ldots, 10\rangle$) are separated from the ground state by Coulomb gap U. Let the tunneling Hamiltonian H_{tun} be a small perturbation, which thus intensifies the energy degeneration mixing the ground and excited states (Fig. 24b).

We will treat the splitting of the ground state related to the tunnel transition of the chain as a whole, which occurs between the two configurations with opposite proton polarizations. To make these coherent tunnel transitions of
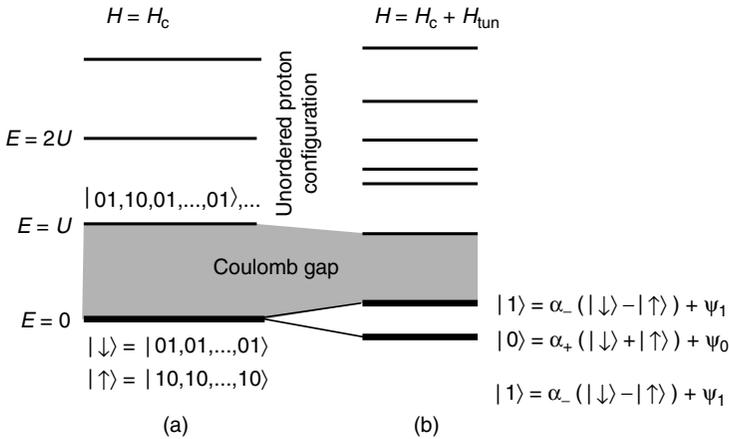
Figure 24. Energy spectrum of the proton subsystem: (a) Energy levels determined only by Coulomb repulsion of protons (H_C) in nearest hydrogen bonds. The doubly degenerated ground level corresponds to the two states of the chain with opposite proton polarizations. (b) The energy splitting caused by a small perturbation H_{tun}. The ground state splitting is associated with the coherent tunnel dynamics of protons. In the case of the strong Coulomb interaction, the Coulomb gap separates the excited state from the ground one, which ensures the coherent tunneling.

protons possible, the energies of the two lowest states must be separated by a gap from excited states. Obviously, when the local tunnel integral J is small in comparison with U, the Coulomb gap preserves such transitions. However, if the kinetic energy of the system has an order of the Coulomb repulsion, the gap between the ground and excited states will be virtually reduced to zero. This in turn will destroy the coherent proton dynamics. Thus an important prerequisite to the correlated tunnel dynamics is the strong Coulomb interaction between protons.

Another important condition for such transitions is low temperature at which thermal fluctuations do not blur the ground state. The ground state will be split when temperature increases, though the value of splitting will still be less than the Coulomb gap U. Thermal fluctuations are also able to generate the possibility of the chain repolarization between configurations $|\uparrow\rangle$ and $|\downarrow\rangle$. Thus, at some temperature the coherent tunnel regime of the cooperative proton oscillations (temperature independent) should change to a classical regime based on the mechanism of over-barrier proton transitions.

The matrix element, or the probability of coherent transition between states, includes the full information about the transition. Let us denote wave functions of the two degenerate ground states (at $J = 0$) as $|\uparrow\rangle = |10, 10, \ldots, 10\rangle$ (the chain's protons are oriented to the left) and $|\downarrow\rangle = |01, 01, \ldots, 01\rangle$ (the chain's

protons are oriented to the right). Let $|l\rangle$ be the eigenstate of the Hamiltonian $H = H_C + H_{tun}$, $H|l\rangle = E_l|l\rangle$. The probability corresponding to the transition from $|\uparrow\rangle$ to $|\downarrow\rangle$ is

$$|\langle\uparrow|e^{-\frac{i}{\hbar}Ht}|\downarrow\rangle|^2 = \sum_l |\langle\uparrow|l\rangle\langle l|\downarrow\rangle|^2$$

$$+ 2\sum_{l>n} \langle\uparrow|l\rangle\langle l|\downarrow\rangle\langle\uparrow|n\rangle\langle n|\downarrow\rangle \cos\left(\frac{E_n - E_l}{\hbar}t\right) \quad (440)$$

As can readily be seen, at low temperature the oscillations between the $|\uparrow\rangle$th and the $|\downarrow\rangle$th states take place with the frequency that corresponds to the energy splitting of the ground state:

$$\Gamma^2 \sim \langle\uparrow|0\rangle\langle 0|\downarrow\rangle\langle\uparrow|1\rangle\langle 1|\downarrow\rangle\cos\left(\frac{E_1 - E_0}{\hbar}t\right) \quad (441)$$

where $|0\rangle$ and $|1\rangle$ are the two lowest levels. The transitions $|\uparrow\rangle \leftrightarrow |\downarrow\rangle$ include both the single-domain repolarization and transitions through unordered proton configurations. The wave functions of the two lowest levels have the following forms:

$$\begin{aligned} |0\rangle &= \alpha_+(|\uparrow\rangle + |\downarrow\rangle) + \Psi_0 \\ |1\rangle &= \alpha_-(|\uparrow\rangle - |\downarrow\rangle) + \Psi_1 \end{aligned} \quad (442)$$

Terms Ψ_0 and Ψ_1 describe unordered proton configurations in the bonds, so that the probability of single-domain chain oscillations becomes $\sim |\alpha_+|^2|\alpha_-|^2$ $\cos[(E_1 - E_0)t/\hbar]$. When Ψ_0 and Ψ_1 are small in comparison with the α terms, one can treat the chain repolarization as that of a single domain. Contribution of Ψ_0 and Ψ_1 in (442) becomes more appreciable at the increasing of the integral J that leads to the destroying the correlated proton dynamics. For example, in the case of a chain consisting only of two bonds, which is characterized by periodical boundary conditions, we have

$$\begin{aligned} |0\rangle &= \alpha_+(|\uparrow\rangle + |\downarrow\rangle) + \beta_+(|01, 10\rangle + |10, 01\rangle) \\ |1\rangle &= \frac{1}{\sqrt{2}}(|\uparrow\rangle - |\downarrow\rangle) \end{aligned} \quad (443)$$

where

$$2\alpha_+^2 + 2\beta_+^2 = 1, \qquad \beta_+ = \alpha_+\frac{E_0}{2J}, \qquad E_2 = \tfrac{1}{2}[U + J - ((U + J)^2 + 8J^2)]^{1/2} \quad (444)$$

If the local tunnel integral J is small compared with Coulomb interaction U, the contribution on the side of the term proportional to β_+ in expression (443) is negligible (its contribution is of the order of $J/U \ll 1$). Hence in this case we can consider the tunnel repolarization of the chain as a repolarization of a single domain. Increasing of γ involves an increase of the β term, which will suppress the coherent tunneling of protons.

In such a manner the coherent oscillation is restricted by two factors. First, it is the strong Coulomb correlation between particles which suppresses the local tunneling of separate protons ($U \gg J$). Second, the small value of J decreases the proton mobility. However, the increase of the proton mobility due to the enlargement of the J will diminish the coherence in proton oscillations. Note that similar correlated tunneling of particles can occur in the systems with the strong Coulomb interaction—for instance, in small ferroelectric clusters and chain-like structures with charge-ordering (Coulomb crystals). Another example of a molecular system in which similar tunnel oscillations can be observed is a short chain of *trans*-isomeric polyacetylene that features the periodic change of single and double bonds, [326,327] (Fig. 25).

Having estimated the tunneling rate of the aforementioned proton transitions, we shall draw the analogy to ferroelectric systems. For this purpose we should represent the system of hydrogen bonds in the framework of the pseudo-spin formalism (see Section II.D). However, before the detailed consideration of the chain repolarization, let us touch upon the effect of the coherent quantum tunneling in small magnetic grains and the quasi-classical approach to the calculation of the tunneling rate, which is employed below.

Let us briefly state the most important features associated with small magnetic grains [306–309,328–330]. Small ferromagnetic particles with size about 15 nm usually consist of a single magnetic domain. The total magnetization is fixed in one of several possible directions of the so-called easy magnetization, which is determined by the crystalline anisotropy and the shape of a magnetic particle. In the particular case of the easy-axes anisotropy, the total magnetization $\mathbf{M}$ can be specified by two equilibrium states, which differ only by the vector orientation. Transitions of the particle magnetization between these states occur spontaneously. At high temperature T, the moment jumps from one orientation to another over the anisotropy barrier. Below some $T = T_c$, thermal processes are essentially frozen, but oscillating of the total magnetization does not disappear. Quantum mesoscopic tunneling in the systems in question was evidenced by the magnetic relaxation measurements with a sharp

Figure 25. Possible tunnel transitions between the two different configurations of a *trans*-polyene chain.

crossover to the temperature-independent magnetic relaxation for low temperature [306–309,328–330]. The magnetic relaxation time that characterized the oscillations did not depend on temperature and was finishing when T trends to zero. Measurements of the susceptibility conducted on small antiferromagnetic grains with size 7 nm showed (a) the coherent quantum tunneling of the sublattice magnetization through the anisotropy barrier even below $T_c \simeq 0.2$ K [328,329] and (b) the tunneling of the total magnetic moment of the mesoscopic $Mn_{12}O_{12}$ magnetic molecule below 2 K [307,308]. Thus, the mentioned experiments in fact demonstrated the total magnetic moment (in ferromagnetics) or the Néel vector (in antiferromagnetic) tunnels between the two energy minima. The phenomenon of mesoscopic (macroscopic) quantum tunneling (or the decay of a metastable state) and the mesoscopic quantum coherence (or the resonance between degenerate states) arise owing to the coherent behavior of individual magnetic moments, whose quantity is rather macroscopic as it varies from 10^4 to 10^6. Typical frequencies of coherent tunneling fall in the range 10^6 to 10^8 s^{-1} (see, e.g., Refs. 331 and 332), though in the case of the hydrogen-bonded chain the frequency of coherent tunneling of protons can reach 10^{12} s^{-1} [249,288,289].

Such a tunnel switching of the magnetization can be described by the so-called "one-domain" approximation, when the total magnetization vector $\mathbf{M}$ is taken as a main dynamic variable with fixed absolute value M_0. Then the total energy density, or the anisotropy energy E, is obtained from the spin-Hamiltonian H using a spin coherent state $|n\rangle$ chosen along the direction $\mathbf{n}$ [332,333]:

$$\langle n|H|n\rangle = \mathscr{V} \cdot E(\theta, \varphi) \tag{445}$$

where $\mathscr{V}$ is the volume of a magnetic particle (i.e., domain), and θ and φ are polar coordinates of the vector $\mathbf{n}$. Minima of the E correspond to equilibrium directions of the particle magnetization, $\mathbf{n}_1$, $\mathbf{n}_2, \ldots$, which are separated by the appropriate energy barriers. In order to calculate the probability of the magnetization tunneling between the aforementioned equilibrium directions, we have to consider a matrix element of type (440), which can be represented by the spin-coherent-path integral [332,333]

$$\Gamma = \langle n_1|e^{-\frac{i}{\hbar}Ht}|n_2\rangle = C \int \{d\mathbf{n}\}\exp\left\{-\frac{\mathscr{S}_E[\mathbf{n}(\tau)]}{\hbar}\right\} \tag{446}$$

where C is a normalization factor and $\mathscr{S}[\mathbf{n}(\tau)]$ is the imaginary time, or Euclidean action [306,332,333]

$$\mathscr{S}_E[\mathbf{n}(\tau)] = v \int_{-T/2}^{T/2} d\tau\left\{-i\frac{M_0}{\lambda}\frac{d\varphi}{d\tau}(\cos\theta - 1) + E(\theta, \varphi)\right\}, \qquad t = i\tau \tag{447}$$

where $\lambda \equiv e\gamma/2mc$ and γ is the gyromagnetic ratio. Below we restrict our consideration by the quasi-classical approximation, which allows expression (446) to be rewritten as follows:

$$\Gamma \approx Ae^{-\frac{\mathscr{S}_E}{\hbar}} \tag{448}$$

$\mathscr{S}_E$ is the Euclidean action written for a classical trajectory corresponding to the sub-barrier rotation of the particle magnetization **M**. This is a typical instanton trajectory that satisfies the equations of motion

$$\begin{aligned} i\frac{M_0}{\lambda}\sin(\theta)\dot\theta &= \frac{\partial E(\theta, \varphi)}{\partial \varphi} \\ i\frac{M_0}{\lambda}\sin(\theta)\dot\varphi &= -\frac{\partial E(\theta, \varphi)}{\partial \theta} \end{aligned} \tag{449}$$

Prefactor A (i.e., the Van Vleck determinant) in Eq. (448) relates to fluctuations around the classical path. It should be noted that the utilization of the "single-domain" approximation (445) partly ignores a contribution on the side of unordered spin configurations to wave functions of the ground states; that is, any term similar to Ψ_0 in expression (442), the decoherence factor, is omitted. Thus, the spin–spin interaction results in the coherent behavior of a magnetic one-domain particle.

Being interested in the effect of tunnel repolarization, one can apply the semiclassical approximation, which is the most general, though is more crude at the same time. The essence of the approach is the following. We are not interested in forces, which hold a hydrogen-bonded chain. We are interested only in the possibility of transition of the polarization of the chain from the state when the polarization vector is directed to the right of the state when that is vectorial to the left. The two states are characterized by the same energy. However, in order that the polarization comes from one state to the other, the polarization should overcome some barrier. It can be made by means of either the over-barrier transition or tunnel one. We will not take an interest in a substructure (local barriers) of the aforementioned super barrier. The barrier will be determined from the anisotropy dependence of the polarized energy on the polarization vector, much as in the case of the magnetization tunneling in ferromagnetics. This allows the direct calculation of the probability of repolarization in the quasi-classical approximation, and then parameters that characterize the barrier are phenomenological constants.

We assume that the interaction between protons in the neighbor hydrogen bonds plays a role of the exchange pseudo-spin interaction, which gives rise to the coherent proton tunneling. In such a way, we will not treat the combined probability of individual protons, but will consider the probability of coherent

proton tunneling determined by the interference effect. The mesoscopic quantum coherence phenomenon can manifest itself in the measurement of the total dipole moment (i.e., polarization) **P** of a chain.

In the framework of our model, the dipole operator takes the form $P = d \sum_l (\hat{a}_{R,l}^+ \hat{a}_{R,l} - \hat{a}_{L,l}^+ \hat{a}_{L,l})$, where d is the dipole moment of a hydrogen bond. If we drop thermal fluctuations and dissipation, we can write the correlator, which takes into account successive measurements of the P separated by time interval Δt:

$$\langle P(t)P(t + \Delta t)\rangle \sim P_0^2 \Gamma^2 \cos\left(\frac{E_1 - E_0}{\hbar} \Delta t\right) \tag{450}$$

where $\langle P^2\rangle = P_0^2$. Here Γ is the matrix element [Γ^2 is written explicitly in expression (441)], and the angular brackets denote the quantum mechanical averaging.

Short hydrogen-bonded chains are characterized by a large proton polarizability, and they play a role of typical proton channels in biomembranes. That is why it is reasonable to assume that coherent proton transitions in the chain can be involved in the mechanism of real proton transport along the chain [327].

The coherent repolarization can be realized by means of the coherent tunnel proton motion along hydrogen bonds [319,320] (i.e., coherent tunnel repolarization of bonds A—H $\cdots$ A $\leftrightarrow$ A $\cdots$ H—A) and/or owing to the proton rotation around heavy atoms [320,321] (coherent tunnel reorientation of ionic groups A—H $\cdots$ A—H $\leftrightarrow$ H—A $\cdots$ H—A). The latter becomes possible when protons are tightly bound with the ionic groups, so that the probability of proton transfer along the hydrogen bond is lower than that of the orient proton motion around a heavy atom.

From the preceding, it may be seen that the probability of coherent tunneling is specified by a nonmonotonic dependence on J. This brings about an interesting ''isotopic effect'' [322,327]: The probability of coherent tunnel transitions for heavy particles can be higher than that for light particles. An analogous effect occurs in the case of the proton–phonon interaction [320], which, on the one hand, can effectively suppress local proton tunneling J (due to the increasing the effective mass of a particle) and, on the other hand, enlarge the probability of collective tunneling of protons.

Let us now consider these two possibilities and discuss the influence of phonons, which modulate the distance between heavy atoms A $\cdots$ A, on the coherent tunneling rate.

B. Two Possible Mechanisms of Coherent Tunneling of the Repolarization of Hydrogen-Bonded Chain

Let us calculate the tunneling rate of correlated proton dynamics associated with oscillations of the chain's total polarization using the quasi-classical (WKB)
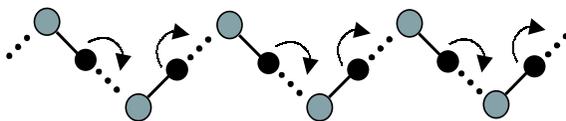
Figure 26. Chain repolarization as the coherent proton tunneling.

approximation [319,320]. We can distinguish the two following options: (i) The chain repolarization is realized owing to the coherent tunneling of protons along hydrogen bonds, and (ii) the chain repolarization occurs due to the rotation of protons around heavy backbone atoms.

In the first case (Fig. 26) a quasi-one-dimensional hydrogen-bonded chain is characterized by the two different configurations of the chain, $|\uparrow\rangle$ and $|\downarrow\rangle$ (Fig. 23), which possess the same energy. Let us assume that the hydrogen bonds are exemplified by the two-well potential, and let the two-level model in which protons are distributed between the ground state and an excited state be achieved. We can then introduce the Fermi operators of creation (annihilation) of a proton in the right and the left well of the kth hydrogen bond, $\hat{a}_{R,l}^+(\hat{a}_{R,l})$ and $\hat{a}_{L,l}^+(\hat{a}_{L,l})$, respectively. Since one hydrogen bond is occupied by only one proton—that is, $n_{R,l} + n_{L,l} = \hat{1}$, where $n_{R,l}(n_{L,l})$ is the proton number operator in the right (left) well of the lth hydrogen bond—we can pass to the pseudo-spin presentation of the proton subsystem as expressions (70)–(72) prescribe.

In this presentation, the bond polarization can be written as $p^z = 2S^z d$, where d is the dipole moment of the hydrogen bond. Then the Hamiltonian (437) of the proton subsystem is transmitted to [compare with expression (73)]

$$H = -\hbar\Omega \sum_l S_l^x - U \sum_l S_{l-1}^z S_l^z \tag{451}$$

where Ω is the tunneling frequency of a proton in the hydrogen bond [note that $\hbar\Omega = 2J$, where J is the tunnel integral written in expression (439)] and U is the Coulomb energy of a couple of protons located in neighbor hydrogen bonds. If the chain satisfies the periodical boundary conditions, the following equations of motion for the operator $\mathbf{S}_l$ are obtained:

$$\hbar \frac{dS_l^x}{dt} = U(S_l^y S_{l+1}^z + S_{l-1}^z S_l^y) \tag{452}$$

$$\hbar \frac{dS_l^y}{dt} = \hbar\Omega S_l^z - U(S_l^x S_{l+1}^z + S_{l-1}^z S_l^x) \tag{453}$$

$$\hbar \frac{dS_l^z}{dt} = -\hbar\Omega S_l^y \tag{454}$$

We recall that our key interest is the study of the tunneling dynamics of the chain polarization or, equivalently, the total pseudo-spin $\mathbf{S}$ of the chain. Following Ref. 332, we can estimate, using the quasi-classical approximation, the tunneling rate $\hbar\tau$, or the splitting energy between the states $|\uparrow\rangle$ and $|\downarrow\rangle$:

$$\hbar\tau = p\hbar\omega_p \left(\frac{\mathscr{S}_E}{2\pi\hbar}\right)^{1/2} \exp\left(-\frac{\mathscr{S}_E}{\hbar}\right) \tag{455}$$

where ω_p is the oscillating frequency of the $\mathbf{S}$ in the well, (i.e., the so-called small-angle pseudo-spin precession), p is the dimensionless prefactor, which can be about 10, and I_E is the Euclidean action for the sub-barrier rotation of the $\mathbf{S}$. Using the time-dependent mean field approximation and taking into account our assumption that the chain is a single domain, we can write the classical equation for the $\mathbf{S}$ in the following form [96]:

$$\hbar\frac{d\mathbf{S}}{dt} = -\mathbf{S} \times \frac{\partial E}{\partial \mathbf{S}} \tag{456}$$

where the anisotropy energy

$$E = -\hbar\Omega S^x - U \cdot (S^z)^2 \tag{457}$$

Vector $\mathbf{S}$ characterizes the polarization of one-domain chain. In the spherical coordinate system we have $\mathbf{S} = S(\sin\theta\cos\phi, \sin\theta\sin\phi, \cos\theta)$ and equation (456) is reduced to

$$\begin{aligned} \hbar S \frac{d\theta}{dt}\sin\theta &= \frac{\partial E}{\partial\phi} \\ \hbar S \frac{d\phi}{dt}\sin\theta &= -\frac{\partial E}{\partial\theta} \end{aligned} \tag{458}$$

The classical action that corresponds to Eqs. (458) has the form

$$\mathscr{S} = N \int dt \left(\hbar S \frac{d\phi}{dt}(\cos\theta - 1) - E(\theta, \phi)\right) \tag{459}$$

where N is the number of hydrogen bonds. The anisotropy energy

$$E(\theta, \phi) = US^2 \sin^2\theta - \hbar\Omega S \sin\theta\cos\phi + \frac{\hbar^2\Omega^2}{4U} \tag{460}$$

reaches minima at the following values of the pseudo-spin: $S_\uparrow = S(\sin\theta_0,\ 0,\ \cos\theta_0)$ and $S_\downarrow = S(\sin\theta_0,\ 0,\ -\cos\theta_0)$, where

$$\sin\theta_0 = \frac{\hbar\Omega}{2US} \tag{461}$$

They are the minima, which determine the two equilibrium polarizations of the chain. The minima are equal in magnitude but opposite in sign and direction to each other. The energy of the states is chosen to be equal to zero.

In such a way we have reduced our consideration to the problem of one-domain ferromagnetic particle with anisotropy energy described by equations (457) or (460). The problem of the macroscopic and mesoscopic quantum coherence which correspond to the tunnel switching of the magnetic moment between the two equilibrium directions was studied by Garg and Kim [332] in detail. This means that we may apply their results to calculate the tunneling frequency in the case of the hydrogen-bonded chain. Thus the Euclidean action $\mathscr{S}_E$ becomes

$$\mathscr{S}_E = N\int d\tau\left(-i\hbar S\frac{d\phi}{d\tau}(\cos\theta - 1) + E(\theta,\phi)\right) \tag{462}$$

where $\tau = it$ and the extremum of $\mathscr{S}_E$ is reached at the solution of equations

$$i\hbar S\frac{d\theta}{d\tau}\sin\theta = \frac{\partial E}{\partial\phi} \tag{463}$$

$$i\hbar S\frac{d\phi}{d\tau}\sin\theta = -\frac{\partial E}{\partial\theta} \tag{464}$$

Using the energy conservation law written for a classical path, $E = 0$, one can obtain the relationship between $\sin\theta$ and $\cos\phi$:

$$\sin^2\left(\frac{\phi}{2}\right) = -\frac{(\sin\theta - \sin\theta_0)^2}{4\sin\theta\sin\theta_0} \tag{465}$$

The sub-barrier path that conforms to the switching the motion of $\mathbf{S}$ from the state $S_\uparrow$ at $\tau = -\infty$ to the state $S_\downarrow$ at $\tau = \infty$ is defined by the instanton solution of Eqs. (464) and (465):

$$\cos\theta = -\cos\theta_0\tanh(\omega_p\tau) \tag{466}$$

$$\sin\phi = \frac{i}{2}\frac{\cot^2\theta_0\ \mathrm{sech}^2(\omega_p\tau)}{[1 + \cot^2\theta_0\ \mathrm{sech}^2(\omega_p\tau)]^{1/2}} \tag{467}$$

where $2\omega_p = \Omega \cot \theta_0$ is the small oscillation frequency in the well. Calculating the action for this trajectory, we get

$$\frac{1}{\hbar} \mathscr{S}_E(\cos \theta_0) = 2\, SN \left(-\cos \theta_0 + \frac{1}{2} \ln \left(\frac{1 + \cos \theta_0}{1 - \cos \theta_0} \right) \right) \tag{468}$$

where N is the number of hydrogen bonds in the chain. The tunneling rate is determined by the WKB exponent dependent only on $\mathscr{S}_E$ and the prefactor calculated in Ref. 332. Using these results, we can represent the splitting energy $\hbar \tau_N$ for such transitions as

$$\hbar \tau_N = 8US \left(\frac{SN}{\pi} \right)^{1/2} \left(\frac{x^5}{1 - x^2} \right)^{1/2} \left(\frac{1 - x}{1 + x} \right)^{x/2} \exp \left\{ -\frac{\mathscr{S}_E}{\hbar} \right\}, \qquad x = \cos \theta_0 \tag{469}$$

The behavior of τ_N / Ω as a function of $\hbar \Omega / U$ is demonstrated in Fig. 27. It can easily be seen that the frequency of the coherent tunnel repolarization may come close to the frequency of an individual proton that tunnels in the hydrogen bond. Note that the coherent tunnel repolarization depends nonmonotonically on Ω.

The critical temperature T_c, which correlates with the crossover from the thermal to the quantum repolarization mechanism, can be easy to estimate. The
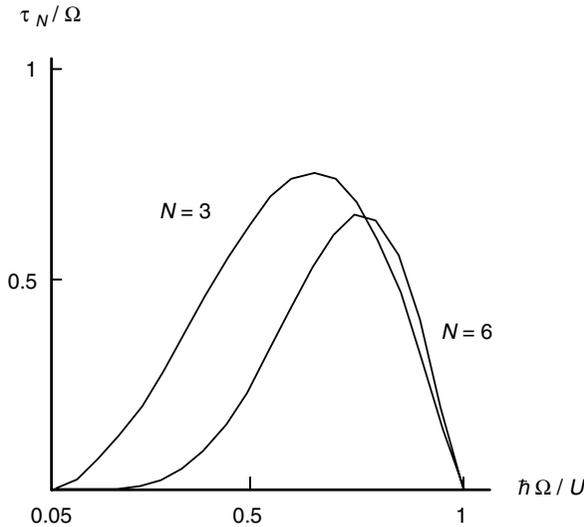

Figure 27. Normalized coherent tunneling rate τ_N / Ω as a function of the parameter $\hbar \Omega / U$. N is the number of hydrogen bonds in the chain.

probability of switching of the chain polarization via the thermal activation is proportional to $\exp(-\Delta E/k_B T)$, where $\Delta E = S^2 N(1 - \sin\theta_0)^2$ is the barrier height. When this expression is compared with that of the tunneling probability, it is apparent that

$$\exp(-\Delta E/k_B T_c) \approx \exp(-\mathscr{S}_E/\hbar) \tag{470}$$

and we immediately gain the critical temperature

$$T_c \approx \frac{\hbar \Delta E}{k_B \mathscr{S}_E} \tag{471}$$

Let us now proceed to a study of the second scenario of cooperative proton transitions, namely, the coherent tunnel motion of protons around heavy ions [320,321]. The pattern is schematically shown in Fig. 28. Such a motion of protons can be realized if protons are tightly bound with the ion groups, so that the probability of proton transfer along the hydrogen bond becomes lower than that of orientational proton motion of the group A—H. To illustrate the feasibility of such transitions, we shall treat simplest models of orientation oscillations of the ionic groups in the hydrogen-bonded chain [135,323–325]. In the two-level approximation, these models can be reduced to the model of an easy-axes ferromagnetic with the transversal external field. In Ref. 325 a model of the orientational kink defect in a quasi-one-dimensional ice crystal was proposed. In the model, the main dynamic variable was the angle between the direction of O—H bond and the principal axis of the chain. The potential energy was determined by the interaction of neighbor water molecules, which were specified by the two-well potentials, and the potential minima corresponded to the equilibrium orientations ($\cdots$O—H$\cdots$ and $\cdots$H—O$\cdots$) of water molecules in the chain. In the pseudo-spin representation, the secondary quantized Hamiltonian of such a system can be reduced to a model of the easy-axes ferromagnetic with the transversal external field [96].

However, the model by Stasyuk et al. [135] described in Section II.A is more attractive because it allows an estimation of the frequency of coherent orientational tunnel transitions taking into account both the proton dynamics of the hydrogen bonds and the reorientational processes of A—H groups. Let us
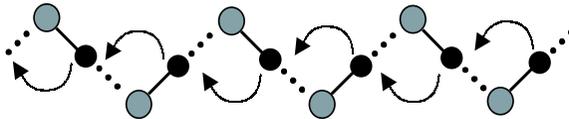

Figure 28. Cain repolarization caused by the motion of protons around backbone heavy atoms.

treat transitions between the chain configurations $|\uparrow\rangle$ and $|\downarrow\rangle$ caused by the coherent tunnel reorientation of groups A—H starting from their Hamiltonian [135] [see expression (120)]. We may choose the Hamiltonian in the form

$$H = H_0 + H_{\text{tun}} + H_{\text{rot}} + H_C \tag{472}$$

$$H_0 = \sum_l [w'(1 - n_{R,l})(1 - n_{L,l+1}) + w n_{R,l} n_{L,l+1}$$

$$+ \,\varepsilon(1 - n_{R,l}) n_{L,l+1} + \varepsilon n_{R,l}(1 - n_{L,l+1})] \tag{473}$$

Here w, w', and ε are the energies of proton configurations in the minima of the potential near an ionic group; $n_{R,l}(n_{L,l})$ is the proton number operator that characterizes the occupation of the right (left) well of lth hydrogen bond. The Hamiltonian H_{tun} in expression (472) describes the tunnel transition between two proton states in the same hydrogen bond:

$$H_{\text{tun}} = -J \sum_l (\hat{a}_{L,l}^+ \hat{a}_{R,l} + \hat{a}_{R,l}^+ \hat{a}_{L,l}) \tag{474}$$

where J is the tunnel integral. Orientational transitions of ionic groups—that is, (A—H) $\leftrightarrow$ (H—A), Fig. 28—can be described as a pseudo-tunnel effect. So the corresponding Hamiltonian is

$$H_{\text{rot}} = -\Upsilon_{\text{rot}} \sum_l (\hat{a}_{R,l}^+ \hat{a}_{L,l+1} + \hat{a}_{L,l+1}^+ \hat{a}_{R,l}) \tag{475}$$

where Υ_{rot} is the pseudo-tunnel integral caused by the orientational transitions of protons. The term H_C in expression (472) includes the Coulomb interaction between protons and electron pairs in the same hydrogen bonds (see Section II.A) [135,334]:

$$H_C = U_{(D\text{-})} \sum_l n_{R,l} n_{L,l} + U_{(L\text{-})} \sum_l (1 - n_{R,l})(1 - n_{L,l}) \tag{476}$$

Let the chain obey the periodical boundary conditions and let protons be strongly connected with heavy atoms, so that tunnel proton transitions along the hydrogen bond are negligible in comparison with the reorientation motion of A—H groups. This means that only one proton is localized near each heavy atom in the chain; that is, equality $n_{R,l} + n_{L,l+1} = \hat{1}$ holds, which makes it possible to introduce the following pseudo-spin operators:

$$S_l^x = \tfrac{1}{2}(\hat{a}_{R,l}^+ \hat{a}_{L,l+1} + \hat{a}_{L,l+1}^+ \hat{a}_{R,l}) \tag{477}$$

$$S_l^y = \tfrac{1}{2}(\hat{a}_{R,l}^+ \hat{a}_{L,l+1} - \hat{a}_{L,l+1}^+ \hat{a}_{R,l}) \tag{478}$$

$$S_l^z = \tfrac{1}{2}(\hat{a}_{R,l}^+ \hat{a}_{R,l} - \hat{a}_{L,l+1}^+ \hat{a}_{L,l+1}) \tag{479}$$

This allows us to construct the Hamiltonian for the orientational motion of ionic groups in the hydrogen-bonded chain:

$$H_{\rm rot} = -\hbar\Omega_{\rm rot}\sum_l S_l^x - U_{\rm rot}\sum_l S_{l-1}^z S_l^z \qquad (480)$$

where $\hbar\Omega_{\rm rot} = 2\Upsilon_{\rm rot}$ and $U_{\rm rot} = U_{(D\text{-})} + U_{(L\text{-})}$ specifies the energy of Bjerrum's D and L defects.

The Hamiltonian (480) of orientational oscillations of ionic groups in the hydrogen-bonded chain can be related to the model of easy-axis ferromagnetic in transversal external field $2\Upsilon_{\rm rot}$. The Hamiltonian (480) resembles the Hamiltonian (451) in outward appearance, and this means that we can reduce the problem to the previous one. However, we are interested in the explicit form of parameters $\Omega_{\rm rot}$ and $U_{\rm rot}$. For this purpose we should start from the appropriate classical Hamiltonian that describes the motion of an oriental defect in the hydrogen bonded chain [325]:

$$H = \frac{1}{2}\sum_l mr^2\dot{\vartheta}_l^2 + \chi(\vartheta_{l+1} - \vartheta_l)^2 + U[1 - (\vartheta_l/\vartheta_0)^2]^2 \qquad (481)$$

where ϑ_l is the angle of orientation of lth A—H group, as illustrated in Fig. 29; $\pm\vartheta_0$ are the angles that conform to the two different equilibrium orientations of the A—H group in the chain; m is the reduced mass of a proton in the A—H dipole; r is the length of the aforementioned dipole; U denotes the barrier height between the two equilibrium orientations of the dipole; and χ is the constant that characterizes the interaction of neighbor dipoles. Quantization of the Hamiltonian (481) by the scheme described above results in the Hamiltonian form (480).

Thus starting from the simplest pseudo-spin model of proton dynamics in the hydrogen bond, we have studied a possibility of spontaneous tunnel oscillations of the polarization of a short hydrogen-bonded chain. The phenomenon can be affected by two reasons: (a) the coherent motion of protons along the hydrogen bonds and (b) the coherent motion of protons around heavy backbone atoms.
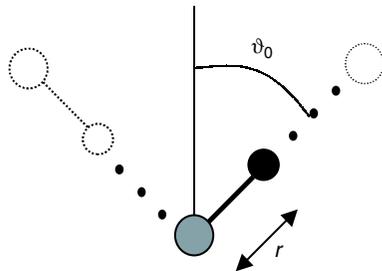

Figure 29. Orientation of the group A—H in the hydrogen-bonded chain. The angle $\pm\vartheta_0$ corresponds to two different equilibrium orientations of the A—H group.

The phenomenon is a typical example of the mesoscopic quantum coherence, which has been observed in small magnetic grains [305,309,328,329,332,335] and mesoscopic magnetic molecules [307,308]. Besides, a large proton polarizability of the hydrogen-bonded chain revealed by Zundel and co-workers [6] is the direct empirical corroboration of the coherent proton motion in the chain. The frequency of the coherent tunnel motion can be close to that of the tunnel motion of a proton in the single hydrogen bond, 5×10^{12} s^{-1}. Experimental estimation of the tunneling rate of a hydrogen-bonded chain, $\tau_{exper} \geq 10^{12}$ s^{-1}, was achieved by Zundel and collaborators [249,288,289]. The maximum value of the tunneling rate calculated in the framework of our model is also about $\tau \sim 10^{12}$ s^{-1}. The value of τ significantly depends on the number N of hydrogen bonds in the chain. For instance, assigning typical numerical values to the parameters $U/\hbar \sim 8 \times 10^3$ cm^{-1}, $\Omega \simeq 50$ to 200 cm^{-1}, and $N = 3$, we obtain the following estimate from expression (469): $\tau \sim 10^5$ to 10^{11} s^{-1}.

C.   Can Coherent Tunneling of Heavy Particles Be More Probable than That of Light Particles? The Role of Proton–Phonon Coupling

The tunneling rate (469) as a function of the tunnel integral is specified by a nonmonotone behavior (Fig. 27). Such a dependence of the probability of tunneling of the chain polarization can produce an interesting effect, namely, that the coherent tunneling of heavier particles becomes greater than that of light particles. It seems reasonable that only a part of the total energy—namely, the kinetic energy, which induces the resonance tunnel integral J—depends on the particle's mass ($J \propto \exp(-\sqrt{m}\ldots)$). However, the smaller the mass of a particle, the greater its mobility—that is, greater the value of J. Light particles are more sensitive to fluctuations, which are able to destroy the strong correlation between particles. That is why, in the case of the lightest particles, when $J \sim U$, fluctuations will strongly drop the probability of coherent tunnel transitions. On the other hand, the mobility of heavy particles is rather small, which should result in a low frequency of coherent transitions. Thus, the probability of coherent tunnel dynamics tends virtually to zero for both the lightest and the heaviest particles and, consequently, should have a maximum in an intermediate range, giving rise to a peculiar isotope effect. A similar phenomenon may appear due to the potential coupling of protons with local vibrations.

Since dissipation can bring about the degradation of the tunneling rate, we shall investigate a possible coupling of protons with backbone atoms. In some instances, for example, in the case of a mesoscopic magnetic molecule $Mn_{12}O_{12}$, the coherent spin tunneling occurs with exchange of phonons [336]. In the case of the hydrogen-bonded chain, we can take into account the interaction between protons and acoustic vibrations of hydrogen bonds, which

modulate the distance $A \cdots A$ [320]. The modulations alter the anisotropy energy (see, e.g., Ref. 96).

The interaction potential between the protons and the atom vibrations can be written as [323]

$$H_{\text{p-ph}} = \sum_l V(x_l)\rho_l, \qquad V(x_l) = \chi(x_l^2 - x_0^2) \qquad (482)$$

where χ is the coupling constant, ρ_l is the additional stretching of the lth hydrogen bond, x_l is the proton coordinate with relation to the center of the two-well potential, and $\pm x_0$ are the coordinates of the minima of the wells. In the mean field approximation the Hamiltonian of the spin–phonon system can be written as

$$H = -\hbar\Omega \sum_l S_l^x - U \sum_l S_{l-1}^z S_l^z + \sum_q \hbar\omega_q \hat{b}_q^+ \hat{b}_q$$
$$+ \sum_{l;q} (2V_{RL}S_l^x + V_{RR})\tau_{q,l}(\hat{b}_{-q}^+ + \hat{b}_q) \qquad (483)$$

where $\hat{b}_q^+ (\hat{b}_q)$ is the Bose operator of creation (annihilation) of a phonon with the wavenumber q and the frequency ω_q:

$$V_{RL} = \langle \psi_R | V(x) | \psi_L \rangle$$
$$V_{RR} = \langle \psi_R | V(x) | \psi_L \rangle \qquad (484)$$

are the matrix elements of the interaction potential $V(x)$ (482); here $|\psi_R\rangle$, $|\psi_L\rangle$ are the wave functions of a proton localized in the right and the left potential well, respectively. The interaction parameter $\tau_{q,l}$ is expressed as

$$\tau_{q,l} = \sqrt{\hbar/2MN\omega_q} \exp(iglq) \qquad (485)$$

where g is the chain constant, M is the atom (or heavy ion) mass, and N is the number of hydrogen bonds in the chain.

The effective anisotropy energy of the chain takes the form [320]

$$E^{\text{eff}} = -\hbar(\Omega + \Omega_0)S^x - U(S^z)^2 - B(S^x)^2 \qquad (486)$$

where

$$\hbar\Omega_0 = 2\frac{V_{RR}V_{RL}}{M\omega_0^2}, \qquad B = 2\frac{V_{RL}^2}{M\omega_0^2} \qquad (487)$$

The energy (486) can be rewritten in the spherical coordinates

$$E^{\text{eff}}(\theta, \phi) = (U - B)S^2(\sin\theta - \sin\theta_*)^2 + BS^2(1 - \cos^2\phi)\sin^2\theta$$
$$+ 2(U - B)S^2(1 - \cos\phi)\sin\theta\sin\theta \tag{488}$$

where

$$\sin\theta_* = \frac{\hbar(\Omega + \Omega_0)}{2S(U - B)} = \sin\theta_0 \frac{1 + \Omega_0/\Omega}{1 - B/U} \tag{489}$$

and $\sin\theta_0$ is defined in expression (461).

The spin–phonon interaction renormalizes the tunneling frequency of a proton, $\Omega \to \Omega + \Omega_0$ (the sign of the Ω_0 can be both positive and negative), which, in turn, changes the interaction between the spins. The effective anisotropy energy (488) has two minima: the first one at $\phi = 0$, $\theta = \theta_*$ and the second one at $\phi = 0$, $\theta = \pi - \theta_*$. These two solutions determine the two possible equilibrium directions of the chain polarization at the same value of the energy. We may set $E^{\text{eff}} = 0$ along the aforementioned directions.

The energy conservation law makes it possible to obtain the following expression for the classical path of the polarization:

$$\cos\phi = \frac{\sqrt{1+s}\sqrt{s\sin^2\theta + \sin^2\theta_*} - \sin\theta_*}{s\sin\theta} \tag{490}$$

where $s = B/(U - B)$. Expression (490) is reduced to expression (465) if one puts B, $\Omega_0 \to 0$. Combining (490) with the equation of motion (463), we get the instanton that moves from θ_* to $\pi - \theta_*$:

$$\cos\theta(\tau) = \cos\theta_* \tanh(\omega_*\tau)\frac{\cosh(\omega_*\tau)}{\cosh(\omega_*\tau) + \eta} \tag{491}$$

where

$$\eta = \sqrt{\frac{(1+s)\sin^2\theta_*}{s + \sin^2\theta_*}} \quad \text{and} \quad \omega_* = (\Omega + \Omega_0)\sqrt{1+s}\cot\theta_* \tag{492}$$

The instanton obtained corresponds to the subbarrier path of the tunnel switching of the vector $\mathbf{S}$ moving between the two equilibrium directions, defined by the anisotropy energy (488). The imaginary-time action associated with the solution obtained takes the form

$$\frac{\mathscr{S}_E^{\text{eff}}}{\hbar} = 2SN\left[-\delta^{-1/2}\arcsin\left(\frac{\delta^{1/2}}{(1+\delta)^{1/2}}\cos\theta_*\right) + \frac{1}{2}\ln\frac{1 + \sqrt{1 - B/U}\cos\theta_*}{1 - \sqrt{1 - B/U}\cos\theta_*}\right] \tag{493}$$

where

$$\delta = \frac{1}{\sin^2 \theta_0} \frac{B}{U} \left(1 - \frac{B}{U} \right) \tag{494}$$

The behavior of the normalized action $\mathscr{S}_E^{\text{eff}}/\mathscr{S}_E$ as a function of the ratio Ω_0/Ω at different values of B/U is shown in Fig. 30. The function $\mathscr{S}_E$ determined in expression (468) is the imaginary-time action that has been obtained without an influence of phonons on the tunneling of the polarization. In general case, the values of Ω_0 and B cannot be treated as independent parameters; the smaller the value of Ω_0, the smaller that of B. Assuming that inequalities $\Omega_0/\Omega \ll 1$ and $B/(U\sin^2 \theta_0) \ll 1$ hold, the action $\mathscr{S}_E^{\text{eff}}$ can be rewritten in the form

$$\mathscr{S}_E^{\text{eff}} \approx \mathscr{S}_E - 2\hbar SN \left[\frac{\Omega_0}{\Omega} + \frac{B}{U} \left(1 + \frac{1}{6} \cot^2 \theta_0 \right) \right] \tag{495}$$

It is obvious from expression (495) that the chain vibrations effect a decrease of the tunneling rate when $\hbar\Omega_0 \geq -B/3 \sin \theta_0$ (note that $\sin \theta_0 \ll 1$; for typical material parameters we have $\sin \theta_0 \sim 10^{-2}$–$10^{-3}$). In particular, expression
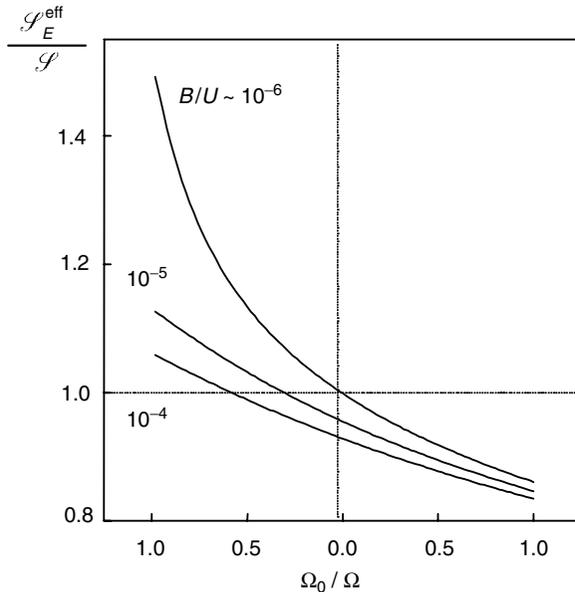
Figure 30. Role of the proton–phonon interaction in the coherent tunnel repolarization of a short chain. $\mathscr{S}_E^{\text{eff}}$ is the Euclidean renormalized action of phonons, and $\mathscr{S}_E$ is their nonrenormalized action. The bond vibrations can effectively decrease the local proton tunneling ($\Omega_0/\Omega < 0$) and at the same time increase the coherent tunneling of protons ($\mathscr{S}_E^{\text{eff}} < \mathscr{S}_E$).

(489) shows that the distance between the energy minima is reduced ($\sin \theta_* \geq \sin \theta_0$) if the spin–phonon interaction is accounted for. As this takes place, the barrier height between the minima is dropped on the value of

$$\Delta E(\Omega_0, B) = S^2 N(U - B)(1 - \sin \theta_*)^2 \leq S^2 N U(1 - \sin \theta_0)^2 = \Delta E$$

While B is always positive, Ω_0 can change in sign. The sign of Ω_0 depends on the type of the wave function $\psi_R(x)(\psi_L(x))$ of a proton localized in the right (left) potential well. The reason for the sign change can be roughly understood if we analyze the proton–phonon potential (482). The behavior of values $(x^2 - x_0^2)$, $\psi_R(x)\psi_L(x)$, and $\psi_R^2(x)$ as functions of x is schematically shown in Fig. 31. It is easily seen that the matrix element $V_{RL} = \langle \psi_R | x^2 - x_0^2 | \psi_L \rangle$ is always negative, while $V_{RR} = \langle \psi_R | x^2 - x_0^2 | \psi_R \rangle$ changes in sign: $V_{RR} < 0$ when the maximum of $\psi_R^2(x)$ is close to $x = 0$ and $V_{RR} > 0$ when the function $\psi_R^2(x)$ is shifted toward the right to the well minimum x_0. $\Omega_0 \leq 0$ when V_{RR} and V_{RL} are not the same sign. Therefore, the introduction of phonons decreases the tunneling frequency of individual protons; however, the coherent tunneling frequency can increase as it follows from the action (495).

Thus, the proton–phonon coupling being inserted into the initial Hamiltonian is able to suppress or enlarge the coherent tunnel repolarization of the chain. The realization of this or that option depends not only on the spin–phonon interaction, but also on the form of the two-well potential of the hydrogen bond.
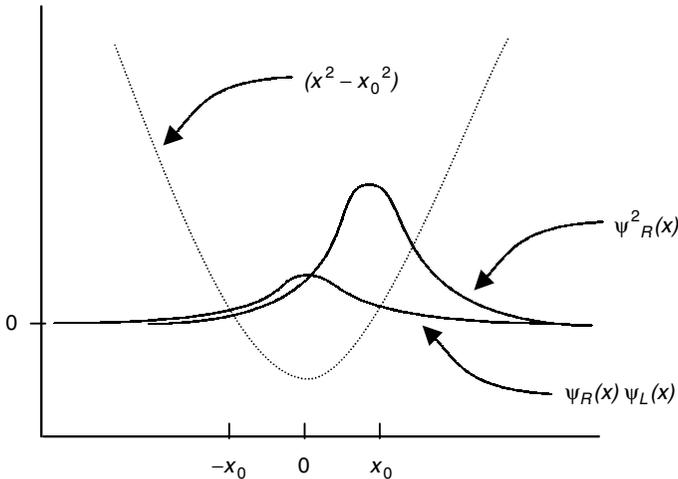

Figure 31. Schematic behavior of the functions $\psi_l(x)$, $\psi_r(x)$, $\psi_R^2(x)$, and $(x^2 - x_0^2)$, where $\psi_L(x)$ and $\psi_R(x)$ are wave functions of a proton localized in the left and right wells of the two-well potential, respectively; $\pm x_0$ are coordinates of the minimums of the right and the left wells.

When protons are tightly bound with the backbone ions, phonons will reduce the coherent tunnel rate. By contrast, when protons are localized near the potential barriers, the coherent tunnel rate will increase.

VII.   UNUSUAL PROPERTIES OF AQUEOUS SYSTEMS

A.   Organization and Thermodynamic Features of Degassed Aqueous Systems

The remarkable treatise by Eisenberg and Kauzman [139], early computer simulations based on realistic intermolecular potentials like Rahman's and Stillinger's [337,338], and the detailed random network model by Sceats and Rice [339], which took into account important peculiarities of the intermolecular interaction, allowed a significant advance in the study of water, which is believed to be a very nonordinary substance. A detailed quantitative theory of the structure of water rests on the model of a continuous tetrahedrally coordinate network of hydrogen bonds [339–342] (see also Ref. 343). The structural features of the model of a disordered network are specified in the description of the short-range order of liquid water. Changes in the potential energy of OH oscillators under the effect of the hydrogen bonds are interpreted as a result of action of a certain potential field: the potential of the disordered network. It depends only on the water molecules of the instantaneous configuration of the water molecules. In other words, it is assumed that the network of hydrogen bonds is quasi-static within the time interval of approximately 10^{-11} s (so-called V structure). The model of the disordered network leaves out of account the existence of large fluctuations brought about by cooperative motion of the water molecules, though such cooperative fluctuations, as was emphasized by Sceats and Rice, [340] must exist.

It has recently been pointed out by Rønne et al. [344] that ''the structure and dynamics of liquid water constitute a central theme in contemporary natural science [345–353].'' Modern theoretical considerations are aimed at (a) a detailed description of an electronic structure model of hydrogen bonding, applied to water molecules (see, e.g., Ref. 354), (b) models that involve a certain critical temperature where the thermodynamic response functions of water diverge (see, e.g., Ref. 353), and (c) models that presuppose a coexistence between two liquid phases [344]: a low-density liquid phase at the low-pressure side and a high-density liquid phase at the high-pressure side (see also Refs. 355–357).

Meanwhile, experimentalists have measured and analyzed, in particular, the dielectric response of liquid water in the frequency range from 10 up to 1000 cm^{-1} [344,358]. An analysis of the dielectric spectra of water shows the availability of complex permittivity in the microwave region and two absorption

bands in the far-infrared region (the maxima are recorded at 200 and 700 cm^{-1}). Generally, two-component models provide a simple way of accounting for many thermodynamic anomalies of liquid water [344]. The major results obtained are the following [344]: The dielectric relaxation is successfully represented by a biexponential model with a fast (< 300 fs) and a slow (> 2ps) decay time; the slow decay time is consistent with structural relaxation of water; and the temperature dependence of the slow relaxation time allows the modeling from a singularity point at 228 K.

Below we would like to state results [359,360] obtained on samples of bidistilled water (and exceptionally pure water obtained by means of ionic gum), which were partly degassed. These results correlate very well with the recent study on the two-component water model, the existence of a singularity temperature point, and the existence of thermodynamic anomalies of water.

In 1987, Zelepukhin and Zelepukhin [361,362] established that the removal of part of the gases dissolved in water under normal temperature and pressure conditions change biological activity of the water. Degassed water is absorbed appreciably better by the leaves of plants; and when acting on biological objects, such water stimulates their respiration and enzymatic activity. The stimulating effect manifests itself even if only a few percent of the gases contained in the aqueous system are removed from it (under normal conditions, water contains approximately 30 mg/liter of air gases). In order to elucidate the biophysical and physiological mechanisms of action of degassed water, some of its physical and electrophysical properties were studied [359,360].

The starting component was distilled water that reached equilibrium with the gases of the air (usually this takes 3 days). Degassed water was prepared in two modifications: by heating to 90°C and subsequent cooling down to 20°C (a flask was cooling with running water), or by boiling for 30 minutes and subsequent cooling down to 20°C. Different modifications of water contained the following quantities of oxygen at 20°C: the starting (equilibrium) water, 9.05 mg/liter; water degassed at 90°C, 5.2 mg/liter; water degassed by boiling for 30 minutes, 2–3 mg/liter.

1. *Experimental Results*

Since the resonance bandwidth in the proton nuclear magnetic resonance (^{1}H NMR) spectrum is in inverse dependence on the mobility of the molecules [363], this technique can provide reliable information on the degree of structurization of different modifications of water. The width of the ^{1}H NMR spectrum lines for different modifications of water was measured with a high-resolution spectrometer (Bs-467, Tesla). The resolving power of the instrument was 2×10^{-8}, and the sensitivity expressed by the signal-to-noise ratio for 1% C_6H_6-CH_2CH_3 is 100:1 at the working frequency of 60 MHz. The averaged results are presented in Table I. As is seen in Table I, the samples of the water degassed at 90°C have a

TABLE I
Magnetic Resonance Studies

Modification of Water	Bandwidth (Hz)	The Experimental Error
Equilibrium (control)	3.6	0.18
Degassed (at 90°C)	4.3	0.19
Degassed (by boiling for 30 minutes)	3.5	0.18

reliable greater width of the resonance absorption band, approximately by 20%, compared with the equilibrium water. Consequently, the mobility of the H_2O molecules of this modification of water is lower by the same percentage; hence, structurization in this modification is more pronounced. There are some grounds to suppose that water subjected to prolonged boiling features a somewhat smaller structurization than the equilibrium water (the measured error did not allow one to make a more definite statement).

Water degassed at 90°C with the following cooling was called degassed structural water. Water subjected to prolonged boiling and subsequently cooled was called degassed water with disordered structure. We will use these definitions below.

The optical density of the aforementioned water modifications was measured in the ultraviolet region with the help of a spectrometer at 188.6, 189, and 190 nm wavelengths. At these wavelengths the difference in the optical density of the degassed and equilibrium water proved to be maximum. The optical density was measured in absolute units on a control sample (equilibrium water) and on a test samples in succession. The results are presented in Table II. As can easily be seen from Table II, the optical density of degassed structural water decreases with certainty in the ultraviolet region. When degassed water was kept in thermostat in contact with air for 2–3 days, the optical density of the samples gradually approaches the values of equilibrium water.

TABLE II
Optical Density

Wavelength (nm)	Unit of Optical Density		
	Equilibrium Water (Control)	Degassed Water (at 90°C)	Degassed Water with Disordered Structure (Boiled for 30 minutes)
188.6	0.218	0.200	0.186
189.0	0.189	0.174	0.158
190.0	0.130	0.117	0.104

The electrical conductivity of the water samples was measured with the help of a slide wire bridge on D.C. in an electrolytic cell with platinized electrodes. The value of the electrical conductivity of degassed water was approximately equal to that of equilibrium water (the difference is not certain), 2.49×10^{-7} S/cm.

The pH value and the redox potential ($E_{r.p.}$, in mV) were measured as well and then the values of $E_{r.p.}$ was converted into the hydrogen index. The pH value in degassed water increases reliably compared with the control sample (Table III). In degassed structured water these changes are insignificant, whereas in degassed water with disordered structure they are significant (10%). When degassed water is kept in closed glass flask for 3 days, its pH remains higher than that of equilibrium water. When degassed water is kept for 3 days in an open glass flask, elevated pH values are preserved in structured water, whereas in water with a disordered structure the pH value practically reaches equilibrium. The growth of the water pH after degassing may be connected with the removal of the CO_2 gas; therefore, the connection between the changes of the water pH and the changes of the structure of the water may only be indirect.

The redox potential $E_{r.p.}$ of degassed water reliably declines (Table III). The greatest difference is observed in degassed water with a disordered structure. The lowered value of the redox potential is preserved in degassed water also on the third day of its remaining in a closed or open vessel.

Note that the change of the redox potential in degassed water is indicative of a change in its thermodynamic properties. There is a direct relationship between the value of $E_{r.p.}$ and the change of the free energy of the system studied [364]:

$$\Delta G = -nFE_{r.p.} \qquad (496)$$

where n is the number of the electrons transported in the redox reaction, and F is the Faraday number. Calculations in accordance with formula (496) show that the value of free electrochemical energy of equilibrium water at 19°C is equal to 13.4 kJ/mol, that of degassed structural water is 12.73 kJ/mol, and that of degassed water with a disordered structure is 10.22 kJ/mol.

TABLE III
pH and Redox Potential

Index	Modification of Water		
	Equilibrium	Degassed, Structured	Degassed with Disordered Structure
pH	5.29	5.44	5.82
E, mV	340	322	307

Consequently, the change of the redox potential makes it possible to determine the change of the free energy, the thermodynamic state of water on transition from the equilibrium state to the activated one. These changes for degassed water are essential and reliable. It was the major sensitive test that the Zelepukhins exploited for an indication of biologically active water working in the area of crop production.

2.   Thermodynamics

The conception of configuration (relaxation) contributions to the thermodynamic properties that are caused by structural changes of liquid water at different temperature and pressure is well known [301,304]. On the other hand, structural changes in water are caused by the change in the potential energy connected with interaction of the molecules—that is, with the change in the energy of hydrogen bonds.

Water subjected to experimental investigations always contains gases of the air. As a rule, the effect produced by this factor on the structure and properties of water is not taken into account. However, gases can be taken into consideration within the scope of thermodynamic solutions. Zelepukhins [359, 361] proposed to consider water that is kept in a thermostat and has reached equilibrium with the gases of the air at atmospheric pressure (usually this takes several days) as the standard state of liquid water. Kittel [365] and Pauling [366] employed such standardization of water for the thermal function and freezing point of water. From chemical thermodynamics it is known (see, e.g., Refs. 367 and 368) that the formation of solutions is accompanied by a reduction of free energy and is a spontaneous process. Therefore, when gases are removed from water, which is in equilibrium with the air, the free energy and thermodynamic activity of the water must increase. Hence, particular calculations of the thermodynamic parameters of degassed water should be performed just from this standpoint. The role of gases dissolved in the water should be regarded as the fundamental condition for the aqueous system to be in equilibrium with the environment.

The change of the free energy and the enthalpy are connected by the Gibbs–Helmholtz equation

$$\Delta G = \Delta H - T\Delta S \qquad (497)$$

which is essential for the direction of chemical reactions. The chemical system can change its state spontaneously only if this change is accompanied by the negative quantity ΔG—that is, if reversible reactions do the work. The condition of chemical equilibrium of the system is $\Delta G = 0$; then from Eq. (497) follows the equation

$$\Delta H = T\Delta S \qquad (498)$$

which relates the enthalpy factor ΔH and the entropy factor ΔS. According to the conception of Karapetiants [368], the change in the system enthalpy ΔH reflects, in the main, the tendency of molecular interactions to combine particles into aggregates (associates), whereas the change in the entropy ΔS reflects the opposite tendency toward chaotic disposition of the particles—that is, toward their disaggregation (disassociation). Thus, according to Karapetiants, these two tendencies compensate for each other in the state of chemical equilibrium defined by Eq. (498).

On the other hand, the tendency to association displayed by the molecules depends exclusively on the magnitude of their intermolecular interaction; and the measure of energy of intermolecular interaction is, apparently, the heat capacity C of the system, because it is just the heat capacity that characterizes the degree of heating of the substance. Therefore, it would be more appropriate to regard the product $C\Delta T$ as the associating index of the substance (for instance, at $p = $ const, the increment of enthalpy $\Delta H = C_p\Delta T$). Then, since the entropy determines directly the degree of the system disorder, the product $S\Delta T$ can be referred to as disordering index. If we could write an equation that combines terms $C_{p(V)}\Delta T$ and $S\Delta T$, we would be able to examine a peculiar order/disorder of water system based on the weight of each of the said terms.

It should be noted that quite recently Langner and Zundel [369] have proposed an approach to the description of proton transfer equilibria in hydrogen bonds, which in some aspects is similar to that stated herein. They have treated the proton transfer equilibria $AH \cdots B \rightleftarrows A^- \cdots H^+B$ as a function of the ΔpK_a—that is, the pK_a of the base minus the pK_a of the acid. They represented ΔH and ΔS as the sum of the intrinsic quantities ΔH_0 and ΔS_0, which describe the behavior of the systems studied in gas phase, and the external quantities ΔH_I and ΔS_I, which depicted the influence of environment. This allowed them to investigate the transition from $\Delta H = 0$ to $\Delta G = 0$ [note that ΔH and ΔG are linked by Eq. (497)] with increasing ΔpK_a and accounted for the reason of this effect. The effect appeared owing to the large negative interaction entropy term ΔS_I arising from the large order around the polar structure, which shifts the equilibria strongly to the left-hand side. In another system a single-minimum potential has been found; the proton potential has, on average, been symmetrical, whereas the proton is still largely on the left-hand side. In this case the large negative interaction entropy ΔS_I due to the order of the environment has also been drawn to explain the result (the proton is found at the acceptor B).

Coming back to our consideration, let us treat the Gibbs potential

$$G = H - TS \tag{499}$$

As it directly follows from expression (499), the total change of G has the form

$$\Delta G = \Delta H - S\Delta T - T\Delta S \tag{500}$$

Replacing ΔH for $C_p\Delta T$, we get instead of Eq. (500)

$$\Delta G = (C_p - S)\Delta T - T\Delta S \tag{501}$$

(it is assumed here that $p = $ const, but we can write down an analogous equation for the process at $V = $ const). The first summand in Eq. (501), that is,

$$\Delta G_{\text{in.in.}} = (C_p - S)\Delta T \tag{502}$$

can formally be called [359] the change of the Gibbs potential associated with intermolecular interaction (or the configuration potential), which should be taken into account at nonisothermic processes. Equation (502) is very convenient for the determining the degree of structurization of aqueous system caused by its heating and/or cooling. Indeed, $\Delta G_{\text{in.in.}}$ is directly connected with entropy S, but the residual entropy that is a part of the total entropy of the system studied is just a property of amorphous compounds.

It is easy to find numerical values of $\Delta G_{\text{in.in.}}$ from Eq. (502) by using the tabular data for C_p [370] and S [339,367,371,372]. The calculation performed in accordance with Eq. (502) has shown that for equilibrium water, $\Delta G_{\text{in.in.}}$ has positive values up to the temperature of 318 K (45°C), above which the sign of the potential change becomes negative. In other words, in the aqueous system, changes take place in the thermodynamic parameters of the intermolecular interaction (the second ''melting'' point, i.e. the melting point of the associates present in the liquid).

For equilibrium water, $\Delta G_{\text{in.in.}}$ turns to zero at 318 K, and at this temperature the curves of S and C_p intersect (Fig. 32). At the point of equilibrium obtained, the increment of the enthalpy, according to Eq. (498), is equal to

$$\Delta H|_{\text{eq.}} = T_{c0}\Delta S = 3.39 \, \text{kJ/mol} \tag{503}$$

The absolute value of the equilibrium enthalpy at 318 K is given by

$$H|_{\text{eq.}} = \Delta H|_{\text{eq.}} \frac{T_{c0}}{\Delta T} - n\Delta H_{\text{m}} = 17.92 \, \text{kJ/mol} \tag{504}$$

(the numerical value of ΔH_{m} was borrowed from Ref. 139). The value $H|_{\text{eq.}}$ exactly coincides with the value of the activation energy of self-diffusion for the molecules of water, employed in Ref. 373, and is close to the value of the hydrogen bond in water, equal to 18.84 kJ/mol, cited in Ref. 366.
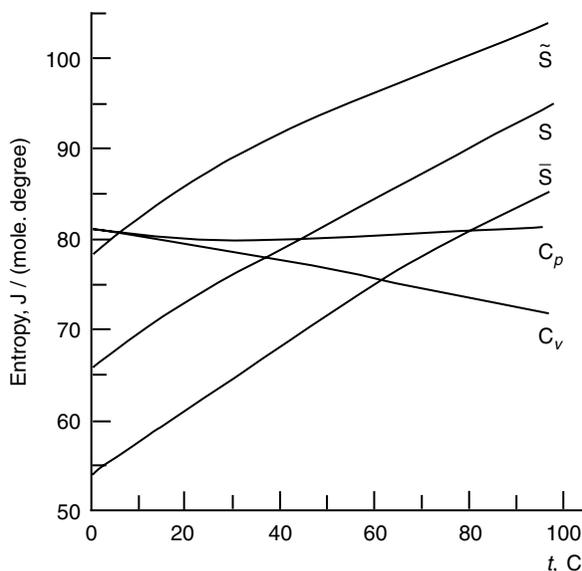
Figure 32. Entropy as a function of temperature for different modifications of water: equilibrium (S), degassed structured ($\bar{S}$), degassed with disordered structure ($\tilde{S}$). The heat capacities of water C_p and C_V as functions of T are plotted as well. (From Ref. 359.)

This approach enables the introduction of the concept of structurization of fluid—in particular, of water—with the help of the parameters C_p and S, whose numerical values for different liquids can be found in the chemical engineers' handbooks. The coefficient $\mathscr{K}$ of fluid structurization can be determined from Eq. (502); that is, putting $\Delta G_{\text{in.in.}} = 0$ we have

$$\mathscr{K} = C_p/S \qquad (505)$$

For equilibrium water, $\mathscr{K} > 1$ up to $T_{c0} = 318$ K; at $T > T_{c0}$ the inequality $\mathscr{K} < 1$ takes place. Consequently, at $T < T_{c0}$, equilibrium water as a whole is structured (the enthalpy factor prevails over the entropy factor), whereas at $T > T_{c0}$ it is nonstructured (the entropy factor prevails over the enthalpy factor). For comparison, we shall cite the values of $\mathscr{K}$ for some liquids, calculated from the published reference data for C_p and S at 25°C [374]: 1.14 for heavy water; 0.815 for hydrogen peroxide; 0.19 for ammonia. At this temperature, $\mathscr{K} = 1.073$ for equilibrium water.

Let us temporarily introduce the notion of a certain "structurization potential" and apply it for the consideration of thermodynamic parameters of degassed water. This notion must be based on the main thermodynamic

potentials and should include such peculiarities as strong intermolecular interaction, thermal expansion, and so on. In the past, theoretical [375] and experimental [376] investigations of the macrophysics properties of liquid water made it possible to establish considerable strengthening of water (by several orders of magnitudes!) in the case of specific degassing, namely, when large bubbles of gases and air present in the water were dissolved under the effect of applied pressure. A more compact arrangement of the water molecules upon application of pressure is pointed out also in monographs [377,378]. At normal conditions, incorporation of gases into the solvent disturbs the mutual ordering of the solvent molecules and is accompanied by increase of entropy [367]. Thus, on degassing of the aqueous system, its entropy must reduce in the main, and the intermolecular interaction must increase.

In the general case, not all the energy of the system during an isochoric process can be transformed into work $(-\Delta G)$. Part of the energy ("bound" energy, proportional to the residual entropy δS) is not used [368]; then we may write

$$\delta S \Delta T = V \Delta p - (-\Delta G_{\text{in.in.}}) \tag{506}$$

Let us denote the entropy of the maximum-degassed aqueous system by $\bar{S}$. Then, insofar as the residual entropy δS is greater than 0, in the first, linear approximation we have $\delta S \simeq S - \bar{S}$. In the case of an isochoric process the work $V \Delta p$ can be represented as

$$V \Delta p = T \Delta S - \Delta U \tag{507}$$

In the linear approximation $\Delta \bar{S} = \Delta S$; in the same approximation at $V = \text{const}$ the change of internal energy can be estimated as $\Delta U = C_V \Delta T$. Substituting expressions (502) and (507) with regard to explicit forms of δS and ΔU into Eq. (506), we derive the expression for the entropy of the maximum-degassed associated aqueous system

$$\bar{S} \simeq 2S - C_p + C_V - \Delta S \frac{T}{\Delta T} \tag{508}$$

From here on we shall call the maximum-associated aqueous system maximum-structured, whereas the "bound" energy $\delta S \Delta T$ can be spoken of as of "structurization potential" $\Delta \alpha$. The calculation of the value $\Delta \alpha$ from formula (506) shows that $\Delta \alpha \simeq R \Delta T$, where R is the gas constant. The calculation of the entropy from formula (508) yields the estimate $\bar{S} \simeq S - R$ (the $\bar{S}$ versus T plot is presented in Fig. 32).

The change of the Gibbs "potential" $\Delta G_{\text{in.in.}}$ in the discussed modification of water can be written in a form analogous to expression (441):

$$\Delta G_{\text{in.in.}} = (C_p - \bar{S})\Delta T \tag{509}$$

Since $\bar{S} < S$ and $\bar{C}_p = C_p$, the structurization coefficient (505) for the given aqueous system at one and the same temperature will be greater than the equilibrium system.

The plots of $\bar{S}$ and C_p as functions of temperature intersect at 85°C (see Fig. 32). Thus, at $T_c = 358$ K we have $\Delta G_{\text{in.in.}} = 0$; consequently, in this state the equilibrium value of the enthalpy increment [see (498)] is expressed as

$$\Delta \bar{H}|_{\text{eq.}} = T_c \Delta \bar{S} = 6.41 \text{ kJ/mol} \tag{510}$$

The absolute value of equilibrium enthalpy at 358 K is given by

$$\bar{H}|_{\text{eq.}} = H|_{\text{eq.}} + (\Delta \bar{H}|_{\text{eq.}} - \Delta H|_{\text{eq.}}) \tag{511}$$

where $\Delta H|_{\text{eq.}}$ and $H|_{\text{eq.}}$ are determined in expressions (503) and (504), respectively. Substituting the numerical values into (511), we get

$$\bar{H}|_{\text{eq.}} = 20.93 \text{ kJ/mol} \tag{512}$$

Thus the enthalpy of intermolecular bonding—that is, energy of the hydrogen bond in the equilibrium state in the maximum-structured water—is 3 kJ/mol greater than in the case of equilibrium water.

In the case of degassing carried out by way of long-term boiling, degassed water becomes disordered, hydrogen bonds become deformed, and the structural phase must be nearly absent. Water activated in such a manner has an enhanced dissolvability with respect to different salts (see also, e.g., Ref. 379) and is characterized by higher Gibbs potential. Consequently, we can presume that compared with equilibrium water, the entropy increases: $S \rightarrow \tilde{S} > S$ in degassed water with a disordered structure.

The maximum possible increase of entropy can be arrived at from the energy conservation law:

$$V\Delta p - (-\Delta \tilde{G}_{\text{in.in.}}) = 0 \tag{513}$$

where the change of the Gibbs "potential" of intermolecular interaction for the given modification of water is given by

$$\Delta \tilde{G}_{\text{in.in.}} = (C_p - \tilde{S})\Delta T \tag{514}$$

Let us put $\tilde{S} = S + \delta S$ and substitute this expression into Eq. (514). Then combining Eqs. (514) and (513), and taking Eq. (507) into account, we obtain the expression for estimating the entropy of a maximum-degassed disordered aqueous system:

$$\tilde{S} \simeq \Delta S \frac{T}{\Delta T} + C_p - C_V \tag{515}$$

The calculation shows that $\tilde{S} \simeq S + R$. The structurization coefficient for the given water $\mathcal{K} = 1$ at about 6°C. At this temperature, $T_c = 279$ K, the curves $\tilde{S}$ and C_p in Fig. 32 intersect and

$$\Delta\tilde{H}|_{\text{eq.}} = T_c \Delta\tilde{S} = 0.64\,\text{kJ/mol} \tag{516}$$

correspondingly, $\tilde{H}|_{\text{eq}} = 15.16$ kJ/mol, i.e., the energy of hydrogen bond of water with a disordered structure is 2.76 kJ/mol smaller than in the case of equilibrium water.

To better understand the changes taking place in the intermolecular interactions in the aqueous system, Table IV gives the calculated values of the coefficient $\mathcal{K}$ (the index of a peculiar structurization) for different modifications of water. The value $\mathcal{K}$ for equilibrium water was calculated from formula (505); for degassed structural water it was calculated from the formula $\mathcal{K} = C_p/\bar{S}$; and for degassed water with disordered structure, it was calculated from the formula $\mathcal{K} = C_p/\tilde{S}$.

It is nearly impossible to degas water completely and preserve its structure. In order to evaluate experimentally the degree of structurization of the aqueous system and, consequently, evaluate the parameters of intermolecular interaction

TABLE IV
Coefficient of Water Structurization $\mathcal{K}$

Temperature of Water (°C)	Coefficient $\mathcal{K}$			
	Equilibrium Water	Degassed, Structured Water	Snowmelt Water	Degassed Water with Disordered Structure
0	1.19	1.41	1.29	1.03
10	1.14	1.26	1.22	0.98
20	1.09	1.27	1.16	0.94
30	1.05	1.22	1.12	0.91
40	1.02	1.16	1.08	0.89
50	0.99	1.11	1.04	0.88
60	0.96	1.07	1.00	0.86
80	0.91	1.02	0.95	0.83
100	0.87	0.97	0.91	0.80

as well, the characteristics of the heat of evaporation were employed [359]. It was comparatively easy to investigate artificially prepared snowmelt water (samples contained 6.9 mg/liter oxygen at 20°C). It was found that for this modification of water, $\Delta G_{\text{in.in.}}^{(\text{exper})} = 0$ at 60°C; in this situation, $\Delta \bar{H}^{(\text{exper})}|_{\text{eq}} = 4.69$ kJ/mol and $\bar{H}^{(\text{exper})}|_{\text{eq}} = 19.26$ kJ/mol. It will readily be seen that the enthalpy in snowmelt water is greater by approximately 2 kJ/mol than that in equilibrium water. The values of the coefficient $\mathscr{K}$ for snowmelt water are listed in Table IV; the equality $\mathscr{K} = 1$ is attained at about 60°C. This is a direct indication that the degree of structurization of snowmelt water is greater than that in equilibrium water.

3.   Organization of Water System

Recent studies partly mentioned in the introduction to this section adhere chiefly to two liquid phase models, one of which is similar to the *V*-structure that appeared in the coordinate network of hydrogen bonds in Refs. 139 and 339. Spectral investigation (see, e.g., Refs. 341,342, and 380) allowed one to subdivide tentatively the diversity of hydrogen bonds in a single network into an ensemble of strong, approximately tetrahedrally directed hydrogen bonds and an ensemble of weak, appreciably disordered hydrogen bonds. Quite recently, Kaivarainen [381] has constructed a quantitative theory of liquid state, mesoscopic molecular Bose condensation in water and ice in the form of coherent clusters. Mechanisms of the first- and second-order phase transitions, related to such clusters formation, their assembly, and symmetry change, have been suggested as a consequence of computer calculation (300 parameters have been taken into account). His theory, indeed, unifies dynamics and thermodynamics on microscopic, mesoscopic, and macroscopic scales. Chaplin [382] is an advocate of the icosahedron structure of water; he presents an icosahedral cluster model and has made all explanations for 37 anomalies of water. In the past, a peculiar kind of clusters in the single network of hydrogen bonds of water was also recorded (by X-ray technique [383] and neutron scattering technique [384,385]). Very interesting results were obtained by Gordeev and Khaidarov [385]: They detected density fluctuations, supposedly globules to 3 nm in size comprising up to 10^3 molecules, and noted that the bulk water could be regarded as a polycrystal-ferroelectric with a domain structure in time ~100 ps (see also Luck [386]).

Thus many investigations support an idea about ordered regions in water. Since the water–gaseous solution is characterized by the temperature of structurization T_c discussed above, we can hypothesize that the water network features an order parameter. As a first crude approximation, in Ref. 359 an ordering of OH groups of water molecules was treated in the framework of a simplified model in which water molecules were located in knots of the Ising lattice. The model was based on the Blinc's formalism stated briefly in

Section II.D above. The pseudo-spin operator S_l^z [see formulas (68) and (72)] corresponded to two possible projections of the coordinate of the ith proton onto the z axis. The order parameter obeyed the equation

$$\langle S^z \rangle = \frac{1}{2} \tanh \frac{\langle S^z \rangle (\mathscr{J} + \delta\varepsilon)}{2k_B T} \tag{517}$$

where $2\mathscr{J}$ is the energy of cooperation of the protons and

$$2\delta\varepsilon = (\Delta\bar{H}|_{\text{eq.}} - \Delta\tilde{H}|_{\text{eq.}}) = 5.77 \, \text{kJ/mol} \tag{518}$$

is the difference between the energy of hydrogen bond in the maximum-structured water (510) and maximum-nonstructured water (516). Tending $\langle S^z \rangle$ to zero, we obtain from Eq. (517) the sought temperature of structural (phase) transition of the protons from the ordered to the mismatched state:

$$T_c = (2\mathscr{J} + 2\delta\varepsilon)/8k_B \tag{519}$$

The temperature (519) then was successfully compared [359] (with accuracy of about 5%) with the temperature of structurization T_c obtained above for the considered modifications of water.

We will return to the problem of cluster formation in water in Section VIII.

B. Determination of Water Structure by Pulsed Nuclear Magnetic Resonance (NMR) Technique

To verify the results on the existence of the critical temperature T_c in the three different modifications of water, there were measured [360] spin-lattice relaxation rates for protons in water, assuming that the latter contains both tightly and loosely bound molecules.

The spin-lattice relaxation time T_1 as a function of temperature T in liquid water has been studied by many researchers [387–393], and in all the experiments the dependence $T_1(T)$ showed a distinct non-Arrhenius character. Other dynamic parameters also have a non-Arrhenius temperature dependence, and such a behavior can be explained by both discrete and continuous models of the water structure [394]. In the framework of these models the dynamics of separate water molecules is described by hopping and drift mechanisms of the molecule movement and by rotations of water molecules [360]. However, the cooperative effects during the self-diffusion and the dynamics of hydrogen bonds formation have not been practically considered.

The spin-lattice relaxation time was measured with an ISSH-2-13 coherent nuclear quadrupole resonance spectrometer-relaxometer equipped with a Tesla BS 488 electromagnet (magnetic field strength is 1.6×10^5 A/m) to realize the

pulsed NMR regime. The probe pulse duration was several tens of microseconds and tat of the front no more than 0.5 μs. Owing to the use of the water sample volume of 0.6 cm^3, we achieved a signal-to-noise ratio on the order of 50. The signal from the sample was recorded and accumulated in a measuring computing unit. The data array involving the values of signal amplitudes and corresponding values of the pulse repetition rate was processed with a computer by the least squares method to determine spin-lattice relaxation time T_1.

The dependence of the reciprocal of the spin-lattice relaxation time T_1^{-1} on temperature T for water is generally approximated [390–394] by the sum of two exponents:

$$T_1^{-1} = A \exp(E_1/k_B T) + B \exp(E_2/k_B T) \tag{520}$$

where E_1 and E_2 are the activation energies of movement (rotational or translational) of water molecules in the low-temperature and high-temperature regions, respectively; A and B are constants or are functions of T. At the same time, the temperature dependence of T_1 can also be considered in the single-exponential approximation in the high-temperature ($T > 320$ K) and low-temperature ($T < 240$ K) regions. In this case the value of the activation energy at low temperature determined from the slope of dependence of $\ln T_1$ on T approaches the activation energy of ice (60 kJ/mol), whereas at high temperature it nears the energy of the hydrogen bond rupture (14.6 kJ/mol) [392].

Aside of the activation energies E_1 and E_2 characterizing the motion of water molecules in loosely and tightly bound structures (dominating in the high-temperature and low-temperature regions, respectively)—that is, the energy (E_1) of hydrogen bond rupture and the energy (E_2) corresponding to the continuous network of hydrogen bonds—we are interested in the contribution of each structure in the region of moderate temperatures. The study of the influence of the past history of water and of its treatment on the energetic characteristics is also of interest, because it is precisely the effect of the past history of the $T_1(T)$ that can explain the scatter of E_1 and E_2 values observed in different papers (see, e.g., Refs. 389 and 392). However, the use of the two-structure model complicates experimental data processing because one has to consider additionally the contribution from each structure; that is, the temperature dependence of coefficients A and B in Eq. (520) must be taken into account.

To process the non-Arrhenius temperature dependence of T_1, we use an approach different from that described by Eq. (520). The method, which is describing, required data in a wide temperature range (from $-30°$ to $180°$C) and rather prolonged computer calculations. The temperature dependence $T_1(T)$ can be broken in a small temperature range (from $5°$ to $70°$C) into two intervals divided by a temperature T_c and approximated in each interval by a single exponential (Fig. 33). In this case the value of the effective activation energy E_a
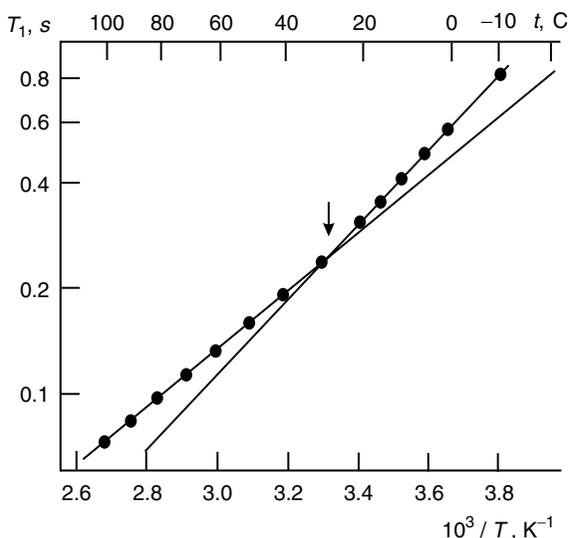
Figure 33. Single-exponential approximation of the temperature dependence of the spin-lattice relaxation rate in two temperature intervals. (From Ref. 360.)

in the region of $T < T_c$ is more than that in the region of $T > T_c$. The point $T = T_c$ plays the role of the critical temperature of water transition from the dominating tightly bound component ($T < T_c$) to the dominating loosely bound component ($T > T_c$).

The large value of E_a suggests that tightly bound water molecules greatly contribute to the spin-lattice relaxation rate in this temperature range. The closer the E_a value to $E_1 \simeq 14.6$ kJ/mol, the closer the water structure involved to the system with a single hydrogen bond per molecule. The greater the E_a, the greater the contribution of the tightly bound molecules that form a structure with an energy value E_a determined in the single-exponential approximation that allows one to estimate the effect of water treatment on the degree of molecule binding.

A glass ampoule 7 mm in diameter was approximately half-filled with water under study. The air was pumped from the ampoule by a vacuum pump, and then the ampoule was sealed and placed into a detector.

Measurements of the spin-lattice relaxation rates for protons in a freshly distilled water (taken from a flask of volume 1 liter) showed that $E_a \simeq 19.5$ kJ/mol and $T_c = 284$ K (or $t_c = 11°C$). On standing in a flask at room temperature, the structuring of the water system increased. Even after several days, measurements showed a considerable increase in the values of E_a and T_c, whereas after 40 days these parameters reached $E_a = 21.9$ kJ/mol and $t_c = 52°C$ (Fig. 34).
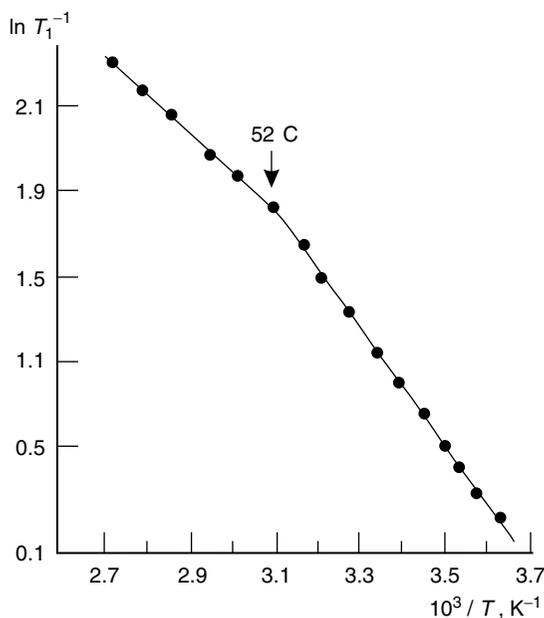
Figure 34. Temperature dependence of the spin-lattice relaxation rate for protons in water settled for 40 days at room temperature and exposed to the surrounding air. (From Ref. 360.)

When water taken from a flask had parameters $E_{a0} = 20.6$ kJ/mol and $t_{c0} = 20°C$, two extra portions of water were taken and the disordering in one of them and the structuring in the other were preformed. The value of the activation energy $\tilde{E}_a$ for the disordered water modification proved to be less than the initial one E_{a0}, namely, $\tilde{E}_a = 19.7$ kJ/mol (disordered by durational boiling), $\tilde{E}_a = 18.9$ (disordering by vacuum pumping), and $\tilde{E}_a = 15.5$ kJ/mol (disordering by passing air). The temperature $\tilde{t}_c$ for these disordered modifications was not determined because of the limitation of our method (it could not have fixed t_c below 10°C).

Water structuring results in an increase of the activation energy ($\bar{E}_a = 22$ kJ/mol) and of the transition temperature ($\bar{t}_c = 28°C$) compared to the initial values of E_{a0} and t_{c0}. Figure 35 shows the results of measurements of the spin-lattice relaxation rates for another series of samples.

In the first crude approximation the transition temperature has been described by Eq. (519). It is obvious that the value $8k_BT$ characterizes the degree of binding of water molecules at $T < T_c$. On the other hand, the energy E_a obtained in this chapter should determine the barrier height for hopping of water molecules during translational diffusion.

Table V presents the values of E_a and $8k_BT$ [see expression (519)] for different water modifications from the first series of samples. If the model [359]
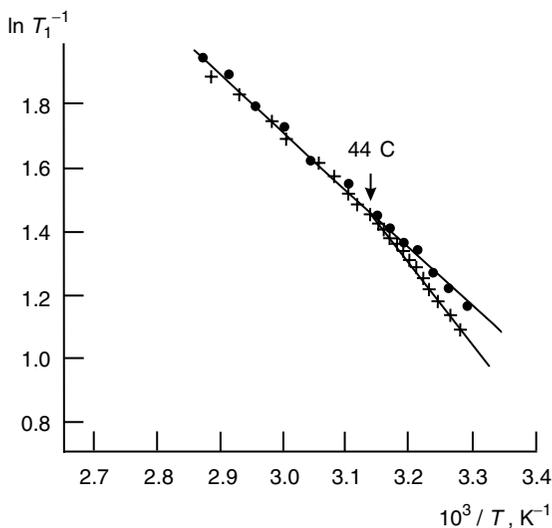
Figure 35. Temperature dependence of the spin-lattice relaxation rate for a freshly distilled water (•) and water allowed to stand in air for several days and thermally treated at 90°C—that is, for degassed structured water (+). (From Ref. 360.)

discussed in the previous subsection is assumed to be valid, inequality $E_a > 8\,k_B T$ can account for the fact that the self-diffusion of water molecule involves the surrounding groups of molecules. In particular, self-diffusion of this type in water was considered in the model of collective molecular motion [395,396]. The possibility of a diffuse random walk of groups of molecules (with a lifetime of about 100 ps) was conjectured in Ref. 385 (see also Ref. 386).

Thus, investigations of the spin-lattice relaxation rates in the water system showed directly that water by its nature is a metastable liquid. The degree of binding of its molecules depends essentially on the past history of the water system involved, and therefore in studies of dynamic parameters one has to take into account the metastable structural state of the water system. The water structure is considerably determined by atmospheric gases. Their removal from water without distortion of its structure results in the ordering of intermolecular interactions (water structuring), whereas bubbling with air, on the contrary,

TABLE V
Numerical Estimates of the Model Parameters

$t_c(°C)$	E_a kJ/mol	$8\,k_B T$ kJ/mol
52	21.9	21.6
11	19.5	18.8
20	20.6	19.5
28	22	20

weakens intermolecular interactions in water (water disordering). The water structure is also disordered after prolonged boiling. The pulsed nuclear magnetic resonance technique allowed the direct determination of the temperature T_c of peculiar structural transition in water. The activation energy E_a is also an important parameter. Its value may indicate the dominating contribution of one or another self-diffusion mechanism of water molecules in each specific modification of the water system.

C. Water-Dependent Switching in Continuous Metal Films

In moist surrounding air, sandwiched diodes Ag/BN/Si/Al [397] and planar diodes with continuous films of Ag [398] and Au [399] are characterized by a switching current that depends on the frequency and form of alternating voltage. For example, in Ref. 399 the voltage frequency was varied in the range from 0.1 to 100 Hz, the voltage reached 4.3 V, the strength of the applied field $\mathscr{E}$ is $\sim 10^4$ V/cm (possibly, $\mathscr{E}$ in the diode was high as a result of the microstructure of the films, i.e., small metallic inlands) [399], current density I is $\sim 10^6$ A/cm^2, and the curve $I(\mathscr{E})$ had the form $I \propto \mathscr{E}^\alpha$, where $0 < \alpha < 1$. The presence of the switching current is associated with the formation of a water layer on the film in the conditions of the moist surrounding space.

Earlier experiments [400,401] (see also Refs. 402 and 403) showed that hydrated colloidal particles are characterized by polarization whose nature is determined by spontaneous orientation of the polar molecules of water on the surface of particles leading to formation of the giant momentum **P**. The energy advantage of formation of **P** is shown in Ref. 404, which is in agreement with a detailed study of the dielectric anomalies in thin water layers conducted in Ref. 405. Spontaneous polarization of the monolayers of polar molecules is theoretically substantiated in Refs. [406,407].

Based on the known properties of layers of water molecules with regions of spontaneous polarization and taking into account the results stated in the section above, we have proposed [408] a detailed microscopic theory of switching current as a polarization surface current in the aforementioned regions (i.e., current of water domains).

In the experiments [397,398] the strength of the field applied to the films was low ($\mathscr{E} \leq 10^4$ V/cm) in comparison with the strength of the intramolecular field ($\mathscr{E} \sim 10^7$ V/cm); therefore, the detected higher switching current cannot be linked with induction of an additional moment (proportional to $\alpha\mathscr{E}$) on water molecules. There is another possibility—to link the switching current with polarization current determined by rotation of the water molecules in the applied field, taking into account the friction of molecules of H$_2$O on the surface of the metallic film.

Spontaneous polarization of the layer of water molecules on the metallic film cannot only be static. Since in bulk water some kinds of polycrystal-

ferroelectric domains with lifetime $\tau_{\mathrm{dom}} \sim 100$ ps were observed by neutron scattering technique [385] (and the literature on dynamic clusters is quite extensive), we assumed that two-dimensional domains could exist as well, and due to the strong bonding with the hydrophilic surface the lifetime of the domains is several orders of magnitude higher (cf. Ref. 409). The vector of polarization **P** of these "twinkling" domains on the surface of the film is the direction of the external fields. This holds only in the case in which the field over the period τ_{dom} is static; that is, the inequality $\Omega \ll \tau_{\mathrm{dim}}^{-1}$ must be fulfilled for the frequency Ω of alternating voltage.

Let us consider the cooperated behavior of the dipoles (i.e., O—H$\cdots$O bonds) in the domain on the film using Ising's model with regard to friction— that is, phonons of the film. In Ising's model the ordering of dipoles is characterized by the mean value of the z component of the pseudospin $\langle S^z \rangle$.

Thus let the electric field that is applied to the film be oriented along the z axis. The polarization current appears as a result of rotation of the dipoles in the direction of the field; that is, the dipoles periodically change the orientation and are now straight and in parallel direction and antiparallel direction in relation to the z axis. These positions of the dipoles in Ising's model are linked with two projections of the zth component of the pseudospin $\langle S^z \rangle$: $1/2$ and $-1/2$, respectively. Since the water molecules are situated on the surface of the film, we should include in the consideration the interaction with the film, which in turns introduces the interaction with the film phonons.

The form of the operators of the pseudospin is given in expressions (66)–(68). The pseudospin operators obey rules (69), which represent the switching relations in this situation studied. The total Hamiltonian for the dipoles in the domain in the mean field approximation is retained in the form

$$H = H_0 + H_{\mathrm{tun}} + H_{\mathscr{E}}(t) \tag{521}$$

$$H_0 = \sum_{l,l'} \mathscr{I}_{ll'} S_l^z \langle S_{l'}^z \rangle + \sum_{\mathbf{q}} \hbar\omega_{\mathbf{q}} \left(\hat{b}_{\mathbf{q}}^+ \hat{b}_{\mathbf{q}} + \frac{1}{2} \right)$$
$$- \sum_{l,l';\mathbf{q}} S_l^z \langle S_{l'}^z \rangle \hbar\omega_{\mathbf{q}} [u_{ll'}(\mathbf{q}) \hat{b}_{\mathbf{q}}^+ + u_{ll'}(\mathbf{q}) \hat{b}_{\mathbf{q}}] \tag{522}$$

$$H_{\mathrm{tun}} = W \sum_l S_l^x \tag{523}$$

$$H_{\mathscr{E}}(t) = -\sum_l S_l^z d_0 \mathscr{E}_0 \exp(-i\Omega t) \tag{524}$$

The first term in expression (522) describes the interaction of dipoles, the second term depicts the phonon energy of the film, and the last term characterizes the interaction of the dipoles with the film and allows for small displacements from

equilibrium positions of water atoms caused by interaction with the film's surface atoms or ions. The Hamiltonian (523) specifies the variation of the dipole spontaneous orientation from parallel to antiparallel in relation to the x axis and vice versa; H_{tun} is regarded as a perturbation. The Hamiltonian (524) describes the interaction of dipoles with the external field $\mathscr{E}(t) = \mathscr{E}_0\exp(-i\Omega t)$, where $\mathscr{E}_0$ and Ω are the amplitude and the frequency of the field. W is the "kinetic" energy required for reorientation of the dipole, and d_0 is the dipole moment of the O−H bond. $\mathscr{J}_{ll'}$ is the interaction energy between the lth and the l'th hydrogen bonds; $u_{ll'}(\mathbf{q}) = u\exp[i\mathbf{q} \cdot (\mathbf{R}_l - \mathbf{R}_{l'})]$; u is the dimensionless value describing the displacement of an atom/ion of the film owing to its hydration; $\mathbf{R}_l$ is the radius vector of the lth dipole; $\hat{b}_{\mathbf{q}}^+(\hat{b}_{\mathbf{q}})$ is the Bose operator of creation (annihilation) of a phonon with the wave vector $\mathbf{q}$ and the energy $\hbar\omega_{\mathbf{q}}$. Since the phenomenon of the water-dependent switching of current was detected [399–401] for films of Ag, Al, and Au, and the ions of these atoms are strongly hydrated, it must be assumed that $u > 1$ or even $u \gg 1$, like in the situation of a small polaron.

Using the small polaron model, we can easily diagonalize the Hamiltonian (521) with respect to the phonon variables by canonical transformation [compare with expression (255)]

$$\bar{H} = e^{-S}He^{S}, \qquad S = \sum_{l,l'} S_l^z[u_{ll'}(\mathbf{q})\hat{b}_{\mathbf{q}}^+ - u_{ll'}^*(\mathbf{q})\hat{b}_{\mathbf{q}}] \qquad (525)$$

This leads us to the following explicit form of the total Hamiltonian:

$$\bar{H} = \bar{H}_0 + \bar{H}_{\text{tun}} + H_{\mathscr{E}}(t) \qquad (526)$$

$$\bar{H}_0 = \sum_{l,l'} 2\bar{\mathscr{J}}_{ll'}S_l^z\langle S_{l'}^z\rangle + \sum_{\mathbf{q}} \hbar\omega_{\mathbf{q}}\left(\hat{b}_{\mathbf{q}}^+\hat{b}_{\mathbf{q}} + \frac{1}{2}\right) \qquad (527)$$

$$H_{\text{tun}} = W\sum_{l} \bar{S}_l^x \qquad (528)$$

where

$$2\bar{\mathscr{J}}_{ll'} = 2\mathscr{J}_{ll'} - \sum_{\mathbf{q}} |u_{ll'}(\mathbf{q})|^2\hbar\omega_{\mathbf{q}} \qquad (529)$$

$$\bar{S}_l^x = e^{-S}S_l^x e^{S} \qquad (530)$$

Thus, it is evident that the fluctuation formation of domains with polarization **P**, oriented along the applied field $\mathscr{E}$ (z axis), is more advantageous from the viewpoint of energy. Variation of the direction of the field is accompanied by the reorientation of the domains; and since the molecules of water are linked with the lattice of the metallic film, this repolarization process is extended in time to

the measured values t. In the Hamiltonian (526) the reorientation of the dipole—that is, the presence of the current of repolarization domains—is caused by operator (528), and the operator $H_\mathscr{E}(t)$ (524) specifies the direction of current. In the case $\bar{H}_{\text{tun}}, H_\mathscr{E}(t) \rightarrow 0$—that is, when the energy W of "spontaneous" reorientation of the dipole, amplitude $\mathscr{E}_0$, and frequency Ω of the field tend to zero—polarization current should not occur.

Current density is calculated by the method described in Sections III.D to III.I:

$$I = \operatorname{Im} \operatorname{Tr}(\rho_\mathscr{E} j) \tag{531}$$

where symbol Im takes into account the phase shift of current in comparison with the field $\mathscr{E}(t)$. In expression (531),

$$j = \frac{1}{\mathscr{V} i\hbar}[H_{\text{tun}}, D] \tag{532}$$

is the operator of current density where $\mathscr{V}$ is the typical volume of an elementary cell,

$$D = -d_0 \sum_l S_l^z \tag{533}$$

is the operator of the dipole moment, and

$$\rho_\mathscr{E} = -\frac{i}{\hbar} e^{i\Omega t} \int_{-\infty}^{t} d\tau e^{-i(t-\tau)\bar{H}/\hbar}[H_\mathscr{E}(t-\tau), \rho_1] e^{i(t-\tau)\bar{H}/\hbar} \tag{534}$$

is the operator of the density matrix. The correction to the density matrix caused by the Hamiltonian $\bar{H}_{\text{tun}}$ (528) is

$$\rho_1 = -\frac{e^{-\bar{H}_0/k_B T}}{\operatorname{Tr} e^{-\bar{H}_0/k_B T}} \int_0^{1/k_B T} d\lambda e^{\lambda \bar{H}_0} H_{\text{tun}} e^{-\lambda \bar{H}_0} \tag{535}$$

Furthermore, in the exponents in Eq. (534) we will ignore the operators $\bar{H}_{\text{tun}}$ and $H_\mathscr{E}$, and we assume that $\bar{H} \rightarrow \bar{H}_0$. Substituting expressions from (532) to (535) into the expression for the current (531), we obtain

$$I = \frac{W^2 d_0^2 \mathscr{E}_0 \sin \Omega t}{\mathscr{V} \hbar^2 \operatorname{Tr} e^{-\bar{H}_0/k_B T}} i \sum_l \int_0^\infty d\tau \int_0^{1/k_B T} d\lambda \operatorname{Tr}\{e^{-\bar{H}_0/k_B T}$$
$$\times (S_l^z e^{(-i\tau/\hbar + \lambda)\bar{H}_0} \bar{S}_l^x e^{-(-i\tau/\hbar + \lambda)\bar{H}_0} \bar{S}_l^y - e^{(-i\tau/\hbar + \lambda)\bar{H}_0} \bar{S}_l^x e^{-(-i\tau/\hbar + \lambda)\bar{H}_0} S_l^z \bar{S}_l^y)\} \tag{536}$$

Here the designations

$$\bar{S}_l^x = \frac{1}{2}(e^{-\hat{\beta}}\hat{a}_{+,l}^+\hat{a}_{-,l} + \hat{a}_{-,l}^+\hat{a}_{-,l}e^{\hat{\beta}})$$

$$\bar{S}_l^x = \frac{1}{2i}(e^{-\hat{\beta}}\hat{a}_{+,l}^+\hat{a}_{-,l} + \hat{a}_{-,l}^+\hat{a}_{+,l}e^{\hat{\beta}}$$

(537)

are introduced [compared with expressions (66)–(68)] where

$$\hat{\beta}_l \equiv \sum_{l;\mathbf{q}}[u_{ll'}(\mathbf{q})\hat{b}_{\mathbf{q}}^+ - u_{ll'}^*(\mathbf{q})\hat{b}_{\mathbf{q}}]$$

(538)

After operator transformations and calculation of the integrals, we obtain for the density current [407]

$$I = \frac{W^2 n d_0^2 \mathscr{E}_0 \sin \Omega t}{\hbar^2 \omega \bar{\mathscr{J}}} \left(\frac{2\pi}{|u|^2 \operatorname{cosech}(\hbar\omega/k_BT)}\right)^{1/2}$$

$$\times \exp\left(-\frac{E_a}{k_BT}\right) \sinh\frac{\langle S^z\rangle \bar{\mathscr{J}}}{2k_BT}$$

(539)

where the activation energy (height of the barrier, separated into opposite orientations of the dipole) is given by

$$E_a = k_BT|u|^2 \tanh\frac{\hbar\omega}{k_BT} - \frac{1}{2}\bar{\mathscr{J}}\langle S^z\rangle$$

(540)

and $2\bar{\mathscr{J}}$ is the energy of a hydrogen bond in the domain (i.e., $2\bar{\mathscr{J}} = 2\bar{\mathscr{J}}_{l,l-1}$).

In calculating expression (539), we examined only the nearest neighbors and ignored the dispersion; consequently, ω is the characteristic frequency of the phonons on the surface of the metallic film, and n is the concentration of the dipoles—that is, O—H bonds in the domain on the film.

The equation for the order parameter is

$$\langle S^z\rangle = \frac{\operatorname{Tr}\{S^z\exp[-(\bar{H}_0 - Nd_0\mathscr{E}_0 S^z)/k_BT]\}}{\operatorname{Tr}\exp[-(\bar{H}_0 - Nd_0\mathscr{E}_0 S^z)/k_BT}$$

$$= \frac{1}{2}\tanh\frac{\langle S^z\rangle\mathscr{J}_{\text{coll}} - Nd_0\mathscr{E}_0}{2k_BT}$$

(541)

Note that in Eq. (541) the Hamiltonian $H_{\mathscr{E}}(t)$ (524) is regarded as written at the saddle point τ_0, since $\operatorname{Re}\exp(-i\Omega\tau) \to \cos\Omega\tau_0 \simeq 1$ and N is the mean number of the dipoles for mean polarization of $\mathbf{P}$ of the domain.

Evaluating I, we shall substitute into (539) the characteristic values of the parameters. The concentration n is approximately $3 \times 10^{28}\,\mathrm{m}^{-1}$ [410], and $d_0 \simeq 10^{-29}\mathrm{C}\cdot\mathrm{m}$. Energy W can be found from the time of direct relaxation of water $\nu^{-1} \simeq 10^{-11}\,\mathrm{s}$ [385], and then $W = h\nu \simeq 6 \times 10^{-23}\,\mathrm{J}$. Like in the problem of a small polaron, we accept $|u|^2 = 10$. In this case, it is realistic to assume that the phonon frequency is $\omega \approx 10^{12}\,\mathrm{s}^{-1}$. The value $2\mathscr{J}$ should correspond to the energy of a hydrogen bond for water, and the presence of spontaneous polarization in the layer should indicate structurization of water. Therefore we put $2\mathscr{J} \simeq 20.93$ kJ/mol (see Section VI.A). Besides we set $T = 300$ K and $\langle S^z \rangle < 1$. Comparing the parameters on the basis of the order of magnitude, we can greatly simplify expression (539) for the required current density

$$I = \frac{\sqrt{2\pi}}{16} \frac{W^2 n d_0^2 \mathscr{E}_0}{|u|\hbar(k_\mathrm{B}T)^2} \langle S^z \rangle \sin \Omega t \qquad (542)$$

The numerical solution of Eq. (541) for the order parameter $\langle S^z \rangle$ as a function of $\mathscr{E}_0$ at $2\mathscr{J} \simeq 20.93$ kJ/mol, $k_\mathrm{B}T = 2.53$ kJ/mol (i.e., $T = 300$ K), $d_0 = 10^{-29}$ C·m, and $N = 100$ is given in Fig. 36. Information regarding the size of the domain can be obtained from the experiments with scattering neutrons in water [387]: They examined stable groupings of water molecules, including up to 10^3 molecules, and estimated their size at 2.5 to 3 nm. Expression (542) describes the density of current in one such domain. In experiment [399] the width of the examined film was equal to 7 mm. Consequently, the maximum number of water domains, which might be distributed along the film
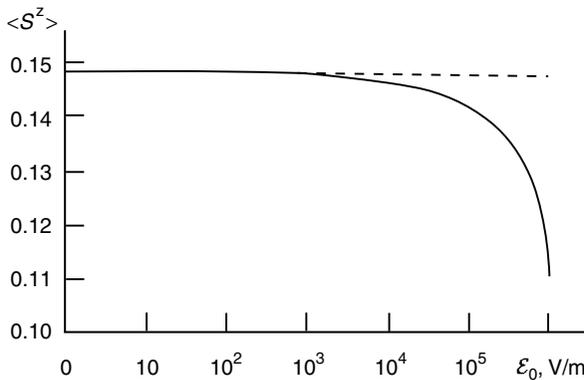

Figure 36. Numerical solution of Eq. (541) for $\langle S^z \rangle$ as a function of applied electric field $\mathscr{E}_0$. (From Ref. 408.)

width, could be evaluated as $\mathcal{N}_{\max} = 7\,\text{nm}/3\,\text{nm} \approx 10^6$. Thus, the maximum total polarization current for the film at $\mathcal{E}_{0\,\max} = 10^6$ V/m is given by

$$I_{\max} = \mathcal{N}_{\max}I \tag{543}$$

Substituting into expressions (542) and (543) all previously mentioned parameters, we obtain an estimate of the maximum current density: $I_{\max} \approx 10^6$ A/cm^2. This value is in complete agreement with the experimental results by Muller and Pagnia [399]. It is evident that the dependence $I_{\max}(\mathcal{E}_0)$ is specified by the dependence of $\langle S^z \rangle$ on $\mathcal{E}_0$ (Fig. 36), and this behavior of polarization current also corresponds to that detected in experiment [399]. It is evident that the number of domains on the surface of the film is a stochastic quantity (it is possible that it can also depend in a certain manner on the voltage applied to the film). In this case, the results (542) and (543) are in agreement with the conclusions drawn by Muller and Pagnia [399], who reported that this phenomenon on the whole is of the statistical nature.

VIII.   CLUSTERING IN MOLECULAR SYSTEMS

A.   Clusterization as Deduced from the Most General Statistical Mechanical Approach

Belotsky and Lev [411] proposed a very new approach to the statistical description of a system of interacting particles, which made allowance for spatial nonhomogeneous states of particles in the system studied. However, in the case when the inverse operator of the interaction energy cannot be determined, one should search for the other method, which, nevertheless, will make it possible to take into account a possible nonhomogeneous particle distribution. In Refs. 412–415, systems of interacting particles were treated from the same standpoint [411]; however, the number of variables describing the systems in question was reduced and a new canonical variable, which characterized the nascent nonhomogeneous state (i.e., cluster), automatically arose as a logical consequence of the particles behavior.

Having considered whether nonhomogeneous states (i.e., clusters) may appear spontaneously in systems with hydrogen bonds, we first should describe the methodology developed in Refs. 411–414. We shall start from the construction of the Hamiltonian for a system of two types of interacting particles (note that systems with hydrogen bonds consist of the minimum of two types of atoms, namely, hydrogen and oxygen).

Let atoms/molecules (called particles below) form a 3D lattice and let $n_s = \{0, 1\}$ be filling number of the sth lattice site. The energy for a system of

two types of particles (sorts A and B) can be written in the form [415]

$$H = \sum_{\mathbf{r},\mathbf{r}'} \mathscr{U}_{AA}(\mathbf{r},\mathbf{r}')c_A(\mathbf{r})c_A(\mathbf{r}') + 2\sum_{\mathbf{r},\mathbf{r}'} \mathscr{U}_{AB}(\mathbf{r},\mathbf{r}')c_A(\mathbf{r})c_B(\mathbf{r}')$$
$$+ \sum_{\mathbf{r},\mathbf{r}'} \mathscr{U}_{BB}(\mathbf{r},\mathbf{r}')c_B(\mathbf{r})c_B(\mathbf{r}') \tag{544}$$

where $\mathscr{U}_{ij}$ is the potential of the interaction of particles of types i and j $(i, j = A, B)$, which occupy notes in Ising's lattice described by the radius vectors $\mathbf{r}$ and $\mathbf{r}'$; $c_{A,B}(\mathbf{r})$ are the random functions $(c = \{0, 1\})$ that satisfy condition

$$c_A(\mathbf{r}) + c_B(\mathbf{r}) = 1 \tag{545}$$

Expression (544) can be written as follows:

$$H = H_0 + \frac{1}{2}\sum_{\mathbf{r},\mathbf{r}'} \mathscr{U}(\mathbf{r},\mathbf{r}')c_A(\mathbf{r})c_A(\mathbf{r}') \tag{546}$$

where

$$H_0 = \frac{1}{2}\sum_{\mathbf{r}}[1 - 2c_A(\mathbf{r})]\sum_{\mathbf{r}'} \mathscr{U}_{BB}(\mathbf{r},\mathbf{r}') + \sum_{\mathbf{r}} c_A(\mathbf{r})\sum_{\mathbf{r}'} \mathscr{U}_{AB}(\mathbf{r},\mathbf{r}') \tag{547}$$

$$\mathscr{U}(\mathbf{r},\mathbf{r}') = \mathscr{U}_{AA}(\mathbf{r},\mathbf{r}') + \mathscr{U}_{BB}(\mathbf{r},\mathbf{r}') - 2\mathscr{U}_{AB}(\mathbf{r},\mathbf{r}') \tag{548}$$

Let us rewrite the Hamiltonian (546) in the form

$$H = H_0 - \frac{1}{2}\sum_{\mathbf{r},\mathbf{r}'} V_{\mathbf{r}\mathbf{r}'}c(\mathbf{r})c(\mathbf{r}') + \frac{1}{2}\sum_{\mathbf{r},\mathbf{r}'} U_{\mathbf{r}\mathbf{r}'}c(\mathbf{r})c(\mathbf{r}') \tag{549}$$

where index A is omitted at the function $c(\mathbf{r})$ and the following definitions

$$V_{\mathbf{r}\mathbf{r}'} = \mathscr{U}_{AB}(\mathbf{r},\mathbf{r}') \tag{550}$$

$$U_{\mathbf{r}\mathbf{r}'} = \frac{1}{2}[\mathscr{U}_{AA}(\mathbf{r},\mathbf{r}') + \mathscr{U}_{BB}(\mathbf{r},\mathbf{r}')] \tag{551}$$

are introduced.

If the potentials $V_{\mathbf{r}\mathbf{r}'}$, $U_{\mathbf{r}\mathbf{r}'}$ are greater than 0, then, as seen from the form of the Hamiltonian (549), the second term on the right-hand side corresponds to the effective attraction and the third term conforms to the effective repulsion. The Hamiltonian (549) can be represented as the model of ordered particles, which

feature a certain nonzero parameter σ:

$$H(n) = \sum_s E_s n_s - \frac{1}{2}\sum_{s,s'} V_{ss'} n_s n_{s'} + \frac{1}{2}\sum_{s,s'} U_{ss'} n_s n_{s'} \qquad (552)$$

where E_s is the additive part of the particle energy in the sth state. The main point of our approach is the initial separation of the total atom/molecular potential into two terms: the repulsion and attraction components. So, in the Hamiltonian (552), $V_{ss'}$ and $U_{ss'}$ are respectively the paired energies of attraction and repulsion between particles located in the states s and s'. It should be noted that the signs before the potentials in expression (552) specify proper signs of the attractive and repulsive paired energies, and this means that both functions $V_{ss'}$ and $U_{ss'}$ in expression (552) are positive. The statistical sum of the system

$$Z = \sum_{\{n\}} \exp(-H(n)/k_B T) \qquad (553)$$

may be presented in the field form

$$Z = \int_{-\infty}^{\infty} D\phi \int_{-\infty}^{\infty} D\psi \sum_{\{n\}} \exp\left[\sum_s (\psi_s + i\phi_s) n_s \right.$$
$$\left. - \sum_s \tilde{E}_s n_s - \frac{1}{2}\sum_{s,s'} (\tilde{U}_{ss'}^{-1}\phi_s\phi_{s'} + \tilde{V}_{ss'}^{-1}\psi_s\psi_{s'}) \right] \qquad (554)$$

due to the following representation known from the theory of Gauss integrals:

$$\exp\left(\frac{\rho^2}{2}\sum_{s,s'} \mathscr{W}_{ss'} n_s n_{s'} \right) = \text{Re}\int_{-\infty}^{\infty} D\vartheta \exp\left[\rho\sum_s n_s\vartheta_s - \frac{1}{2}\sum_{s,s'} \mathscr{W}_{ss'}^{-1}\vartheta_s\vartheta_{s'} \right] \qquad (555)$$

where $D\vartheta \equiv \prod_s \sqrt{\det\|\mathscr{W}_{ss'}\|}\sqrt{2\pi}d\vartheta_s$ implies the functional integration with respect to the field ϑ; $\rho^2 = \pm 1$ in relation to the sign of interaction ($+1$ for attraction and -1 for repulsion). The dimensionless energy parameters $\tilde{V}_{ss'} = V_{ss'}/k_B T, \tilde{U}_{ss'} = U_{ss'}/k_B T$, and $\tilde{E}_s/k_B T$ are introduced into expression (554). Furthermore, we will use the known formula

$$\frac{1}{2\pi i}\oint dz z^{N-1-\sum_s n_s} = 1 \qquad (556)$$

which makes it possible to settle the quantity of particles in the system, $\sum_s n_s = N$, and, consequently, we can pass to the consideration of the canonical ensemble of N particles. Thus the statistical sum (554) is replaced for

$$
Z = \operatorname{Re} \frac{1}{2\pi i} \oint dz \int D\phi \int D\psi \exp\left\{ -\frac{1}{2} \sum_{s,s'} (\tilde{U}_{ss'}^{-1}\phi_s\phi_{s'} + \tilde{V}_{ss'}^{-1}\psi_s\psi_{s'}) \right.
$$
$$
\left. + (N-1)\ln z \right\} \times \sum_{\{n_s\}=0}^{1} \exp\left\{ \sum_s n_s(\psi_s + i\phi_s - \tilde{E}_s) - \ln z \right\} \quad (557)
$$

Summing over n_s, we obtain

$$
Z = \operatorname{Re} \frac{1}{2\pi i} \int D\phi \int D\psi \oint dz e^{\mathscr{S}(\phi,\psi,z)} \quad (558)
$$

where

$$
\mathscr{S} = \sum_s \left\{ -\frac{1}{2} \sum_{s'} (\tilde{U}_{ss'}^{-1}\phi_s\phi_{s'} + \tilde{V}_{ss'}^{-1}\psi_s\psi_{s'}) \right.
$$
$$
\left. + \eta \ln\left| 1 + \frac{\eta}{z} e^{-\tilde{E}_s} e^{\psi_s} \cos\phi_s \right| \right\} + (N-1)\ln z \quad (559)
$$

Here, the symbol η characterizes the kind of statistics: Bose ($\eta = +1$) or Fermi ($\eta = -1$). Let us set $z = \xi + i\zeta$ and consider the action $\mathscr{S}$ on a transit path that passes through the saddle point at a fixed imaginable variable $\operatorname{Im} z = \zeta_0$. In this case, $\mathscr{S}$ may be regarded as the functional that depends on the two field variables ϕ and ψ; and the fugacity ξ equals $e^{-\mu/k_B T}$, where μ is the chemical potential.

In a classical system the mean filling number of the sth energy level obeys the inequality

$$
n_s = \frac{1}{\xi} e^{-\tilde{E}_s} = e^{(\mu - E_s)/k_B T} \ll 1 \quad (560)
$$

(note the chemical potential $\mu < 0$ and $|\mu|/k_B T \gg 1$). By this means, we can simplify expression (559) expanding the logarithm into a Taylor series with respect to the small second member. As a result, we get the action that describes the ensemble of interacting particles, which are subjected to the Boltzmann statistics:

$$
\mathscr{S} \cong \sum_s \left\{ -\frac{1}{2} \sum_{s'} (\tilde{U}_{ss'}^{-1}\phi_s\phi_{s'} + \tilde{V}_{ss'}^{-1}\psi_s\psi_{s'}) + \frac{1}{\xi} e^{-\tilde{E}_s} e^{\psi_s} \cos\phi_s \right\} + (N-1)\ln\xi
$$
$$
\quad (561)
$$

The extremum of functional (561) is realized at the solutions of the equations $\delta\mathscr{S}/\delta\phi = 0$, $\delta\mathscr{S}/\delta\psi = 0$, and $\delta\mathscr{S}/\delta\xi = 0$, or explicitly

$$\sum_{s'} \tilde{U}_{ss'}^{-1}\phi_{s'} = -\frac{2}{\xi}e^{-\bar{E}_s}e^{\psi_s}\sin\phi_s \tag{562}$$

$$\sum_{s'} \tilde{V}_{ss'}^{-1}\psi_{s'} = -\frac{2}{\xi}e^{-\bar{E}_s}e^{\psi_s}\cos\phi_s \tag{563}$$

$$\frac{1}{\xi}\sum_{s'} e^{-\bar{E}_{s'}}e^{\psi_{s'}}\cos\phi_{s'} = N - 1 \tag{564}$$

If we introduce the designation

$$\mathscr{N}_s = \frac{1}{\xi}e^{-\bar{E}_s}e^{\psi_s}\cos\phi_s \tag{565}$$

we will easily see from Eq. (565) that the sum $\sum_s \mathscr{N}_s$ is equal to the number of particles in the system studied. So the combined variable $\mathscr{N}_s$ specifies the quantity of particles in the sth state. This means that one may treat $\mathscr{N}_s$ as the variable of particle number in a cluster. Using this variable we can rewrite the action (561) as a function of only one variable $\mathscr{N}_s$ and the fugacity ξ (see technical details in Ref. 414):

$$\mathscr{S} = -2\sum_{s,s'} \left[\tilde{V}_{ss'}\mathscr{N}_s\mathscr{N}_{s'} + \tilde{U}_{ss'}\mathscr{N}_s\mathscr{N}_{s'}\left(\frac{e^{-2\bar{E}_s+4\sum_{s'}\tilde{V}_{ss'}\mathscr{N}_{s'}}}{\xi^2\mathscr{N}_s^2} - 1\right)\right]$$
$$+ \sum_s \mathscr{N}_s(1+\ln\xi) \tag{566}$$

If we put the variable $\mathscr{N}_s = \mathscr{N} = \text{const}$ in each of the clusters, we may classify the $\mathscr{N}$ as the number of particles in a cluster [413]. Thus the model deals with particles entirely distributed by clusters.

It is convenient now to pass to the consideration of one cluster and change the discrete approximation to the continual one. The transformation means the passage from the summation over discrete functions in expression (566) to the integration of continual functions by the rule

$$\sum_s f_s = \frac{1}{\mathscr{V}}\int_{\text{cluster}} d\vec{x}\, f(\vec{x})$$
$$= \frac{1}{\mathscr{V}}\int_0^{2\pi} d\phi \int_0^{\pi} d\theta \sin\theta \int_1^{R/g+1} dx\, x^2 f(x)$$
$$= \frac{3}{\mathscr{N}}\int_1^{(\mathscr{N}+1)^{1/3}} dx\, x^2 f(x) \tag{567}$$

where $\mathscr{V} = 4\pi R^3/3$ is the volume of a cluster, R/g is the dimensionless radius of a cluster where g is the mean distance between particles in a cluster, and x is the dimensionless variable ($x = [1, R/g]$); therefore, the number of particles in the cluster is linked with R and g by the relation $(R/g)^3 \cong \mathscr{N}$. We assume that $\mathscr{N} \gg 1$ and set the upper limit in the integral (567) equal to $\mathscr{N}^{1/3}$.

If we introduce the designations

$$a = \frac{3}{\mathscr{N}} \int_1^{\mathscr{N}^{1/3}} dx\, x^2 \tilde{U}, \qquad b = \frac{3}{\mathscr{N}} \int_1^{\mathscr{N}^{1/3}} dx\, x^2 \tilde{V} \tag{568}$$

we will arrive at the action for one cluster written in the simple form

$$\mathscr{S} = 2\mathscr{N}(a - b) - 2\frac{1}{\xi^2} a e^{-2\tilde{E} + 4b\mathscr{N}} + \mathscr{N} \ln \xi \tag{569}$$

The second term on the right-hand side of expression (569) is the smallest one (owing to the inequality $e^{-2\tilde{E}}/\xi^2 \ll 1$) and is omitted hereafter.

Thus we shall start from the action

$$\mathscr{S} = 2\mathscr{N}(a - b) + \mathscr{N} \ln \xi \tag{570}$$

The extremum (minimum) of the action (570) is reached at the meaning of $\mathscr{N}$, which is found from the equation $\delta\mathscr{S}/\delta\mathscr{N} = 0$ and satisfies the inequality $\partial^2\mathscr{S}/\delta\mathscr{N}^2 > 0$. The value $\mathscr{N}_{\text{extr}}$ obtained in such a way will correspond to the number of particles that give a cluster.

B. Cluster Formation in Solid Phase of Alkyl- and Alkoxybenzoic Acids

As we mentioned in Section V, near the temperature of phase transition to the metaphase the solid state of alkyl- and alkoxybenzoic acids is unstable in relation to the formation of hydrogen-bonded open associates. The associates merge in polymer chains, which can include over 10 acid molecules. Let us treat how the statistical model described above can account for such a behavior of the associates.

We shall consider potentials that describe the interaction between dimers ($\mathscr{U}_{\text{AA}}$), between dimers and open associates ($\mathscr{U}_{\text{AB}}$), and between open associates ($\mathscr{U}_{\text{BB}}$) [see expressions (548)–(550)]. It is reasonable to assume that the potentials $\mathscr{U}_{\text{AA}}$ and $\mathscr{U}_{\text{AB}}$ are typical van der Waals; that is, $\mathscr{U}_{\text{AA}} = -C_{\text{AA}} \cdot (g/r)^6$ and $\mathscr{U}_{\text{AB}} = -C_{\text{AB}} \cdot (g/r)^6$, where C_{ij} are constants. Notice that the two peculiarities are important: (i) open associates can be regarded as impurities to the main matrix (dimers), and (ii) open associates feature a larger dipole moment in comparison with dimers. These two circumstances (see Ref. 282)

allow us to conclude that open associates interact as dipoles, and hence we can simulate the interaction between them as follows (see also Ref. 177):

$$\mathcal{U}_{BB} = -\frac{2d^2}{4\pi \varepsilon_0 r^3} \tag{571}$$

Here d is the dipole moment of the open associate formed by alkyl- or alkoxybenzoic acid molecules, and r is the distance between two interacting associates.

Now we can construct potentials of effective attraction (550) and repulsion (551), namely, $V(r) = \mathcal{U}_{AB}$ and $U(r) = (\mathcal{U}_{AA} + \mathcal{U}_{BB})/2$. Substituting these parameters into expressions for a and b (568), we get instead of the action (570)

$$\mathcal{S} = -\frac{d^2}{2\pi\varepsilon_0 g^3 k_B T}\ln\mathcal{N} + \frac{C_{AA} - 2C_{AB}}{2k_B T}\left(\frac{1}{\mathcal{N}} - 1\right) + \mathcal{N}\ln\xi \tag{572}$$

where g is the effective distance between molecules.

The equation $\delta\mathcal{S}/\delta\mathcal{N} = 0$ that determines the minimum of the $\mathcal{S}$ as a function of $\mathcal{N}$ is the following:

$$\mathcal{N}^2 - \frac{d^2}{2\pi\varepsilon_0 g^3 k_B T \ln\xi}\mathcal{N} - \frac{C_{AA} - 2C_{AB}}{2k_B T \ln\xi} = 0 \tag{573}$$

In the first approximation the solution to Eq. (573) is equal to

$$\mathcal{N} \cong \frac{d^2}{2\pi\varepsilon_0 g^3 k_B T \ln\xi} \tag{574}$$

The number of ABA/OABA molecules, which enter in the cluster, can be easily estimated. Indeed, let the dipole moment of the open associate be equal to 7D, that is, $(7/3) \times 10^{-29}$ C·m (note that long molecules linked through hydrogen bonds are characterized by a large proton polarizability [6]); the distance between two associates, g, is approximately 0.26 nm; the temperature of the phase transition, T_c, is 320 K. Substituting these values into expression (574) we obtain

$$\mathcal{N} \simeq \frac{130}{\ln\xi} \tag{575}$$

Let us now evaluate the fugacity ξ, which should satisfy the inequality $\xi \gg 1$ since we employ the classical statistics. For the evaluation, let us use the expression for the chemical potential μ of ideal gas (see, e.g., Ref. 416):

$$\mu = 3k_B T \ln(\langle\lambda\rangle n^{1/3}) \tag{576}$$

where $\langle\lambda\rangle = h/(3mk_\mathrm{B}T)^{1/2}$ is the de Broglie thermal wavelength of particles of gas and n is the concentration of the particles. As a particle, we take one open associate; hence the particle mass m is approximately 1500 m_p, where m_p is the proton mass and $n = n_\mathrm{ass} = 1.4 \times 10^{27}$ m^{-3} (see Section V). These meanings allow the calculation of the chemical potential by expression (576): $\mu \simeq -16\,k_\mathrm{B}T$. Consequently, $\ln\xi \equiv \ln[\exp(-\mu/k_\mathrm{B}T)] \simeq 16$. Substituting this value into the expression (575), we get the estimate of the number of open associates that are merged into a cluster: $\mathscr{N} \approx 8$. This result is in good agreement with the observed quantity of ABA/AOBA molecules that enter in a polymer chain (see Section V).

C. Clustering of H₂O Molecules in Water

In the case of ABA/AOBA acids, we have neglected the repulsive interaction between acid molecules due to their large size. In the case of the interaction of water molecules, we can keep the repulsion at least at the first stage of consideration. But what kind of potentials should we choose in the case of water? Since the hydrogen bond in many aspects is similar to the ionic interaction, we may assume that the pair potential between two water molecules combines both van der Waals type of interaction and the electrostatic energy. Let us choose the potential as the sum of the Lennard-Jones potential and the ionic crystal potential:

$$W_{\mathrm{H_2O-H_2O}} = \varepsilon\left[\left(\frac{1}{r/g}\right)^{12} - \left(\frac{1}{r/g}\right)^6\right] + \lambda_{\mathrm{ion\,rep.}}\exp(-r/r_0) - \alpha\frac{e^2}{4\pi\varepsilon_0\varepsilon\,r} \quad (577)$$

Here ε is the bound energy linked oxygen and hydrogen in the water molecule and g is the distance between O and H in the molecule; $\lambda_{\mathrm{ion\,rep.}}$ is the constant that describes short-range repulsion and r_0 is a typical radius of this repulsion force; α is Madelung's constant, which, as a rule, falls within the range from unit to two (see, e.g., Kittel [177]); ε is the dielectric constant (which, however, is absent in the case of ionic crystals). Having chosen the pair potential (577), we can now represent the repulsive potential U and the attractive potential V, which enter the Hamiltonian (552), as follows:

$$U = \varepsilon\left(\frac{1}{r/g}\right)^{12} + \lambda_{\mathrm{ion\,rep.}}\exp(-r/r_0) \quad\quad (578)$$

$$V = \left(\frac{1}{r/g}\right)^6 + \alpha\frac{e^2}{4\pi\varepsilon_0\varepsilon\,r} \quad\quad (579)$$

Thus the functions a and b determined in expression (568) become

$$a = \frac{1}{\mathcal{N}}\left[-\frac{\varepsilon}{3k_\mathrm{B}T}\left(\frac{1}{\mathcal{N}^3}-1\right)\right] \tag{580}$$

$$b = \frac{1}{\mathcal{N}}\left[-\frac{\varepsilon}{k_\mathrm{B}T}\left(\frac{1}{\mathcal{N}}-1\right)+\frac{3\alpha e^2}{8\pi\varepsilon_0\varepsilon gk_\mathrm{B}T}(\mathcal{N}^{2/3}-1)\right] \tag{581}$$

(the term proportional to $\lambda_{\mathrm{ion\,rep.}}$ is omitted owing to its extremely small contribution). If we substitute a (580) and b (581) in expression (570) for the action $\mathscr{S}$, we obtain

$$\mathscr{S} = -\frac{2\varepsilon}{3k_\mathrm{B}T}\left(\frac{1}{\mathcal{N}^3}-1\right)-\frac{2\varepsilon}{k_\mathrm{B}T}\left(\frac{1}{\mathcal{N}}-1\right)$$
$$+\frac{3\alpha e^2}{8\pi\,\varepsilon_0\,\varepsilon gk_\mathrm{B}\,T}(\mathcal{N}^{2/3}-1)+\mathcal{N}\ln\xi \tag{582}$$

Retaining the major terms, expression (582) is reduced to

$$\mathscr{S} \simeq -\frac{3\alpha e^2}{8\pi\varepsilon_0\varepsilon gk_\mathrm{B}T}(\mathcal{N}^{2/3}-1)+\mathcal{N}\ln\xi \tag{583}$$

The equation for the minimum of the $\mathscr{S}$ (i.e., $\delta\mathscr{S}/\delta\mathcal{N}=0$) is

$$-\frac{\alpha e^2}{4\pi\varepsilon_0\varepsilon gk_\mathrm{B}T}\frac{1}{\mathcal{N}^{1/3}}+\ln\xi = 0 \tag{584}$$

The solution to Eq. (584) is

$$\mathcal{N} = \left(\frac{\alpha e^2}{4\pi\varepsilon_0\varepsilon gk_\mathrm{B}T\ln\xi}\right)^3 \tag{585}$$

Let us now assign numerical values to the parameters g (lattice constant), α (Madelung's constant), ε (permittivity), and ξ(fugacity) (other parameters are elementary charge e, dielectric constant ε_0, and the temperature T, which can be set at 300 K). For liquid water we can set $g = 0.281$ nm; for the estimation let α be 1.3 and let ε be 4 (though $\varepsilon = 81$ for bulk water). Stobbe and Peschel [405], based on literature data [417–419] and their own studies, have concluded that the dielectric constant ε varies from 5 to 10 for the absorbed water layer with thickness from 1 nm to 12 nm. A cluster of water molecules with the radius on the order of $10g$ just falls under the aforementioned water layer thickness.

However, as was mentioned in Ref. 405, the water structure near a solid surface owing to its orienting power appears to be anisotropic, and therefore the dielectric constant of oriented water becomes a tensor. In our case we do not deal with any orienting surface, and that is why we may expect that ε is less than 5. Using expression (576), we can evaluate the chemical potential: $\mu \simeq -6.75\,k_B T$ (for water at the normal conditions $n \simeq 3 \times 10^{28}\,\mathrm{m}^{-3}$ and $\langle \lambda \rangle \simeq 0.034$ nm) and hence $\ln \xi \simeq 6.75$. Inserting all these numerical values into expression (585), we obtain $\mathcal{N} \approx 800$. This result is in line with the experimental data [383–386] discussed in Section VII. At the same time, in the case of ice, water molecules do not form any clusters: In the crystal state the interaction between water molecules is significantly stronger and hence the fugacity ξ should approach unity. Therefore, Eq. (584) will not have any cluster solution.

Thus, using methods of statistical mechanics we have shown that the homogeneous water network is unstable and spontaneously disintegrates to the nonhomogeneous state (i.e., peculiar clusters), which can be treated as an ordinary state of liquid water. However, the investigation of the dynamics of clusters is beyond of the approach described. The number $\mathcal{N}$ of water molecules that enter a cluster is a function of several parameters, namely, α, ε, and ξ (ξ, in turn, is a function of μ). It seems reasonable to assume that the main variation should undergo the dielectric constant ε and the chemical potential μ. Indeed, μ depends on temperature, volume, and total number of particles of the system studied (moreover, μ includes, though indirectly, the residual entropy). In a water system the total number of particles varies (in particular, owing to the dilution of gases of air). ε can be altered owing to introduced polar molecules and ions. Besides, external field sources (electromagnetic radiation, ultrasound, temperature, and others) can also strongly influence the water system changing conditions of the cluster formation treated above; in particular, these would cause the time relaxation to change over a long period of time.

IX. SUMMARY

In the present work the specific physical effects in structures with hydrogen bonds have received the bulk of our attention. Starting from the microscopic physics viewpoint, we have analyzed (a) the behavior of protons in a single hydrogen bond embedded in a surrounding matrix, (b) transfer and transport properties of protons in hydrogen-containing compounds, (c) proton dynamics caused by the influence of external fields, (d) the rearrangement of hydrogen bonds stipulated by temperature, (e) coherent phenomena that occur in hydrogen-bonded chains, and (f) clustering in systems with hydrogen bonds. Considerable attention has been given to the description of theoretical methods

developed and employed in resolving the problems, which had their origins in very detailed experimental research.

Particular emphasis has been placed on two antithetical urgent problems: proton transfer incorporating acoustic phonons, which is intensively studied by Trommsdorf and co-workers [15,16,21,22,78–84], and the proton dynamics that is very decoupled from the backbone lattice, which is investigated by Fillaux and collaborators [1,7–11,14,49,110–114].

Much attention has been given to the developmet and application of the small polaron model to problems associated with proton transport in systems with hydrogen bonds; it is this model that the authors have employed for a long time. In the framework of the polaron model, we have studied various aspects connected with the motion of protons both along a hydrogen-bonded chain and in the bulk compounds. In particular, we have treated two different mechanisms of superionic conductivity for the $M_3H(XO_4)_2$ class of crystals and the $NH_4IO_3 \cdot 2NHIO_3$ crystal. The small polaron model has also found use in the problem of rearrangement of hydrogen bonds and the formation of open associates in alkyl- and alkoxybenzoic acids.

The mechanism of the polariton absorption by strong symmetric hydrogen bonds has successfully been applied for the description of anomalous of the infrared spectra of the α-$KIO_3 \cdot HIO_3$ crystal. A complex investigation has been done at the disclosing of the molecular mechanism of the bacteriorhodopsin functioning.

Coherent phenomena experimentally revealed in hydrogen-bonded chains by Zundel and collaborators [3–6] (i.e., the availability of a large proton polarizability in hydrogen-bonded chains) has allowed us to construct the microscopic mechanism of fast oscillations of the chain polarizability considering the phenomenon as a macroscopic tunneling similar to the tunneling of the magnetization in ferromagnetic particles.

Rigorous experimental results obtained on degassed water modifications and the thermodynamic analysis of the corresponding aqueous systems make it possible to conclude that the impact of dissolved air on the structure of aqueous systems is very significant (for instance, though the gases of the air in standard water account only for 0.003% of its mass, the change of entropy after the degassing of water is quite great and can reach 15% [359]). More research should be done to account for a microscopic mechanism of changes brought about by the gases.

A new approach to the problem of clustering of particles (atoms or molecules) in condensed media has been applied to systems with hydrogen bonds. The aforementioned statistical mechanical approach has allowed us to investigate the spatial nonhomogeneous distribution of interacting particles starting from the initially homogeneous particle system. The major peculiarity of the concept is that it separates the paired potential to two independent

components: the attractive potential and the repulsive one, which in turn should feature very different dependence on the distance from particle. We have treated two problems: (a) clusterization of open associates in the solid phase of alkyl- and alkoxybenzoic acids and (b) clusterization of water molecules in liquid water. The method employed has enabled us to calculate the number of molecules that enter the cluster. Besides, the study conducted has revealed an important role of the chemical potential in the problem of clustering in the two mentioned cases.

APPENDIX A: STRETCHING AND BENDING ENERGIES AS FUNCTIONS OF $R_{O\cdots O}$

Novak [70] tabulated the dependence of the $O-H$ stretching excitation energies (ν_{OH}) of many compounds on the distance R_{OH}. The rate of increase of ν_{OH} is greatest in the range $0.24 < R < 0.26$ nm. Ikeda et al. [105] have recently proposed a new model of $H-O-H$ hydrogen bond dynamics, which makes it possible to calculate the hydrogen stretching and bending mode energies as functions of the hydrogen-bond length R. Their result agrees well with the experimental values presented in Ref. 70.

In the model of Ikeda et al. [105] the $O-H-O$ bonds have been considered as fixed at a separation of R, and the hydrogen has interacted with the lattice system through the oxygens. The Hamiltonian was written in the form [106,107]

$$H = H_p + H_q + H'_{pq} \tag{A1}$$

$$H_p = -\frac{\hbar^2}{2m}\frac{d^2}{dx^2} + U_{\text{unperturb}}(X) \tag{A2}$$

$$H_q = -\frac{\hbar^2}{2M}\frac{d^2}{dq^2} + \frac{1}{2}M\omega^2 q^2 \tag{A3}$$

$$H'_{pq} = \gamma q x \tag{A4}$$

Here $X = (x, y, z)$; H_p and H_q are the total Hamiltonians of the hydrogen bond and the lattice, respectively (it is supposed that the $O-H-O$ bond is decoupled from the lattice system); m is the hydrogen mass; q and M are the coordinate in the lattice system and the effective mass of the lattice's atom, respectively. H'_{pq} is an interaction Hamiltonian describing the interaction between the hydrogen and the lattice; x is the coordinate of the hydrogen along the hydrogen bond; γ is a constant.

Adopting the adiabatic approximation, Ikeda et al. [105] derived the wave functions of the hydrogen and the lattice, $\varphi(X; q)$ and $\vartheta(q)$, and the corresponding

eigenvalues (i.e., energies E and ε) from the equations

$$\left[-\frac{\hbar^2}{2m}\frac{d^2}{dX^2} + U_{\text{unperturb}}(X) + \gamma q x\right]\varphi(X;q) = E(q)\varphi(X;q) \qquad (A5)$$

$$\left[-\frac{\hbar^2}{2M}\frac{d^2}{dq^2} + G(q)\right]\vartheta(q) = \varepsilon(q)\vartheta(q) \qquad (A6)$$

Here $G(q)$ is the modified lattice potential that is defined as

$$G(q) = \frac{1}{2}M\omega^2 q^2 + E_0(q) \qquad (A7)$$

where $E_0(q)$ is the ground-state energy of hydrogen. The unperturbed hydrogen potential function is given as [106,108]

$$H_{\text{unperturb}}(x, y, z) = \frac{f}{2}(\alpha_1^2 + \alpha_2^2) + \frac{g}{2}(\beta_1^2 + \beta_2^2) + V([(x-x_1)^2 + y^2 + z^2]^{1/2})$$
$$+ V([(x-x_2)^2 + y^2 + z^2]^{1/2}) \qquad (A8)$$

where x_1 and x_2 are the positions of two oxygen at the equilibrium value $x = \pm R/2$. $\alpha_{1,2}$ and $\beta_{1,2}$ are the bending angles of the hydrogen defined with respect to both oxygens (below $i = 1, 2$):

$$\alpha_i = \sin^{-1}\{y/[(x-x_i)^2 + y^2]^{1/2}\} \qquad (A9)$$

$$\beta_i = \sin^{-1}\{z/[(x-x_i)^2 + z^2]^{1/2}\} \qquad (A10)$$

$V(r)$ is the Morse potential defined as

$$V(r) = V_0[e^{-2a(r-r_0)} - 2e^{-a(r-r_0)}] \qquad (A11)$$

All of the parameters, especially expression (A8), have been determined for KH_2PO_4 shape KD_2PO_4. The shape of $U_{\text{unperturb}}(X)$ in expression (A8) is given as a function of R. Hence $U_{\text{unperturb}}$ depends on $E_0(q; H)$, $E_0(q; D)$ and $\lambda q_c(H)$, $\lambda q_c(D)$. It has been found that λq_c increases with R, and this changes the effective hydrogen potential $[U_{\text{unperturb}}(X) + \lambda q_c x]$.

In order to calculate the R dependence of the stretching excitation energies across a wide range of R ($0.24 < R < 0.29$ nm), they additionally introduced higher-order bending terms, $\zeta(\alpha_1^4 + \beta_1^4 + \alpha_2^4 + \beta_2^4)$, into Eq. (A8). Using calculated values of $\lambda q_c(H)$ and $\lambda q_c(D)$, we have calculated the stretching ν_{OH} and bending δ_{OH} and γ_{OH} energies. The obtained values have been compared with Novak's summary of the experimental data. The calculated values are

indeed totally consistent with the observations. Besides, at $R \approx 0.26$ nm a strong Fermi resonance has been predicted as a general future of any hydrogen bond compound with 0.26 nm.

In the case of the R dependence of ν_{OD} for deuterated compounds, a Fermi resonance is predicted as well, but at $R \cong 0.255$ nm. It has been found that the potential $\lambda q_c(H)$ differs from $\lambda q_c(D)$ greatly; and because of that, the H and D isotopomers feature different properties in the ranges of $R < 0.243$ nm and $R > 0.26$ nm. $\lambda q_c(D) > \lambda q_c(H)$, which means that a stronger effective distortion takes place in the D potentials and in O—H—O bonds. These strong distortions depress the ground-state energy of deuterium and therefore depress the reaction rate of D isotopomers even in the range expected from simple mass consideration conducted in Ref. 109.

APPENDIX B: A POSSIBLE MECHANISM OF SONOLUMINESCENCE

Sonoluminesce is the glow seen from bubbles in a liquid under ultrasound. The experiment [123] allowed the investigation of a single bubble. The band of light is broad, $200 \leq \lambda \leq 800$ nm [124]. The light is radiated during each acoustic cycle, which lasted from 40 to 350 ps [125,126]. A number of studies have been devoted to explain the phenomenon (see, e.g., Refs. 127–134). Willison [122] has considered the motion of a proton in the hydrogen bond in cold water quantum mechanically, and the radiation from the tunneling charge has been treated classically.

The one-dimensional quadratic potential $V = \frac{1}{2}kx^2$ has been used for the description of covalent binding. The ground-state wave functions for a simple harmonic oscillator, ψ_L and ψ_R, have been used to describe the proton in the left and right wells. The force constant k has been determined from the stretch-mode vibrational transitions for water occurring at 3700 cm^{-1}. The ground-state energy for the proton is 0.368×10^{-19} J. The tunneling barrier is $\Delta E = 4 \times 10^{-19}$ J.

First-order perturbation theory makes it possible to estimate the transition rate between ψ_L and ψ_R. Initializing the system in ψ_L, all of the wave function amplitude moves to ψ_R in the 18 ns after the step perturbation is applied as asserted in Ref. 122. Then, reduction of the distance between potential wells by 0.025 nm reduces the time to move all of the population to less than 4 ps. The making and breaking of hydrogen bonds that takes place during a phase transition is a "switch" that turns "on" the tunneling current. It is assumed that the intensity of the radiated light will depend on the number of tunneling events that occur during the phase transition.

The wavelength of the emissions then will depend on the time Δt that the proton needs to tunnel between binding sites. This time may be shorter than

the transition rate. The time can be estimated from the uncertainty principle: $\Delta t \sim 2.2 \times 10^{-16}$ s.

The current impulse of a proton tunneling event is written as a Gausssian impulse:

$$i(t) = \frac{2e}{\sqrt{2\pi}\Delta t} \exp\left(-\frac{2t^2}{\Delta t^2}\right) \tag{B1}$$

The current impulse (B1) can be expressed as Fourier component amplitudes, $2e \exp[-(\pi v \Delta t^2)]$ per second. In such a presentation, v plays the role of frequency (in hertz) of radiated light.

The spectral radiance for the wavelength λ is written as [122]

$$R(\lambda) = \frac{4\pi\sqrt{\mu}\, ce^2\delta^2}{3\sqrt{\varepsilon}\,\lambda^4 e^{\frac{c^2\hbar^2}{2\lambda^2\Delta E^2}}} \tag{B2}$$

where δ is the charge tunneling distance; ΔE is the height of the potential barrier; ε and μ are the permittivity and permeability of a medium (i.e., water in our case), respectively. For the estimated tunneling barrier ($\Delta E = 4.64 \times 10^{-19}$ J) the maximum wavelength is $\lambda_{\text{peak}} = 213$ nm.

All wavelengths are radiated simultaneously by a current impulse. The total number of photons emitted by a single tunneling event is estimated by dividing $R(\lambda)$ by the energy per photon (hc/λ) and integrating over the observed interval of wavelengths. The calculation yields 10^{-9} photons per one tunneling event radiated into a band between 200 and 800 nm.

In the case of sonoluminescence, typically 10^6 photons are radiated for a bubble collapse. This can be satisfied by 10^{15} tunneling events that happen incoherently. The sample of water incorporated by one bubble included approximately 10^{16} molecules of H_2O, which is quite enough for the number of tunneling events needed for the phenomenon of sonoluminescence observed.

APPENDIX C: DIAGONALIZATION OF PHONON VARIABLES

Let us sum over l and q (or k) in the second term of expression (203) with allowance for $\langle n_l \rangle = n = \text{const}$, $u_l(q) = N^{-1/2}u_q \exp(iqR_l)$, and $v_l(k) = N^{-1/2}v_k\exp(ikR_l)$. Then let us write Hamiltonian (192) as the sum of two terms:

$$H = \mathscr{H}_0 + \mathscr{H}_{01} \tag{C1}$$

$$\mathscr{H}_{01} = \sum_l E\hat{a}_l^+ \hat{a}_l + \frac{1}{2}\sum_q \hbar(\omega_0(q) + \omega_{\text{ac}}(q))$$
$$- \sum_l \hbar\omega_0(q)\hat{a}_l^+ \hat{a}_l[u_l(q)\hat{b}_q^+ + u_l^*(q)\hat{b}_q] + \sum_{l,m} J(R_m)\hat{a}_{l+m}^+ \hat{a}_l \tag{C2}$$

The second term in expression (197), symmetrized in q, can be represented as

$$\mathscr{H}_0 = \sum_{\alpha,\beta;q>0} \left\{ \frac{1}{2}[R_{\alpha\beta}(q)\hat{x}_\alpha^+(q)\hat{x}_\beta^+(-q) + R_{\alpha\beta}^*(q)\hat{x}_\alpha^+(-q)\hat{x}_\beta^+(q)] \right.$$
$$+ [S_{\alpha\beta}(q)\hat{x}_\alpha^+(q)\hat{x}_\beta(q) + S_{\alpha\beta}^*(q)\hat{x}_\alpha^+(-q)\hat{x}_\beta(-q)]$$
$$\left. + [R_{\alpha\beta}^*(q)\hat{x}_\alpha(q)\hat{x}_\beta(-q) + R_{\alpha\beta}(q)\hat{x}_\alpha(-q)\hat{x}_\beta(q)] \right\} \qquad (C3)$$

where $\alpha = 1,2$; $\beta = 1,2$; $\hat{x}_1(q) = \hat{b}_q$, $\hat{x}_2(q) = \hat{B}_q$

$$||R_{\alpha\beta}(q)|| = \left\| \begin{array}{cc} 0 & h\chi n u_q v_q \\ h\chi n u_q^* v_q^* & 0 \end{array} \right\|$$
$$\qquad (C4)$$
$$||S_{\alpha\beta}(q)|| = \left\| \begin{array}{cc} \hbar\omega_0(q) & h\chi n u_q v_q \\ h\chi n u_q^* v_q^* & \hbar\omega_{ac}(q) \end{array} \right\|$$

By means of the Bogolyubov–Tyablikov transformation [172,173]

$$\hat{b}_q = \sum_\iota [\hat{b}_\iota(q)f_{q\iota}^{(1)} + \hat{b}_\iota^+(-q)g_{q\iota}^{(1)*}]$$
$$\hat{B}_k = \sum_\iota [\hat{b}_\iota(k)f_{k\iota}^{(2)} + \hat{b}_\iota^+(-k)g_{k\iota}^{(2)*}]$$
$$\qquad (C5)$$

the Hamiltonian (C3) is diagonalized:

$$\mathscr{H}_0 = -\sum_{\iota=1}^{2}\sum_{\alpha=1}^{2}\sum_q \hbar\Omega_\iota(q)|g_{-q\iota}^{(\alpha)}|^2 + \sum_{\iota=1}^{2} \hbar\Omega_\iota(q)\hat{b}_\iota^+(q)\hat{b}_\iota(q) \qquad (C6)$$

The eigenvalues of $\mathscr{H}_0$ are determined from the equations

$$\hbar\Omega_\iota(q)f_{q\iota}^{(\alpha)} = \sum_\beta [S_{\alpha\beta}(q)f_{q\iota}^{(\beta)} + R_{\alpha\beta}(q)g_{-q\iota}^{(\beta)}]$$
$$-\hbar\Omega_\iota(q)f_{q\iota}^{(\alpha)} = \sum_\beta [S_{\alpha\beta}(-q)g_{q\iota}^{(\beta)} + R_{\alpha\beta}(-q)f_{-q\iota}^{(\beta)}]$$
$$\qquad (C7)$$

The functions $f_{q\iota}^{(\alpha)}$ and $g_{q\iota}^{(\alpha)}$, where $\iota = 1,2$, are determined from Eq. (C7). The form of these functions should meet the requirement that passing from the operators $\hat{b}_{1,2}$ back to the operators $\hat{b}_q$, $\hat{B}_q$, the Hamiltonian (C2) in the limit $\chi \to 0$ must be reduced to that without charge carrier interaction with acoustic

phonons; that is, the coefficients of the terms $\hat{a}_l^+ \hat{a}_l (\hat{B}_q^+ + \hat{B}_q)$ must be equal to zero. The explicit form of the function $f_{ql}^{(\alpha)}$ and $g_{ql}^{(\alpha)}$ is presented in Ref. 165.

Returning to Hamiltonian (C1) in which the operator $\mathscr{H}_0$ is given by (C5) and the operator $\mathscr{H}_{01}$ is given by (C2), expressed through the new operators $\hat{b}_\iota$ (here $\iota = 1,\ 2$), we obtain Hamiltonian (205). In expression (205) the energy is counted from

$$\frac{1}{2}\hbar \sum_q \left[\omega_0(q) + \omega_{\mathrm{ac}}(q) - \sum_\iota \hbar\Omega_l(q) \left(1 + \sum_\alpha |g_{-ql}^\alpha|^2 \right) \right]$$

APPENDIX D: PROTON BIFURCATION AND
THE PHONON MIXTURE

In the ammonium triiodate hydrogen $NH_4IO_3 \cdot 2HIO_3$ crystal, the proton bifurcation for $T > T_c = 120$ K is treated as the origin of a mixture of low-frequency phonon mode ($\omega_1 = 99\ \mathrm{cm}^{-1}$) and high-frequency intracellular mode ($\omega_2 = 756\ \mathrm{cm}^{-1}$, which characterizes the collective vibrations of IO_3 pyramids). Following Ref. 47, let us study a mechanism of the change of intensity of the two aforementioned modes with temperature in the range $T_c < T < T_0$, where $T_c = 120$ K and $T_0 = 213$ K.

The interaction between an incident electromagnetic field and a polar crystal has the form $H_{\mathrm{int}} = \mathbf{P} \cdot \mathscr{E}(\mathbf{r},\ t)$, where $\mathscr{E}(\mathbf{r},\ t) = \mathscr{E}_0 e^{i\mathbf{q}\mathbf{r} - i\omega t}$. If the crystal features two active optical modes, the components of its polarization can be presented as follows [47]:

$$P_s(\mathbf{q},\ \omega) = \frac{-1 + \varepsilon_{ss'}(\mathbf{q},\ \omega)}{4\pi} \mathscr{E}_{0s'} \tag{D1}$$

where the permittivity of the crystal is equal to

$$\varepsilon_{ss'}(\mathbf{q},\ \omega) = \varepsilon_{ss'}^{(0)} + \sum_{j=1}^2 d_{js}(\mathbf{q}) d_{js'}(\mathbf{q})$$
$$\times \left[\frac{2\omega(\omega^2 - \omega_j^2(\mathbf{q}))}{(\omega^2 - \omega_j^2(\mathbf{q}))^2 + 4\omega^2\eta^2} + i\eta \frac{4\omega^2}{(\omega^2 - \omega_j^2(\mathbf{q}))^2 + 4\omega^2\eta^2} \right] \tag{D2}$$

Here $d_{js}(\mathbf{q})$ refers to the components of dipole moments of the crystal cell.

Upon the first phase transition ($T > T_c$), when a proton in a unit cell is bifurcated, the proton deforms the lattice and interacts with crystal vibrations. The interaction leads to the rearrangement of the phonon spectrum. Corresponding transformations of the $\omega_j(\mathbf{q})$ values can be obtained in the framework

of the small polaron model. For the crystal studied, the $\omega_{1,2}(\mathbf{q})$ change only by a few cm^{-1} when the temperature passes the point $T = T_c$ on the temperature scale; and further on, for $T > T_c$, they remain constant ($\omega_1 = 99$ cm^{-1} and $\omega_2 = 756$ cm^{-1}). However, according to the experimental results, in the ammonium triiodate hydrogen crystal these two modes that provide the proton polaron motion have anomalous temperature behavior, unlike all the other modes of the crystal. Consequently, in this case the proton should influence the intensity of atomic vibrations of the crystal.

The first phase transition leads to very interesting changes in the lattice of the crystal studied. For $T > T_c$, since each proton is bifurcated, it does not have a strictly fixed position but migrates ceaselessly between two hydrogen bonds. Protons in a polar crystal are strongly connected with the most polarizable longitudinal optic mode—that is, the 99-cm^{-1} mode in our case. Then with two possible positions of the proton the neighboring sites move in different potential wells. However, the frequency of proton jumps is very large, on the order of 10^{13}–10^{14} s^{-1}. Therefore the sites have not managed to occupy new equilibrium positions. So, the stationary state of the lattice is not fixed, but fluctuates uninterruptedly. A similar statement is true for IO$_3$ pyramids in the cell, whose collective behavior is described by the 756 cm^{-1} mode. Thus, the proton bifurcation can be considered as a distinctive fluctuation source that induces an additional displacement $\delta u_{\mathbf{l}}$ of the cellular sites. The intensity $\mathscr{I}_1$ of the source is directly connected with the lattice mode, 99 cm^{-1}; that is, the real fluctuation displacement of the lth site should be described by the term $\delta u_{\mathbf{l}}(\mathscr{I}_1)$. This term can be represented in the form $\delta u_{\mathbf{l}} = u_{2\mathbf{l}} g_{\mathbf{l}}(\mathscr{I}_1)$, where $g_{\mathbf{l}}(\mathscr{I}_1)$ is a function of the intensity of the phonon field of the 99-cm^{-1} mode and $u_{2\mathbf{l}}$ is the value that describes the displacement of pyramid IO$_3$ caused by the 756-cm^{-1} mode. Below these two modes are the first mode and the second mode, respectively.

Let us introduce the Hamiltonian function for a model cubic lattice

$$\Delta \mathscr{H} = K + U \tag{D3}$$

Here the kinetic and potential energies are, respectively,

$$K = \frac{m}{2} \sum_{\mathbf{l}} \delta \dot{u}_{\mathbf{l}}^2, \qquad U = \frac{\gamma}{2} \sum_{\mathbf{l}} \left(\delta u_{\mathbf{l}} - \delta u_{\mathbf{l-a}} \right)^2 \tag{D4}$$

In expression (D4), m is the mass of the IO$_3$ pyramid, γ is the effective elasticity constant of the model lattice, and $\mathbf{a}$ is the lattice vector. The transition to new collective vibrations $A_{\mathbf{q}}$, which characterize a collective fluctuation motion of the IO$_3$ pyramids, could be made by means of the canonical transformation

$$\delta u_{\mathbf{l}} = \frac{1}{\sqrt{N}} \sum_{\mathbf{q}} A_{\mathbf{q}} \exp(i\mathbf{l} \cdot \mathbf{q}) \tag{D5}$$

where $A_{\mathbf{q}} = A_{\mathbf{q}}^*$ and N is the quantity of the IO_3 pyramids in the lattice. In the new representation the kinetic energies take the form

$$K = \frac{m}{2}\sum_{\mathbf{q}} \dot{A}_{\mathbf{q}}\dot{A}_{-\mathbf{q}}, \qquad U = \frac{m}{2}\sum_{\mathbf{l}} \Delta\omega^2(\mathbf{q})A_{\mathbf{q}}A_{-\mathbf{q}} \qquad (D6)$$

where

$$\Delta\omega^2(\mathbf{q}) = 4\frac{\gamma}{m}\sin^2\left(\frac{1}{2}\mathbf{a}\cdot\mathbf{q}\right) \qquad (D7)$$

Furthermore, we can write the Lagrange function as $L = K - U$ and find the generalized momentum $P_{\mathbf{q}} = \partial L/\partial\dot{A}_{\mathbf{q}} = m\dot{A}_{-\mathbf{q}}$. The classical energy (D3) as a function of the generalized variables $A_{\mathbf{q}}$ and $P_{\mathbf{q}}$ has the form

$$\Delta\mathscr{H} = \frac{1}{2}\sum_{\mathbf{q}}\left[\frac{1}{m}P_{\mathbf{q}}P_{-\mathbf{q}} + m\Delta\omega^2(\mathbf{q})A_{\mathbf{q}}A_{-\mathbf{q}}\right] \qquad (D8)$$

A change of variables from $A_{\mathbf{q}}$ and $P_{\mathbf{q}}$ to operators $\hat{A}_{\mathbf{q}}$ and $\hat{P}_{\mathbf{q}}$ transforms the energy (D8) to the energy operator ΔH.

Usually, the permutation relations

$$[\hat{A}_{\mathbf{q}},\ \hat{P}_{\mathbf{q}'}]_- = i\delta_{\mathbf{q}\mathbf{q}'}, \quad [\hat{A}_{\mathbf{q}},\ \hat{A}_{\mathbf{q}'}]_- = [\hat{P}_{\mathbf{q}},\ \hat{P}_{\mathbf{q}'}]_- = 0 \qquad (D9)$$

hold. However, in our case the displacement $\delta u_{\mathbf{l}}$ is a compound value: $\delta u_{\mathbf{l}} = u_{2\mathbf{l}}g_{\mathbf{l}}(I_1)$. Therefore the collective variables $A_{\mathbf{q}}$ should have the same structure; this can be presented as follows:

$$A_{\mathbf{q}} = \mathscr{A}_{2\mathbf{q}}e^{\frac{1}{2}\alpha N_{1\mathbf{q}}} \qquad (D10)$$

where $\mathscr{A}_{2\mathbf{q}}$ is the generalized combined variable of the motion the motion of IO_3 pyramids, $N_{1\mathbf{q}}$ is the quantity of phonons with the wave vector $\mathbf{q}$ of the first mode, and α is the coefficient that characterizes the degree of influence of this lattice mode on the second (i.e., intracellular) mode. In other words, α is the constant of coupling between the two kinds of phonons. Note that the function of the fluctuation intensity $g_{\mathbf{q}}(\mathscr{I}_1)$ written in the $\mathbf{q}$-representation is obviously in complete agreement with the expression for the intensity $\mathscr{I}$ of a normal phonon mode. The expression for $\mathscr{I}$ is determined by the thermodynamic averaging:

$$\mathscr{I} = \prod_{\mathbf{q}}\exp\langle\hat{b}_{\mathbf{q}}^+\hat{b}_{\mathbf{q}}\rangle$$

(see, e.g., Ref. 88). By this means, the transition from variables $A_{\mathbf{q}}$ and $P_{\mathbf{q}}$ to the corresponding operators may be performed in the following manner:

$$A_{\mathbf{q}} \rightarrow \hat{\mathscr{A}}_{2\mathbf{q}} e^{\frac{1}{2}\alpha \hat{N}_{1\mathbf{q}}} \tag{D11}$$

$$P_{\mathbf{q}} \rightarrow m(\hat{\mathscr{A}}_{2,-\mathbf{q}} e^{\frac{1}{2}\alpha \hat{N}_{1\mathbf{q}}})^{\cdot}$$

$$= \hat{\mathscr{P}}_{2\mathbf{q}} e^{\frac{1}{2}\alpha \hat{N}_{1\mathbf{q}}} + \frac{1}{2}\alpha m \hat{\mathscr{A}}_{2,-\mathbf{q}} e^{\frac{1}{2}\alpha \hat{N}_{1\mathbf{q}}} \dot{\hat{N}}_{1\mathbf{q}} \tag{D12}$$

Here one takes into account that the generalized variable $\mathscr{P}_{2\mathbf{q}}$ corresponds to $m\dot{\mathscr{A}}_{2,-\mathbf{q}}$; $\hat{N}_{1\mathbf{q}}$ is the operator of the phonon quantity for the first mode. Using relations (D9), which should be valid for the operators $\hat{\mathscr{A}}_{2\mathbf{q}}$ and $\hat{\mathscr{A}}_{2\mathbf{q}}$, we obtain the permutation relations for compound operators (D11) and (D12):

$$[\hat{\mathscr{A}}_{\mathbf{q}}, \hat{\mathscr{P}}_{\mathbf{q}'}]_{-} = i\hbar\delta_{\mathbf{qq}'}e^{\alpha\hat{N}_{1\mathbf{q}}}, \qquad [\hat{\mathscr{A}}_{\mathbf{q}}, \hat{\mathscr{A}}_{\mathbf{q}'}]_{-} = [\hat{\mathscr{P}}_{\mathbf{q}}, \hat{\mathscr{P}}_{\mathbf{q}'}]_{-} = 0 \tag{D13}$$

(here one sets $\dot{\hat{N}}_{1\mathbf{q}} = i\hbar[\hat{N}_{1\mathbf{q}}, \sum_{j;\mathbf{q}} \hat{b}_{j\mathbf{q}}^{+}\hat{b}_{j\mathbf{q}}]_{-} = 0$). Then one can pass from these operators $\hat{\mathscr{A}}_{\mathbf{q}}$ and $\hat{\mathscr{P}}_{\mathbf{q}}$ to the Bose operators for phonons $\hat{b}_{j\mathbf{q}}^{+}$ and $\hat{b}_{j\mathbf{q}}$ ($j = 1, 2$), which satisfy standard permutation relations

$$[\hat{b}_{j\mathbf{q}}^{+}, \hat{b}_{j'\mathbf{q}'}]_{-} = \delta_{jj'}\delta_{\mathbf{qq}'}, \qquad [\hat{b}_{j\mathbf{q}}, \hat{b}_{j'\mathbf{q}'}]_{-} = 0 \tag{D14}$$

The transition can be made via the following rules:

$$\hat{\mathscr{A}}_{\mathbf{q}} = \left(\frac{\hbar}{2m\Delta\omega(\mathbf{q})}\right)^{1/2} (\hat{b}_{2,-\mathbf{q}}^{+} + \hat{b}_{2\mathbf{q}}) e^{\frac{1}{2}\alpha\hat{b}_{1,\mathbf{q}}^{+}\hat{b}_{1\mathbf{q}}} \tag{D15}$$

$$\hat{\mathscr{P}}_{\mathbf{q}} = i\left(\frac{m\hbar\Delta\omega(\mathbf{q})}{2}\right)^{1/2} (\hat{b}_{2\mathbf{q}}^{+} - \hat{b}_{2,-\mathbf{q}}) e^{\frac{1}{2}\alpha\hat{b}_{1,\mathbf{q}}^{+}\hat{b}_{1\mathbf{q}}} \tag{D16}$$

Substitution of the variables $A_{\mathbf{q}}$ and $P_{\mathbf{q}}$ on the right-hand side of the Hamiltonian (D8) the operators $\hat{\mathscr{A}}_{\mathbf{q}}$ and $\hat{\mathscr{P}}_{\mathbf{q}}$ from expressions (D15) and (D16) converts the Hamiltonian function (D3) into the fluctuation Hamiltonian

$$\Delta\mathscr{H} = \sum_{\mathbf{q}} \hbar\Delta\omega(\mathbf{q})\left(\hat{b}_{2\mathbf{q}}^{+}\hat{b}_{2\mathbf{q}} e^{\frac{1}{2}\alpha\hat{b}_{1,\mathbf{q}}^{+}\hat{b}_{1\mathbf{q}}} + \frac{1}{2}\right) \tag{D17}$$

Since the unperturbed Hamiltonian of the crystal is

$$\mathscr{H}_0 = \sum_{j;\mathbf{q}} \hbar\omega_j(\mathbf{q})\left(\hat{b}_{j\mathbf{q}}^{+}\hat{b}_{j\mathbf{q}} + \frac{1}{2}\right) \tag{D18}$$

the total Hamiltonian becomes

$$\mathscr{H} = \mathscr{H}_0 + \Delta\mathscr{H} \tag{D19}$$

Now we can consider the electromagnetic field absorption by the lattice mode (the first mode) and the intracellular one (the second mode) when the modes are perturbed by described fluctuations. We suppose that the operator $\Delta\mathscr{H}$ in the Hamiltonian (D19) is a small perturbation; that is, the fluctuation energy is smaller than the energy of regular vibrations.

The absorption of the lattice mode is derived by the formula

$$\langle \mathbf{P}(\mathbf{r},\ t)\rangle = \mathrm{Tr}\{\rho_{\mathrm{int}}\hat{\mathbf{P}}(\mathbf{r},\ t)\} \tag{D20}$$

where the operators of the crystal polarization and the correction to the statistical operator are, respectively,

$$\hat{\mathbf{P}}(\mathbf{r}) = \frac{1}{\mathscr{V}}\sum_{j;\mathbf{q}}\left(\frac{\hbar}{2\gamma_j(\mathbf{q})\omega_j(\mathbf{q})}\right)^{1/2}\frac{\mathbf{q}}{|\mathbf{q}|}e^{i\mathbf{q}\cdot\mathbf{r}}(\hat{b}_{j\mathbf{q}}^+ + \hat{b}_{j\mathbf{q}}) \tag{D21}$$

$$\rho_{\mathrm{int}} = \rho_0 - \frac{i}{\hbar}\int_{-\infty}^{t}[H_{\mathrm{int}}(\tau),\rho_0]\,d\tau, \qquad \rho_0 = \frac{e^{-H_0/k_{\mathrm{B}}T}}{\mathrm{Tr}\,e^{-H_0/k_{\mathrm{B}}T}} \tag{D22}$$

where the operator of the interaction between the incident electromagnetic field and the operator of the crystal polarization is given by

$$H_{\mathrm{int}} = \hat{\mathbf{P}}\cdot\mathscr{E}(t) \tag{D23}$$

Having calculated the absorption by the lattice mode, we should substitute the operator ρ_0 for the following:

$$\tilde{\rho}(\mathscr{H}_0 + \Delta\mathscr{H}) \simeq \rho_0(\mathscr{H}_0) - \rho_0(\mathscr{H}_0)\int_0^{1/k_{\mathrm{B}}T} d\lambda e^{\lambda\mathscr{H}_0}\Delta\mathscr{H}e^{-\lambda\mathscr{H}_0} \tag{D24}$$

Then calculations by formula (D20) have shown [47] that the permittivity that represents the lattice mode—that is, the term with $j = 1$ in expression (D2)—should be supplemented with the factor $1 + f_1(\mathbf{q}, T)$, where

$$f_1(\mathbf{q},\ T) = -\frac{\hbar\Delta\omega(\mathbf{q})}{k_{\mathrm{B}}T[\exp(\hbar\omega_2(\mathbf{q})/k_{\mathrm{B}}T) - 1]}\exp\left(\alpha\coth\frac{\hbar\omega_1(\mathbf{q})}{2k_{\mathrm{B}}T}\right) \tag{D25}$$

The Hamiltonian of the interaction between the electromagnetic wave and the fluctuations of the intercellular mode in the crystal has the form analogous to

expression (D23):

$$H_{\text{int}}^{(\text{fl})}(t) = -\sum_{\mathbf{q}} \mathbf{d}_{\text{fl}}(\mathbf{q}) \cdot \mathscr{E}_0(\hat{V}_{\mathbf{q}}^+ - \hat{V}_{\mathbf{q}})e^{i\omega t + \eta t} \tag{D26}$$

Here $\hat{V}_{\mathbf{q}}^+(V_{\mathbf{q}})$ is the effective operator for the creation (annihilation) of fluctuations of the intracellular mode:

$$\hat{V}_{\mathbf{q}} = \hat{b}_{2\mathbf{q}} e^{\alpha \hat{b}_{1\mathbf{q}}^+ \hat{b}_{1\mathbf{q}}} \tag{D27}$$

The operator of the fluctuation dipole moment is

$$\hat{\mathbf{P}}_{\text{fl}}(\mathbf{r}, t) = \sum_{\mathbf{q}} \mathbf{d}_{\text{fl}}(\mathbf{q}) e^{i\mathbf{q} \cdot \mathbf{l}}(\hat{V}_{\mathbf{q}}^+ + \hat{V}_{\mathbf{q}}) \tag{D28}$$

In expressions (D26) and (D28), $\mathbf{d}_{\text{fl}}(\mathbf{q})$ is the effective dipole moment of the fluctuations of the intracellular mode. In this case the polarization is defined as

$$\langle \mathbf{P}_{\text{fl}}(\mathbf{r}, t) \rangle = \text{Tr}\{\rho_{\text{fl}} \hat{\mathbf{P}}_{\text{fl}}(\mathbf{r}, t)\} \tag{D29}$$

where the statistical operator is expressed as

$$\tilde{\rho}_{\text{fl}} = \tilde{\rho}_0 - \frac{i}{\hbar} \int_{-\infty}^{t} d\tau [H_{\text{int}}^{(\text{fl})}(\tau), \tilde{\rho}_0] \tag{D30}$$

In the present case we may neglect secondary effects of an expansion of $\tilde{\rho}_0(\mathscr{H})$ in terms of $\Delta\mathscr{H}$. Hence we assume that in Eq. (D30), $\tilde{\rho}_0 \simeq \rho_0$. This approximation allows the calculation of the polarization (D29). The result shows that the dielectric function of the intracellular mode fluctuation obtained from expression (D29) differs of the second term in expression (D2) for the permittivity only by the factor

$$f_2(\mathbf{q}, T) = \frac{d_{(\text{fl})2j}(\mathbf{q}) \, d_{(\text{fl})2j'}(\mathbf{q})}{d_{2j}(\mathbf{q}) \, d_{2j'}(\mathbf{q})} \exp\left(\alpha \coth \frac{\hbar\omega_1}{2k_\text{B}T}\right) \tag{D31}$$

Thus, the overall result for the imaginary part of the permittivity is

$$\text{Im}\,\varepsilon(\mathbf{q}, \, \omega, \, T) = \frac{4\omega^2}{(\omega^2 - \omega_1^2(\mathbf{q}))^2 + 4\omega^2\eta^2}[1 + f_1(\mathbf{q}, \, T)]$$
$$+ \frac{4\omega^2}{(\omega^2 - \omega_2^2(\mathbf{q}))^2 + 4\omega^2\eta^2}[1 + f_2(\mathbf{q}, \, T)] \tag{D32}$$

The investigation of the absorption [47] has shown that in the temperature interval between two phase transitions ($T_c = 120$ K to $T_0 = 213$ K) the relative intensities of the absorption maximum (for the lattice 99-cm^{-1} mode) and the scattering maximum (for the intracellular 756-cm^{-1} mode) have changed very markedly. The first mode decreased by approximately a factor of two at 213 K. The second one increased by approximately a factor of five at 213 K. Since the imaginary part of the permittivity defines the absorption (scattering) maximum, the expression (D32) has to describe the real temperature behavior of the two aforementioned anomalous modes.

The analysis of the behavior of $Im\varepsilon_{1(2)}$ conducted in Ref. 47 in fact correlates very well with the experimental data. Consequently, in the $NH_4IO_3 \cdot 2HIO_3$ crystal the phonon–phonon coupling between the active lattice mode and the intracellular one is realized due to the proton bifurcation. The availability of moderate phonon–phonon coupling α ($\alpha = 0.95$ [47]) permits the intracellular mode to ''live'' on the energy of phonons of the lattice mode. Since the lattice mode is more powerful than the intracellular mode [47], the latter has taken energy out of the former through the phonon–phonon coupling. So, at the second phase transition (i.e., 213 K), the power of the lattice mode can no longer hold proton polarons very strongly and they become more mobile. Thus, the crystal goes into a superionic state in which the band polaron conductivity prevails (see Section III.I).

Acknowledgments

References

1. F. Fillaux and J.-P. Perchard, *J. Chim. Phys.* **Hors série**, 91 (1999).

2. E. D. Isaacs, A. Shukla, P. M. Platzman, D. R. Hamann, B. Barbiellini, and C. A. Tulk, *Phys. Rev. Lett.* **82**, 600 (1999).

3. G. Zundel, *Hydration and Intermolecular Interaction—Infrared Investigations of Polyelectrolyte Membranes*, Academic Press, New York, 1969 and Mir, Moscow, 1972.

4. G. Zundel and H. Metzger, *Z. Physik. Chem.* (*Frankfurt*) **58**, 225 (1968).

5. G. Zundel and H. Metzger, *Z. Physik. Chem.* (*Leipzig*) **240**, 50 (1969).

6. G. Zundel, *Adv. Chem. Phys.* **111**, 1 (2000).

7. F. Fallaux, J. Tomkinson, and J. Penfold, *Chem. Phys.* **124**, 425 (1988).

8. F. Fallaux, J. P. Fontaine, M. H. Baron, G. J. Kearly, and J. Tomkinson, *Chem. Phys.* **176**, 249 (1993).

9. F. Fallaux, J. P. Fontaine, M. H. Baron, G. J. Kearly, and J. Tomkinson, *Biophys. Chem.* **53**, 155 (1994).

10. F. Fillaux, N. Leygue, J. Tomkinson, A. Cousson and W. Paulus, *Chem. Phys.* **244**, 387 (1999).

11. F. Fillaux, *J. Mol. Struct.* **511**–**512**, 35 (1999).

12. T. Horsewill, M. Johnson, and H. P. Trommsdorff, *Europhys. News* **28**, 140 (1997).

13. C. Rambaud, and H. P. Trommsdorff, *Chem. Phys. Lett.* **306**, 124 (1999).

14. F. Fillaux, *Physica D* **113**, 172 (1998).

15. H. P. Trommsdorff, *Adv. Photochem.* **24**, 147 (1998).

16. H. P. Trommsdorff, *Optoélectronique Moléculaire*, Observatoire Français des Techniques Avancées, Arago 13, Masson, Paris, 1993, Chapter VIII, p. 247.

17. C. Rambaud, A. Oppenlander, M. Pierre, H. P. Trommsdorff, and J. C. Vial, *Chem. Phys.* **136**, 335 (1989).

18. J. Bardeen, *Phys. Rev. Lett.* **6**, 57 (1961).

19. C. Herring, *Rev. Mod. Phys.* **34**, 341 (1970).

20. C. P. Flynn and A. M. Stoneham, *Phys. Rev. B* **1**, 3967 (1970).

21. J. L. Skinner and H. P. Trommsdorff, *J. Chem. Phys.* **89**, 897 (1988).

22. R. Silbey and H. P. Trommsdorff, *Chem. Phys. Lett.* **165**, 540 (1990).

23. V. Benderskii, V. I. Goldanskii, and D. E. Makarov, *Phys. Rep.* **233**, 195 (1993).

24. G. N. Robertson and M. C. Lawrence, *Chem. Phys.* **62**, 131 (1981).

25. A. V. Skripov, J. C. Cook, T. J. Udovic, and V. N. Kozhanov, *Phys. Rev. B* **62**, 14099 (2000).

26. R. Baddour-Hadjean, F. Fillaux, F. Floquet, S. Belushkin, I. Natkaniec, L. Desgranges, and D. Grebille, *Chem. Phys.* **197**, 81 (1995).

27. H. J. Morowitz, *Am. J. Physiol.* **235**, R99 (1978).

28. J. Teissié, M. Prats, P. Soucaille, and J. F. Tocanne, *Proc. Natl. Acad. Sci. USA* **82**, 3217 (1985).

29. J. Vanderkooy, J. D. Cuthbert, and H. E. Petch, *Can. J. Phys.* **42**, 1871 (1964).

30. A. D. Reddy, S. G. Sathynarayan, and G. S. Sastry, *Solid State Commun.* **43**, 937 (1982).

31. J. D. Cuthbert and H. E. Petch, *Can. J. Phys.* **41**, 1629 (1963).

32. S. Suzuki and Y Makita, *Acta Crystallogr. B* **34**, 732 (1978).

33. P. M. Tomchuk, N. A. Protsenko, and V. Krasnoholovets, *Biol. Membr.* **1**, 1171 (1984) (in Russian).

34. P. M. Tomchuk, N. A. Protsenko, and V. Krasnoholovets, *Biochem. Biophys. Acta* **807**, 272 (1985).

35. V. Krasnoholovets, N. A. Protsenko, P. M. Tomchuk, and V. S. Guriev, *Int. J. Quant. Chem.* **33**, 327 (1988).

36. V. Krasnoholovets, N. A. Protsenko and P. M. Tomchuk, *Int. J. Quant. Chem.* **33**, 349 (1988).

37. V. Krasnoholovets, V. B. Taranenko, P. M. Tomchuk, and N. A. Protsenko, *J. Mol. Struct.* **355**, 219 (1995).

38. I. V. Stasyuk, N. Pavlenko, and D. Hilczer, *Phase Transitions* **62**, 135 (1997).

39. I. V. Stasyuk, N. Pavlenko, and M. Polomska, *Phase Transitions* **62**, 167 (1997).

40. N. Pavlenko, M. Polomska, and B. Hilczer, *Cond. Matter. Phys.* **1**, 357 (1998).

41. I. V. Stasyuk and V. Pavlenko, *J. Phys. Cond. Matter* **10**, 7079 (1998).

42. V. Stasyuk, V. Pavlenko, and B. Hilczer, *J. Korean Phys. Soc.* **32**, S24 (1998).

43. G. A. Puchkovska and Yu. A. Tarnavski, *J. Mol. Struct.* **267**, 169 (1992).

44. Yu. Tarnavski, G. A. Puchkovska, and J. Baran, *J. Mol. Struct.* **294**, 61 (1993).

45. Yu. Tarnavski, Thesis, Institute of Physics, Kyiv, Ukraine, 1993.

46. V. Krasnoholovets, G. A. Puchkovska, and Tarnavski, *Khim. Fiz.* **12**, 973 (1993) (in Russian); English translation: *Sov. J. Chem. Phys.* **12**, 1434 (1994).

47. V. Krasnoholovets, *J. Phys. Cond. Matter* **8**, 3537 (1996).

48. G. A. Puchkovska and Yu. A. Tarnavski, *J. Mol. Struct.* **403**, 137 (1997).

49. F. Fillaux, *Solid State Ionics* **125**, 69 (1999).

50. W. A. P. Luck and M. Fritzsche, *Z. Phys. Chem.* **191**, 71 (1995).

51. P. L. Huyskens, *J. Mol. Struct.* Special Issue Sandorfy **297**, 141 (1993).

52. P. L. Huyskens, D. P. Huyskens, and G. G. Siegel, *J. Mol. Liquids* **64**, 283 (1995).

53. K. Nelis, L. Van den Berge-Parmentier, and F. Huyskens, *J. Mol. Liquids* **67**, 157 (1995).

54. W. A. P. Luck, *Angew. Chem.* **29**, 92 (1980).

55. W. A. P. Luck, *Opt. Pur. Appl.* 18, 71 (1985).

56. W. A. P. Luck, in *Intermolecular Forces. An Introduction to Modern Methods and Results*, P. L. Huyskens, W. A. P. Luck, and T. Zeegers-Huyskens, eds., Springer-Verlag, Berlin, 1991, p. 317.

57. V. Krasnoholovets, G. A. Puchkovska, and A. A. Yakubov, *Ukr. Fiz. Zh.* **37**, 1508 (1992) (in Russian).

58. V. Krasnoholovets, G. A. Puchkovska, and A. A. Yakubov, *Khim. Fiz.* **11**, 806 (1992) (in Russian).

59. V. Krasnoholovets and B. Lev, *Ukr. Fiz. Zh.* **39**, 296 (1994) (in Ukrainian).

60. V. Krasnoholovets, G. A. Puchkovska, and A. A. Yakubov, *Mol. Cryst. Liq. Cryst.* **265**, 143 (1995).

61. L. M. Babkov, E. Gabrusenoks, V. Krasnoholovets, G. A. Puchkovska, and I. Khakimov, *J. Mol. Struct.* **482–483**, 475 (1998).

62. V. Krasnoholovets, I. Khakimov, G. Puchkovska, and E. Gabrusenoks, *Mol. Cryst. Liq. Cryst.* **348**, 101 (2000).

63. N. D. Gavrilov and O. V. Mukina, *Neorg. Mater.* **33**, 871 (1997) (in Russian).

64. M. A. Kovner and V. A. Chuenkov, *Izv. Akad. Nauk SSSR Ser. Fiz.* **14**, 435 (1950).

65. D. Hadzi, *Hydrogen Bonding*, Papers Symposium, Ljubljana 1957 (1959).

66. Y. Marechal and A. Witkowski, *J. Chem. Phys.* **48**, 3697 (1968).

67. E. R. Lippinkott and R. Schröder, *J. Am. Chem. Soc.* **78**, 5171 (1956).

68. T. Matsubara and E. Matsubara, *Prog. Theor. Phys.* **67**, 1 (1982).

69. S. Tanaka, *Phys. Rev. B.* **42**, 1088 (1990).

70. A. Novak, *Struct. Bond.* (Berlin) **18**, 177 (1977).

71. J. P. Sethna, *Phys. Rev. B* **24**, 698 (1981).

72. J. P. Sethna, *Phys. Rev. B* **25**, 5050 (1982).

73. A. J. Bray and M. A. Moore, *Phys. Rev. Lett.* **49**, 1545 (1982).

74. A. L. Fetter and J. D. Walecka, *Quantum Theory of Many-Particle Systems*, McGraw-Hill, New York, 1971, p. 390.

75. S. Nagaoka, T. Terao, F. Imashiro, A. Saika, N. Hirota, and S. Hayashi, *J. Chem. Phys. Lett.* **79**, 4694 (1983).

76. J. M. Clemens, R. M. Hochstrasser, and H. P. Trommsdorff, *J. Chem. Phys.* **80**, 1744 (1984).

77. G. R. Holtom, R. M. Hochstrasser, and H. P. Trommsdorff, *Chem. Phys. Lett.* **131**, 44 (1986).

78. D. F. Brougham, A. J. Horsewill, and H. P. Trommsdorff, *Chem. Phys.* **243**, 189 (1999).

79. V. A. Benderskii, E. V. Vetoshkin, S. Yu. Grebenshchikov, L. von Laue, and H. P. Trommsdorff, *Chem. Phys.* **219**, 119 (1997).

80. V. A. Benderskii, E. V. Vetoshkin, L. von Laue, and H. P. Trommsdorff, *Chem. Phys.* **219**, 143 (1997).

81. V. A. Benderskii, E. V. Vetoshkin, and H. P. Trommsdorff, *Chem. Phys.* **234**, 153 (1998).

82. V. A. Benderskii, E. V. Vetoshkin, *Chem. Phys.* **234**, 173 (1998).

83. V. A. Benderskii, E. V. Vetoshkin, and H. P. Trommsdorff, *Chem. Phys.* **244**, 299 (1999).

84. V. A. Benderskii, E. V. Vetoshkin, I. S. Irgibaeva, and H. P. Trommsdorff, *Chem. Phys.* **262**, 369 (2000); 262, 393 (2000).

85. A. C. Legon, *Chem. Soc. Rev.* **22**, 153 (1993).

86. H. Haken, *Quantenfieldtheorie des Festkörpers*, B. G. Teubner, Stuttgart, 1973; Russian translation: *Quantum Field Theory of Solids*, Nauka, Moscow, 1980, p. 47.

87. T. Holstein, *Ann. Phys.* (*NY*) **8**, 325 (1959); **8**, 343 (1959).

88. Yu. A. Firsov, ed., *Polarons*, Nauka, Moscow, 1975 (in Russian).

89. S. F. Fischer, G. L. Hofacker, and M. A. Rather, *J. Chem. Phys.* **52**, 1934 (1970).

90. I. I. Roberts, N. Apsley, and R. W. Munn, *Phys. Rep.* **60**, 59 (1980).

91. A. O. Azizyan and M. I. Klinger, *Doklady Acad. Nauk SSSR* **242**, 1046 (1978) (in Russian); *Theor. Math. Fiz.* **43**, 78 (1980) (in Russian).

92. M. I. Klinger and A. O. Azizyan, *Fiz. Tekhn. Poluprovodn.* **13**, 1873 (1979) (in Russian).

93. D. L. Tonks and R. N. Silver, *Phys. Rev. B* **26**, 6455 (1982).

94. R. Bilnc and D. Hadzi, *Mol. Phys.* **1**, 391 (1958).

95. R. Blinc, *J. Chem. Phys. Solids* **13**, 204 (1960).

96. R. Blinc and B. Žecš, *Soft Mode in Ferroelectrics and Antiferroelectrics*, North-Holland, Amsterdam, American Elsevier, New York, 1974.

97. P. G. de Genn, *Solid State Commun.* **1**, 150 (1963).

98. M. Tokunaga and T. Matsubara, *Prog. Theor. Phys.* **35**, 581 (1966).

99. R. Silbey and H. P. Trommsdorff, *Chem. Phys. Lett.* **165**, 540 (1990).

100. S. S. Rozhkov, E. A. Shadchin, and S. P. Sirenko, *Teoret. Eksperim. Khim.* **35**, 343 (1999) (in Russian).

101. E. D. Isaacs, A. Shukla, and P. M. Platzman, *Phys. Rev. Lett.* **82**, 600 (1999).

102. T. Matsubara and K. Kamiya, *Prog. Theor. Phys.* **58**, 767 (1977).

103. A. P. Petrov and A. B. Khovanski, *Zh. Vyssh. Mat. Mat. Fiz.* **14**, 292 (1974) (in Russian).

104. E. A. Shadchin and F. I. Barabash, *J. Mol. Struct.* **325**, 65 (1993).

105. S. Ikeda, H. Sugimoto, and Y. Yamada, *Phys. Rev. Lett.* **81**, 5449 (1998).

106. Y. Yamada and S. Ikeda, *J. Phys. Soc. Jpn.* **63**, 3691 (1994).

107. Y. Yamada, *J. Phys. Soc. Jpn.* **63**, 3756 (1994).

108. H. Sugimoto and S. Ikeda, *Phys. Rev. Lett.* **67**, 1306 (1998).

109. R. P. Bell, *Tunnel Effect in Chemistry*, Chapman and Hall, London, 1980.

110. F. Fillaux, B. Nicolaï, M. H. Baron, A. Lautié, J. Tomkinson, and G. J. Kearly, *Ber. Bunsenges. Phys. Chem.* **102**, 384 (1998).

111. F. Graf, R. Meyer, T. K. Ha, and R. R. Ernst, *J. Chem. Phys.* **75**, 1914 (1981).

112. B. H. Meier, F. Graf, and R. R. Ernst, *J. Chem. Phys.* **76**, 767 (1982).

113. R. Meyer and R. R. Ernst, *J. Chem. Phys.* **86**, 784 (1987).

114. S. Nagaoka, T. Terao, F. Imashiro, A. Saika, and S. Hayashi, *J. Chem. Phys.* **79**, 4694 (1983).

115. A. J. Pertsin and A. I. Kitaigorodsky, *The Atom–Atom Potential Method*, Springer Series in Chemical Physics, Springer, Berlin, 1987.

116. A. Griffin and H. Jobic, *J. Chem. Phys*. **75**, 5940 (1981).

117. H. Jobic and H. Lauter, *J. Chem Phys*. **88**, 5450 (1988).

118. S. W. Lovesey, *Theory of Neutron Scattered from Condensed Matter*, Vol. I: *Nuclear Scattering*, Clarendon Press, Oxford, 1984.

119. F. Fillaux, *Chem. Phys*. **74**, 405 (1983).

120. C. Cohen-Tannoudji, B. Diu, and F. Laloë, *Méchanique Quantique*, Vol. 1, Herman, Paris, 1977, p. 576.

121. S. Ikeda and F. Fillaux, *Phys. Rev. B* **59**, 4134 (1999).

122. J. R. Willison, *Phys. Rev. Lett*. **81**, 5430 (1998).

123. D. F. Gaitan, L. A. Crum, C. C. Church, and R. A. Roy, *J. Acoust. Soc. Am*. **91**, 3166 (1992).

124. R. Hiller, S. J. Putterman, and B. P. Barber, *Phys. Rev. Lett*. **69**, 1182 (1992).

125. B. Compf, R. Günther, G. Nick, R. Pecha, and W. Eisenmenger, *Phys. Rev. Lett*. **79**, 1405 (1997).

126. R. A. Hiller, S. J. Putterman, and K. R. Weninger, *Phys. Rev. Lett*. **80**, 1090 (1998).

127. L. A. Crum and T. J. Maluta, *Science* **276**, 1348 (1997).

128. J. Schwinger, *Proc. Natl. Acad. Sci. USA* **90**, 2105 (1993).

129. C. Eberlein, *Phys. Rev. Lett*. **76**, 3842 (1996).

130. A. Lambrecht, M. T. Jaekel, and S. Reynaud, *Phys. Rev. Lett*. **78**, 2267 (1997).

131. N. Garsia and A. P. Levanyuk, *JETP Lett*. **64**, 907 (1996); *Phys. Rev. Lett*. **78**, 2268 (1997).

132. L. S. Bernstein and M. R. Zakin, *J. Phys. Chem*. **99**, 14619 (1995).

133. T. Lepoint et al., *J. Acoust. Soc. Am*. **101**, 2012 (1997).

134. A. Prosperetti, *J. Acoust. Soc. Am*. **101**, 2003 (1997).

135. I. V. Stasyuk, O. L. Ivankiv, and N. I. Pavlenko, *J. Phys. Studies* **1**, 418 (1997).

136. M. Hubman, *Z. Physik B* **32**, 127 (1979).

137. R. Hassan and E. Campbell, *J. Chem. Phys*. **97**, 4326 (1992).

138. I. V. Stasyuk and A. L. Ivankiv, *Ukr. Fiz. Zhurn*. **36**, 817 (1991) (in Ukrainian); *Mod. Phys. Lett. B* **6**, 85 (1992).

139. D. Eisenberg and W. Kauzman, *The Structure and Properties of Water*, Gidrometeoizdat, Leningrad, 1975 (Russian translation).

140. M. Kunst and J. M. Warman, *Nature* **288**, 465 (1980).

141. N. Sone, M. Yoshida, H. Hirata, and Y. Kagava, *J. Biol. Chem*. **252**, 2956 (1977).

142. H. Okamoto, N, Sone, H. Hirata, and Y. Kagawa, *J. Biol. Chem*. **252**, 6125 (1977).

143. K. Sigrist-Nelson and A. Azzi, *J. Biol. Chem*. **255**, 10638 (1980).

144. B. Hilczer and A. Pawłowski, *Ferroelectrics* **104**, 383 (1990).

145. A. Pawłowski, Cz. Pawlaczyk, and B. Hilczer, *Solid State Ionics* **44**, 17 (1990).

146. A. Pietraszko, K. Łukaszewicz, and M. A. Augusyniak, *Acta Crystallogr. C* **48**, 2069 (1992); **49**, 430 (1993).

147. T. Fukami, K. Tobaru, K. Kaneda, K. Nakasone, and K. Furukawa, *J. Phys. Soc. Jpn*. **63**, 2829 (1994).

148. W. Salejda and N. A. Dzhavadov, *Phys. Status Solidi B* **158**, 119 (1990); **158**, 475 (1990).

149. N. Pavlenko, ICMP-98-26E Preprint of the Institute for Condensed Matter Physics National Academy of Science of Ukraine, 1998 (see also on http://www.icmp.lviv.ua).

150. I. V. Stasyuk and N. Pavlenko, ICMP-98-30U Preprint of the Institute for Condensed Matter Physics National Academy of Science of Ukraine, 1998 (see also on http://www.icmp.lviv.ua).

151. B. V. Merinov, N. B. Bolotina, A. I. Baranov, and L.A. Shuvalov, *Cristallografiya* **33**, 1387 (1988) (in Russian).

152. B. V. Merinov, A. I. Baranov, and L. A. Shuvalov, *Cristallografiya* **35**, 355 (1990) (in Russian).

153. B. V. Merinov, M. Yu. Antipin, A. I. Baranov, A. M. Tregubchenko, and L.A. Shuvalov and Yu. T. Struchko, *Cristallografiya* **36**, 872 (1992) (in Russian).

154. R. Kubo, *Can. J. Phys.* **34**, 1274 (1956); *J. Phys. Soc. Jpn.* **12**, 570 (1957).

155. A. Pawlowski, Cz. Pawlaczyk, and B. Hilczer, *Solid State Ionics* **44**, 17 (1990).

156. J. Grigas, *Microwave Dielectrics spectroscopy of Ferroelectrics and Related Materials*, Gordon and Beach Publishers, 1996.

157. A. V. Belushkin, C. J. Carlile, and L. A. Shuvalov, *Ferroelectrics* **167**, 83 (1995).

158. J. Nagle, M. Mille, and H. J. Morowitz, *J. Chem. Phys.* **72**, 3959 (1980).

159. J. F. Nagle and H. J. Morowitz, *Proc. Natl. Acad. Sci. USA* **75**, 298 (1978).

160. E.-W. Knapp, K. Schulten, and Z. Schulten, *Chem. Phys.* **46**, 215 (1980).

161. V. Ya. Antonchenko, A. S. Davydov, and A. V. Zolotariuk, *Phys. Status Solidi B* **115**, 631 (1983).

162. S. Yomosa, *J. Phys. Soc. Jpn.* **51**, 3318 (1982); **52**, 1866 (1983).

163. P. M. Tomchuk, V. Krasnoholovets, and N. A. Protsenko, *Ukr. Fiz. Zh.* **28**, 767 (1983) (in Russian).

164. V. Krasnoholovets, P. M. Tomchuk, and N. A. Protsenko, Preprint 9/83, Institute of Physics Akademie Nauk UkrSSR, Kyiv, 1983 (in Russian).

165. V. Krasnoholovets and P. M. Tomchuk, *Phys. Status Solidi B* **123**, 365 (1984).

166. N. D. Sokolov, in *Hydrogen Bond*, Nauka, Moscow, 1975, p. 65 (in Russian).

167. H. Merz and G. Zundel, *Biochim. Biophys. Res. Commun.* **101**, 540 (1981).

168. S. Scheiner, *J. Chem. Soc. Faraday Trans. II* **103**, 315 (1981).

169. E. G. Weidemann and G. Zundel, *Z. Naturforsch.* **25a**, 627 (1970).

170. R. Janoschek, E. G. Weidemann, H. Pfeiffer, and G. Zundel, *J. Am. Chem. Soc.* **94**, 2387 (1972).

171. A. S. Davydov, *The Theory of Solid*, Nauka, Moscow, 1976 (in Russian).

172. S. V. Tyablikov, *Methods of Quantum Theory of Magnetism*, Nauka, Moscow, 1965.

173. K. Hattori, *Phys. Rev. B* **23**, 4246 (1981).

174. H. Eigelhardt and N. Riel, *Phys. Lett.* **14**, 20 (1965).

175. M. A. Lampert and P. Mark, *Current Injection in Solids*, Academic Press, New York, 1970.

176. V. Krasnoholovets and P. M. Tomchuk, *Phys. Status Solidi B* **131**, K177 (1985).

177. C. Kittel, *Introduction to Solid State Physics*, Nauka, Moscow, 1978 (Russian translation).

178. V. Krasnoholovets and P. M. Tomchuk, *Phys. Status Solidi B* **130**, 807 (1985).

179. V. Krasnoholovets and P. M. Tomchuk, *Phys. Status Solidi B* **138**, 727 (1986).

180. V. N. Schmidt, J. E. Drumcheller, and F. L. Howell, *Phys. Rev. B* **12**, 4582 (1971).

181. Z. Schulten and K. Schulten, *Eur. Biophys. J.* **11**, 149 (1985).

182. B. I. Stepanov and V. P. Gribkovskii, *Introduction to the Theory of Luminescence*, (Academic Science Belorus SSR Publishing, Minsk, 1963 (in Russian).

183. V. L. Gurevich, *The Kinetics of Phonon System*, Nauka, Moscow, 1980 (in Russian).

184. J. W. Tucker and V. W. Rampton, *Microwave Ultrasonic in Solid State Physics*, Mir, Moscow, 1975 (Russian translation).

185. A. S. Bakay and N. P. Lazarev, *Fiz. Tverd. Tela* **26**, 2504 (1984).

186. Yu. M. Kagan, in *Defects in Insulating Crystals*, V. M. Tushkevich and K. K. Shvarts, eds., Zinatne Publishing House, Riga; Springer-Verlag, Berlin, 1981, p. 17.

187. P. S. Peercy, *Phys. Rev. B* **12**, 2725 (1975).

188. M. C. Laurence and G. N. Robertson, *J. Phys. C* **13**, L1053 (1980).

189. V. V. Bryksin, *JETP* **100**, 1556 (1991) (in Russian).

190. Yu. Kagan and M. I. Klinger, *JETP* **70**, 255 (1976) (in Russian).

191. V. Krasnoholovets, *Ukr. Fiz. Zhurn.* **38**, 740 (1993) (in Ukrainian).

192. H. Haken, *Quantenfeldtheorie des Festkörpers*, B. G. Teubner, Stuttgart, 1973; Russian translation: Nauka, Moscow, 1980.

193. A. I. Baranov, G. F. Dobrzhanskii, V. V. Ilyukhin, V. S. Ryabkin, N. I. Sorokina, and L. A. Shuvalov, *Kristallografiya* **26**, 1259 (1981) (in Russian).

194. A. I. Baranov, L. A. Muadyan, A. A. Loshmanov, L. E. Fykin, E. E. Rider, G. F. Dobrzhanskii, and V. I. Simonov, *Kristallografiya* **29**, 220 (1984) (in Russian).

195. A. I. Baranov, G. F. Dobrzhanskii, V. V. Ilyukhin, V. I. Kalinin, V. S. Ryabkin, and L. A. Shuvalov, *Kristallografiya* **24**, 280 (1979) (in Russian).

196. G. A. Puchkovska and Yu. A. Tarnavski, *J. Mol. Struct.* **267**, 169 (1992).

197. D. F. Baisa, A. I. Barabash, E. A. Shadchin, A. I. Shanchuk, and V. A. Shishkin, *Kristallografiya* **34**, 1025 (1989) (in Russian).

198. Z. M. Alekseeva, G. A. Puchkovska, and Yu. A. Tarnavski, *Structural Dynamic Processes in Disordered Media*, abstracts of papers read at the conference, Samarkand, 1992, Pt. 1, p. 91 (in Russian).

199. I. P. Aleksandrova, Ph. Colomban, F. Denoyer, et al., *Phys. Status Solidi A* **114**, 531 (1989).

200. Ph. Colomban and J. C. Batlot, *Solid State Ionics* **61**, 55 (1993).

201. A. Baranov, *Izvestia AN SSSR*, *Ser. Fiz.* **51** 2146 (1987) (in Russian).

202. D. F. Baisa, E. D. Chesnokov, and Shamchuk, *Fiz. Tverd. Tela* **32**, 3295 (1990) (in Russian).

203. M. B. Salamon, ed., *Superionic Conductor Physics*, Zinatne, Riga, 1982 (in Russian).

204. Yu. Gurevich and Yu. I. Kharkats, *Advances in Science and Technology*, Vol. 4, Series in Solid-State Chemistry, VINITI, Moscow, 1987, (in Russian).

205. D. Hadzi, *Chimia* **26**, 7 (1972).

206. S. Bratos, J. Lascombe, and A. Novak, in *Molecular interactions*, Vol. 1, H. Ratajczak and W. J. Orville-Thomas, eds., Wiley, New York, 1980, p. 301.

207. J. Baran, *J. Mol. Struct.* **162**, 211 (1987).

208. M. Szafran and Z. Dega-Szafran, *J. Mol. Struct.* **321**, 57 (1994).

209. S. Bratos and H. Ratajczak, *J. Chem. Phys.* **76**, 77 (1982).

210. K. Unterderweide, B. Engelen, and K. Boldt, *J. Mol. Struct.* **322**, 233 (1994).

211. H. Ratajczak and A. M. Yaremko, *Chem. Phys. Lett.* **243**, 348 (1995).

212. G. Zundel, in *The Hydrogen Bond*, P. Schuster, G. Zundel, and C. Sandorfy, eds., North Holland, Amsterdam, 1972, p. 685.

213. A. Barabash, T. Gavrilko, V. Krasnoholovets, and G. Puchkovska, *J. Mol. Struct.* **436–437**, 301 (1997).

214. A. S. Davydov, *Theory of Molecular Excitons*, Nauka, Moscow, 1968 (in Russian).

215. M. P. Lisitsa and A. M. Yaremko, *Fermi-Resonance*, Naukova Dumka, Kyiv, 1984 (in Russian).

216. D. Ostrovski, M. Ya. Valakh, T. A. Karaseva, Z. Latajka, H. Ratajczak, and M. A. Yaremko, *Opt. Spektrosk*. **78**, 422 (1995) (in Russian).

217. A. Barabash, J. Baran, T. Gavrilko, K. Eshimov, G. Puchkovska, and H. Ratajczak, *J. Mol. Struct*. **404**, 187 (1997).

218. A. M. Petrosian, A. A. Bush, V. V. Chechkin, A. F. Volkov, and Yu. N. Venevtsev, *Ferroelectrics* **21**, 525 (1878).

219. E. N. Treshnikov, A. A. Loshmanov, V. R. Kalinin, V. V. Ilyukhin, I. I. Yamzin, L. E. Fykin, V. Ya. Dudarev, and S. P. Solov'ev, *Koordinat. Khimia* **4**, 1903 (1978); **5**, 263 (1979) (in Russian).

220. D. Oesterhelt and W. Stoeckenius, *Nature* **233**, 149 (1971); *Proc. Natl. Acad. Sci. USA* **70**, 2853 (1973).

221. R. H. Lozier, W. Niederberger, R. A. Bogomolni, S. Hwang, and W. Stoeckenius, *Biochim. Biophys. Acta* **440**, 545 (1976).

222. W. Stoeckenius, R. H. Lozier, and R. A. Bogomolni, *Biochim. Biophys. Acta* **505**, 215 (1979).

223. R. Henderson, J. M. Baldwin, R. A. Ceska, F. Zemlin, E. Beckmann, and K. H. Downin, *J. Mol. Biol*. **213**, 899 (1990).

224. A. N. Dencher, G. Papadopoulos, D. Dresselhaus, and G. Büldt, *Biochim. Biophys. Acta* **1026**, 51 (1990).

225. G. Papadopoulos, A. N. Dencher, D. Oesterhelt, H. J. Plöhn, G. Rapp, and G. Büldt, *J. Mol. Biol*. **214**, 15 (1990).

226. A. N. Dencher, D. Dresselhaus, G. Zaccai, and G. Büldt, *Proc. Natl. Acd. Sci. USA* **86**, 7876 (1989).

227. M. H. Koch, A. N. Dencher, D. Oesterhelt, H. J. Plöhn, G. Rapp, and G. Büldt, *EMBO J*. **10**, 521 (1991).

228. T. Mogi, L. J. Stern, T. Marti, B. H. Chao, and H. G. Khorana, *Proc. Natl. Acad. Sci. USA* **85**, 4148 (1988).

229. J. Soppa, J. Otomo, J. Straub, J. Tittor, S. Meessen, and D. Oesterhelt, *J. Biol. Chem*. **264**, 13049 (1989).

230. R. Rammelsberg, G. Huhn, M. Lübben, and K. Gerwert, *Biochemistry* **37**, 5001 (1998).

231. S. Stoeckenius and R. A. Bogomolni, *Annu. Rev. Biochem*. **51**, 587 (1982).

232. R. R. Birge and T. M. Cooper, *Biophys. J*. **42**, 61 (1983).

233. J. Olejnik, B. Brzezinski, and G. Zundel, *J. Mol. Struct*. **271**, 157 (1992).

234. G. Zundel, *J. Mol. Struct*. **322**, 33 (1994).

235. H. G. Khorana, *J. Biol. Chem*. **263**, 7439 (1988).

236. D. Oesterhelt, *Biochem. Int*. **18**, 673 (1989).

237. S. P. A. Fodor, J. B Ames, R. Gebhard, E. M. M. Van der Berg, W. Stoeckenius, J. Lugtenburg, and R. A. Mathies, *Biochemistry* **27**, 7097 (1988).

238. R. R. Birge, *Biochem. Biophys. Acta* **1016**, 293 (1990).

239. J. F. Nagle and S. Tristran-Nagle, *J. Membr. Biol*. **74**, 1 (1983).

240. A. Lewis, *Proc. Natl. Acad. Sci. USA* **75**, 549 (1978).

241. H. Merz and G. Zundel, *Biochem. Biophys. Res. Commun*. **101**, 540 (1981).

242. P. Tavan, K. Schulten, and D. Oesterhelt, *Biophys. J*. **47**, 415 (1985).

243. D. Oesterhelt and J. Tittor, *Trends Biochem. Sci.* **14**, 57 (1989).

244. M. A. El-Sayed, in *Biophysical Studies of Retinal Proteins*, University of Illinois Press, Champaign, 1987, p. 174.

245. S. P. Balashov, R. Govindjee, and T. G. Ebrey, *Biophys. J.* **60**, 475 (1991).

246. S. W. Lin and R. A. Mathies, *Biophys. J.* **56**, 633 (1989).

247. A. Ikagami, T. Kouyama, K. Kinosita, H. Urabe, and J. Otomo, in *Primary Processes in Photobiology*, Springer-Verlag, New York, 1987, p. 173.

248. B. Brzezinski, J. Olejnik, and G. Zundel, *J. Chem. Soc. Faraday Trans.* **90**, 1095 (1994).

249. G. Zundel and B. Brzezinski, *Proton Transfer in Hydrogen-Bonded Systems*, Plenum, New York, 1992, p. 153.

250. M. P. Heyn, R. J. Cherry, and U. Muller, *J. Mol. Biol.* **117**, 607 (1977).

251. J. Y. Huang and A. Lewis, *Biophys. J.* **55**, 835 (1989).

252. K. J. Rothschild, P. Roepe, P. L. Ahl, T. N. Earnest, R. A. Bogomolni, S. K. Das Gupta, C. M. Mulliken, and J. Herzfeld, *Proc. Natl. Acad. Sci. USA* **83**, 347 (1986).

253. L. Eisenstein, S.-L. Lin, G. Dollinger, K. Odashima, J. Termini, K. Konno, W.-D. Ding, and K. Nakanishi., *J. Am. Chem. Soc.* **109**, 6860 (1987).

254. B. Brzezinski, H. Urjasz, and G. Zundel, *Biochem. Biophys. Res. Commun.* **89**, 819 (1986).

255. H. Richter, L. Brown, J. Needleman, and R. Lany, *Biochem.* **35**, 4054 (1996).

256. J. Hebrle and N. A. Dencher, *FEBS Lett.* **277**, 277 (1990).

257. P. Hildebrandt and M. Stockburger, *Biochemistry* **23**, 5539 (1984).

258. G. Popandopoulos, N. A. Dencher, Zaccai, and G. Buld, *J. Mol. Biol.* **214**, 15 (1990).

259. G. Dollinger, L. Eisenstein, S.-L. Lin, K. Nakanishi, and J. Termini, in *Biophysical Studies of Retinal Proteins*, Univiversity of Illinois Press, Champaign, IL, 1987, p. 120.

260. M. S. Braiman, T. Mogi, T. Marti, L. J. Stern, H. G. Khorana, and K. J. Rotshild, *Biochemistry*, **27**, 8516 (1988).

261. L. Eisenstein, S.-N. Lin, G. Dollinger, J. Termini, K. Odashima, and K. Nakanishi, in *Biophysical Studies of Retinal Proteins*, Univiversity of Illinois Press, Champaign, IL, 1987, p. 149.

262. R. R. Birge, *Computer*, November, 56 (1992).

263. L. Eisenstein, S.-N. Lin, G. Dollinger, K. Odashima, J. Termini, K. Konno, W.-D. Ding, and K. Nakanishi, *J. Am. Chem. Soc.* **109**, 6860 (1987).

264. K. Bagley, G. Dollinger, L. Eisenstein, A. K. Singh, and L. Linanyi, *Proc. Natl. Acad. Sci. USA* **79**, 4972 (1982).

265. N. A. Dencher, *Photochem. Photobiol.* **38**, 753 (1983).

266. J. E. Drahein and J. Y. Cassim, *Biophys. J.* **41**, 331 (1983).

267. J. Czege, *FEBS Lett.* **242**, 89 (1988).

268. L. A. Drachev, A. D. Kaulen, and V. V. Zorina, *FEBS Lett.* **243**, 5 (1989).

269. J. Czege and L. Reinisch, *Photochem. Phobiol.* **54**, 923 (1991).

270. M. Sheves, A. Albeck, N. Friedman, and M. Ottolenghi, *Proc. Natl. Acad. Sci. USA* **83**, 3262 (1986).

271. M. Engelhard, K. Gerwert, B. Hess, W. Kreutz, and F. Siebert, *Biochemistry* **24**, 400 (1985).

272. K. Gerwert, G. Souvignier, and B. Hess, *Proc. Natl. Acad. Sci. USA* **87**, 9774 (1990).

273. K. J. Rothschild, M. S. Brainman, Y.-W. He, Th. Marti, and H. G. Khorana, *Biochemistry* **29** 18985 (1990).

274. T. Koboyashi, H. Ohtani, J. Iwai, A. Ikegami, and H. Uchiki, *FEBS Lett.* 162, 197 (1983).

275. A. N. Dencher, G. Popadopoulos, D. Dresselhaus, and G. Buld, *Biochim. Biophys. Acta* **1026**, 51 (1990).

276. H. J. Koch, N. A. Dencher, D. Oesterchelt, H.-J. Plohn, G. Rapp, and G. Buld, *EMBO J.* **10**, 521 (1991).

277. J. Y. Huang, Z. Chen, and A. Lewis, *J. Phys. Chem.* **93**, 3324 (1989).

278. R. R. Birge and C.-F. Zhang, *J. Chem. Phys.* **92**, 7178 (1990).

279. T. Ya. Paperno, V. V. Pozdnyakov, A. A. Smirnova, and L. M. Elagin, *Physics–Chemistry Methods of Investigation in Organic and Biological Chemistry*, Prosveshchenie, Moscow, 1977 (in Russian).

280. S. P. Balashov and Litvin, *Biofizika* **26**, 557 (1981) (in Russian).

281. A. I. Akhieser and S. V. Peletminsky, Methods of Statistic Physics Nauka, Moscow, 1977 (in Russian).

282. V. M. Agranovich and M. D. Galanin, *Electronic Excitation Energy Transfer in Condensed Media*, Nauka, Moscow, 1978 (in Russian).

283. A. V. Sharkov, Yu. A. Matveev, S. V. Chekalin, and A. V. Tsakulev, *Doklady Acad. Nauk SSSR* **281**, 466 (1985) (in Russian).

284. J. Dobler, W. Zinth, W. Kaiser, and D. Oesterhelt, *Chem. Phys. Lett.* **144**, 215 (1988).

285. R. A. Mathies, C. H. Brito Cruz, W. T. Pollard, and C. V. Shank, *Science* **240**, 777 (1988).

286. S. L. Dexheimer, Q. Wang, L. A. Peteanu, W. T. Pollard, R. A. Mathies, and C. V. Shank, *Chem. Phys. Lett.* **188**, 61 (1992).

287. R. R. Birge, T. M. Cooper, A. F. Lawrence, M. B. Masthay, and C. Vasilakis, *J. Am. Chem. Soc.* **111**, 4063 (1989).

288. F. Bartl, G. Decker-Hebestreit, K. H. Altendorf, and G. Zundel, *Biophys. J.* **68**, 104 (1995).

289. B. Brzezinski, P. Radzievski, J. Olejnik, and Zundel, *J. Mol. Struct.* **323**, 71 (1993).

290. J. Heberle, J. Riesle, G. Thiedemann, D. Oesterhelt, and N. A. Dencher, *Nature* (*London*) **370**, 379 (1994).

291. G. W. Gray and B. Jones, *J. Chem. Soc.* (*London*) **12**, 4179 (1953).

292. L. M. Babkov, G. A. Puchkovska, S. P. Makarenko, and T. A. Gavrilko, *IR Spectroscopy of Molecular Crystals with Hydrogen Bonds*, Naukova Dumka, 1989 (in Russian).

293. C. Manohar, V. K. Kelkar, and J. V. Yakhmi, *Mol. Cryst. Liquid Cryst.* **49** (Letters), 99 (1978).

294. L. M. Sverdlov, M. A. Kovner, E. P. Krainov, *Vibrational Spectra of Polyatomic Molecules*, Nauka, Moscow, 1970.

295. J. H. Schachtschneider and R. G. Snyder, *Spectrochim. Acta* **19**, 117 (1963).

296. A. V. Iogansen, in *Hydrogen Bond*, Nauka, Moscow, 1981, p. 112 (in Russian).

297. A. S. N. Rao, C. R. K. Murty, and T. R. Reddy, *Phys. Status Solidi A* **68**, 373 (1981).

298. J. D. Bernal and D. Crowfood, *Trans. Farad. Soc.* **29**, 1032 (1933).

299. P. Excoffon and Y. Mareshal, *Spectrochim. Acta A* **28**, 269 (1972).

300. I. V. Bargatin, B. A. Grishanin, and V. N. Zadkov, *Uspekhi Fiz. Nauk* **171**, 625 (2001) (in Russian).

301. D. L. Haycock, P. M. Alsing, I. H. Deutsch, J. Grondalski, and P. S. Jessen, *Phys. Rev. Lett.* **85**, 3365 (2000).

302. J. Clarke et al., *Science* **239**, 992 (1988).

303. D. M. Stamper-Kurn, H.-J. Miesner, A. P. Chikkatur, S. Inouye, J. Stenger, and W. Ketterle, *Phys. Rev. Lett.* **83**, 661 (1999).

304. W. Wernsdorfer, E. Benoit, D. Mailly, O. Kubo, K. Hasselbach, A. Benoit, D. Mailly, O. Kubo, H. Nakamo, and B. Barbara, *Phys. Rev. Lett.* **79**, 4014 (1997).

305. E. M. Chudnovsky and J. Tejada, *Macroscopic Quantum Tunneling of the Magnetic Moment*, Cambridge University Press, Cambridge, England, 1998.

306. E. M. Chudnovsky, L. Gunther, *Phys. Rev. Lett.* **60**, 661 (1988).

307. R. Sessoli, D. Gatteschi, A. Caneschi, and M. Novak, *Nature* (London) **365**, 141 (1993).

308. J. R. Friedman, M. P. Sorchik, J. Tejada, and R. Zilo, *Phys. Rev. Lett.* **76**, 3830 (1996).

309. C. P. Bean and J. D. Livingston, *J. Appl. Phys.* **30**, 120S (1959).

310. W. T. Coffey, *J. Mol. Liq.* **51**, 77 (1992); *J. Chem. Phys.* **99**, 3014 (1993); **107**, 4960 (1997).

311. W. T. Coffey, V. I. Gaiduk, B. M. Tsetlin, and M. E. Walsh, *Physica A* **282**, 384 (2000).

312. P. C. Fannin and W. P. Coffey, *Phys. Rev. E* **52**, 6129 (1995).

313. Yu. P. Kalmykov, W. T. Coffey, and J. T. Waldron, *J. Chem. Phys.* **105**, 2112 (1996).

314. W. T. Coffey, Y. P. Kalmykov, and E. S. Massawe, *Phys. Rev. E* **48**, 699 (1993).

315. W. T. Coffey and Y. P. Kalmykov, *J. Magn. Magn. Mater.* **164**, 133 (1996).

316. H. Kachkachi, W. T. Coffey, D. S. F. Crothers, A. Ezzir, E. C. Kennedy, M. Noguès, and E. Tronc, *J. Phys. Condens. Matter* **12**, 3077 (2000).

317. W. T. Coffey, D. S. F. Crothers, J. L. Dormann, L. J. Geoghegan, E. C. Kennedy, and W. Wernsdorfer, *J. Phys. Condens. Matter* **10**, 9093 (1998).

318. W. T. Coffey, D. S. F. Crothers, J. L. Dormann, L. J. Geoghegan, E.C. Kennedy, *J. Magn. Magn. Mater.* **173**, L219 (1997).

319. P. M. Tomchuk and V. Krasnoholovets, *J. Mol. Struct.* **416**, 161 (1997).

320. P. M. Tomchuk and S. P. Lukyanets, *J. Mol. Struct.* **513**, 35 (1999).

321. P. M. Tomchuk and S. P. Lukyanets, *Cond. Matter Phys.* **1**, 203 (1998).

322. P. M. Tomchuk and S. P. Lukyanets, *Phys. Status Solidi B* **218**, 291 (2000).

323. A. S. Davydov, *Solitons in Molecular Systems*, Reidel, Dordrecht, 1986.

324. A. I. Sergienko, *Phys. Status Solidi B* **144**, 471 (1987).

325. O. E. Yanovskii and E.S. Kryachko, *Phys. Status Solidi B* **147**, 69 (1988).

326. R. B. Laughlin, *Rev. Mod. Phys.* **71**, 863 (1999).

327. R. D. Fedorovich, D. S. Inosov, O. E. Kiyaev, S. P. Lukyanets, P. M. Tomchuk, A. G. Naumovets, *Proc. SPIE* (2001), in press.

328. D. D. Awschalom, J. F. Smyth, G. Grinstein, D. P. DiVinchenzo, and D. Loss, *Phys. Rev. Lett.* **68**, 3092 (1992).

329. J. Tejada, X. X. Zhang, E. del Barco, J. M. Hernandez, and E. M. Chudnovsky, *Phys. Rev. Lett.* **79**, 1754 (1997).

330. M. J. O'Shea and P. Perera, *J. Appl. Phys.* **76**, 6174 (1994).

331. S. Washburn, R. A. Webb, and S. M. Faris, *Phys. Rev. Lett.* **54**, 2712 (1985).

332. A. Garg and G.-H. Kim, *Phys. Rev. B* **45**, 12921 (1992).

333. H.-B. Braun and D. Loss, *Phys. Rev. B* **53**, 3237 (1996).

334. R. Hassan and E. Campbell, *J. Chem. Phys.* **97**, 4326 (1992).

335. L. Weil, *J. Chem. Phys.* **51**, 715 (1954).

336. P. Politi, A. Rettori, F. Hartmann-Boutrn, and J. Villain, *Phys. Rev. Lett.* **75**, 537 (1995).

337. A. Rahman and F. H. Stillinger, *J. Am. Chem. Soc.* **95**, 7943 (1973).

338. F. H. Stillinger, *Adv. Chem. Phys.* **31**, 1 (1975).

339. M. G. Sceats and S. A. Rice, *J. Chem. Phys.* **72**, 3236 (1980); **72**, 3248 (1980); **72**, 3260 (1980).

340. M. G. Sceats and S. A. Rice, *Water and Aqueous Solutions at Temperature Below 0°C*, Naukova Dumka, Kyiv, 1985, pp. 76, 346 (Russian translation).

341. G. G. Malenkov, *Physical Chemistry. Contemporary Problems*, Ya. M. Kolotyrkin, ed., Khimia, Moscow, 1984, p. 41 (in Russian).

342. Y. I. Naberukhin, *Zh. Strukt. Khim.* **25**, 60 (1984) (in Russian).

343. V. Y. Antonchenko, A. S. Davydov, and V. V. Ilyin, *The Essentials of Physics of Water*, Naukova Dumka, Kyiv, 1991 (in Russian).

344. C. Rønne, P.-O. Åstrand, and S. R. Keiding, *Phys. Rev. Lett.* **82**, 2888 (1999).

345. *Water: A Comprehensive Treatise*, Vols. 1–7, F. Franks, ed., Plenum Press, New York, 1972, p.181.

346. C. A. Angell, *Annual Review of Physical Chemistry*, Vol. 34, Annual Reviews, Palo Alto, 1983, p. 593.

347. C. A. Angell, *Nature* (*London*) **331**, 206 (1988).

348. P. H. Poole, F. Sciorino, U. Essmann, and H. E. Stanley, *Nature* (*London*) **360**, 324 (1992).

349. N. Agmon, *J. Phys. Chem.* **100**, 1072 (1996).

350. H. Tanaka, *Nature* (*London*) **380**, 328 (1996).

351. *Supercooled Liquids*, Vol. 676, J. T. Fourkas, D. Kivelson, U. Mohanty, and K. A. Nelson, eds., American Chemical Society, Washington, D.C., 1997.

352. S. Woutersen, U. Emmerichs, and H. J. Bakker, *Science* **278**, 658 (1997).

353. O. Mishina and H. E. Stanley, *Nature* (*London*) **392**, 164 (1998); **396**, 329 (1998).

354. J. Ortega, J. P. Lewis, and O. F. Sankey, *Phys. Rev. B* **50**, 10516 (1994).

355. P. H. Poole, F. Sciortino, T. Grande, H. E. Stanley, and C. A. Angell, *Phys. Rev. Lett.* **73**, 1632 (1994).

356. F. Scortino, P. H. Poole, U. Essmann, and H. E. Stanley, *Phys. Rev. E* **55**, 727 (1997).

357. C. T. Moynhian, *Mater. Res. Soc. Symp. Proc.* **455**, 411 (1997).

358. V. I. Gaiduk and V. V. Gaiduk, *Russ. J. Phys. Chem.* **71**, 1637 (1997).

359. V. D. Zelepukhin, I. D. Zelepukhin, and V. Krasnoholovets, *Khimich. Fiz.* **12**, 992 (1993) (in Russian); English translation: *Sov. J. Chem. Phys.* **12**, 1461 (1994).

360. A. V. Kondrachuk, V. Krasnoholovets, A. I. Ovcharenko, and E. D. Chesnokov, *Khimich. Fiz.* **12**, 1006 (1993) (in Russian); English translation: *Sov. J. Chem. Phys.* **12**, 1485 (1994).

361. V. D. Zelepukhin and I. D. Zelepukhin, *A Clue to "Live" Water*, Kaynar, Alma-Ata, 1987 (in Russian).

362. T. H. Maugh II, *Science* **202**, 414 (1978).

363. D. Freifelder, *Physical Biochemistry*, Mir, Moscow, 1980 (Russian translation).

364. L. I. Antropov, *Theoretical Electrochemistry*, Vysshaya Shkola, Moscow, 1980 (in Russian).

365. C. Kittel, *Statistical Thermodynamics*, Nauka, Moscow, 1977 (Russian translation).

366. L. Pauling, *Nature of the Chemical Bond and the Structure of Molecules and Crystals: An Introduction to Modern Structural Chemistry*, 3rd ed., Cornell University Press, New York, 1960.

367. G. A. Krestov, *The Thermodynamics of Ionic Processes in Solutions*, Khimia, Leningrad, 1973 (in Russian).

368. M. K. Karapetiants, *Introduction to the Theory of Chemical Processes*, Vysshaya Shkola, Moscow, 1981 (in Russian).

369. R. Langner and G. Zundel, *Can. J. Chem.* **79**, 1376 (2001).

370. A. A. Aleksandrov and M. S. Trakhtenberg, *The Thermophysical Properties of Water at Atmospheric Pressure*, Izdatel'stvo Standartov, Moscow, 1980 (in Russian).

371. S. L. Rivkin and A. A. Aleksandrov, *The Thermophysical Properties of Water and Water Vapor*, Energia, Moscow, 1977 (in Russian).

372. N. B. Vargaftik, *Handbook on the Thermophysical Properties of Fluids* Nauka, Moscow, 1972 (in Russian).

373. O. Y. Samoilov, *The Structure of Aqueous Solutions of Electrolytes and Hydration of Ions*, Izdatel'stvo AN SSSR, Moscow, 1955 (in Russian).

374. V. A. Rabinovich and Z. Y. Khavin, *Concise Chemical Handbook*, Khimiya, Moscow, 1978 (in Russian).

375. Y. B. Zeldovich, *Zh. Exp. Teor. Fiz.* **12**, 525 (1942) (in Russian).

376. E. N. Harvey, W. D. McElroy, and A. H. Whiteley, *J. Appl. Phys.* **18**, 162 (1947).

377. Y. E. Geguzin, *Bubbles*, Nauka, Moscow, 1985 (in Russian).

378. A. M. Blokh, *The Structure of Water and Geological Processes*, Nedra, Moscow, 1969 (in Russian).

379. N. F. Bondarenko and E. Z. Gak, *Electromagnetic Phenomena in Natural Water*, Gidrometeoizdat, Leningrad, 1984 (in Russian).

380. G. V. Yuknevich, *Zh. Struct. Khim.* **25**, 60 (1984); Preprint No. 86-102P, (Institute Theoretical Physics Ukrainian Academy of Science, Kyiv, 1986 (in Russian).

381. A. Kaivarainen, *Am. Inst. Phys. Conf. Proc.* (*New York*) **573**, 181 (2001); *arXiv.org e-print archive* physics/0102086.

382. M. Chaplin, http://www.sbu.ac.uk/water.

383. I. Z. Fisher and B. N. Adamovich, *Zh. Strukt. Khim.* **4**, 818 (1963) (in Russian).

384. P. A. Egelstaff, *Adv. Phys.* **11**, 203 (1962).

385. G. P. Gordeev and T. Khaidarov, *Water in Biological Systems and Their Components*, Leningrad State University, Leningrad, 1983, p. 3; (in Russian).

386. W. A. R. Luck, *Angew. Chem. Int. Engl.* **19**, 28 (1980).

387. R. Hausser, *Z. Naturforsch.* **18**, 1143 (1963).

388. D. W. G. Smith and J. G. Powles, *Mol. Phys.* **10**, 451 (1966).

389. J. C. Hindman, Svirmickas, and M. Wood, *J. Chem. Phys.* **59**, 1517 (1973).

390. J. C. Hindman, *J. Chem. Phys.* **60**, 4483 (1974).

391. J. Jonas, T. De Fries, and D. J. Wilbur, *J. Chem. Phys.* **65**, 582 (1976).

392. E. W. Lang and H. D. Ludeman, *J. Chem. Phys.* **67**, 718 (1977).

393. N. A. Melnichenko and V. I. Chizhik, *Zh. Strukt. Khim.* **22**, 76 (1981).

394. V. V. Mank and Lebovka, *NMR Spectroscopy of Water in Heterogeneous Systems*, Naukova Dumka, Kyiv, 1988 (in Russian).

395. V. I. Jaskichev, *Adv. Mol. Relaxation Interact. Processes* **24**, 157 (1982).

396. V. I. Jaskichev, V. P. Sanygin, and Y. P. Kalmukov, *Zh. Fiz. Khim.* **57**, 645 (1983).

397. T. Kimura, K. Yamamoto, T. Shimizu, and S. Yugo, *Thin Solid Films* **70**, 351 (1980).

398. K. Nanaka and M. Iwata, *Thin Solid Films* **81**, L85 (1981); **86**, 279 (1981).

399. R. Muller and H. Pagnia, *Matt. Lett.* **2**, 283 (1984).

400. N. A. Tolsoi, *Dokl. Akad. Nauk SSSR* **110**, 893 (1955) (in Russian).

401. N. A. Tolstoi and A. A. Spartakov, *Kolloid. Zh.* **28**, 580 (1966) (in Russian).

402. E. McCafferty and A. C. Zettlemoyer, *Discuss. Farad. Soc.* **52**, 239 (1971).

403. R. McIntosh, *Dielectric Behavior of Physically Absorbed Gases*, Marcel Dekker, New York, 1966.

404. N. A. Tolstoi, A. A. Spartakov, and A. A. Tolstoi, *Kolloid. Zhurn.* **28**, 881 (1966) (in Russian).

405. H. Stobbe and G. Peschel, *Colloid. Polym. Sci.* **275**, 162 (1997).

406. B. V. Deriagin and Y. V. Shulepov, *Surf. Sci.* **81**, 149 (1979).

407. I. R. Yukhnovsky and Y. V. Shulepov, Preprint ITP No. 83-103E, Institute of Theoretical Physics, Kyiv (1983).

408. V. Krasnoholovets and P. M. Tomchuk, *Ukr. Fiz. Zh.* **36**, 1392 (1991) (in Russian); English translation: *Ukr. J. Phys.* **36**, 1106 (1991).

409. W. Drost-Hansen, *Phys. Chem. Liquids* **7**, 243 (1978).

410. N. I. Lebovka and V. V. Mank, in *The State of Water in Different Physical Chemical Conditions*, Leningrad University, Leningrad, 1986, p. 84 (in Russian).

411. E. D. Belotsky and B. I. Lev, *Theor. Math. Phys.* **60**, 120 (1984) (in Russian).

412. V. Krasnoholovets and B. Lev, *Ukr. Fiz. Zh.* **33**, 296 (1994) (in Ukrainian).

413. B. I. Lev and A. Y. Zhugaevich, *Phys. Rev. E* **57**, 6460 (1998).

414. V. Krasnoholovets and B. Lev, *Cond. Math. Phys.*, submitted (also cond-mat/0210131).

415. A. G. Khachaturian, *The Theory of Phase Transitions and the Structure of Solid Solutions*, Nauka, Moscow, 1974 (in Russian).

416. V. B. Kobyliansky, *Statistical Physics*, Vyscha Schkola, Kyiv, 1972 (in Ukrainian).

417. J. S. Metzik, V. D. Perevertaev, V. A. Liopo, G. T. Timoshchenko, and A. B. Kiselev, *J. Colloid Interface Sci.* **43**, 662 (1973).

418. A. Gupta and M. M. Shamura, *J. Colloid Interface Sci.* **149**, 392 (1992).

419. W. A. P. Luck, *Structure of Water and Aqueous Solutions*, Verlag Chemie, Weinheim, 1974.